871179
CONF-87119--Vol. 1

* Research sponsored by the Office of Fusion Energy, U.S. Department of Energy, under contract DE-AC05-84OR21400 with Martin Marietta Energy Systems, Incorporated.

Proceedings of

U.S.–Japan

Heliotron-Stellarator

Workshop

Volume I

held at

Oak Ridge National Laboratory
Oak Ridge, Tennessee, U.S.A.

November 9-13, 1987

AGENDA FOR US-JAPAN STELLARATOR/HELIOTRON WORKSHOP

FUSION ENGINEERING DESIGN CENTER, OAK RIDGE

NOVEMBER 9–13, 1987

Table of Contents

CONF-871179--Vol.1

DE88 004790

Monday, November 9

8:30 A.M. Registration

8:45 A.M. Welcome – M. W. Rosenthal (ORNL)

Opening Remarks – K. Uo (Kyoto PPL)

9:00 A.M. Overviews – K. Uo, Chairman Volume I

Overview of the Heliotron E Experiment – O. Motojima (Kyoto PPL)

Overview of CHS Program – K. Matsuoka (Nagoya IPP)

Status of ATF Project – G. H. Neilson (ORNL)

Status of W VII-AS – H. Renner (IPP Garching)

TJ-II Program Status – A. P. Navarro (CIEMAT, Madrid)

12:30 P.M. Lunch

2:00 P.M. Tour of ATF and private discussions, Fusion Energy Division

Tuesday, November 10

8:30 A.M. Programs, Device Preparation - J. L. Shohet, Chairman

ATF Experimental Plans – M. Murakami (ORNL)

ATF Diagnostics – R. C. Isler (ORNL)

Machine of Compact Helical Syste – K. Matsuoka (Nagoya IPP)

CHS Experimental Program and Diagnostics – S. Okamura (Nagoya IPP)

Transport Studies in IMS – J. L. Shohet (U. Wisc.)

11:30 A.M. Lunch

Tuesday, November 10

1:00 P.M. Confinement - O. Motojima, Chairman Volume II

Ripple Transport at Arbitrary Collision Frequency – W.N.G. Hitchon (U. Wisc.)

Transport Scaling in the Collisionless–Detrapping Regime – E. C. Crume (ORNL)

Transport Analysis for Heliotron E – T. Mutoh (Kyoto PPL)

Transport Analysis for ATF – H. C. Howe (ORNL)

Simulation Analysis of Heating and Transport – T. Amano (Nagoya IPP)

Analysis of W VII-A Data – H. Renner (IPP Garching)

7:00 P.M. Reception - Home of W. R. Wing

Wednesday, November 11

8:30 A.M. ECH and NBI - M. Murakami, Chairman

Numerical Study of Fast Ion Confinement – K. Hanatani (Kyoto, PPL)

Benchmarks of NBI Codes for Stellarators – R. H. Fowler (ORNL)

ECH Commissioning and Plans for ATF – T. L. White (ORNL)

ECH and ICH Startup Analysis – M. D. Carter (ORNL)

11:30 A.M. Lunch

1:00 P.M. Ion Cyclotron Heating - T. Amano, Chairman Volume III

Heliotron E ICRF Heating Experiment – T. Mutoh (Kyoto PPL)

CHS Heating Systems (NBI, ECH, ICH) – K. Nishimura (Nagoya IPP)

ICH Program for ATF – F. W. Baity (ORNL)

ICRF Wave Propagation – D. B. Batchelor (ORNL)

The HBQM Heliac Work – B. A. Nelson (U. Washington)

Volume III (continued)

Thursday, November 12

8:30 A.M. Configuration Studies - G. H. Neilson, Chairman

Configuration Studies – K. Nishimura (Nagoya IPP)

Compact Torsatron Studies – B. A. Carreras (ORNL)

Low Aspect Ratio Torsatron Design – J. Hanson (Auburn)

Optimized Small Stellarator Designs – D. T. Anderson (U. Wisc.)

Configuration Studies for ATF – J. H. Harris (ORNL)

11:30 A.M. Lunch

1:00 P.M. Configuration Studies - K. Matsuoka, Chairman

Currents in ATF – B. A. Carreras (ORNL)

Computations of 3-D Equilibria with Islands – A. Reiman (PPPL)

Magnetic Surface Mapping Studies – D. G. Swanson (Auburn)

Magnetic Field Alignment and Mapping on ATF – F.S.B. Anderson (U. Wisc.)

Divertor Experiments in IMS – D. T. Anderson (U. Wisc.)

Friday, November 13

8:30 A.M. General Experimental - H. Renner, Chairman

PMI Program and Wall Conditioning for ATF – P. K. Mioduszewski (ORNL)

Hard X-ray Suppression on ATF – D. A. Rasmussen (ORNL)

Plasma Rotation and Potential Measurement – O. Motojima, (Kyoto PPL)

Status of Heavy Ion Beam Probe for ATF – A. Carnevali (RPI)

11:30 A.M. Lunch

1:00 P.M. Private discussions, Fusion Energy Division

Visit to Large Coil Facility?

OVERVIEW OF HELIOTRON E EXPERIMENT

O.MOTOJIMA

1. INTRODUCTION OF HELIOTRON E DEVICE

2. EXPERIMENT IN FY 1987 (FROM APRIL 1987 TO MARCH 1988)

ICF	APRIL - SEPTEMBER, 1987
ECRH	OCTOBER - JANUARY, 1988
PLASMA-WALL	FEBRUARY - MARCH, 1988

3. RESULTS OF CARBONIZATION EXPERIMENT

4. NEAR FUTURE PROGRAM

Heating Ex. (ECH, NBI, ICRF)

Confinement Study (Neoclassical Transport)

MHD (High β Ex.)

Plasma Wall (Carbon Tile, Carbonized Diverter)

LIST OF SCIENTIFIC STAFF

K. UO, A. IIYOSHI, T. OBIKI, M. WAKATANI, O. MOTOJIMA

S. MORIMOTO, M. SATO, S. SUDO, F. SANO, T. MUTOH, K. ITOH,
T. AKAISHI, M. NAKASUGA, K. KONDO, K. HANATANI, H. ZUSHI,
H. KANEKO, T. MIZUUCHI, H. OKADA, Y. TAKEIRI, N. NODA

K. OHTAKE, Y IJIRI, M. IIMA, N. KAWABATA, T. SENJU, K. YAGUTI,
T. BABA, S. KOBAYASHI

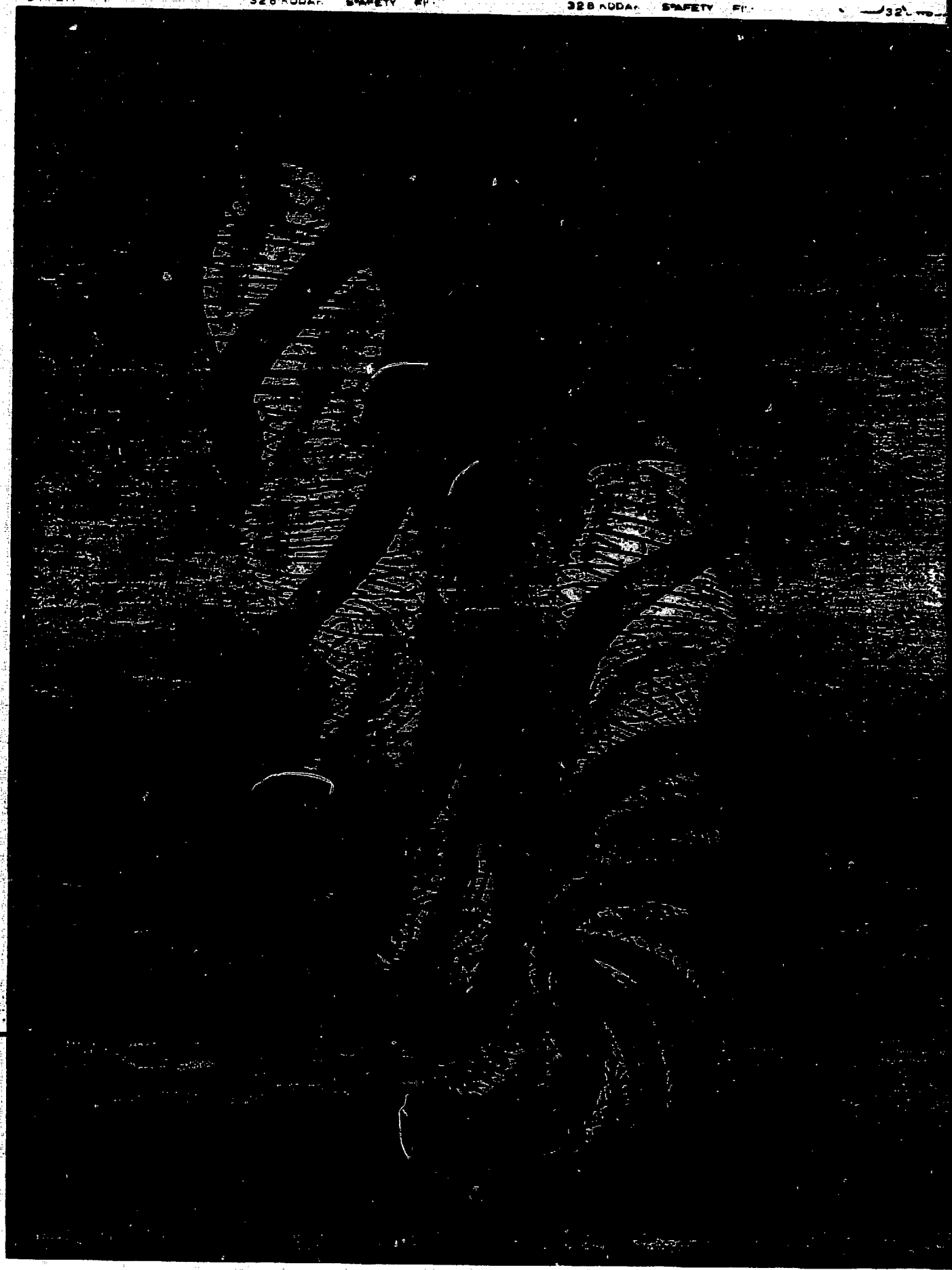

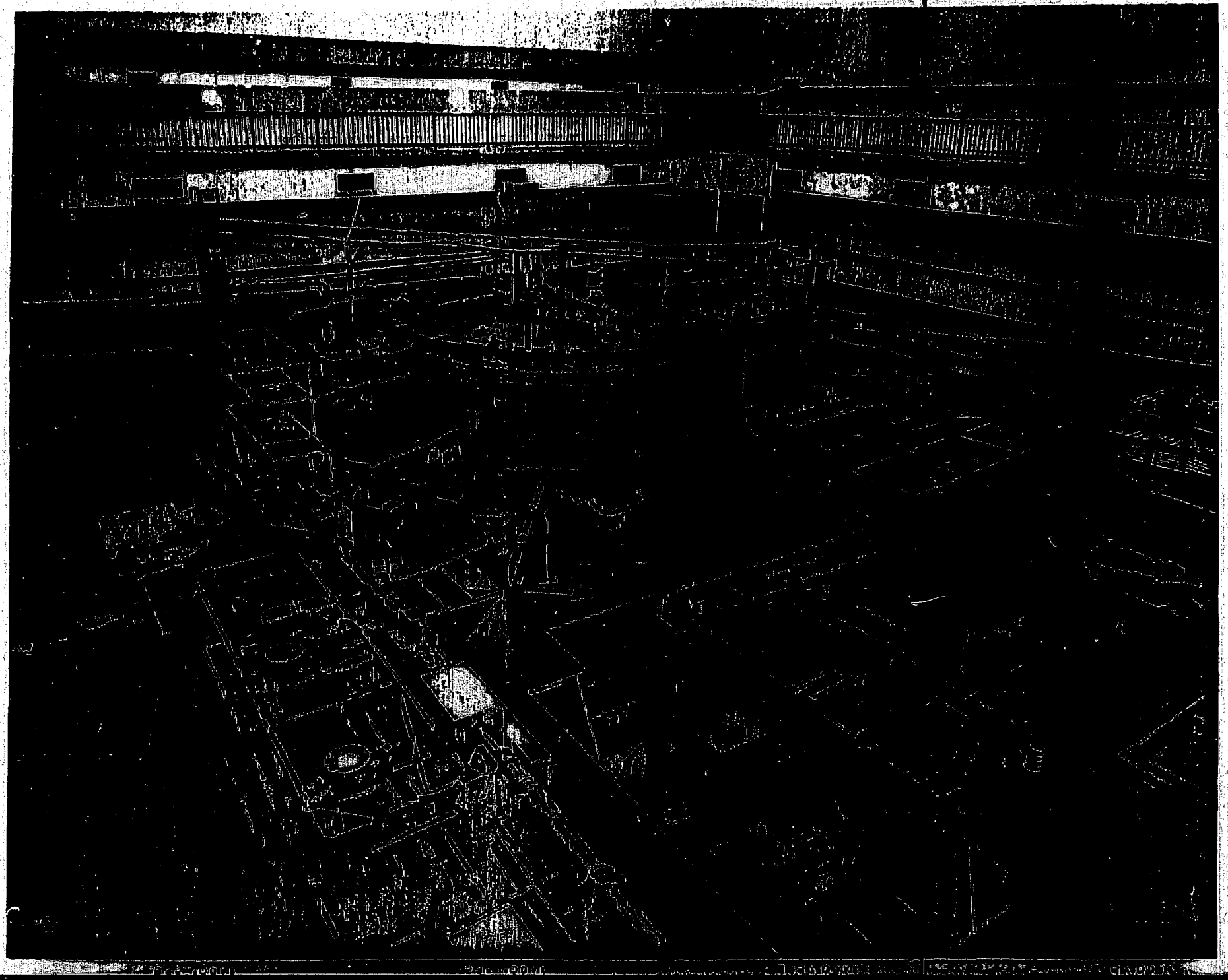

SPECIFICATION OF HELIOTRON E DEVICE

$R = 2.2\text{m}$

$a_c = 0.293\text{m}$

$\bar{a}_p = 0.2\text{m}$

$V_p = 1.7\text{m}^3$

$B_h(0) = 2\text{T}$

$\iota_0 = 0.51, \ \iota_a = 2.5$

HIGH SHEAR MAGNETIC SYSTEM, LARGE ROTATIONAL TRANSFORM MAGNETIC LIMITER CONFIGURATION

HEATING SYSTEM

1. ECRH

FIVE GYROTRONS (AT PRESENT)

200 KWx5

53.2 GHz

TWO INLET PORTS #13.5(x4, VLASOV-MIRROR FOCUSED)

(→ OCTOBER, 1987) #28.5(x1, VLASOV-MIRROR FOCUSED)

↓

TE02x5 (TOROIDALLY DISTRIBUTED)

(NOW)

2. NBI

THREE BEAM LINES

$V_{acc} \leq 30$ KV

4 MW

0^{o} ; 5 ION SOURCES 1.9 MW

11^{o} ; 3 ION SOURCES 1.2 MW

28^{o} ; 2 ION SOURCES 0.9 MW

3. ICRF

FOUR ANTENNA SETS

26.7 MHz, 28.22 MHz, 17.8 MHz

2 MW

FAST WAVE AND SLOW WAVE MODES

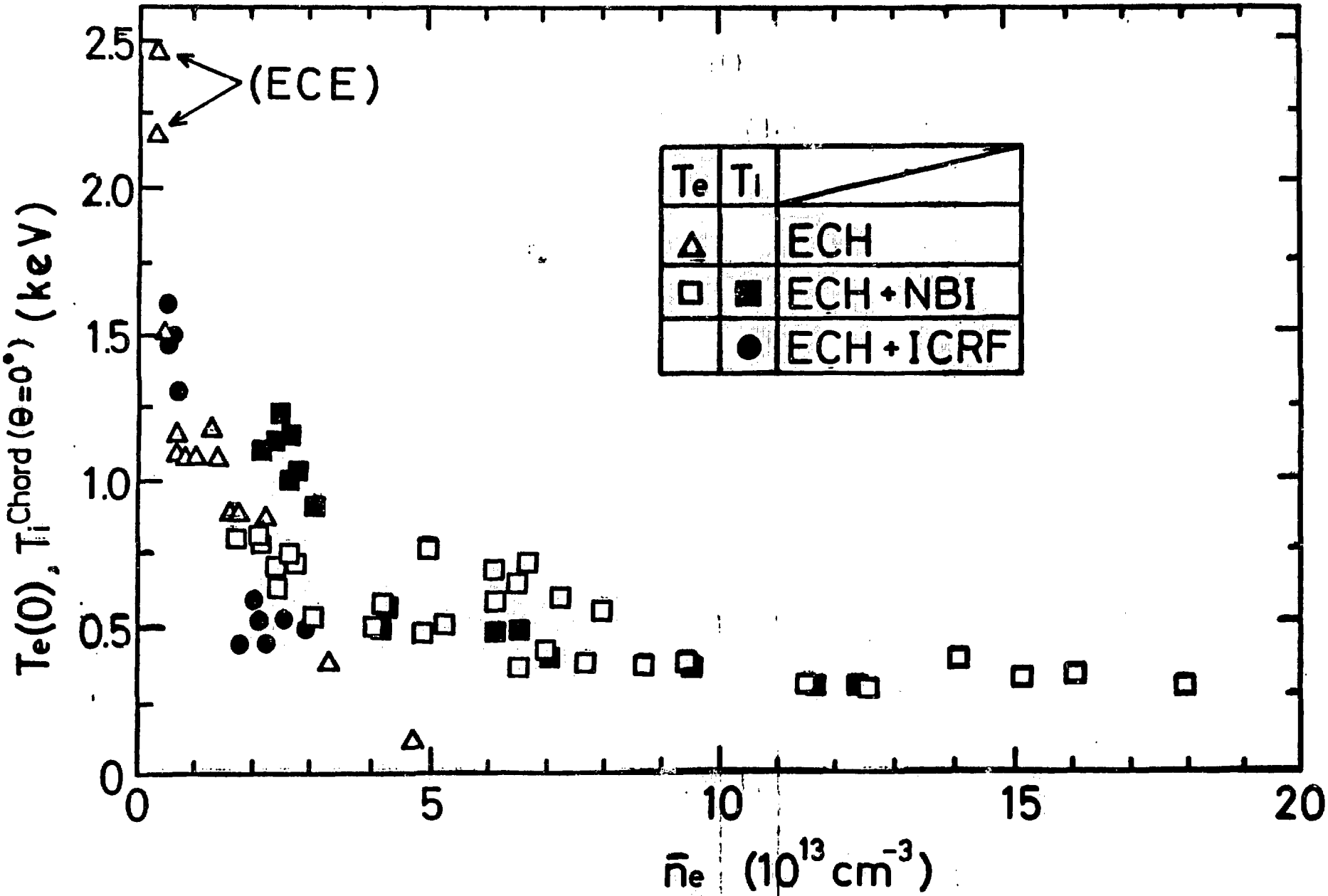
(ECE)
Te
Ti
ECH
ECH+NBI
ECH+ICRF
Te(0), Ti^Chord (θ=0°) (keV)
n̄e (10^13 cm^-3)
0
0.5
1.0
1.5
2.0
2.5
5
10
15
20

Experimental Plans

0033

now ↓

FY1987

4/1 5/1 6/1 7/1 8/1 9/1 10/1 11/1 12/1 1/1 2/1 3/1

ICRF

ECRH

Carbon Tile

NBI

Carbonization

FY1988

4/1 5/1 6/1 7/1 8/1 9/1 10/1 11/1 12/1 1/1 2/1 3/1

Carbon Tile

NBI

Helical Divertor

ECH, NBI

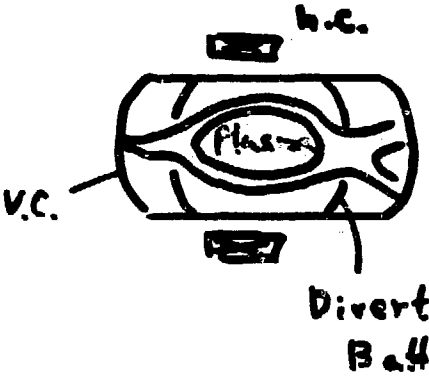

T_a. n_{ed}, T_{ed},

Field Optimization

ECH, NBI (Toroidal Coil)

19 TC (1 TC/Field Period)

t, Θ, $\bar{a}_p$

τ_E, $\bar{\beta}$

T_e

T_i

Scaling

STUDY OF PLASMA-WALL INTERACTION (FEBRUARY 1988-MARCH 1988)

(a) CARBONIZATION EXPERIMENT (CONTINUED)

(b) CARBON-TILE EXPERIMENT

TO REDUCE THE METALLIC IMPURITY OF THE PLASMA

→ HYDROGEN CONTENT OF THE CARBON FILM

TO CONTROL RECYCLING COEFFICIENT OF THE WALL

PHYSICAL OBJECTIVES OF ICRF HEATING EXPERIMENT (FROM APRIL TO SEPTEMBER, 1987)

By Mutch, Wednesday Afternoon

(a) HEATING EXPERIMENT
<<MAX T_i, T_e, HEATING EFFICIENCY>>

(b) CONFINEMENT STUDY OF HIGH ENERGY IONS ACCELERATED BY ICRF
<<HIGH ENERGY PARTICLE ORBIT, SLOWING DOWN AND HEATING PROCESS>>

(c) MEASUREMENTS OF POLOIDAL ROTATION AND PLASMA POTENTIAL
<<NEOCLASSICAL TRANSPORT, ELECTRIC FIELD EFFECT>>

MODE OF ICRF HEATING	B[T]	[MHz]	$\bar{n}_e$[cm^{-3}]	T_o[keV]
(a) MINORITY (H, He^3)/D	1.9	26.7/17.8 -28.2	$2\text{-}3\times10^{13}$	$\leq$1keV
(b) SLOW WAVE H	1.9	26.7-28.2	0.5×10^{13}	$\leq$1.6

Top View of Heliotron E Device

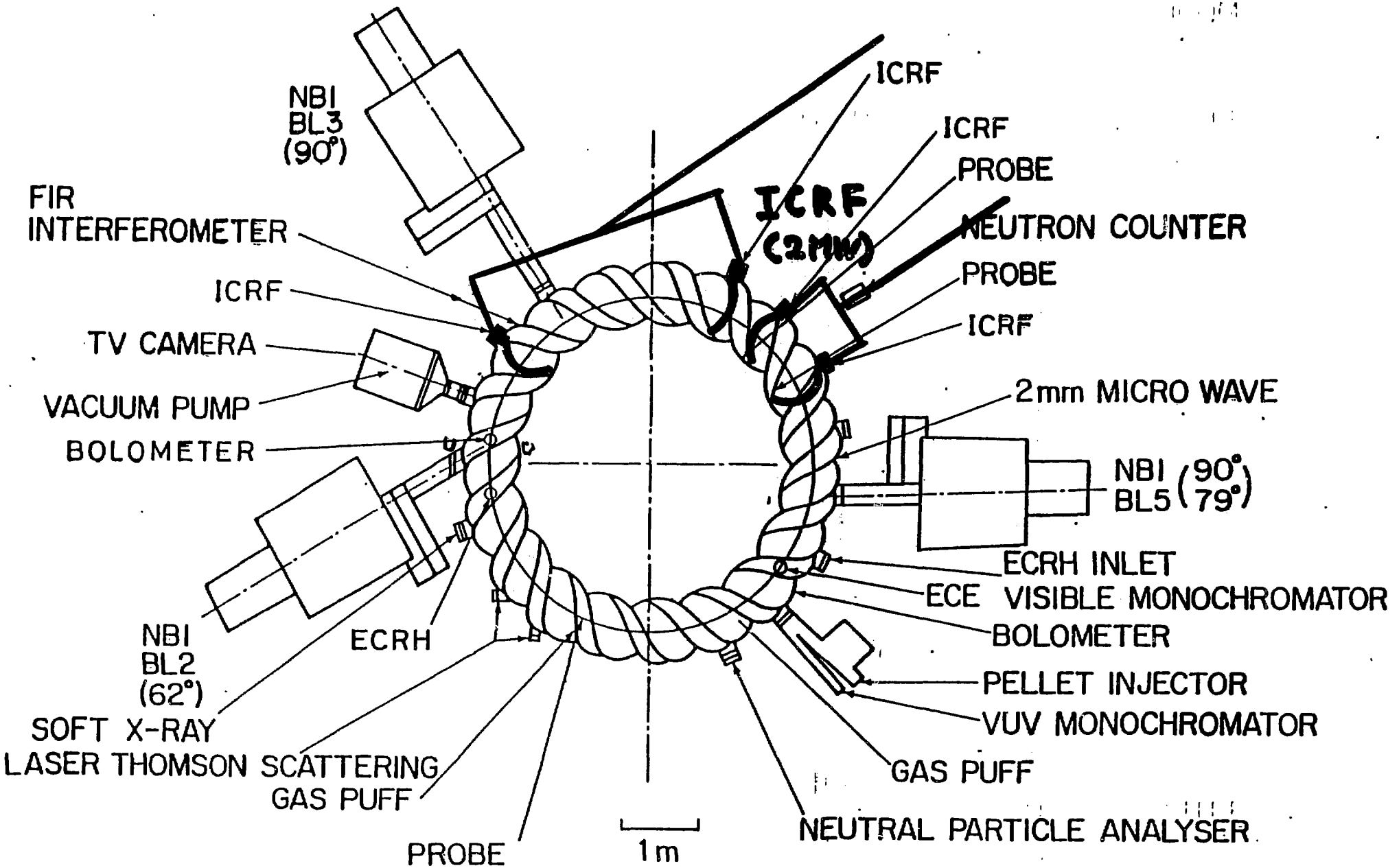

Time Traces of Plasma Parameters

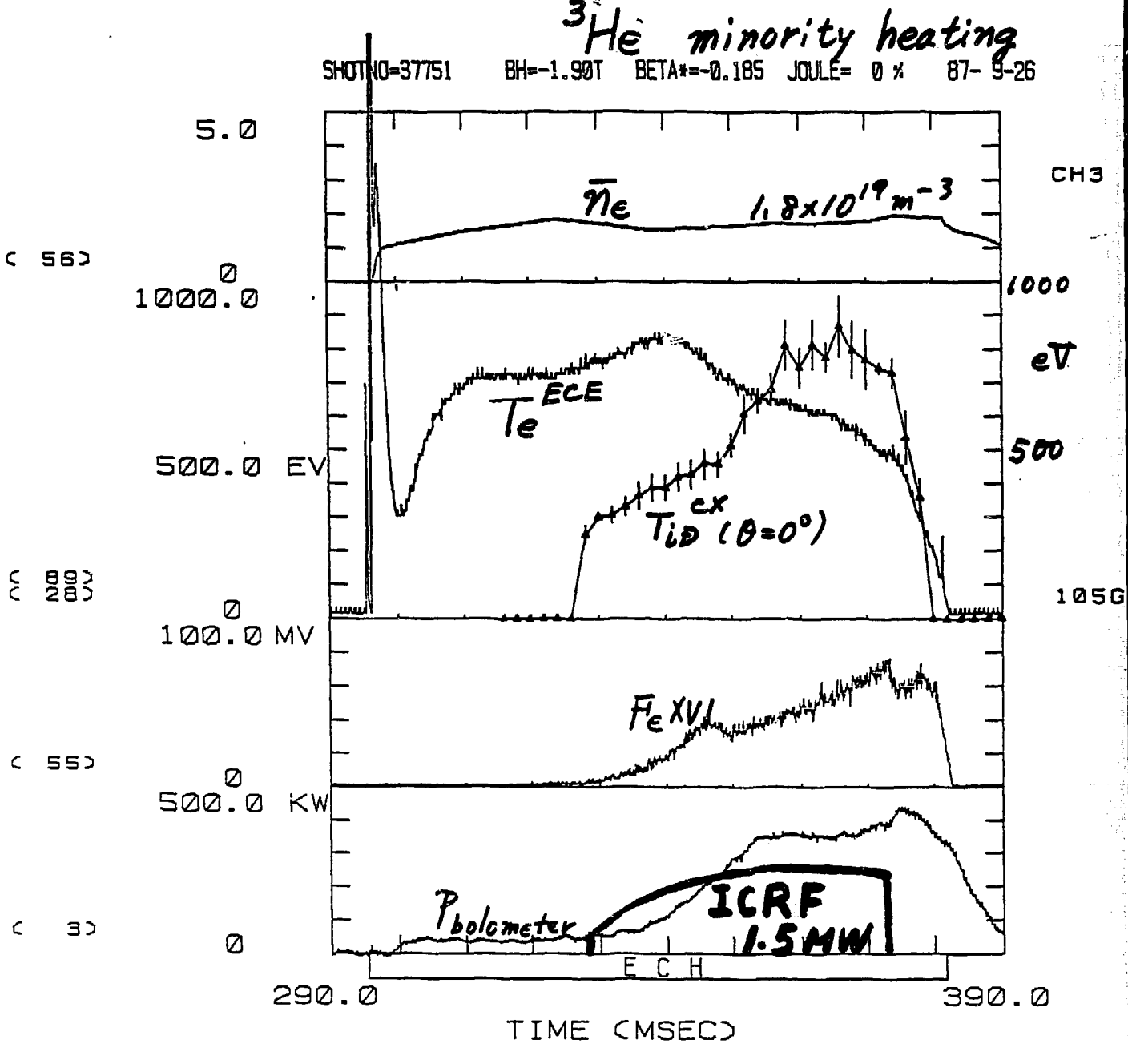

Bulk Ion Temperature Rise (D^+) by ICRF

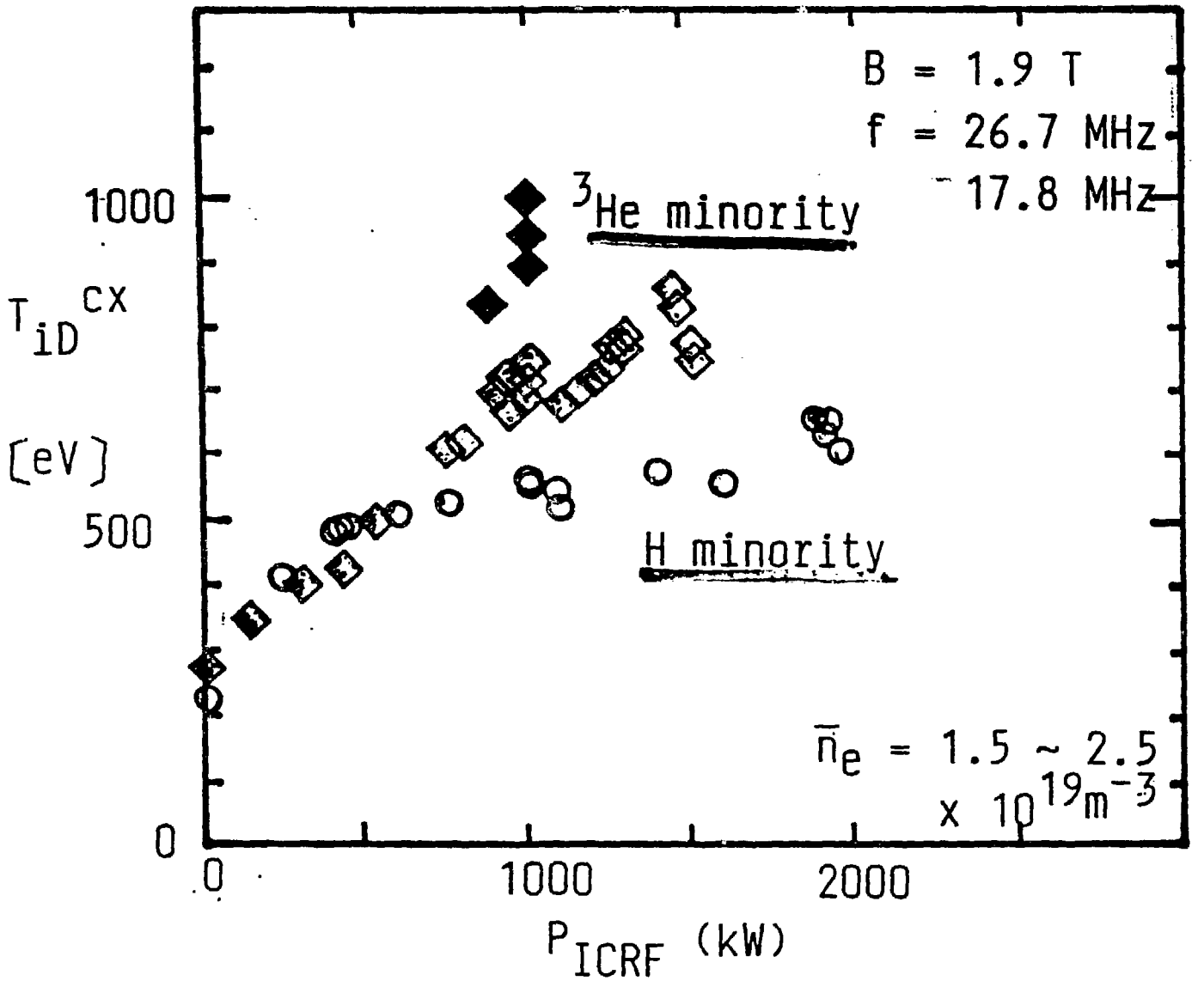

High Energy Newtral Particle Analys

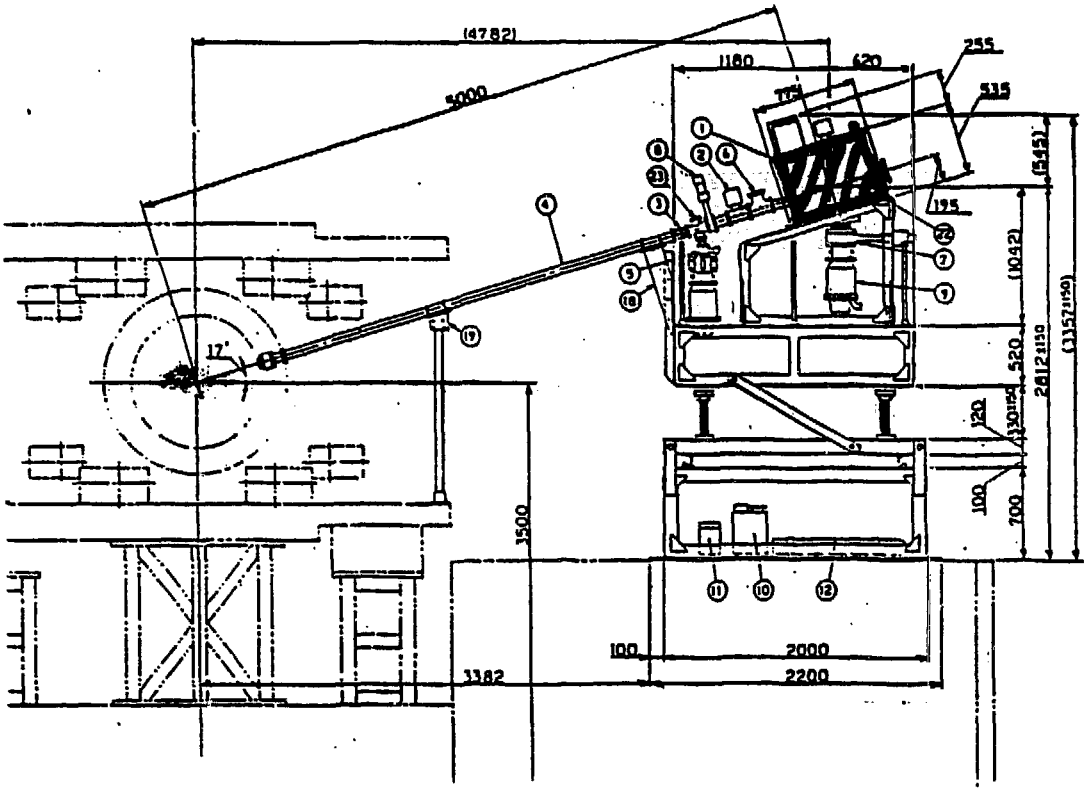

HNPA (EIIB Type)

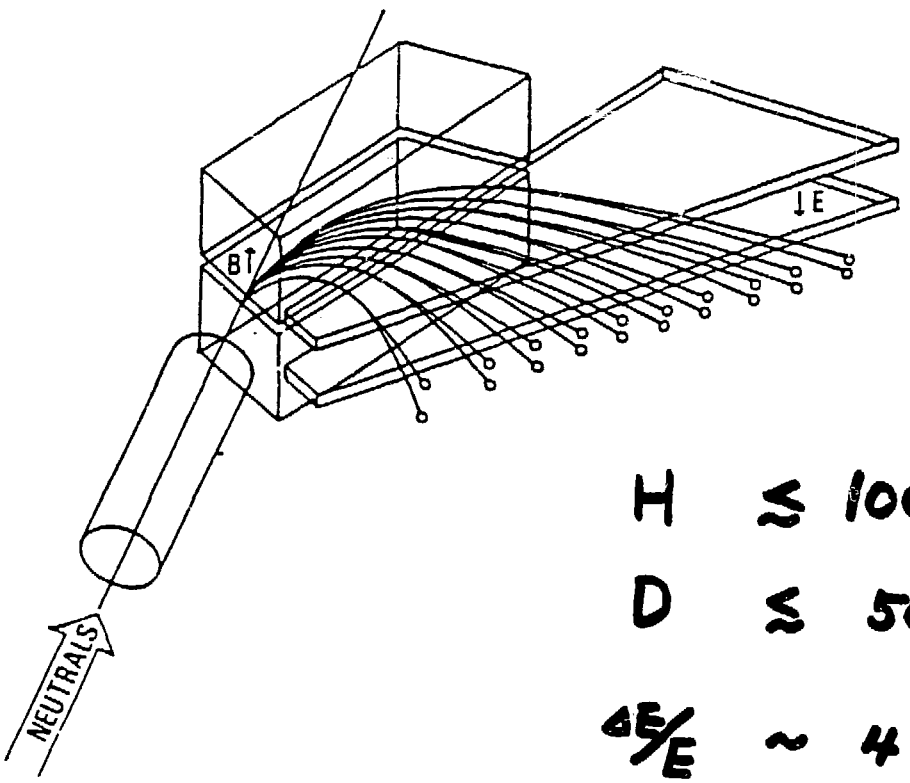

$H \lesssim 100$ keV

$D \lesssim 50$ keV

$\Delta E/E \sim 4 \div 9\%$

FIG. 1. Schematic of analyzer concept.

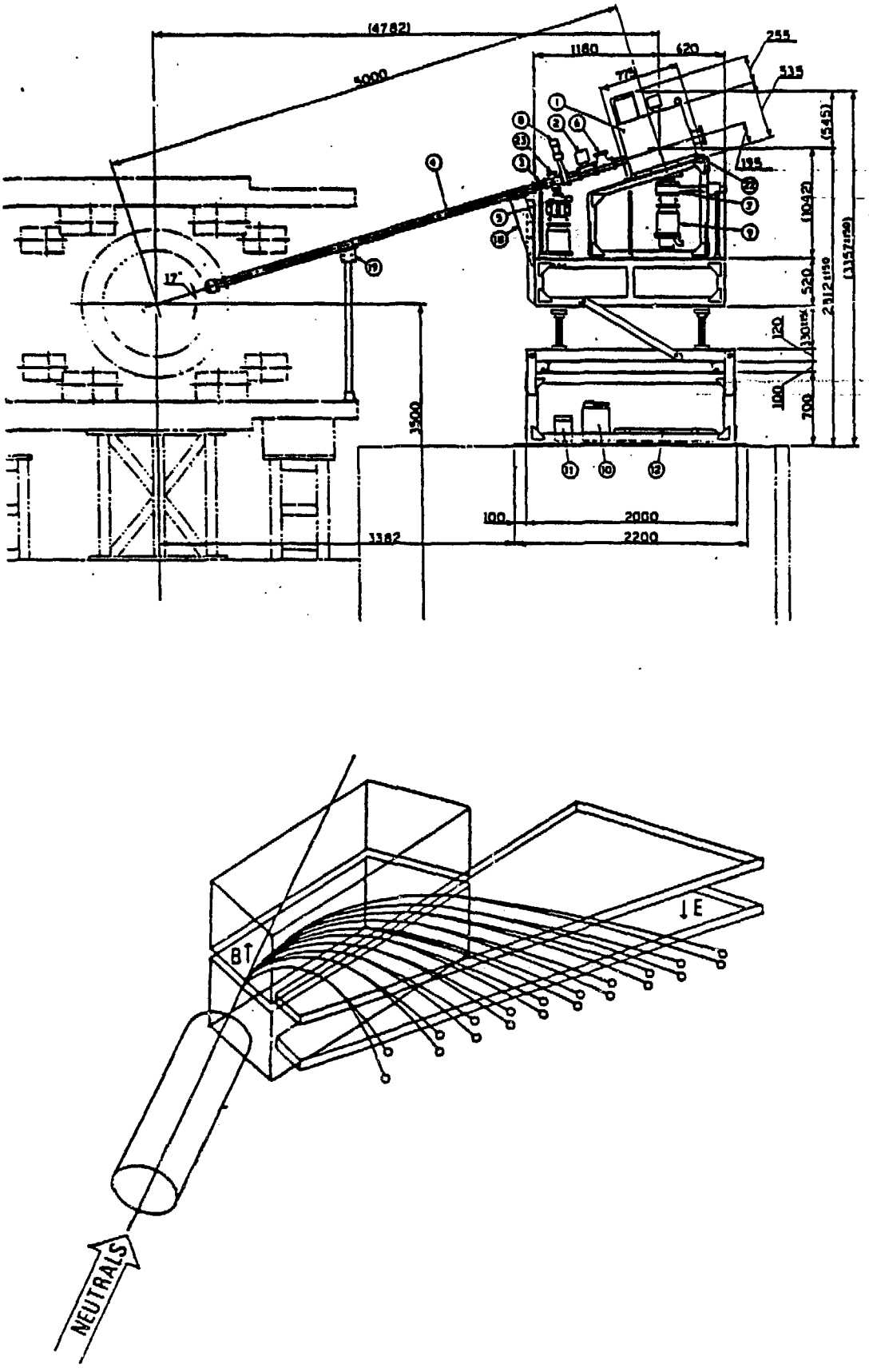

FIG. 1. Schematic of analyzer concept.

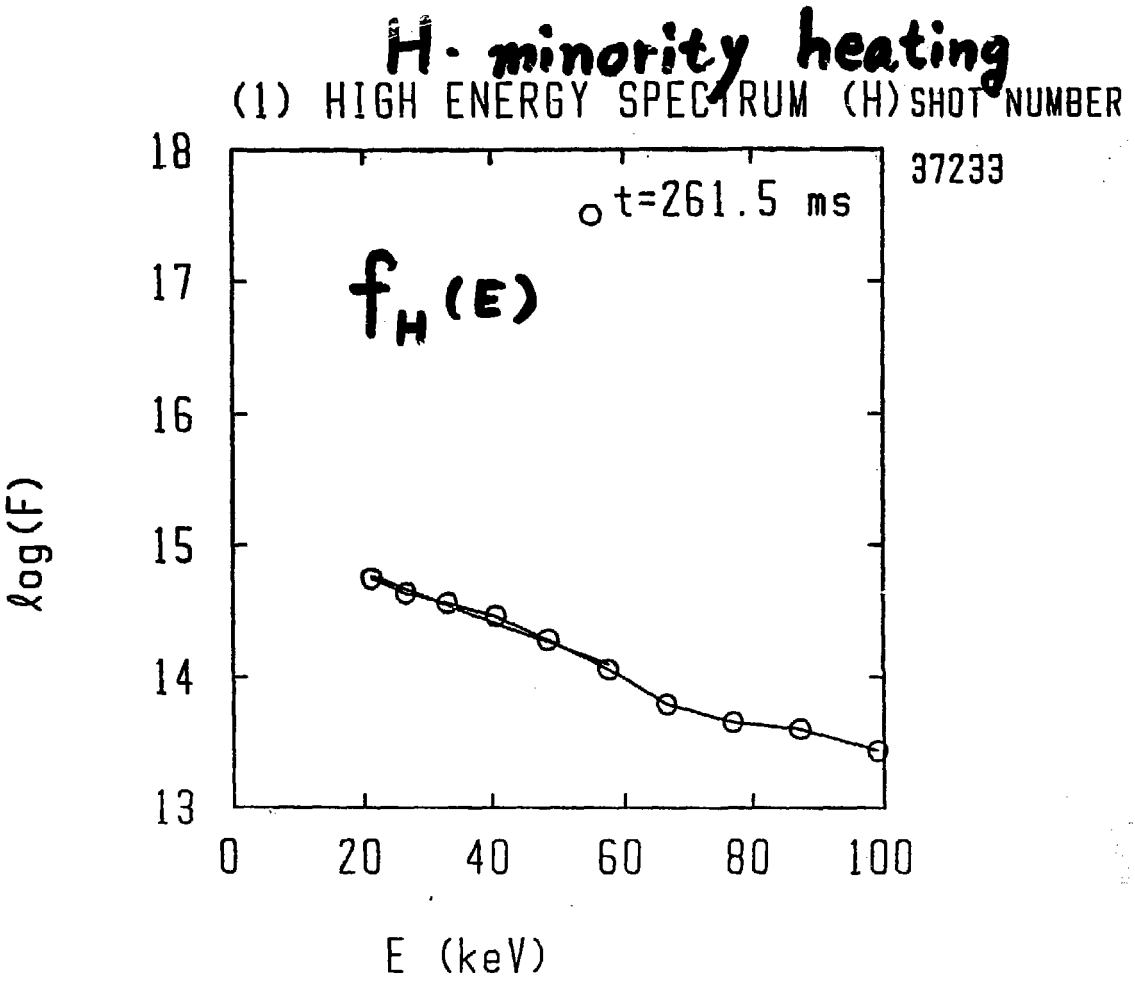
H-minority heating
(1) HIGH ENERGY SPECTRUM (H)
SHOT NUMBER
37233
t=261.5 ms
$f_H(E)$
log(F)
18
17
16
15
14
13
0
20
40
60
80
100
E (keV)

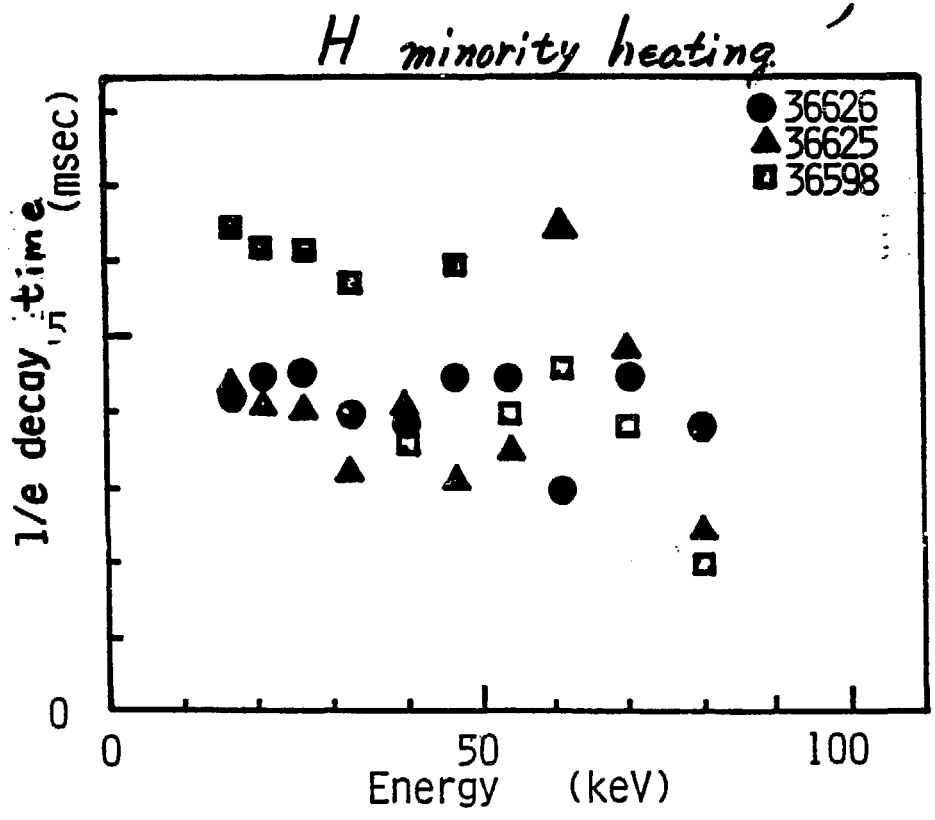
H minority heating
36626
36625
36598
1/e decay time (msec)
0
0
50
100
Energy (keV)

SUMMARIZING THE ICRF EXPERIMENT

(1) HEATING EXPERIMENT

EFFECTIVENESS OF THE ICRF HEATING IN STELLARATOR/HELIOTRON SYSTEM WAS DEMONSTRATED USING MINORITY AND SLOW WAVE HEATING MODES.

HIGH T_i(1.6keV)/LOW DENSITY($0.5\times10^{13}cm^{-3}$) -- SLOW WAVE
T_e-T_i-1keV/$2\text{-}3\times10^{13}cm^3$ -- MINORITY

(2) HIGH ENERGY ION TAIL CONFINEMENT

(a) HIGH ENERGY ION UP TO 100keV IS TRAPPED IN HELIOTRON E FIELD (ε_h-0.3, ε_t-0.1).

$E_{tail} \propto P_{ICRF}$
$n_{tail} \propto P_{ICRF}$

(b) TAIL ACCELERATION WAS OBSERVED FROM 20keV(NBI) TO 100keV (ICRF)

(c) EXTRAPOLATING THE OBTAINED FACT TO THE REACTOR CONDITION, WE FOUND THE POSSIBILITY TO CONFINE THE α PARTICLE IN HELIOTRON TYPE STEADY-CURRENTLESS REACTOR.

	H-E	REACTOR
$\Delta r/a_p = \varepsilon_t/\varepsilon_h$	0.3	0.3
ρ_α/a_p	$>>1$	$<<1$

POLOIDAL ROTATION MEASUREMENT

MOTIVATION

Friday Morning
Metejima

(1) ACCUMULATING DATA BASE IN THE WIDE RANGE OF COLLISIONALITY $\nu_{**}=2\pi\nu/\epsilon_h^{3/2}\cdot 2\pi R_o/mV_{th}$ WHICH CONTAINS THE $1/\nu$ REGIME AND THE PLATEAU REGIME PLASMAS HEATED BY ECRH, NBI AND ICRF.

(2) ANALYSIS BASED ON THE NEOCLASSICAL THEORY ESTIMATING THE RADIAL ELECTRIC FIELD FROM POLOIDAL ROTATION.

Experimental Setup

Doppler Shift Measurement

(a) Vertical

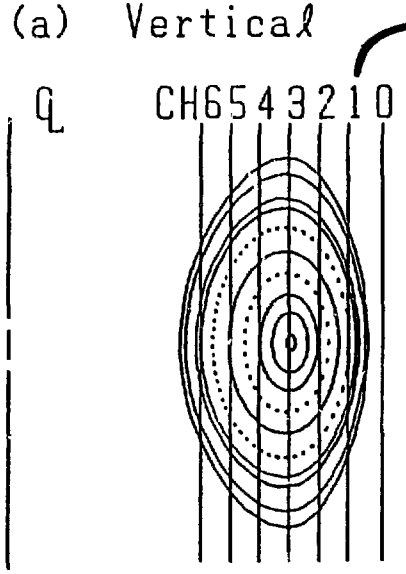

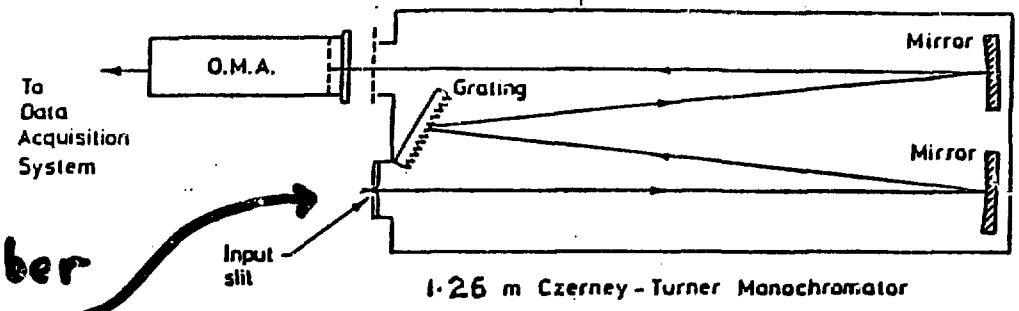

(b) Horizontal

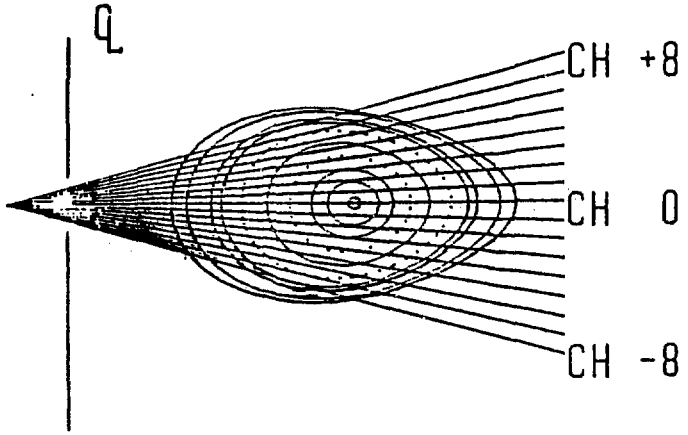

- **Detector :**

  512 ch (Tracor Northern Model 6133)

  Integration time ~ 10÷20 ms

- **Line**

  CV : 2271 Å × 4 th order

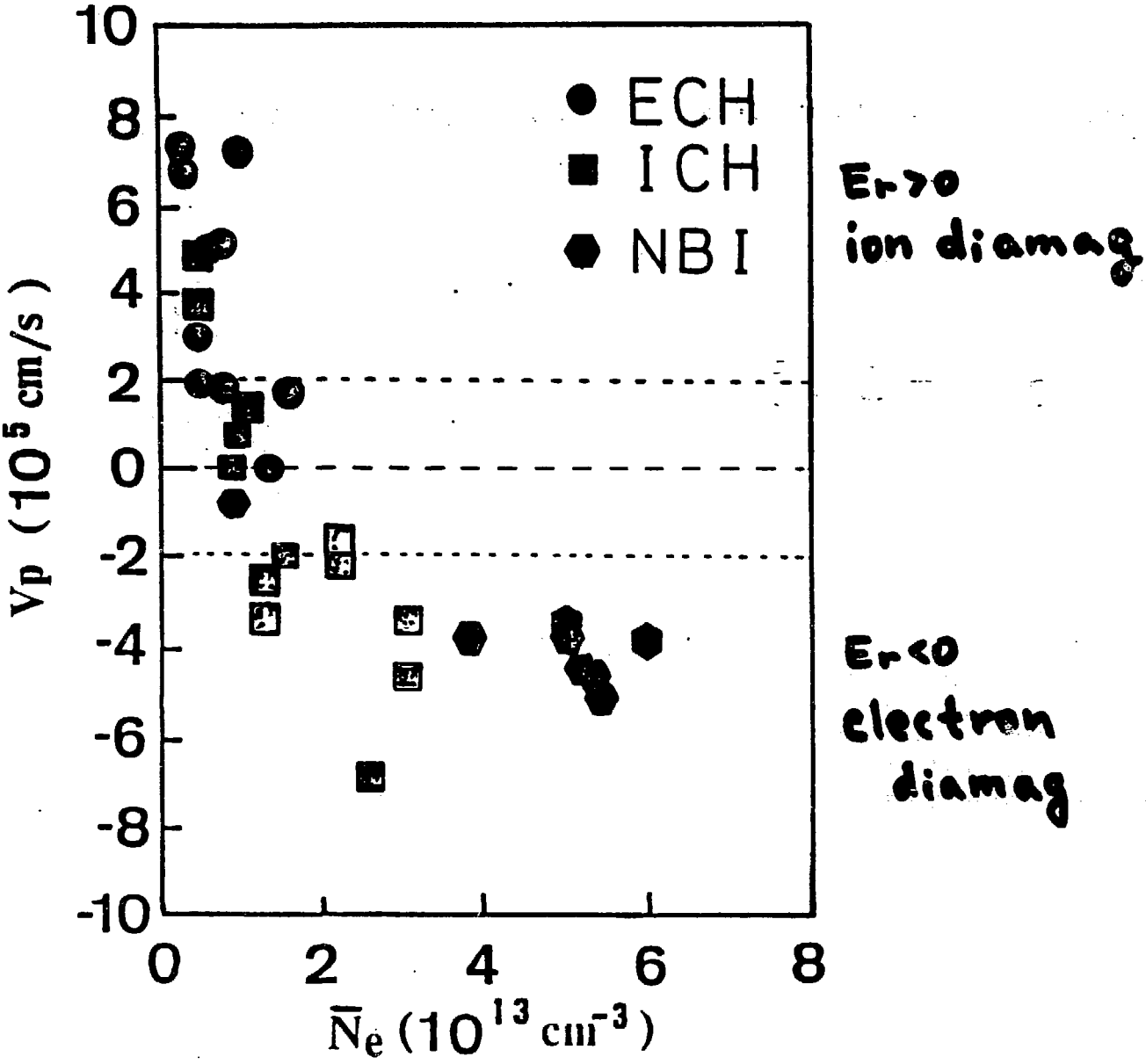
10
8
6
4
2
0
-2
-4
-6
-8
-10
0
2
4
6
8
ECH
ICH
NBI
Vp (10^5 cm/s)
Ne (10^13 cm^-3)
Er>0
ion diamag
Er<0
electron
diamag

NUMERICAL CALCULATION

NEOCLASSICAL FORMULATION WAS APPLIED FOR RIPPLE TRANSPORT.

$$\Gamma_a^{na} = -\epsilon_t^2 \sqrt{\epsilon_h} v_{d_a}^2 n_a \int_0^\infty dx\, x^{5/2} e^{-x} \tilde{\nu}_a(x) \frac{A_a(x)}{\omega_a^2(x)}$$

SHAING, PHYSICS FLUIDS 27 ((1984) 1567

FOR PLATEAU REGIME

$\Gamma_e = \Gamma_i$ (Ambipolarity Condition)

$$\Phi' = -\frac{P_i'}{ne} - \frac{1}{2}\frac{T_i'}{e}.$$

SHAING, HIRSHMAN AND CALLEN, PHYSICS FLUIDS 29 (1986) 521

ION DIAMAGNETIC DRIFT WAS NEGLECTED

$T_e(r)$, $T_i(r)$, $n_e(r)$ PROFILES -- APPROXIMATED WITH POLYNOMIAL ACCORDING TO THE MEASURED PROFILE

(a) ECRH
$T_e(r)/T_{eo} = 1 - r^2$
$T_i(r)/T_{io} = 1 - r^4$
$n_e(r)/n_{eo} = 1 - r^6$

(b) NBI
$T_e(r)/T_{eo} = 1 - r^4$
$T_i(r)/T_{io} = 1 - r^4$
$n_e(r)/n_{eo} = 1 - r^2$

$r = 0.8 \cdot \bar{a}_p$

(c) ICRF
$T_e(r)/T_{eo} = 1 - r^2$
$T_i(r)/T_{io} = 1 - r^4$
$n_e(r)/n_{eo} = 1 - r^6$

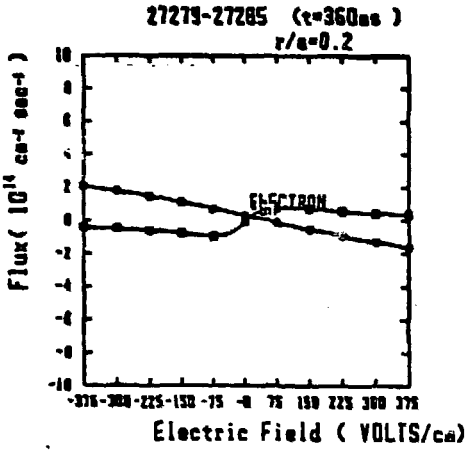
27279-27285 (t=360ms)
r/a=0.2
ELECTRON
Flux(10^14 cm-2 sec-1)
Electric Field (VOLTS/cm)

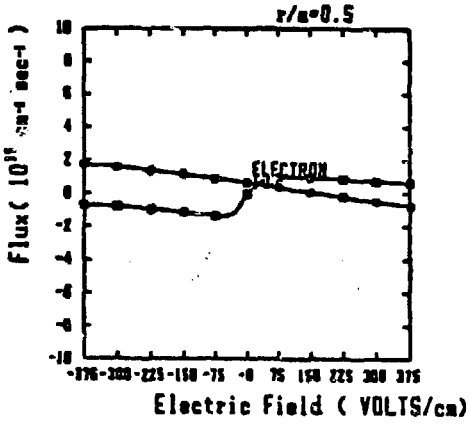
r/a=0.5
ELECTRON
Flux(10^14 cm-2 sec-1)
Electric Field (VOLTS/cm)

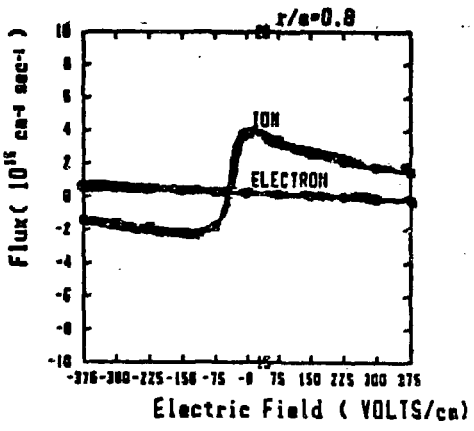
r/a=0.8
ION
ELECTRON
Flux(10^14 cm-2 sec-1)
Electric Field (VOLTS/cm)

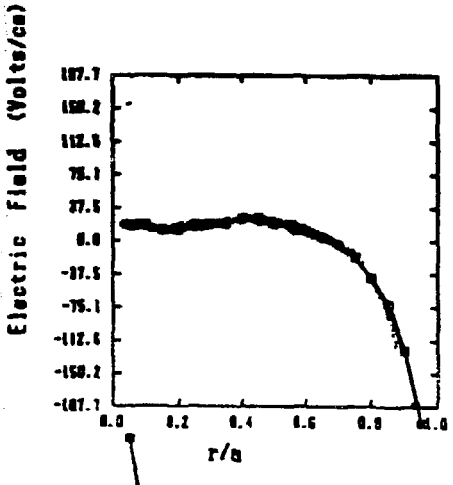
Electric Field (Volts/cm)
r/a

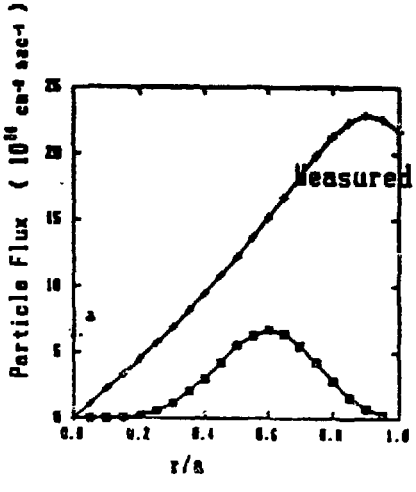
Measured
Particle Flux (10^18 cm-2 sec-1)
r/a

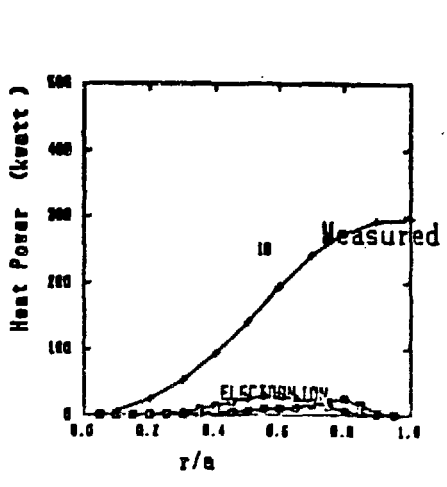
Measured
Heat Power (kwatt)
r/a

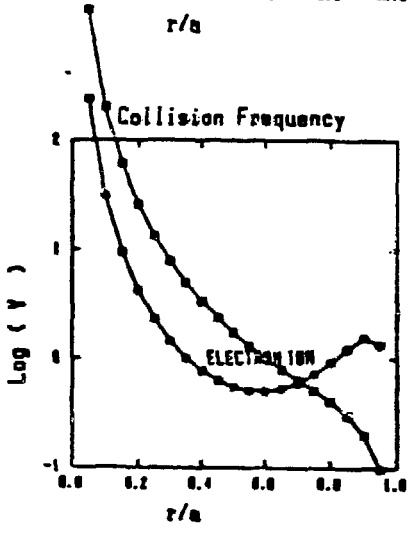
Collision Frequency
Log (V)
r/a

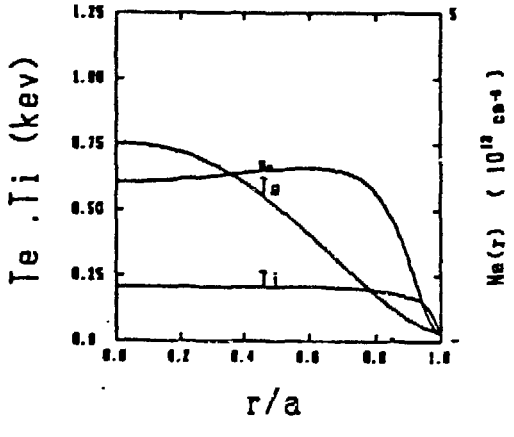
Te ,Ti (kev)
Ne(r) (10^12 cm-3)
Te
Ti
r/a

ECR Plasma

ECRH Plasma

Experiment

ion diamag

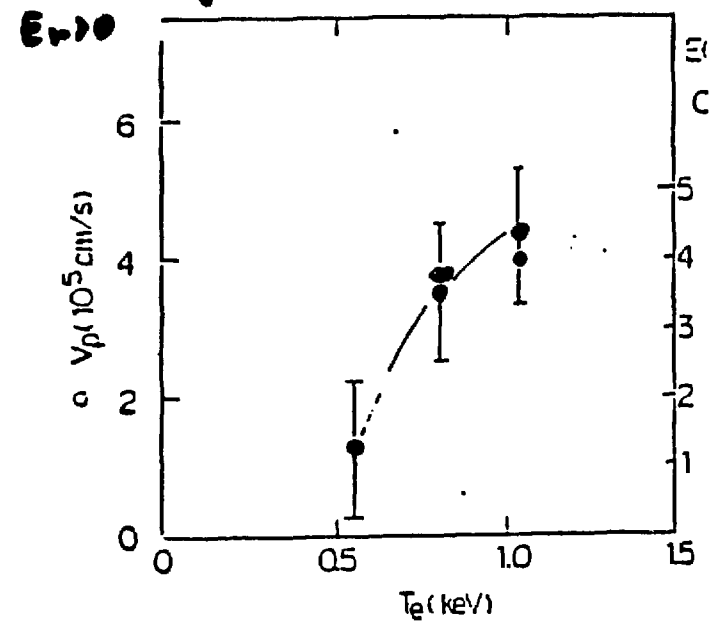

$\bar{n}_e = 0.8 \times 10^{13}\ cm^{-3}$

Calculation

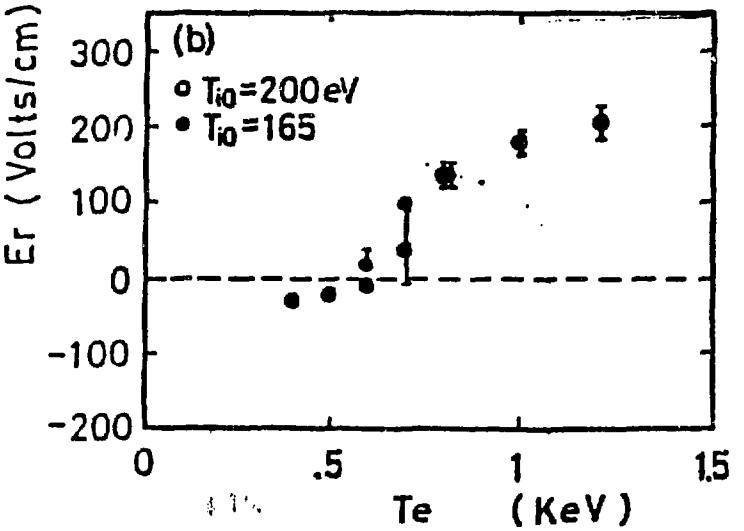

SUMMARIZING

(1) THE ELECTRIC FIELD WAS ESTIMATED FROM V_p AND SURVEYED IN A WIDE RANGE OF COLLISIONALITY OF $0.01 \leq \nu^e_{**}, \nu^i_{**} \leq 1$ AT r/a=0.7-0.9.

(2) OBSERVED DEPENDENCE OF E_r ON PLASMA PARAMETERS OF DIFFERENT PLASMAS (ECR, NBI, ICRF) WAS WELL EXPLAINED BY THE AMBIPOLAR ELECTRIC FIELD BASED ON THE NEOCLASSICAL TRANSPORT PROCESS.

(3) THE POWER DEPENDENCE OF V_p WAS NOT OBSERVED (ICRF, AND NBI).

(4) DIRECT (ORBIT) LOSS EFFECT OF THE HIGH ENERGY PARTICLE DID NOT APPEAR EXPLICITLY IN THE NUMERICAL ANALYSIS.

(5) THE ANOMALY TRANSPORT IS DOMINANT IN THIS OBSERVED REGION. (W-VIIA)

PHYSICAL OBJECTIVES OF ECRH EXPERIMENT (OCTOBER-JANUARY 1988)

<<UNDER PREPARATION>>

(a) HEATING EXPERIMENT TO GET HIGHER ELECTRON TEMPERATURE

(b) TRANSPORT STUDY OF LOW COLLISIONAL REGIME OF ELECTRON (AND ION)

(c) ENGINEERING DEVELOPMENT OF POWER TRANSMISSION FOR FUTURE DEVICE (IN THE CASE OF 106 GHz NFW GYROTRON)

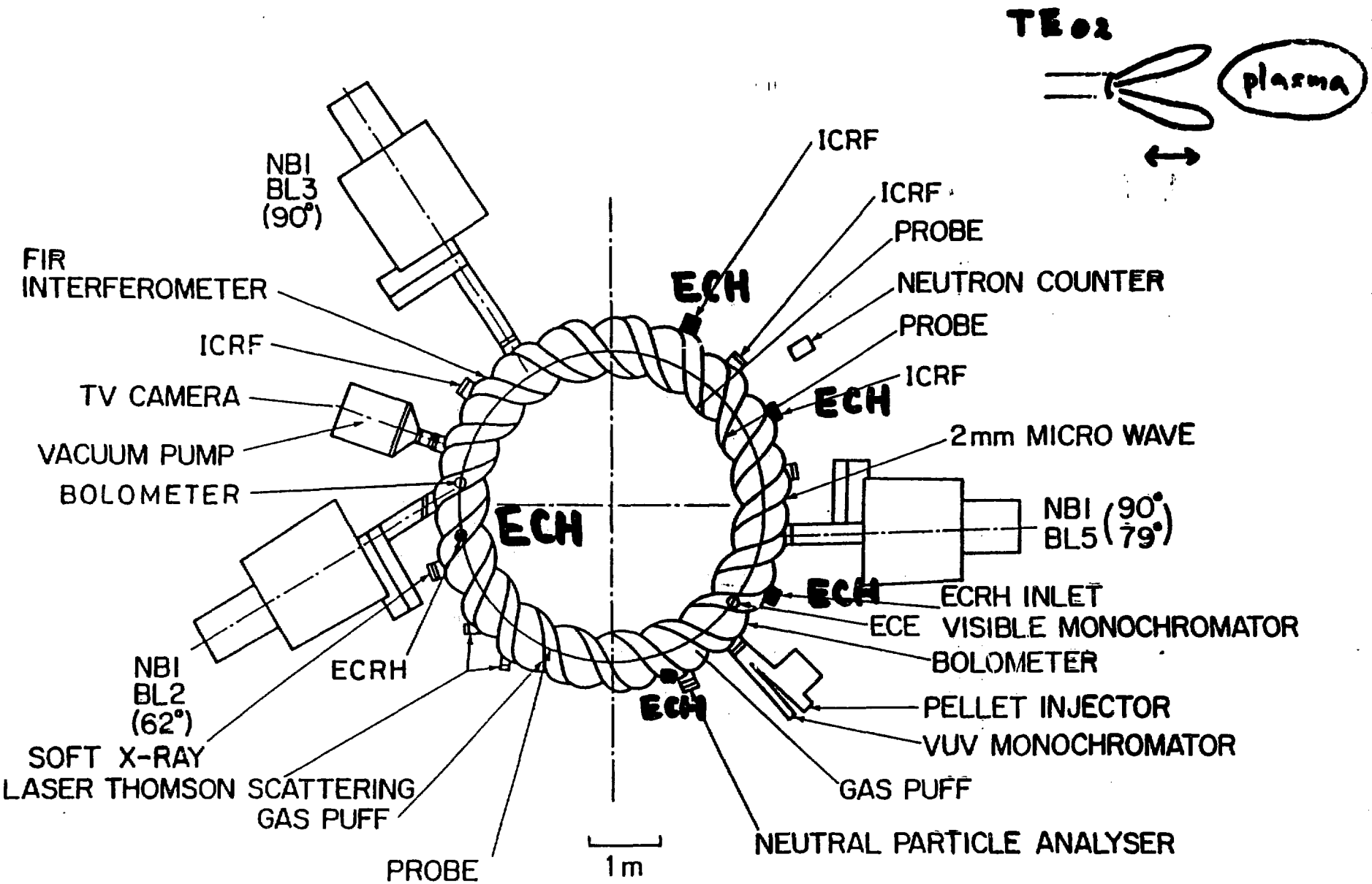

Five Distributed ECH Ports

STUDY OF PLASMA-WALL INTERACTION (FEBRUARY 1988-MARCH 1988)

(a) CARBONIZATION EXPERIMENT (CONTINUED)

(b) CARBON-TILE EXPERIMENT (NEW EXPERIMENT)

TO REDUCE THE METALLIC IMPURITY OF THE PLASMA &
HYDROGEN CONTENT OF THE CARBON FILM
TO CONTROL RECYCLING COEFFICIENT OF THE WALL

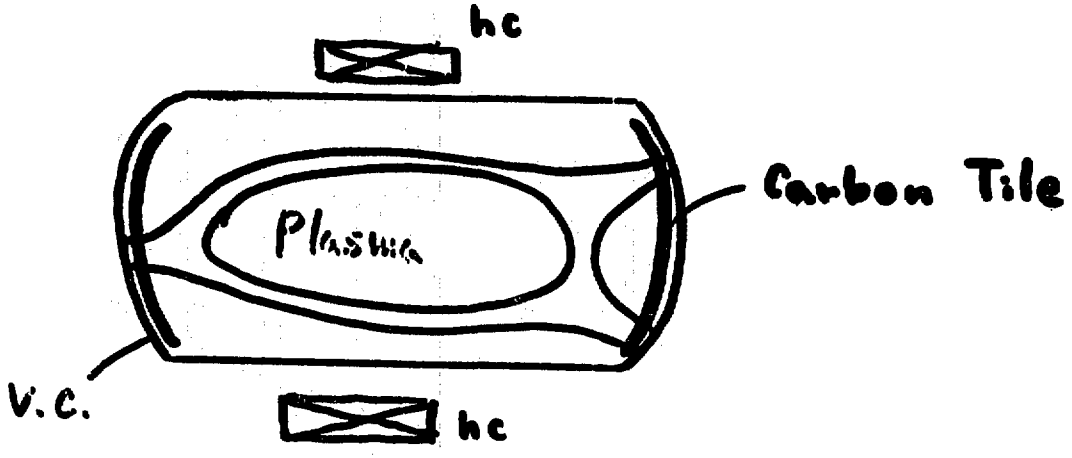
hc
Plasma
Carbon Tile
V.C.
hc

TYPICAL PARAMETERS ON CARBONIZATION

METHOD

D.C. GLOW DISCHARGE WITH CH_4/H_2 GAS MIXTURE.
INSERTION OF POSITIVELY BIASED LIMITER (ANODE) AGAINST WALL (CATHODE) WITH GROUND POTENTIAL.

PARAMETERS

ANODE VOLTAGE :	350 V
ANODE CURRENT :	1.5 A
TOTAL PRESSURE :	10 mTorr
$P(CH_4)/P(H_2)$:	0.1 - 0.2
WALL TEMPERATURE :	ROOM TEMPERATURE
INNER-SURFACE AREA OF THE WALL :	4×10^5 cm^2

RESULTS

THICKNESS OF THE C LAYER AT NBI EXPERIMENTS :	100 - 200 Å
TYPICAL COATING RATE :	180 Å/HOUR (1.1 MONOLAYER/MIN.)
ATOM NUMBER DENSITY :	0.17 ± 0.03 g ATOM/cm^3
MASS DENSITY :	1.5 ± 0.1 g/cm^3
AREA DENSITY OF CARBON :	$(1.7 \pm 0.2) \times 10^{15}$ /cm^2·MONOLAYER
MEAN DISTANCE OF C-C :	2.4 ± 0.1 Å
RATIO OF H TO C :	0.1 - 0.2

Experimental Setup

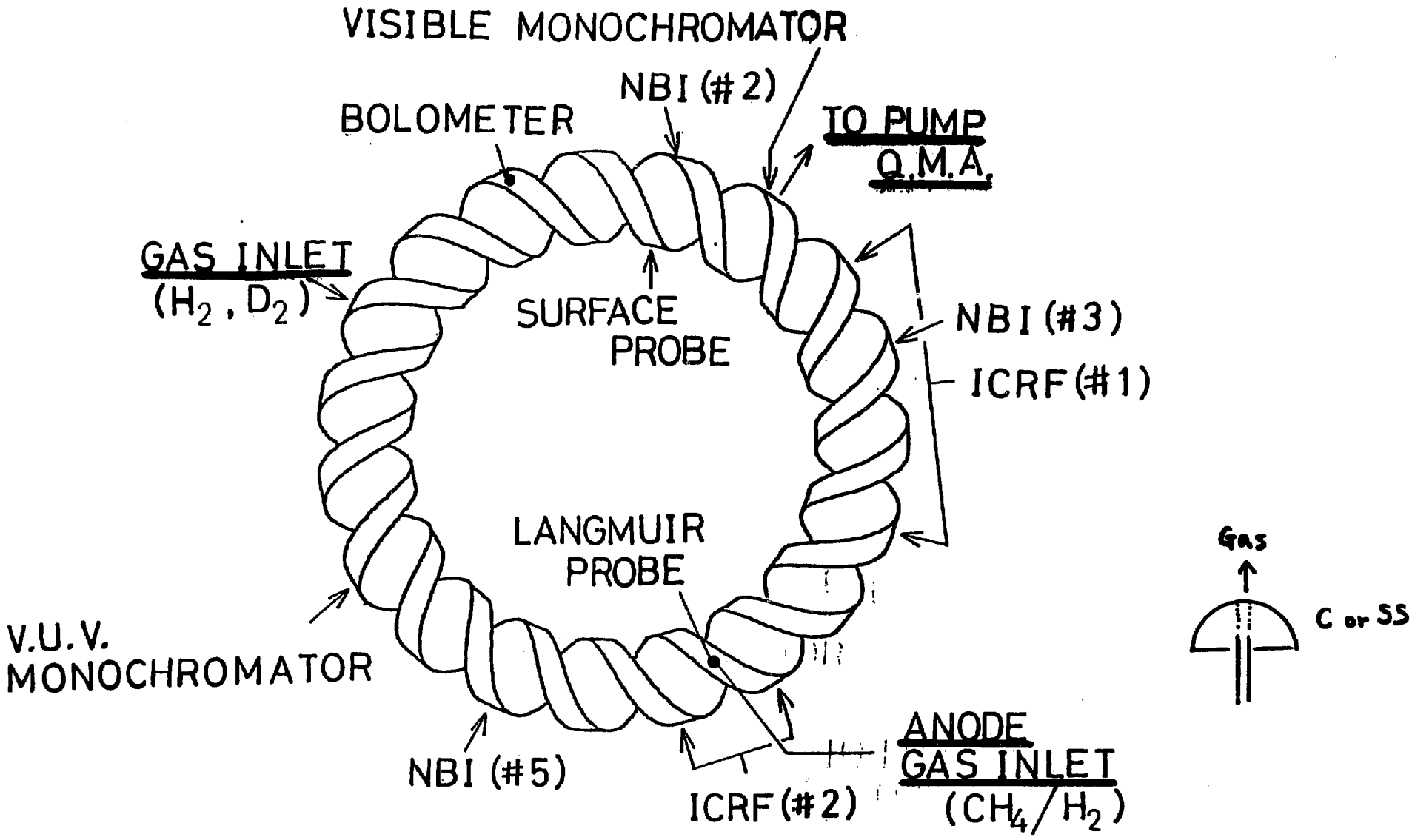

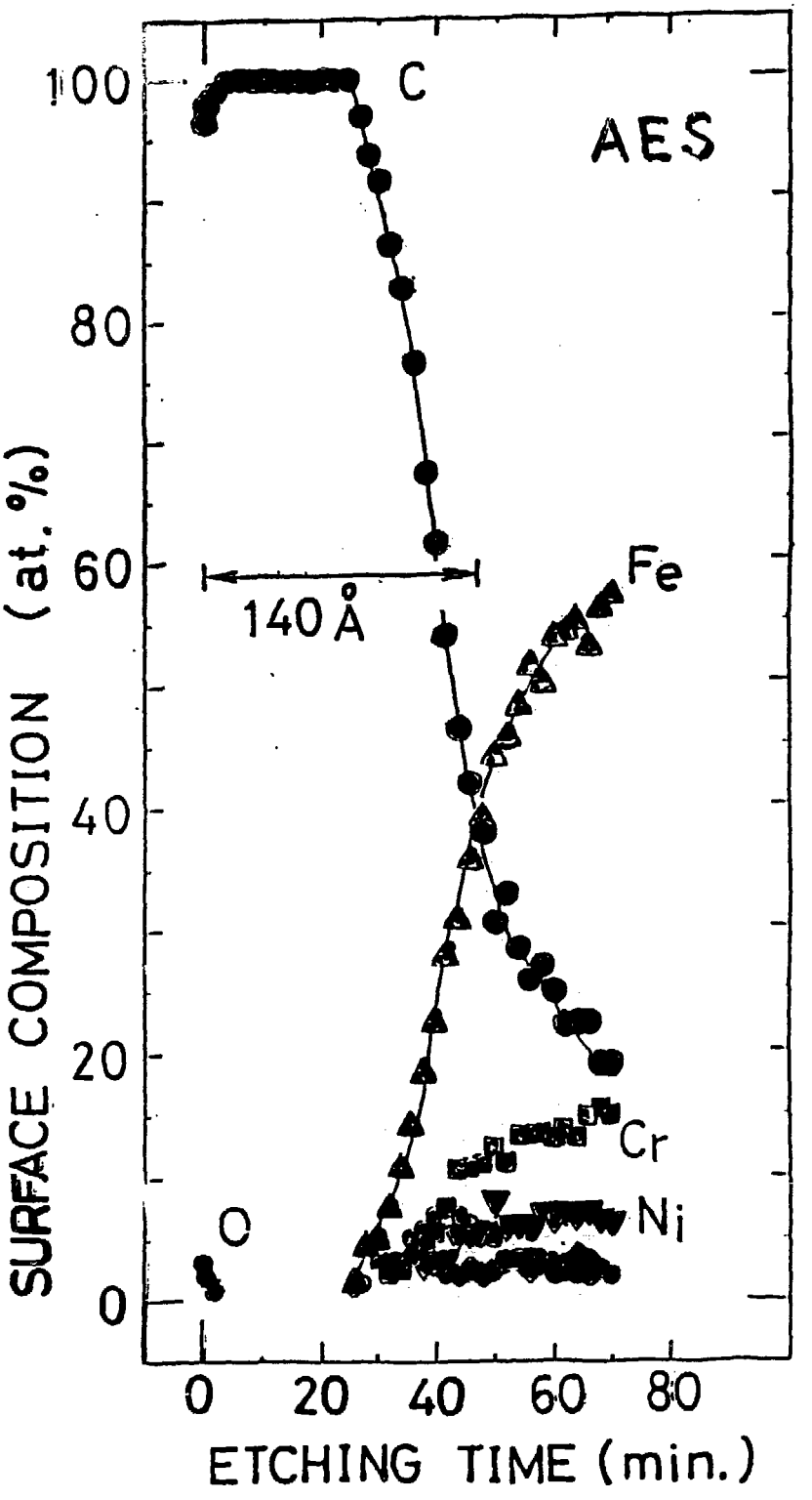
AES
C
Fe
Cr
Ni
O
140 Å
100
80
60
40
20
0
0
20
40
60
80
SURFACE COMPOSITION (at.%)
ETCHING TIME (min.)

← | → After

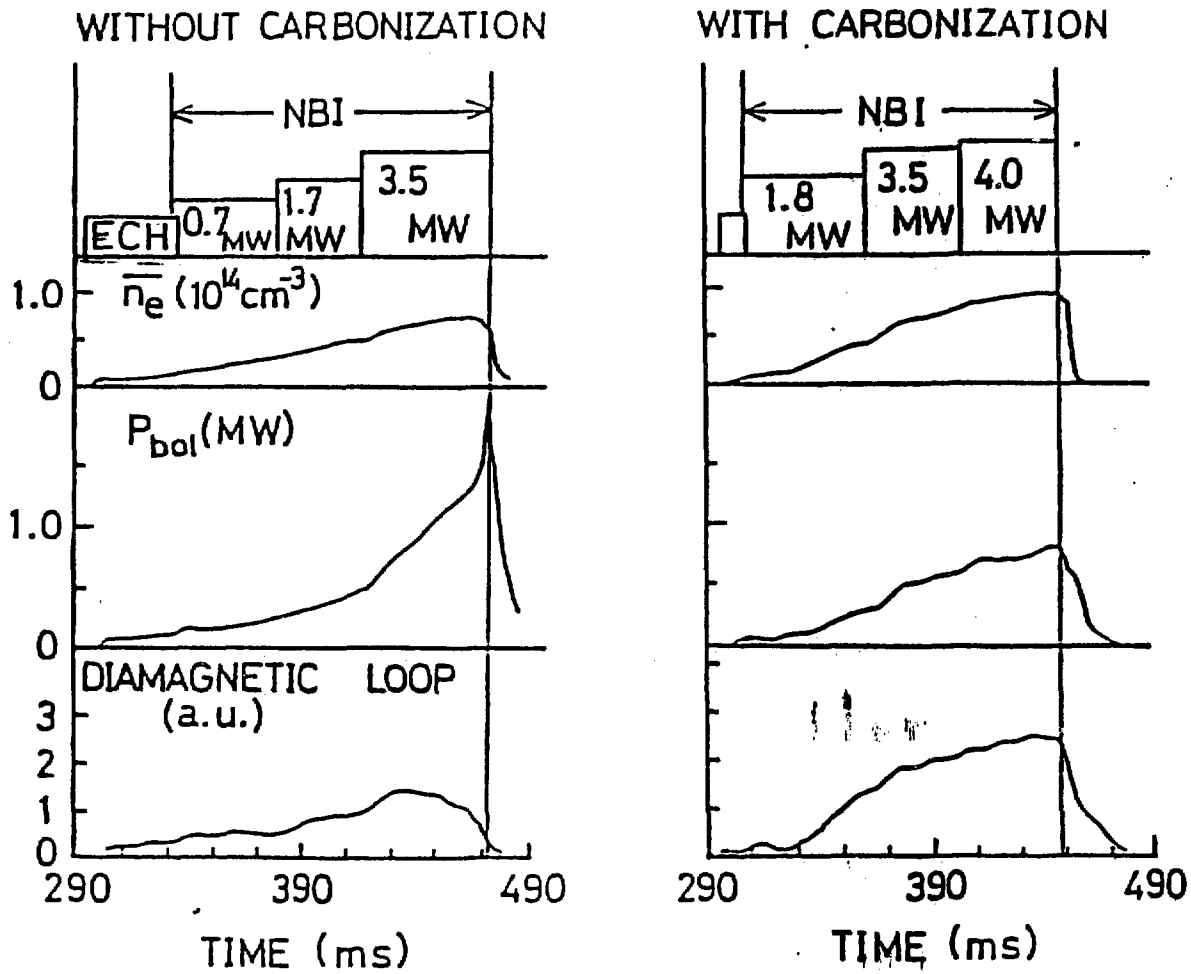
WITHOUT CARBONIZATION
WITH CARBONIZATION
NBI
ECH
0.7 MW
1.7 MW
3.5 MW
1.8 MW
4.0 MW
$\bar{n}_e$ (10^{14}cm^{-3})
1.0
0
P_{bol}(MW)
DIAMAGNETIC LOOP
(a.u.)
3
2
1
290
390
490
TIME (ms)

Improvement of Gross Energy Confinement Time

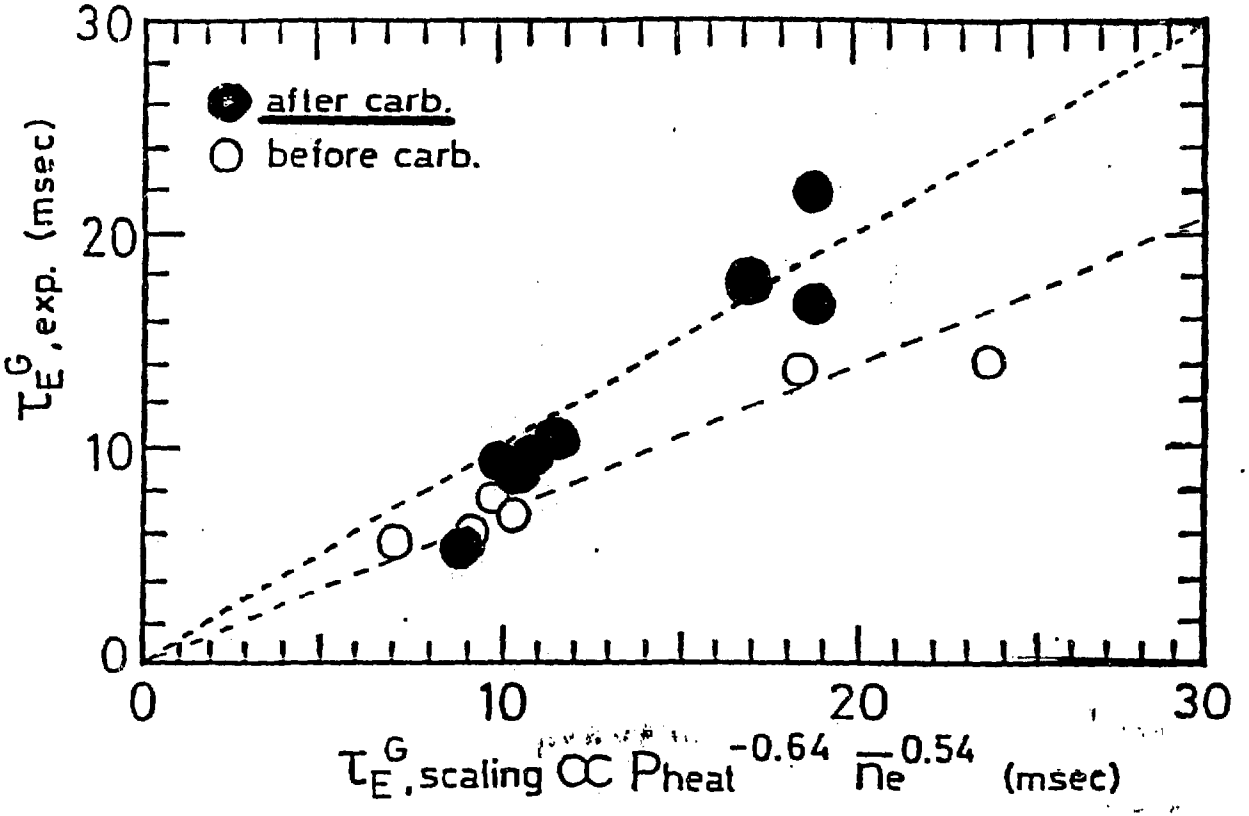

OVERVIEW OF COMPACT HELICAL SYSTEM

CHS group (presented by K.Matsuoka)

Institute of Plasma Physics, Nagoya University, Nagoya 464, Japan

Compactness of machine and steady state operation of high-β plasma are major research objectives from standpoint of engineering and physics for toroidal plasma confinement. In the helical system compactness is attractive because of low construction cost and high stability β limit. Plasma transport, however, is predicted to get worse because of the enhanced toroidicity. We should investigate experimentally transport phenomena and after that we may pave the way for the recipe how to improve the transport in such magnetic field configuration. Compact helical system(CHS) now under construction was planned last year in Institute of Plasma Phisics, Nagoya University. Construction started this June and will be finished next March. Experiment is expected to start next April.

Torsatron-type machine without toroidal field coil has been selected because we can keep good access for heating and diagnostics. The pole number l=2 is determined from finite rotational transform in the plasma center. Taking account of reasonable plasma size which gives meaningful experimental results, we have selected minor and major plasma radii of 20 cm and 1 m respectively and accordingly determined the period number m of 8. After surveying magnetic field characteristics the pitch parameter γ_c of 1.25 and pitch modulation α^* of 0.3 have been selected to get large clean magnetic surface which are necessary to realize the plasma with the aspect ratio of 5. Field strength on axis of 1.5 T is determined to get proof of principle plasma parameters estimated from the neoclassical transport and will be strengthened to 2 Tesla in the near future. To avoid dangerous resonances, especially m/n=1/1, rotational transform profile has central and edge transforms of about 0.33 and < 1 respectively. Resonance with m/n=2/1 is expected to be stabilized by the magnetic well. Pulse length of 2 second is sufficiently long compared with the heating pulse length.

Poloidal field(PF) coils consist of outer vertical field(OVF), trimming vertical field(TVF), shaping field(SF) and inner vertical field(IVF) coils. The freedom of PF coil is 3, hence we can control independently 1) dipole and 2) quadrupole magnetic field components, and 3) poloidal flux linked with the plasma or stray field at diagnostics and heating region:

$-3.0\% < \delta B_D/B < 4.5\%$, $-1.7\% < \delta B_Q/B < 1.8\%$, $\delta\varphi < 0.2$ volt.sec,

where B_D, B_Q and φ refer to the dipole and quadrupole magnetic field components normalized with the field strength, and the poloidal flux linked with plasma respectively. These values correspond to displacement of magnetic axis by about +/- 4cm, cancelling/augmenting the quadrupole component of HF coil by about 70%, these values being sufficient for experiments.

ECH(28GHz,200kW and 56GHz,200kW) and RF(7-40MHz) are being prepared for plasma production and heating. OH plasma production is also possible for NI target plasma. Two beam lines(40kV,3MW each) are injected tangentially. One of them has flexible injection angle to study high-energy particle loss mechanism and beam induced plasma current.

US-Japan Stellarator/Heliotron
Workshop (Nov.9-13,1987)

Overview of Compact Helical System

CHS group (presented by K.Matsuoka)
Institute of Plasma Physics
Nagoya Univ., Nagoya, Japan

1. Objectives
2. Magnetic Configuration and Operational Range
3. Others

Compact Helical System (CHS)

-low A_p system-

Contributors:

Y. Abe
T. Amano
J. Fujita
M. Fujiwara
M. Hosokawa
K. Ida
H. Iguchi
K. Kadota
T. Kamimura
O. Kaneko
S. Kitagawa
S. Kubo
K. Masai
K. Matsuoka
S. Morita
K. Nishimura
A. Nishizawa
T. Ozaki
S. Okamura
H. Sanuki
M. Sasao
T. Shoji
S. Tanahashi
J. Todoroki
H. Yamada
K. Yamazaki

Institute of Plasma Physics

Nagoya Univ., Nagoya, Japan

Objectives of CHS

- To extend data base of helical system
  - Transport
    - B - dependence -- plasma production by RF independent of B
    - Potential -- ECH, NI
      - electron root
      - ion root
  - MHD properties
    - equilibrium β
    - stability β
      - shear, magnetic well/hill -- dipole field
      - control of plasma shape --- quadrupole field
    - helical axis configuration
  - Plasma - wall interaction
    - distance between the outermost magnetic surface and the wall
    - single-null configuration

DRIFT SURFACE IN POLOIDAL PLANE

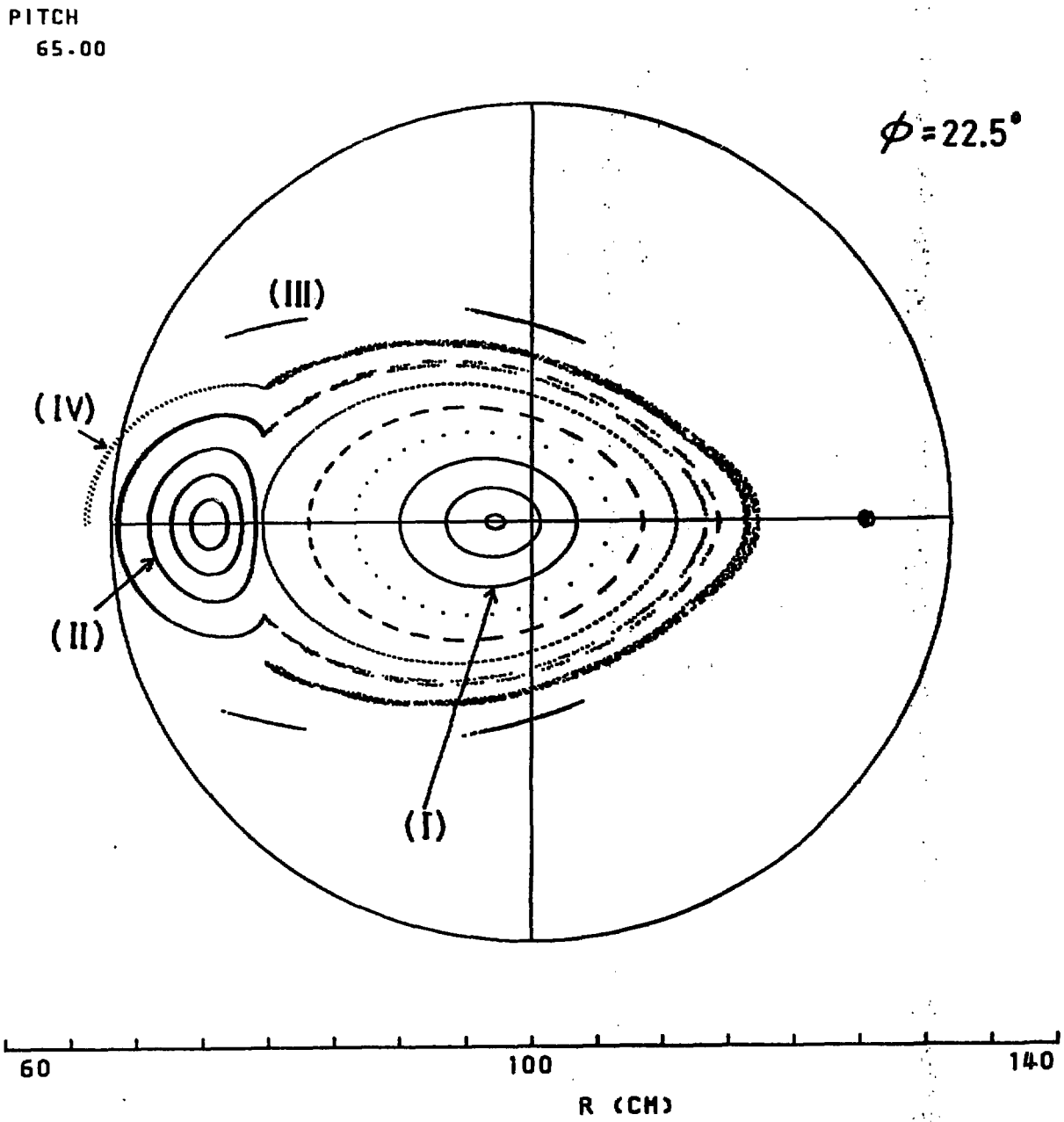

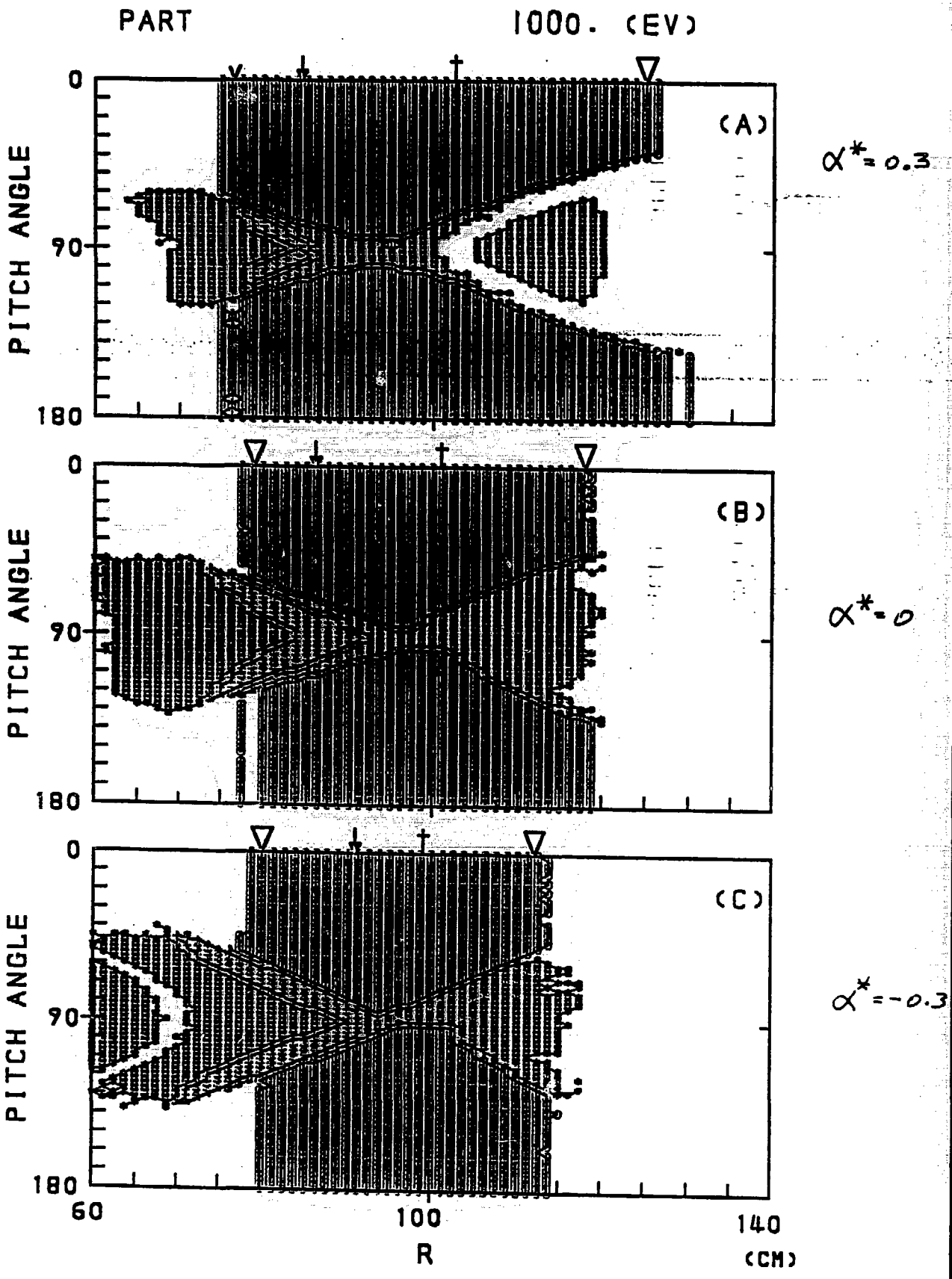
PART
1000. (EV)
(A)
(B)
(C)
PITCH ANGLE
0
90
180
α*=0.3
α*=0
α*=-0.3
60
100
140
R
(CM)

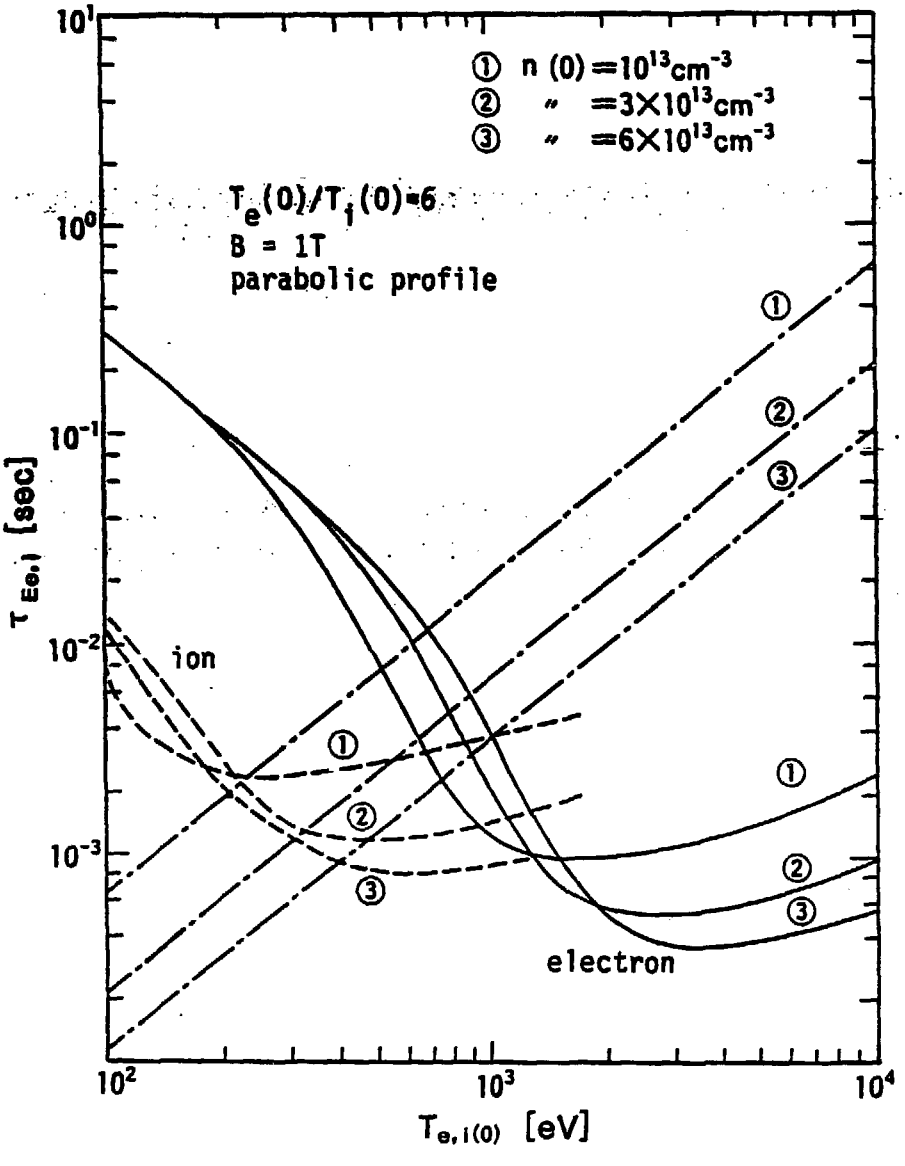
① n (0) =10¹³cm⁻³
② 〃 =3×10¹³cm⁻³
③ 〃 =6×10¹³cm⁻³
Te(0)/Ti(0)=6
B = 1T
parabolic profile
ion
electron
τE(e,i) [sec]
Te,i(0) [eV]
10¹
10⁰
10⁻¹
10⁻²
10⁻³
10²
10³
10⁴

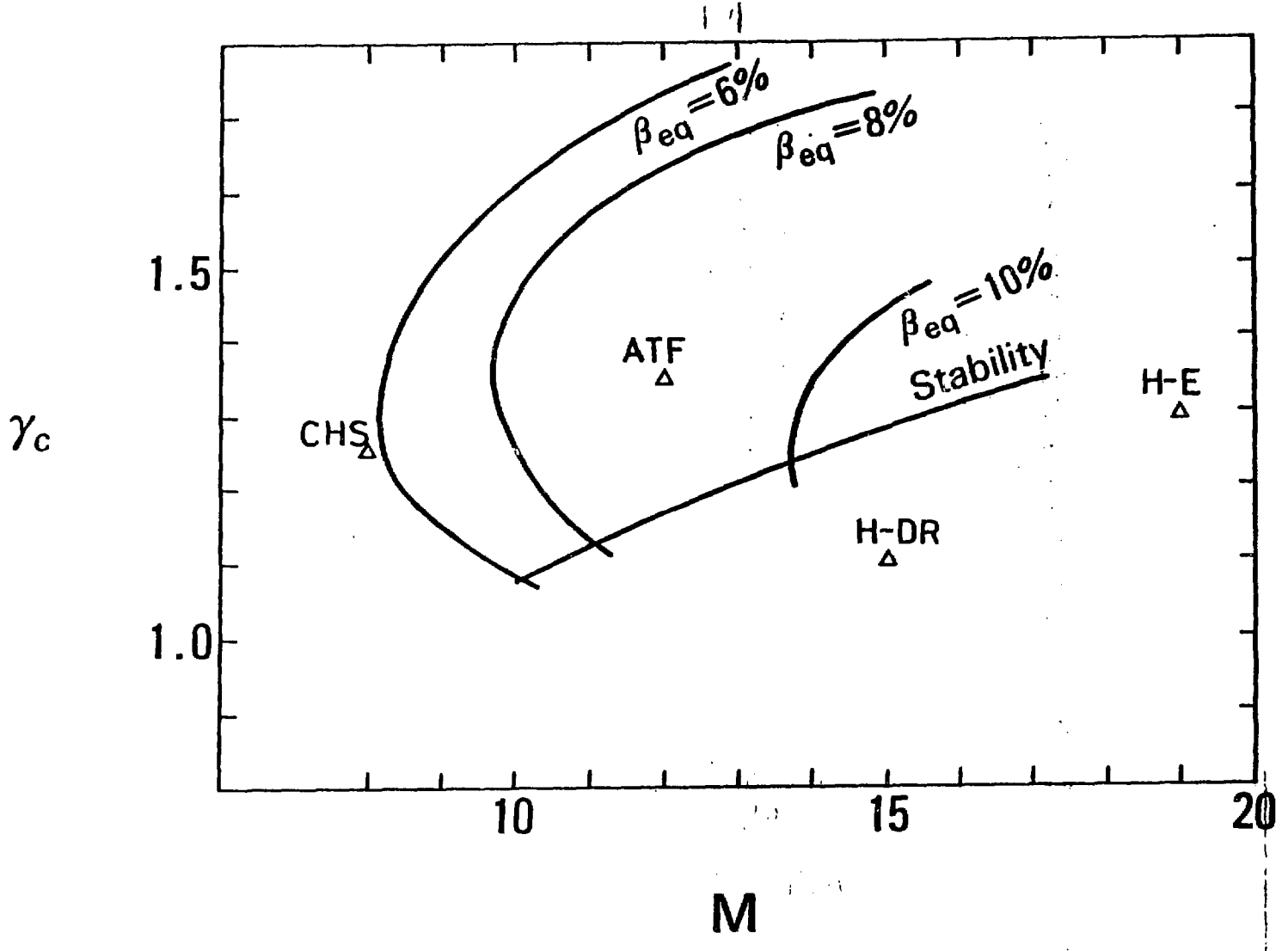
β_{eq}=6%
β_{eq}=8%
β_{eq}=10%
Stability
ATF
CHS
H-E
H-DR
1.5
1.0
γ_c
10
15
20
M

Helical Axis Configuration

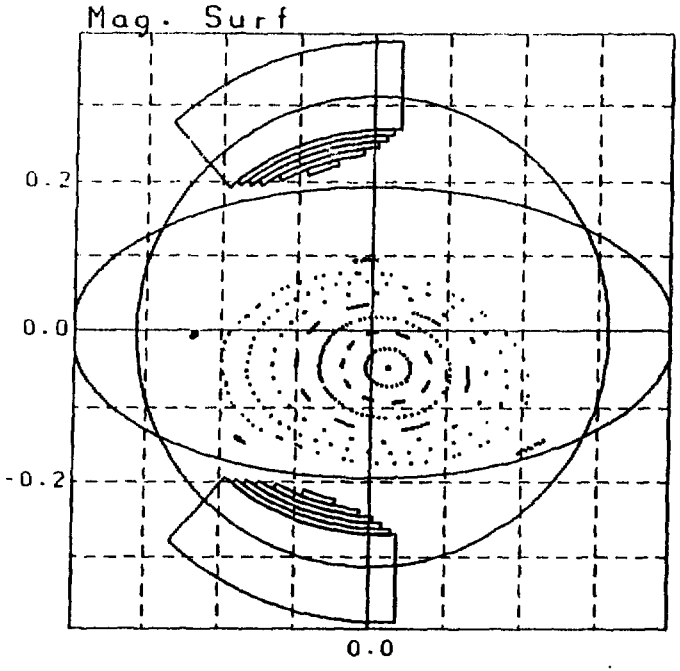

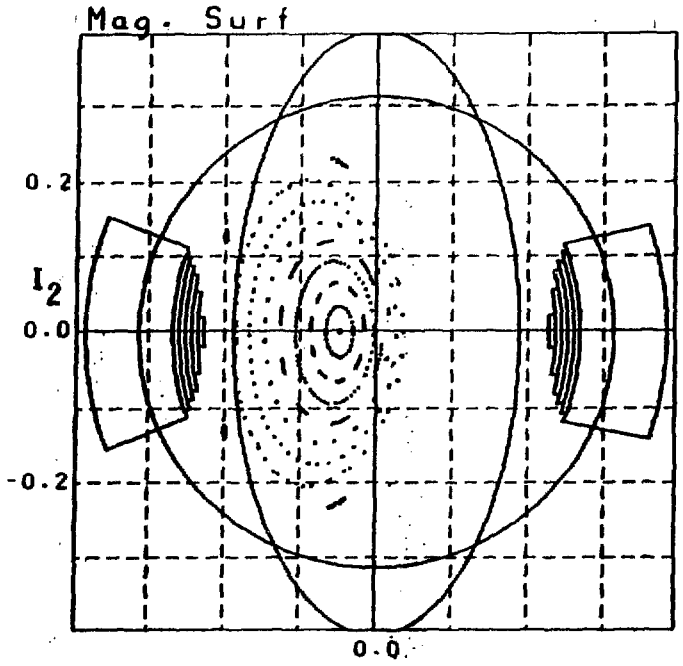

$I_2/I_1 = 1/2$

I_1

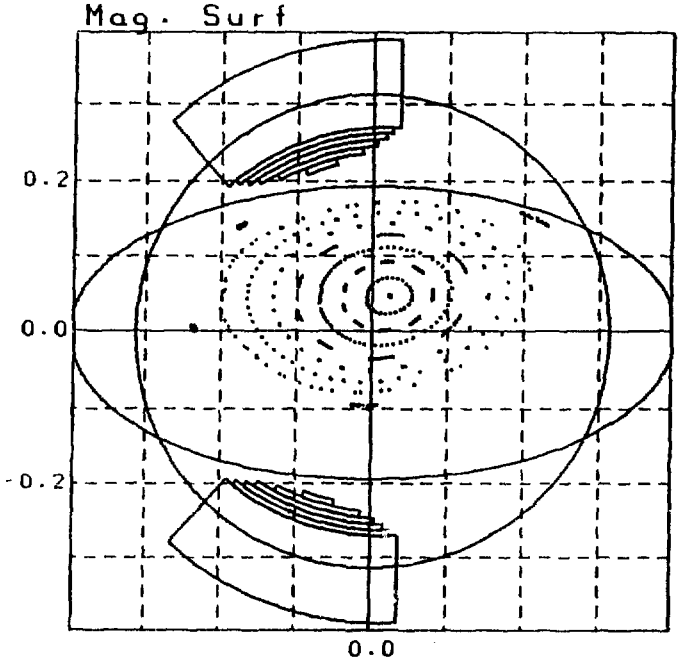

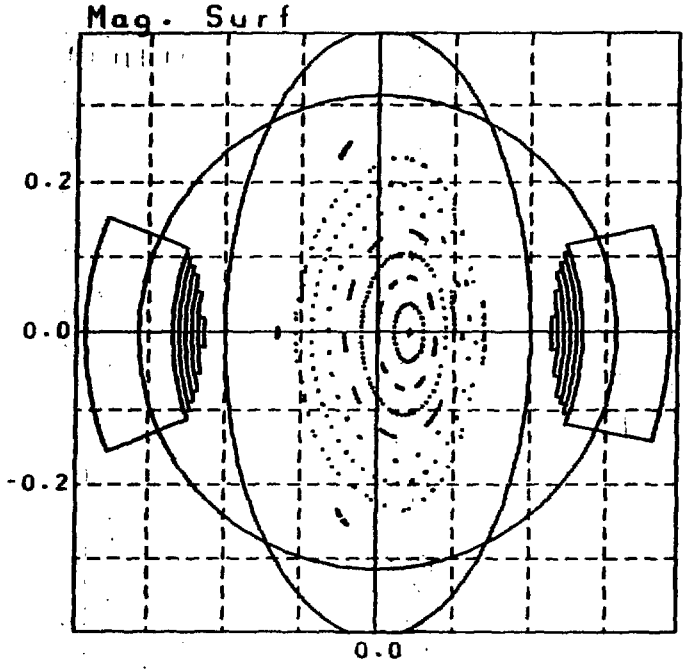

Single Null Configuration

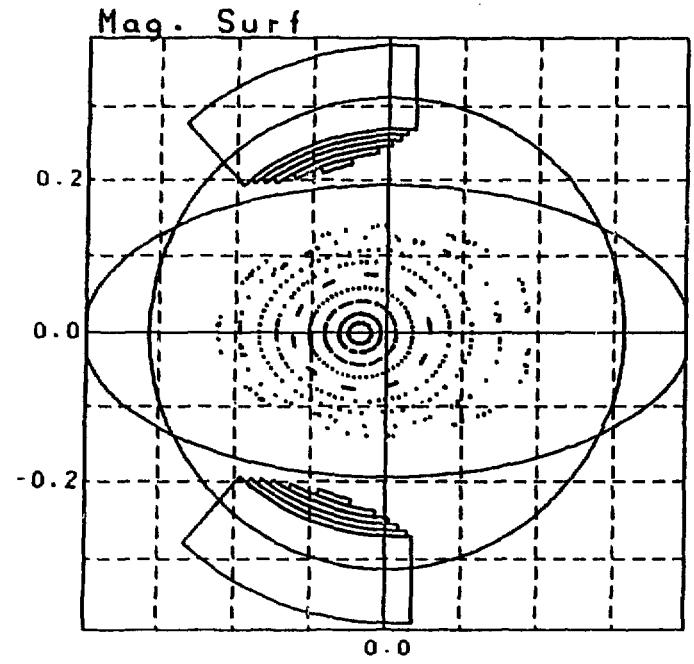

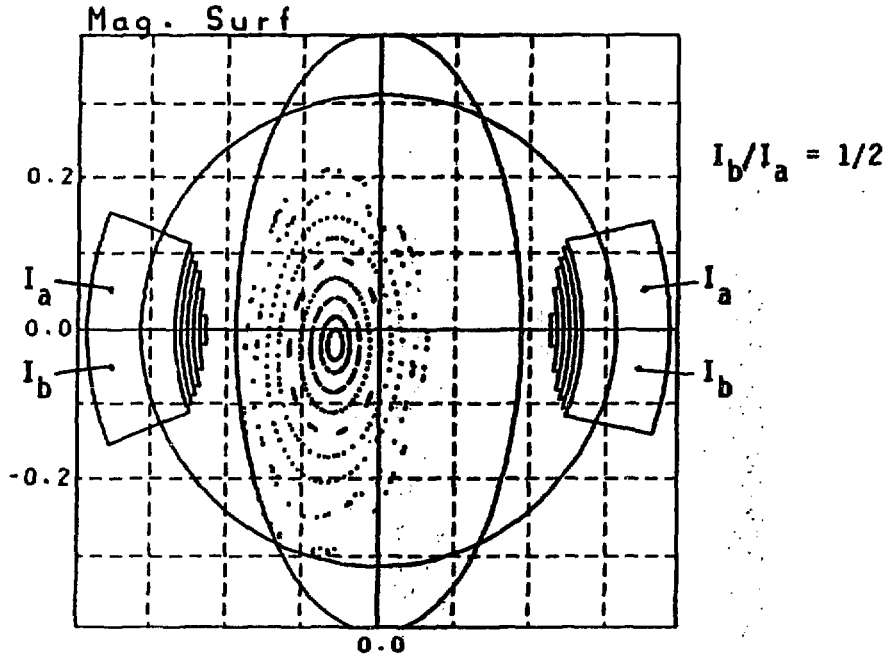

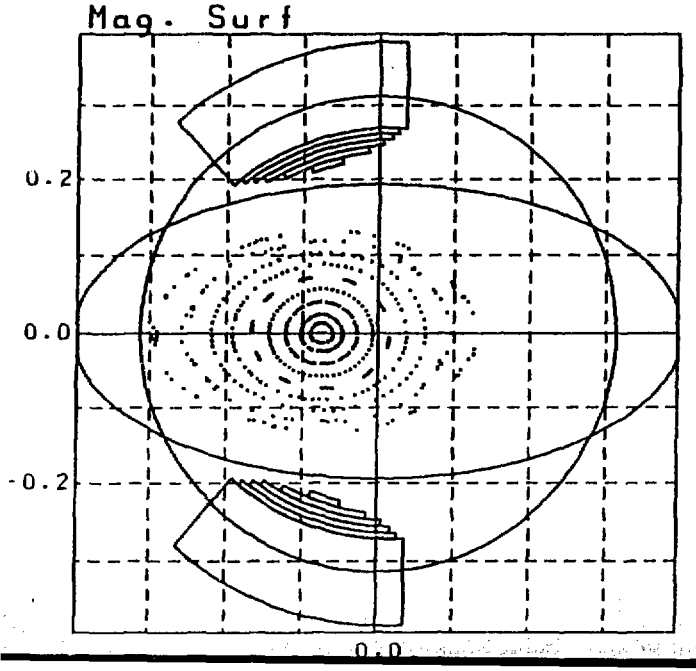

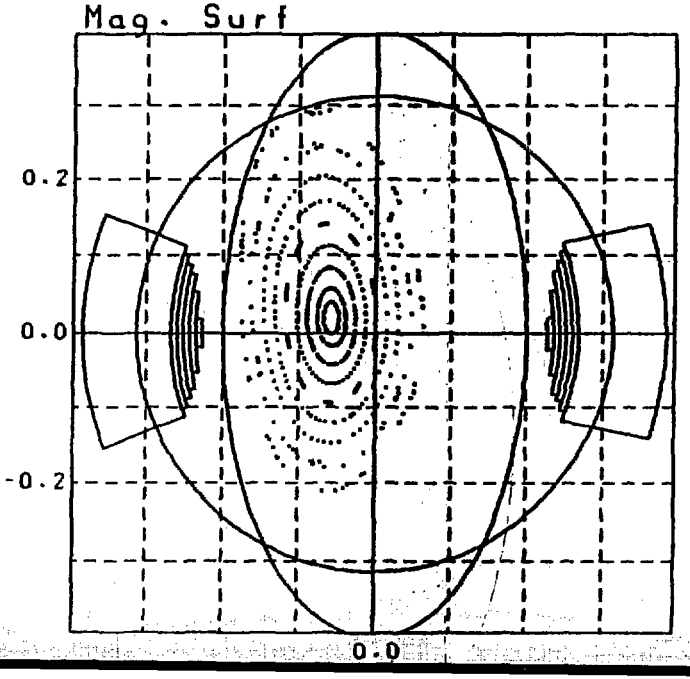

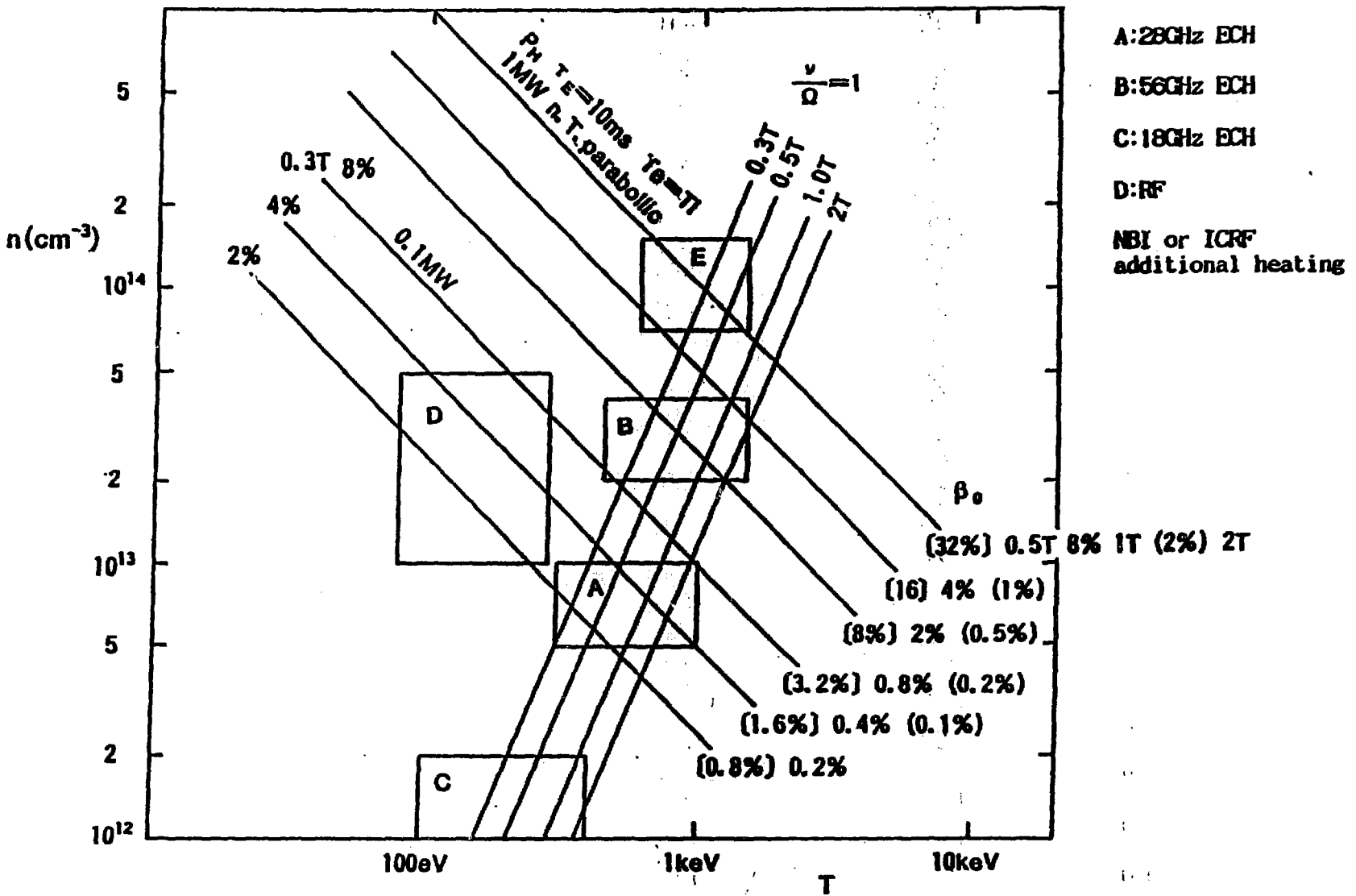
A:28GHz ECH
B:56GHz ECH
C:18GHz ECH
D:RF
NBI or ICRF additional heating
n(cm⁻³)
T
100eV
1keV
10keV
5
2
10¹⁴
5
2
10¹³
5
2
10¹²
A
B
C
D
E
P_M τ_E=10ms Te=Ti
1MW n.T.parabolic
ν/Ω=1
0.3T
0.5T
1.0T
2T
0.3T 8%
4%
2%
0.1MW
β₀
(32%) 0.5T 8% 1T (2%) 2T
(16) 4% (1%)
(8%) 2% (0.5%)
(3.2%) 0.8% (0.2%)
(1.6%) 0.4% (0.1%)
(0.8%) 0.2%

Table 1. Major parameters of CHS

Parameter	Value
Major radius R	1.0m
Helical coil radius a	0.313m
Average plasma radius a	0.2m
Plasma Aspect Ratio	5
Multipolarity ℓ	2
Number of Field Period m	8
Pitch parameter	1.25
Pitch modulation α	0.3
Field Strength on axis B	1.5T−2.0T
Plasma current	0
Central transform ι	0.33
Edge transform ι	0.8~1.0
Pulse length	2s at 1.5T
Access port diameter	30cm$^{\phi}$, 63cm ×38cm, ...
Number of ports	68
Neutral beam power	3~4 MW at 40kV (2 beam lines)
N.I. pulse length	1s
ECH power	60kW at 18GHz cw
	200kW 28GHz 75ms
	200kW 60GHz 100ms
ICRF power	500kW
ICRF frequency	6~28MHz
ICRF pulse length	10ms

<< Compact Helical System >> 87-03-07 <17:40:20>

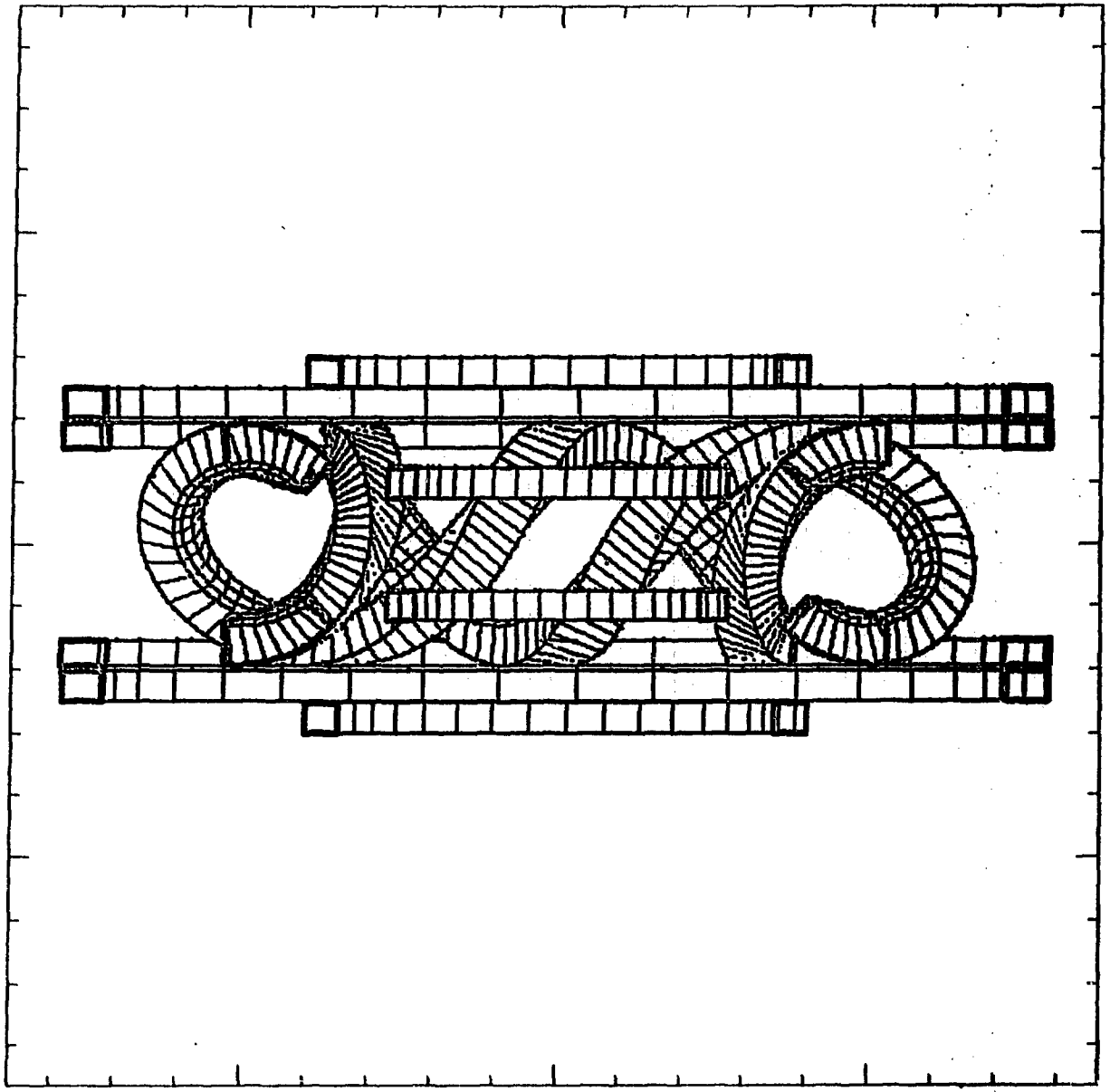

Helical coil parameter

Rc = 100.00 (cm)
Ac = 31.30 (cm)
M = 8
L = 2
alfa* = 0.30

HCw(cm)	HCh(cm)
9.20	7.01
9.20	-5.39
7.00	-7.29
3.40	-9.07

PR/PZ	PCW/PCH
150.00	7.25
35.00	3.95
150.00	6.55
45.00	4.80
75.00	5.30
55.00	4.60
50.00	4.60
20.00	4.60

Theta 1. = 22.50 (deg.)
Theta 2. = 90.00 (deg.)

CPU = 53.308 (sec.)

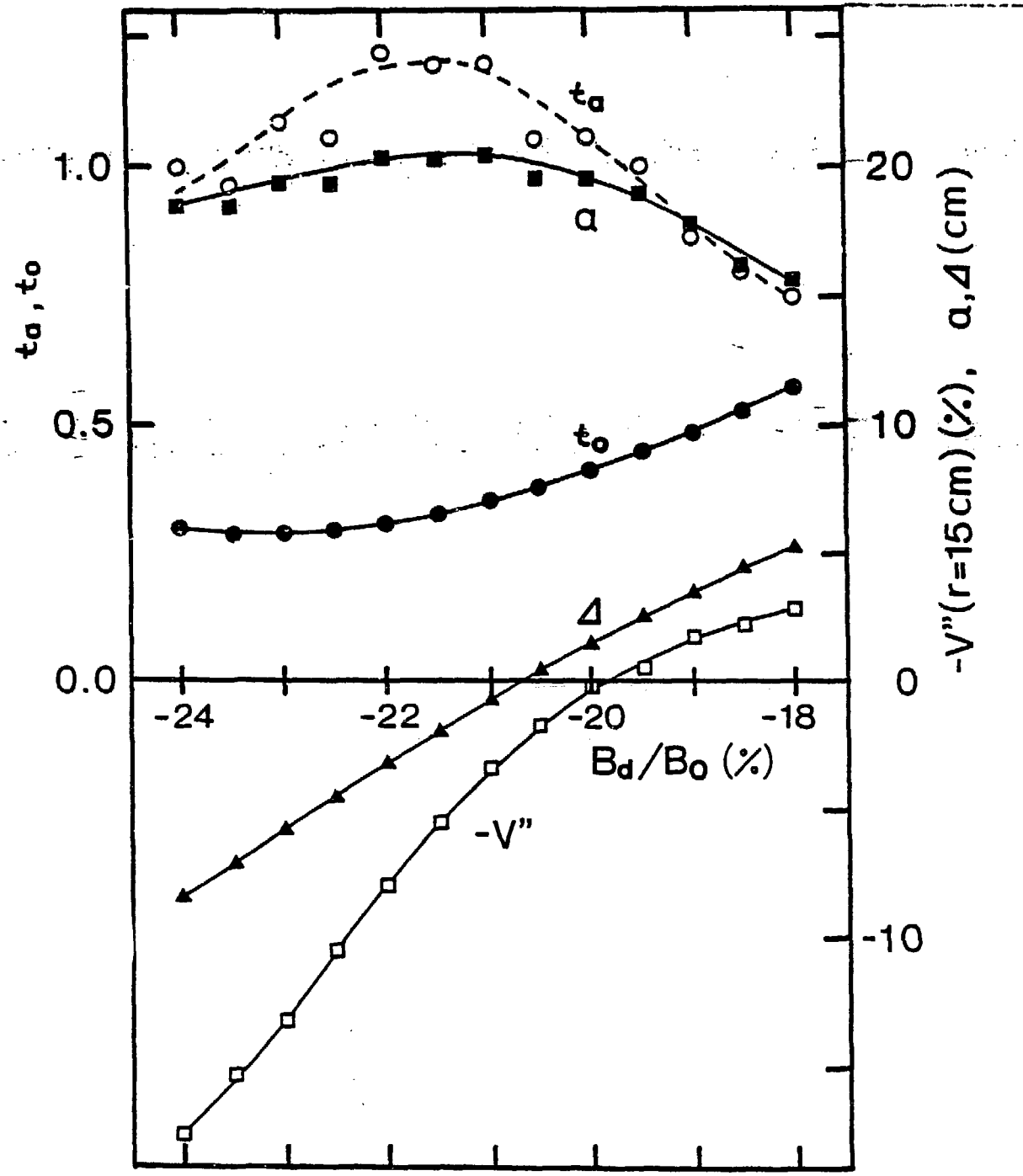
t_a
a
t_o
Δ
-V"
1.0
0.5
0.0
20
10
0
-10
-24
-22
-20
-18
B_d/B_o (%)
t_a, t_o
-V"(r=15cm)(%), a,Δ(cm)

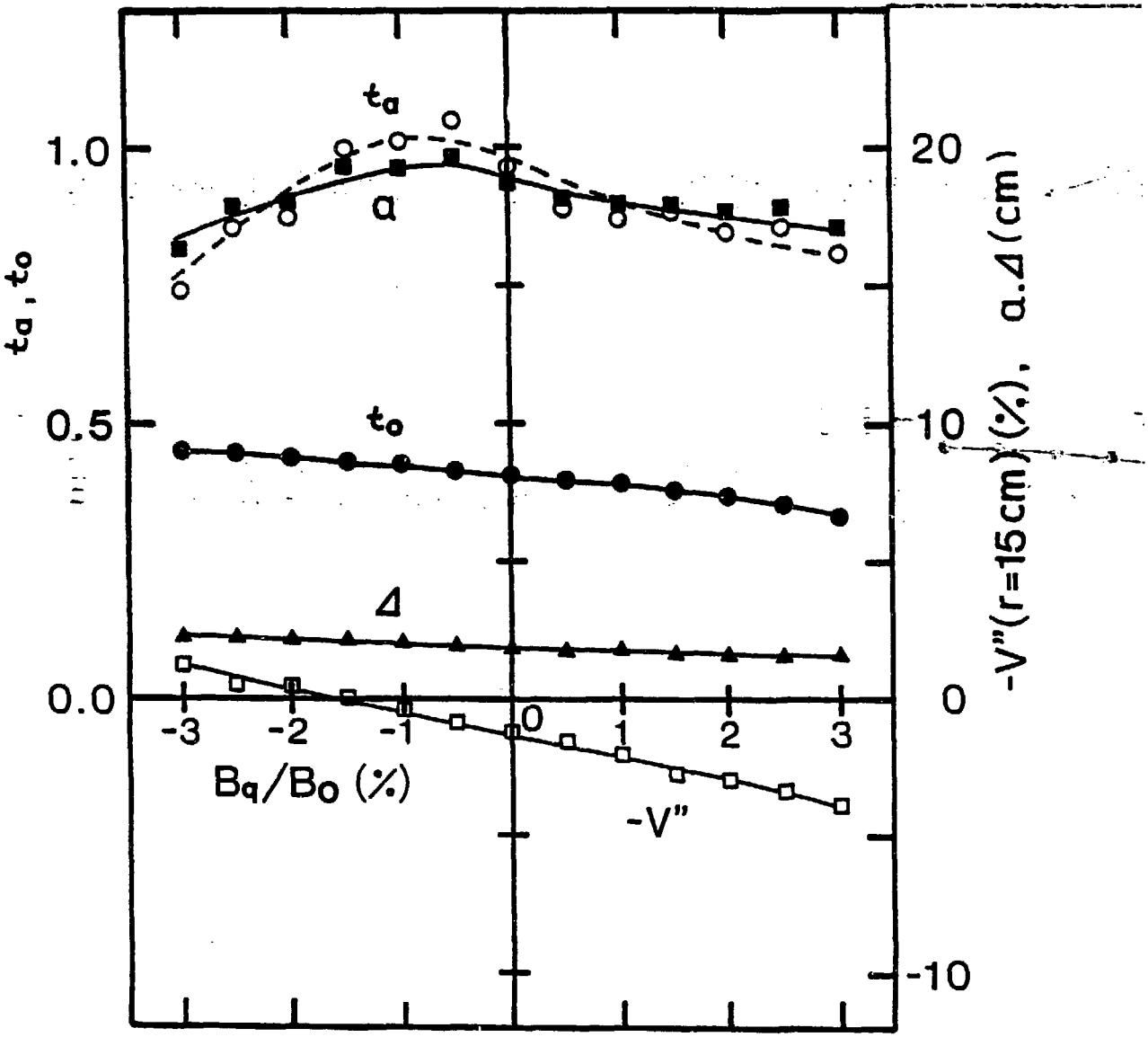
t_a
1.0
0.5
0.0
t_a, t_o
t_o
Δ
-3
-2
-1
0
1
2
3
B_q/B_o (%)
-V"
20
10
0
-10
-V"(r=15cm)(%), a.Δ(cm)

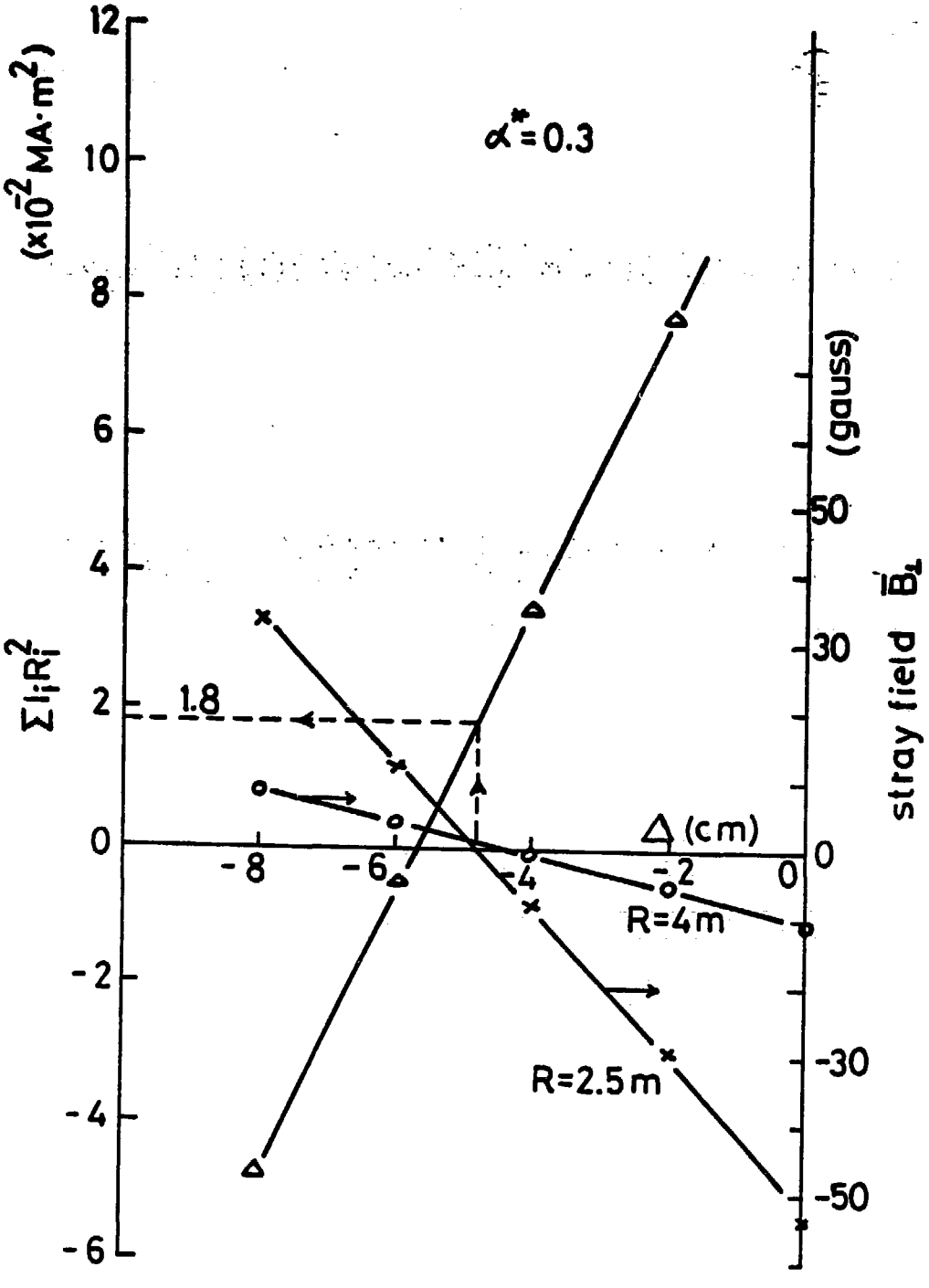
$\alpha^* = 0.3$
$(\times 10^{-2}\,MA\cdot m^2)$
$\Sigma I_i R_i^2$
stray field $\bar{B}_\perp$ (gauss)
Δ (cm)
1.8
R=4m
R=2.5m
12
10
8
6
4
2
0
-2
-4
-6
50
30
-30
-50
-8
-6
-4
-2
0

DIPOLE MOMENT=-3.86 (100KA*M*M)

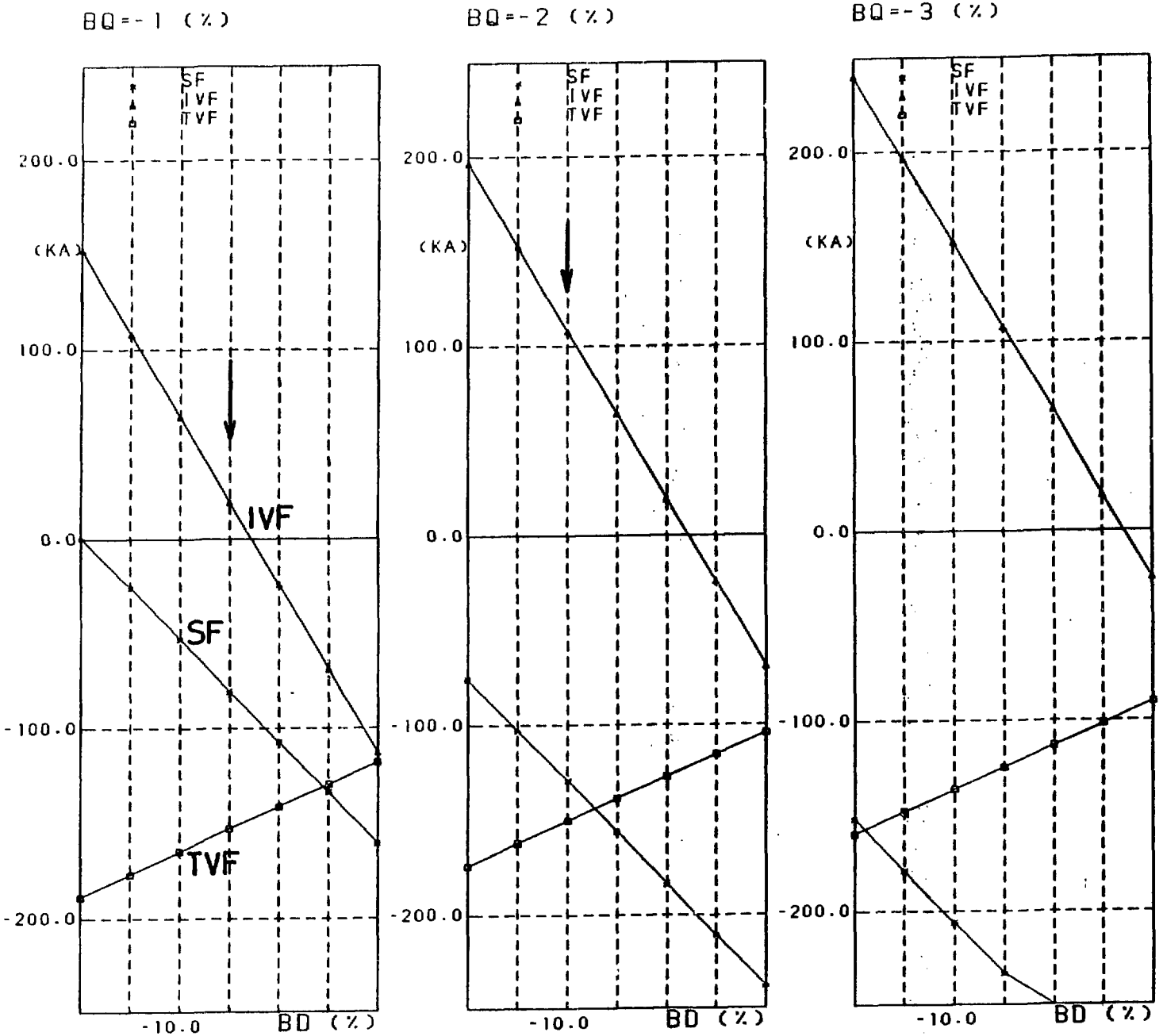

Magnetic Axis Swing

ΔB_D = - 3.0 %

ΔR_{axis} = - 6.0 cm

ΔB_Q = 0

$\Delta \phi$ = 0

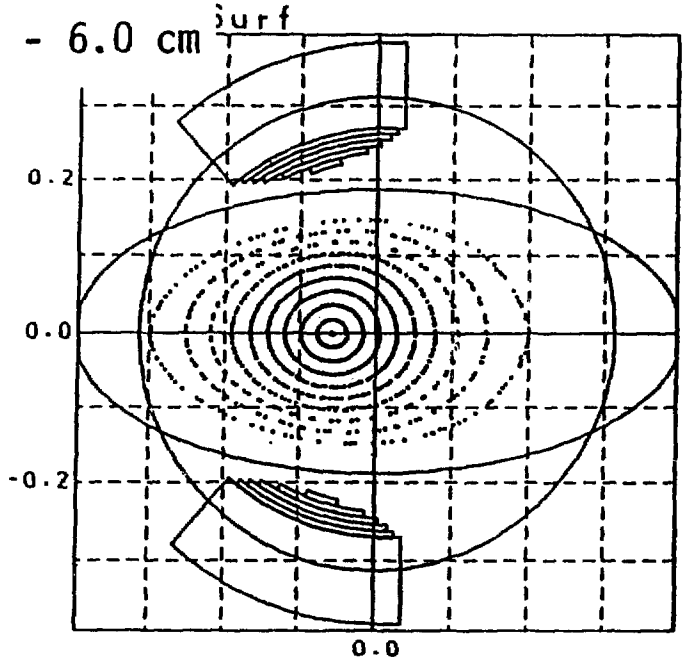

ΔB_D = + 4.5 %

ΔR_{axis} = + 11.5 cm

ΔB_Q = 0

$\Delta \phi$ = 0

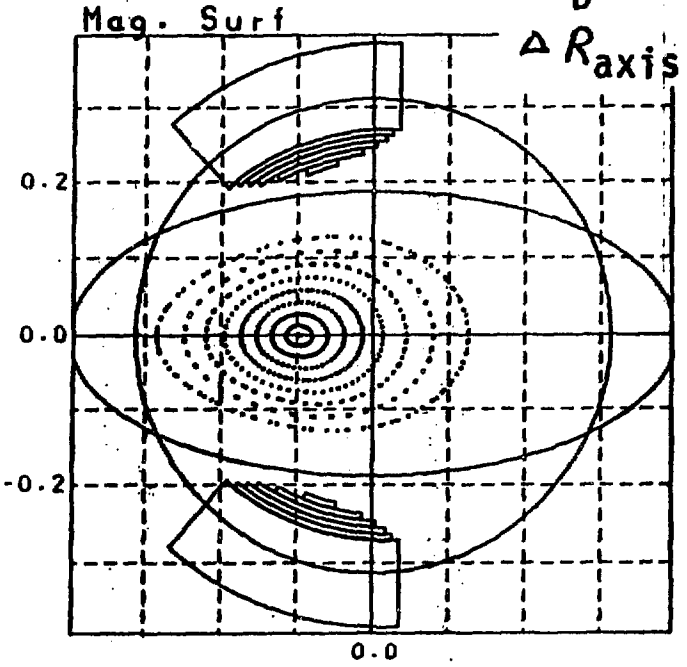

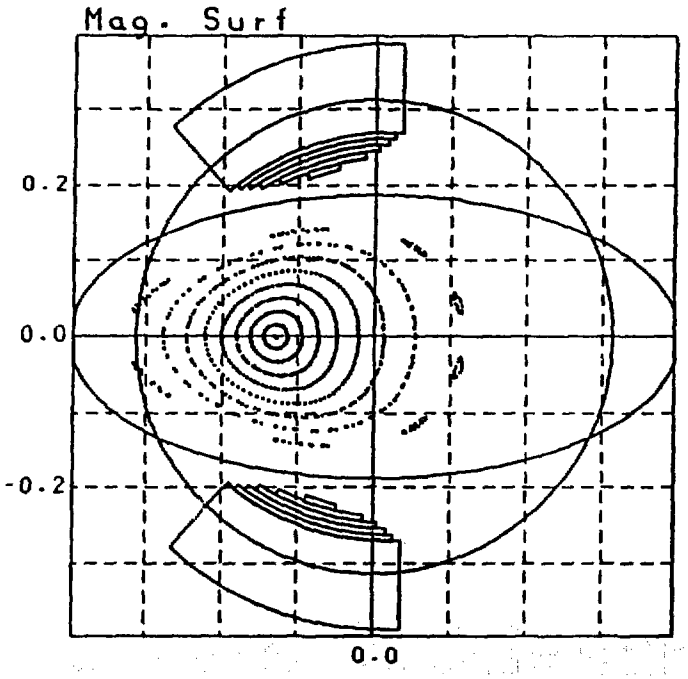

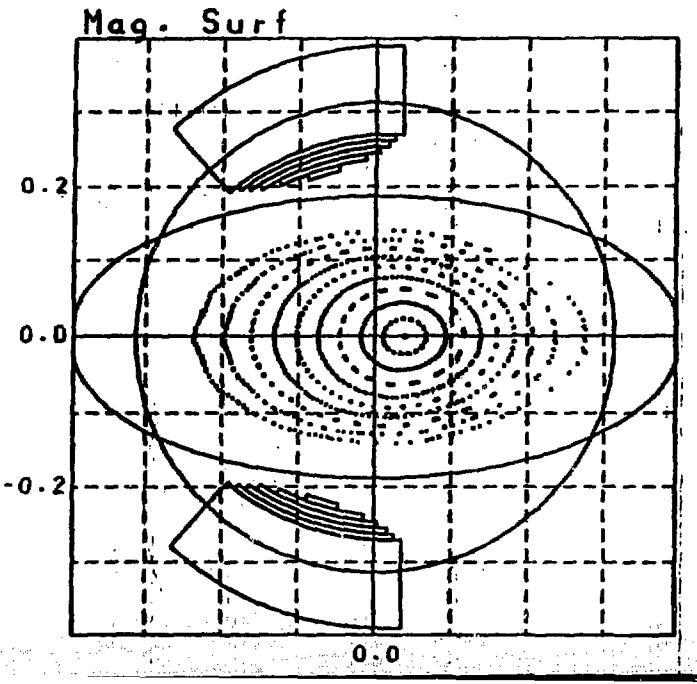

Quadrupole Field Swing

$\Delta B_Q = -1.7\ \%$

$\Delta B_D = 0$

$\Delta \phi = 0$

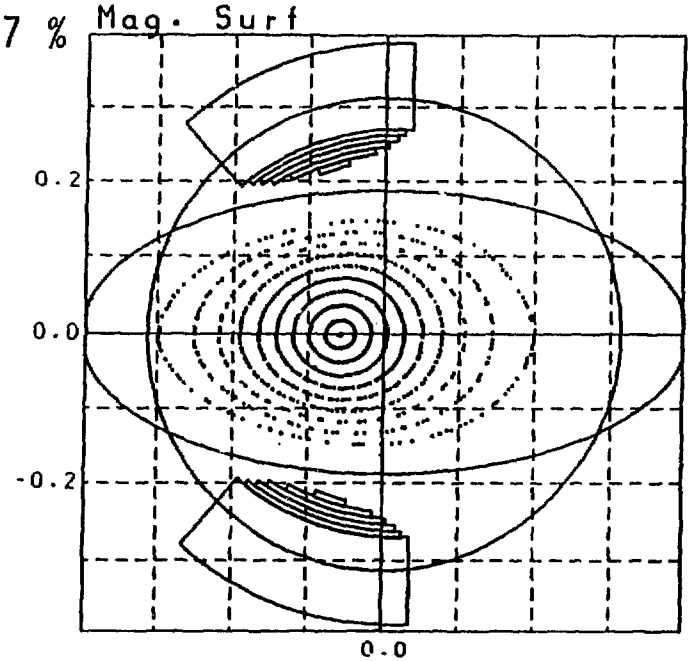

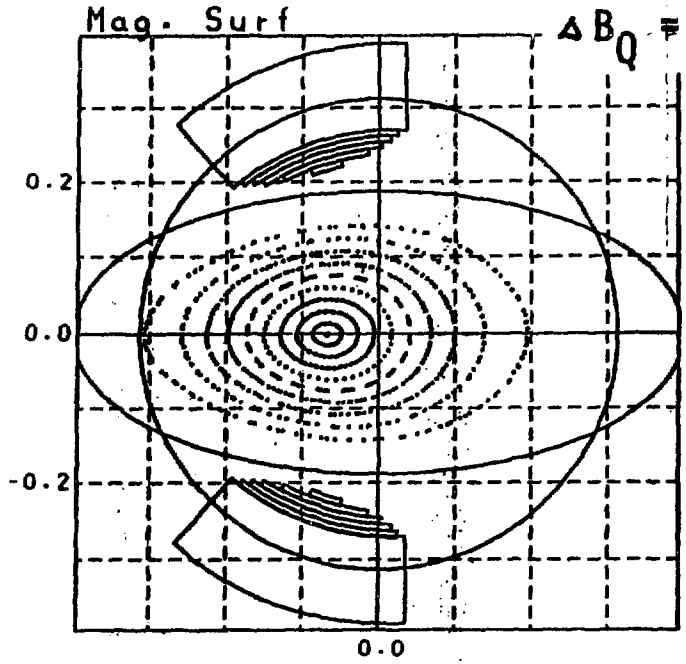

$\Delta B_Q = +1.8\ \%$

$\Delta B_D = 0$

$\Delta \phi = 0$

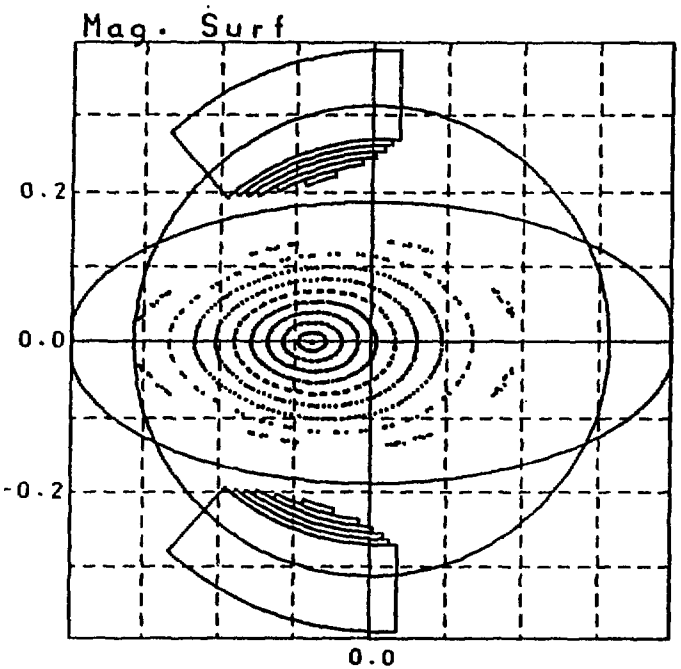

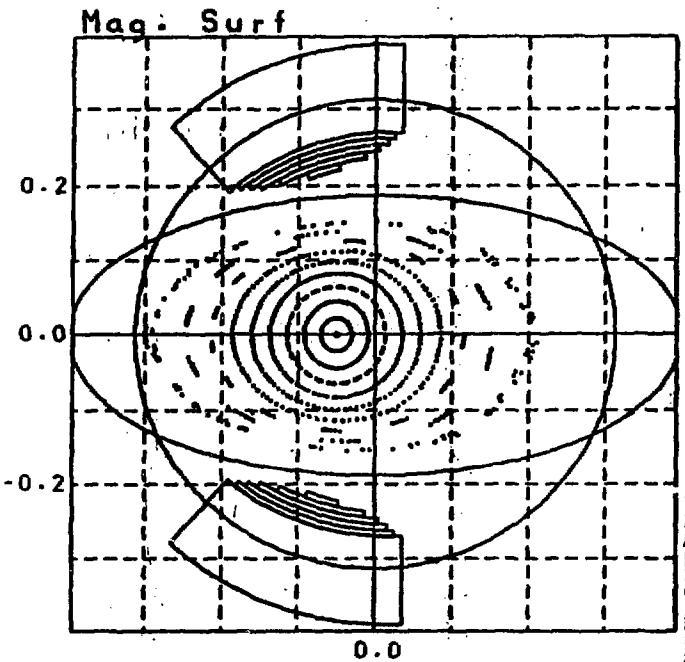

Flux Swing

$\Delta\phi$ = + 0.2 volt.sec

ΔB_D = 0

ΔB_Q = 0

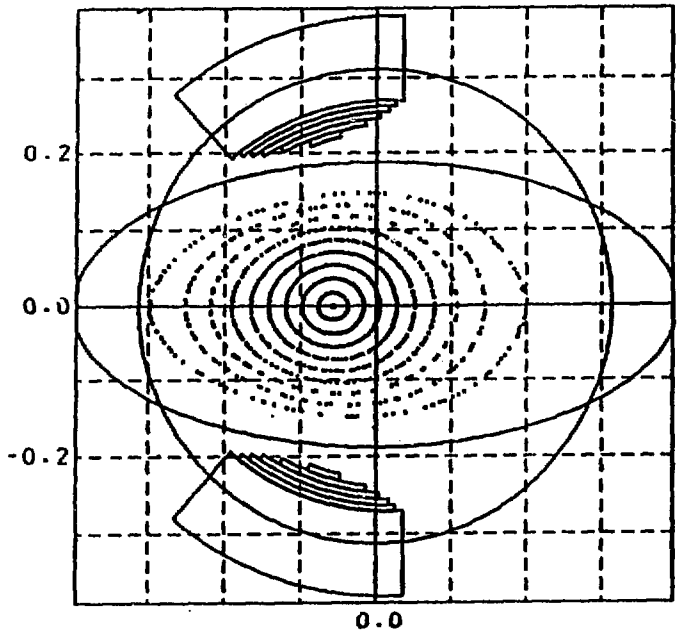

$\Delta\phi$ = - 0.4 volt.sec

ΔB_D = -5.0 %

ΔR_{axis} = - 11.8 c

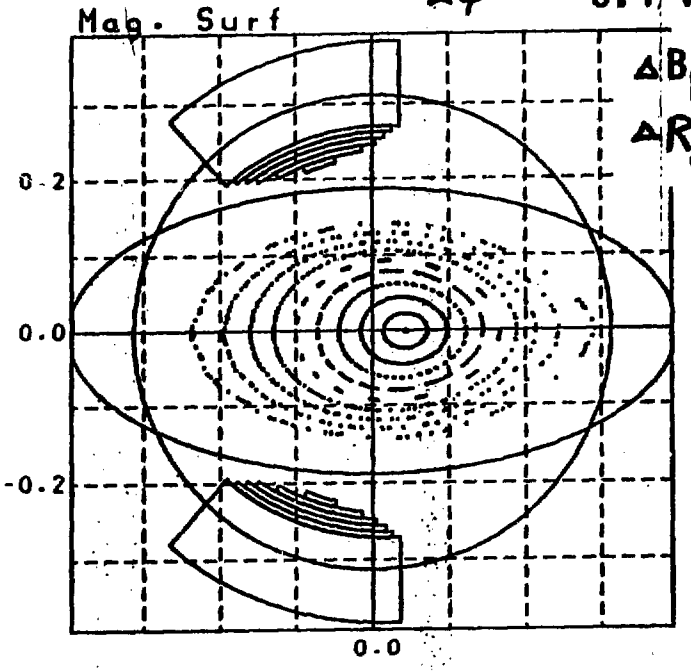

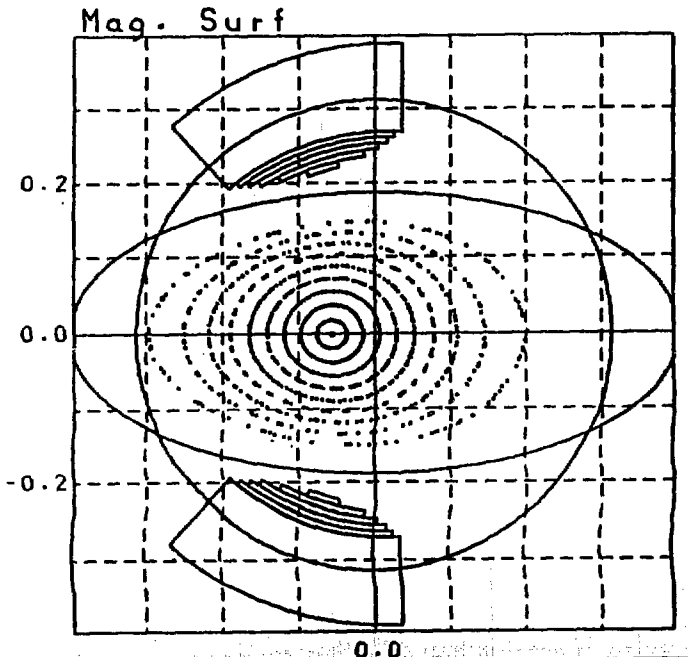

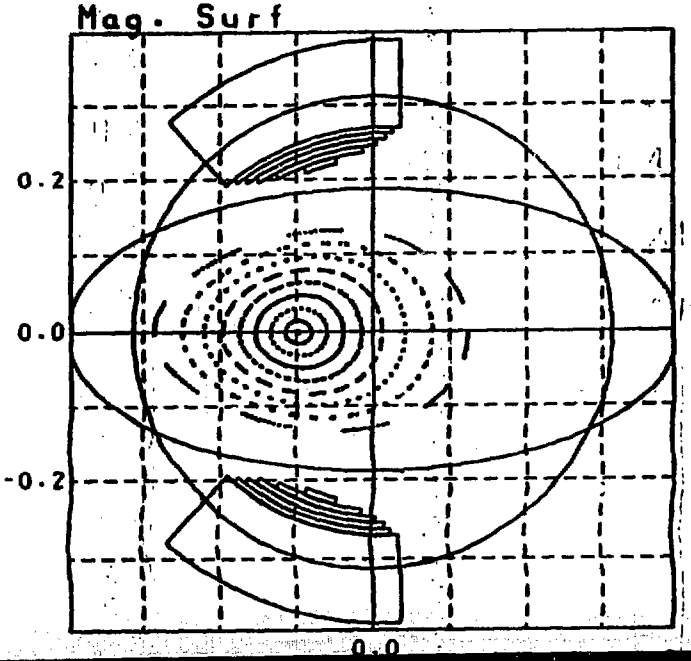

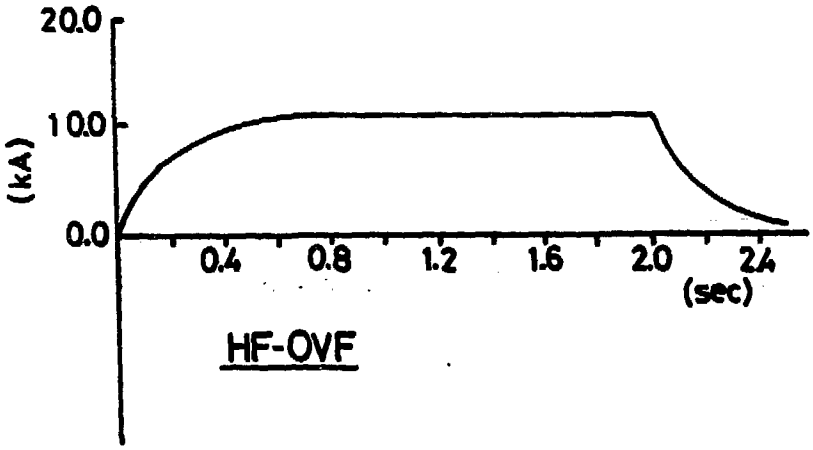
20.0
10.0
0.0
(kA)
0.4
0.8
1.2
1.6
2.0
2.4
(sec)
HF-OVF

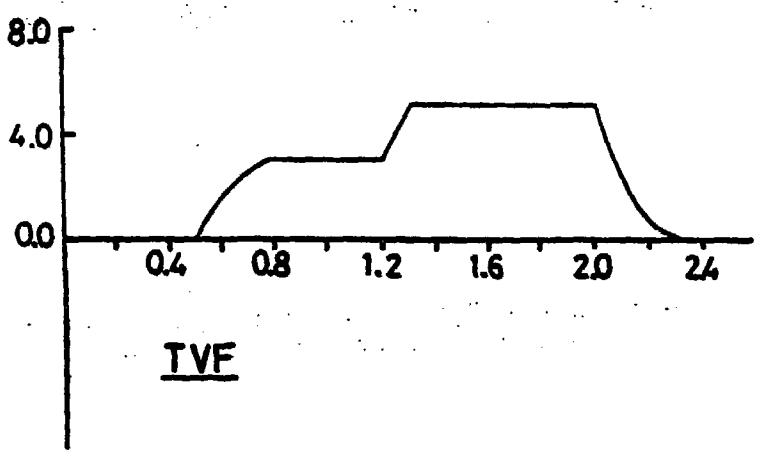
8.0
4.0
0.0
0.4
0.8
1.2
1.6
2.0
2.4
TVF

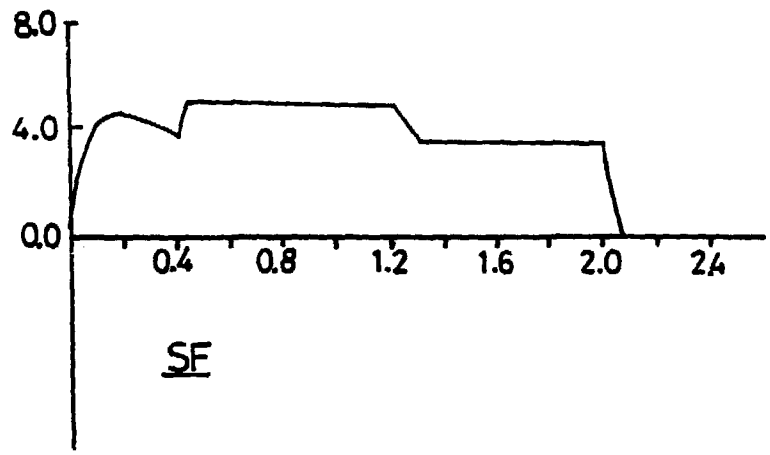
8.0
4.0
0.0
0.4
0.8
1.2
1.6
2.0
2.4
SF

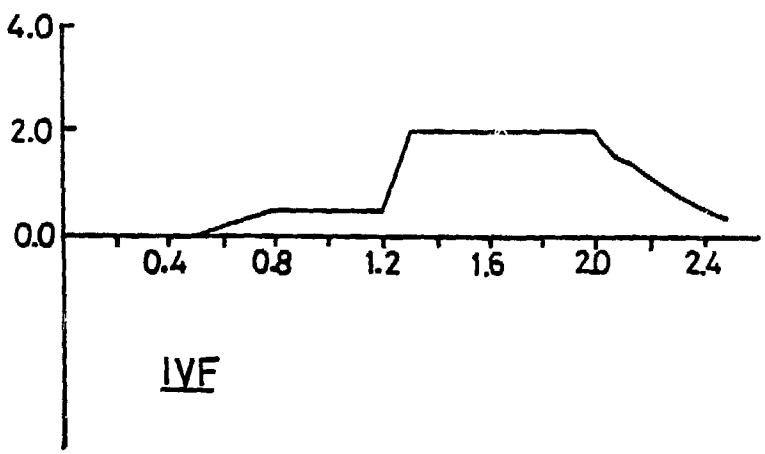
4.0
2.0
0.0
0.4
0.8
1.2
1.6
2.0
2.4
IVF

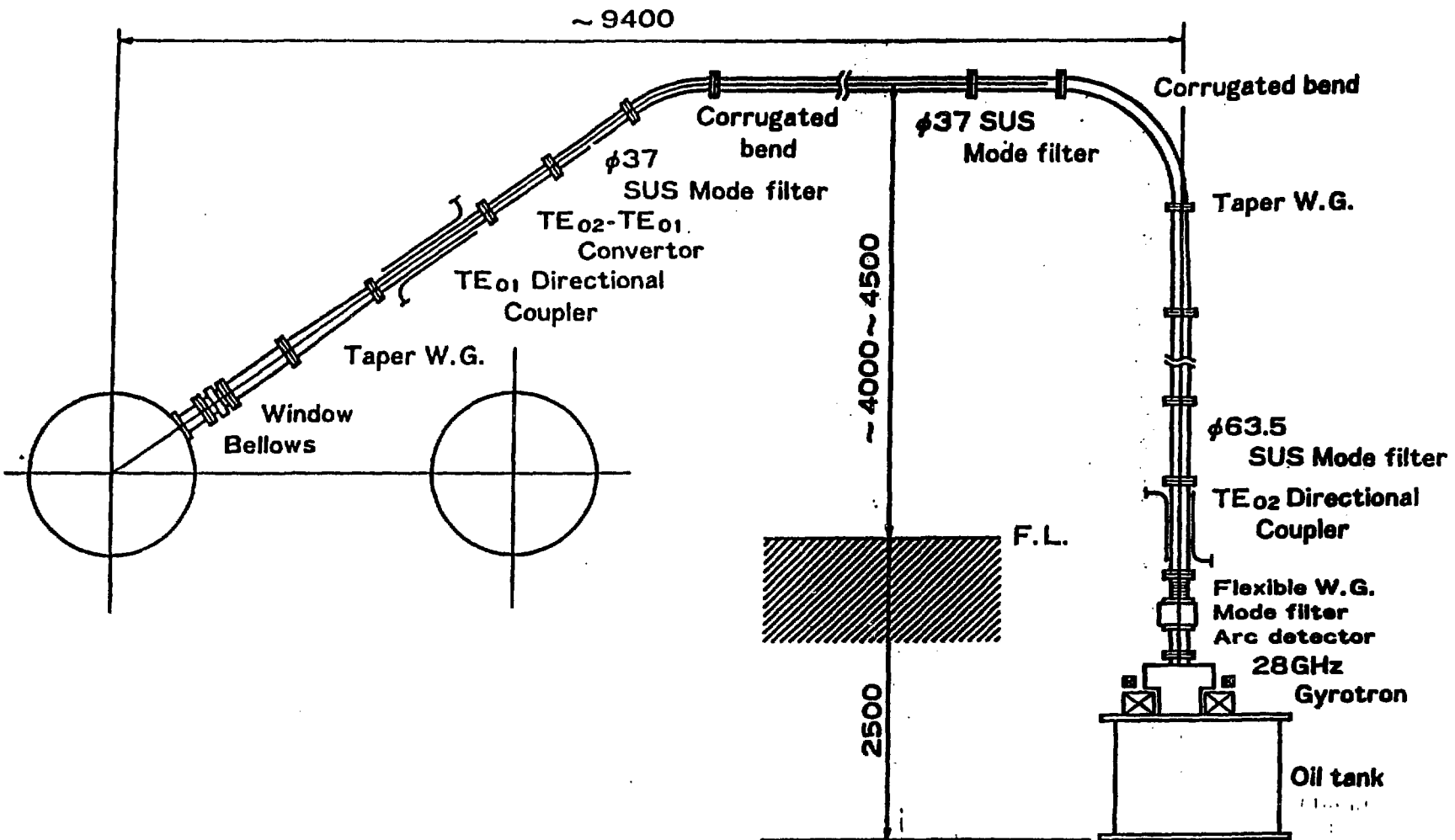
~9400
Corrugated bend
φ37 SUS Mode filter
Corrugated bend
φ37
SUS Mode filter
TE02-TE01 Convertor
TE01 Directional Coupler
Taper W.G.
Window
Bellows
~4000~4500
Taper W.G.
φ63.5
SUS Mode filter
TE02 Directional Coupler
F.L.
Flexible W.G.
Mode filter
Arc detector
28GHz
Gyrotron
2500
Oil tank

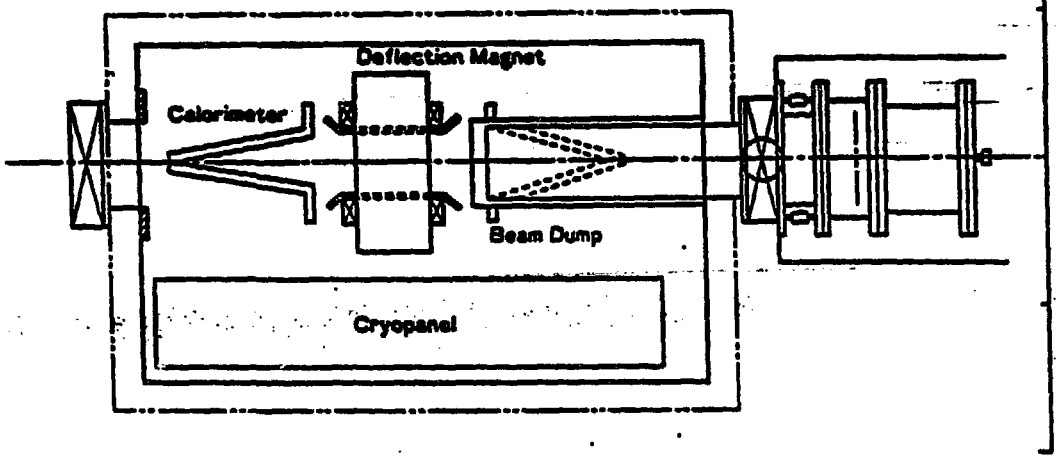
Deflection Magnet
Calorimeter
Beam Dump
Cryopanel

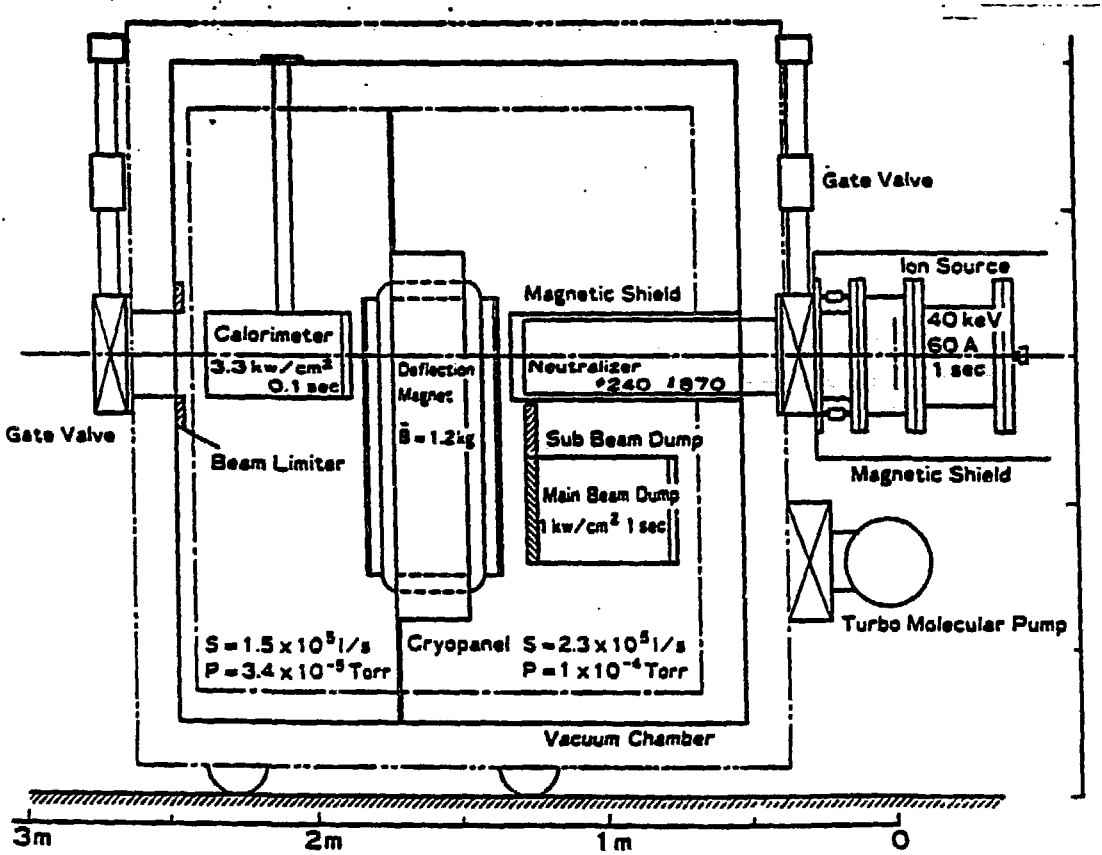
Gate Valve
Ion Source
40 keV
60 A
1 sec
Magnetic Shield
Calorimeter
3.3 kw/cm²
0.1 sec
Deflection
Magnet
B = 1.2kg
Neutralizer
240 1870
Sub Beam Dump
Main Beam Dump
1 kw/cm² 1 sec
Gate Valve
Beam Limiter
Magnetic Shield
Turbo Molecular Pump
S = 1.5 x 10⁵ l/s
P = 3.4 x 10⁻⁵ Torr
Cryopanel
S = 2.3 x 10⁵ l/s
P = 1 x 10⁻⁴ Torr
Vacuum Chamber
3m
2m
1m
0

Plasma production and heating by RF

High density plasma production by Whistler Wave.

* f=40-200 MHz in B=0.5-2 T.
* Adjustable for a change of B_0.
* Cheaper than ECH system.

Ion Bernstein Wave heating.

* Effective heating even in a high density plasma ($10^{14} cm^{-3}$).
  ---------- Alcator
* A little high energy tail. ---------- JIPPT-II, PLT
* Good accessibility of an antenna.
  Installed at low field side.
  Movable antenna.

CHS Diagnostics

Quantity	Diagnostics	Space Resolution
	Monitoring Diagnostics	
N_e	4 mm Microwave Interferometer	Line Average
T_e	Soft X-ray Pulse Height Analysis	
T_i	Time-of-Flight Neutral Particle Analyzer	
Energy	Diamagnetic Loop	Area Average
N_0	H_α Light Monitor	Chord Average
Impurity	VUV Spectrometor	Chord Average
Radiation	Bolometer	Chord Average
Shape	TV Camera	2 D Image
Current	Rogowskii Coil	Area Average
	Profile Diagnostics and others	
N_e	HCN Laser Interferometer	2 D
T_e	Thomson Scattering	Pointwise
	Electron Cyclotron Emission	1 D
T_i	Charge Exchange Neutral Particle Analyzer	
	Charge Exchange Recombination Spectroscopy	Pointwise
Fast Ion Loss	Ion Beam Surface Analysis	Plasma Surface
	Charge Exchange Neutral Particle Analyzer	Pitch Angle
Potential	Spectroscopy (Doppler Shift)	Chord Average
	Heavy Ion Beam Prove	Pointwise
Magnetics	Soft X-ray Detector Array	2 D
Radiation	Bolometer Array	2 D
Diffusion	Instrumented Limiter	Cross section
Edge Region	Lithium Beam Probe	Pointwise

Schedule of CHS

	Apr. 1987 (F.Y.)	1988	1989	1990
Machine	construction	preliminary experiment	heating experiment	
Power Supply	1.5Tesla HF/OVF RF (TVF, IVF, SF)	(upgrade 2T)		
Heating ECH	18GHz 28GHz	56GHz		
NBI		No.1 (2～3MW)	No.2 (2～3MW)	
RF	6～28MHz			
ICRF		2～3MW		
Diagnostics	Basic			

STATUS OF THE ATF PROJECT

by

G. H. Neilson, T. C. Jernigan, R. L. Johnson,
P. H. Edmonds, R. D. Foskett, and M. J. Saltmarsh

presented at
U.S.-Japan Heliotron-Stellarator Workshop
Oak Ridge
November 9, 1987

ORNL-DWG 86-3320 FED

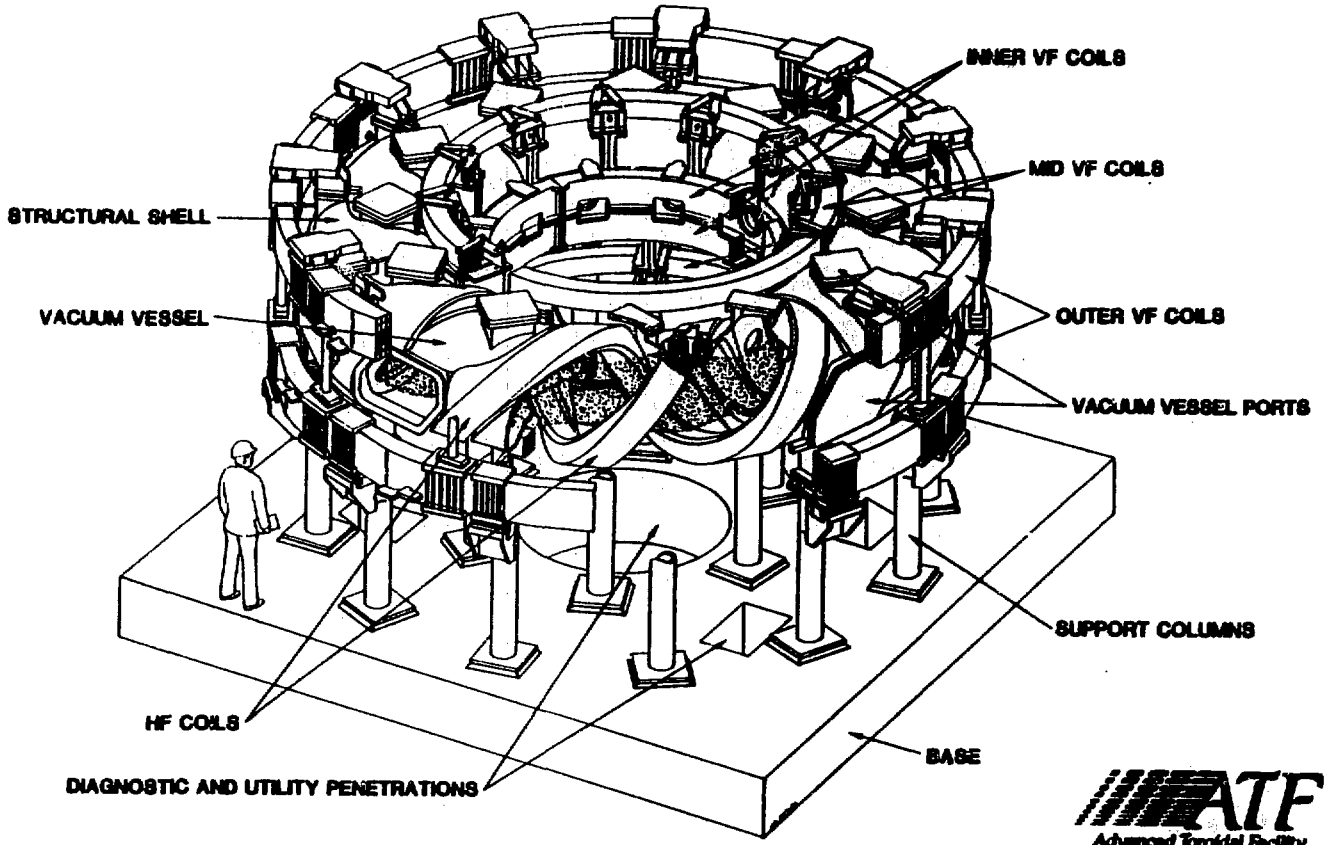

ATF
Advanced Toroidal Facility
Oak Ridge National Laboratory

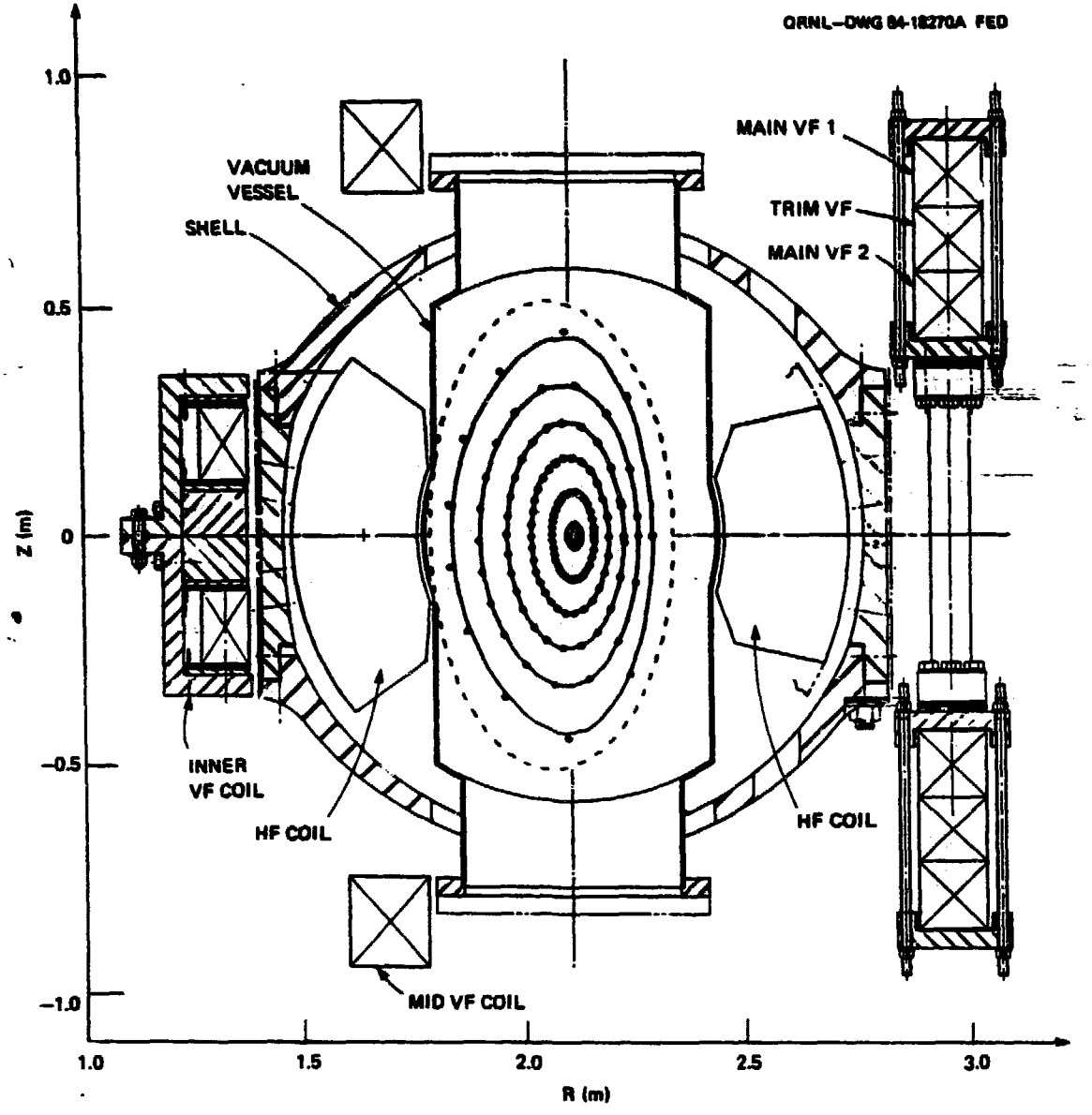
ORNL–DWG 84-18270A FED
MAIN VF 1
TRIM VF
MAIN VF 2
VACUUM VESSEL
SHELL
INNER VF COIL
HF COIL
HF COIL
MID VF COIL
1.0
0.5
0
–0.5
–1.0
Z (m)
1.0
1.5
2.0
2.5
3.0
R (m)

ATF Parameters

Major radius, R_0	2.1 m
Avg. minor radius, $\bar{a}$	0.3 m
Magnetic field on axis, B_0	2 T (5 s)
	1 T (steady state)
Multipole order, ℓ	2
No. field periods, M_0	12
Central rotational transform, $\iota(0)$	0.35 (std. case)
Edge rotational transform, ι(a)	0.95(std. case)
ECH power (st. state)	0.2-0.4 MW @53 GHz
Neutral beam power (0.3 s)	2.0-3.0 MW
ICRF power (st. state)	0.1 MW @5-30 MHz
	0.2 MW @5-15 MHz
	2.0 MW @5-30 MHz ($\sim$1989)

Key ATF Design Features

- Flexible coil system for control of shape, ι profile, V'', magnetic axis.
- Optimized for pure torsatron operation– no OH or TF coil systems.
- Segmented HF coil with bolted joints– for parallel fabrication and demountability.
- Accurate construction of coil and structure. Winding law tolerance ± 1 *mm*.
- Large access for tangential NBI and diagnostics.
- Coil system steady state at B_0=1 T.

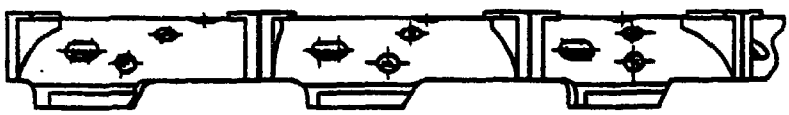

UPPER SHELL

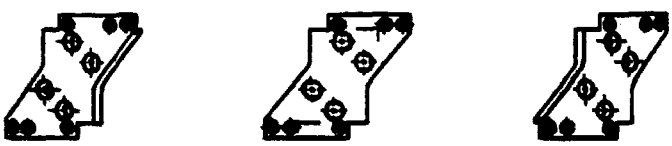

INTERMEDIATE PANELS

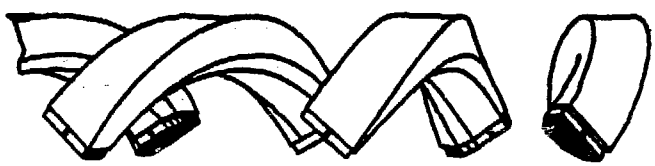

UPPER H.F. COIL SEGMENTS

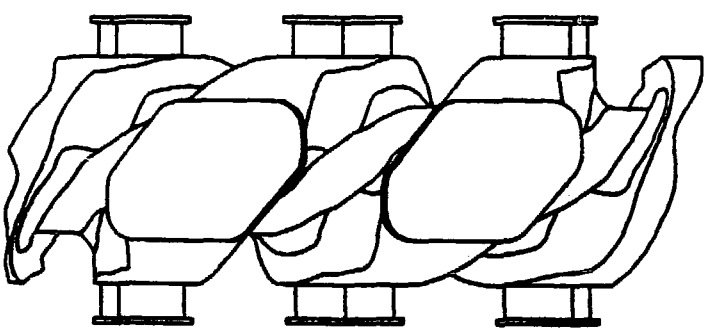

VACUUM VESSEL

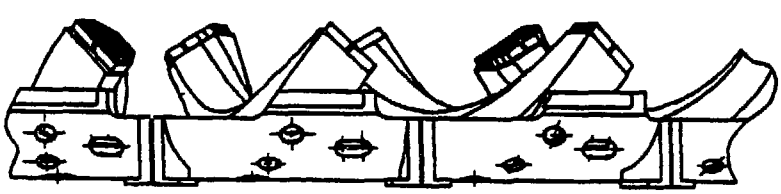

LOWER H.F. COIL SEGMENT POSITIONED IN LOWER SHELL

ATF Construction Progress Since October '86

- Helical field coils were pre-assembled and aligned. Holes for joint bolts were match drilled. Top coils were removed.
- Vacuum vessel was delivered from manufacturer after 17 months' delay.
- Vacuum vessel contour corrections and leak repairs were made by ORNL.
- Vessel, upper HF coils, and joint bolts were installed, and bolts tightened to 12,000 lbs. force.
- Thermal cycle testing of joints was completed. Coils were energized to 15 kA, joints heated to 70°C.
- Epoxy bladders and upper structural shell were installed– HF coil fully supported.
- Upper VF coils installed.
- Bus installation and connection to coils is in progress.
- Construction will be completed by November 25!

ORNL–DWG 85-3623 FED

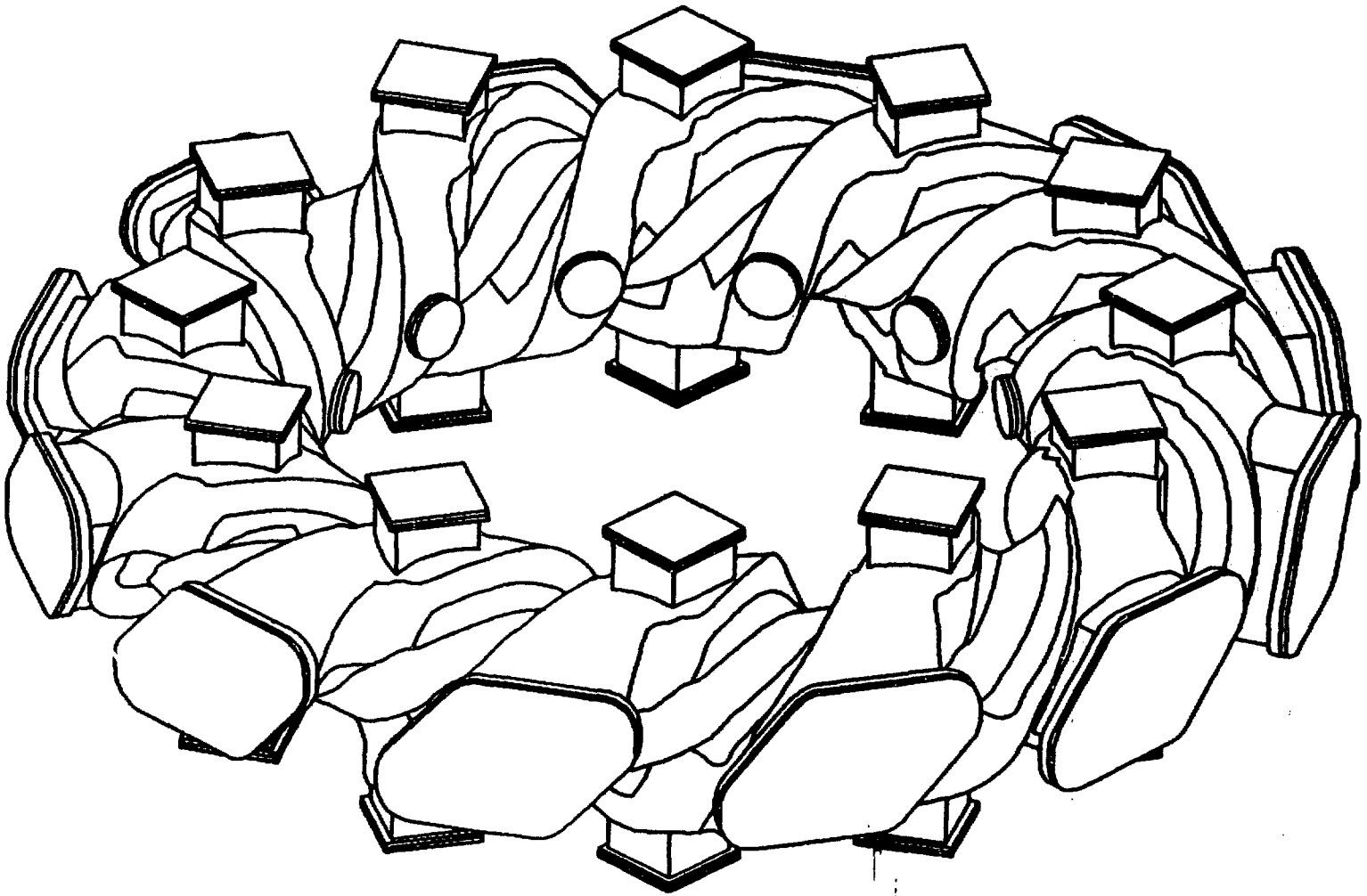

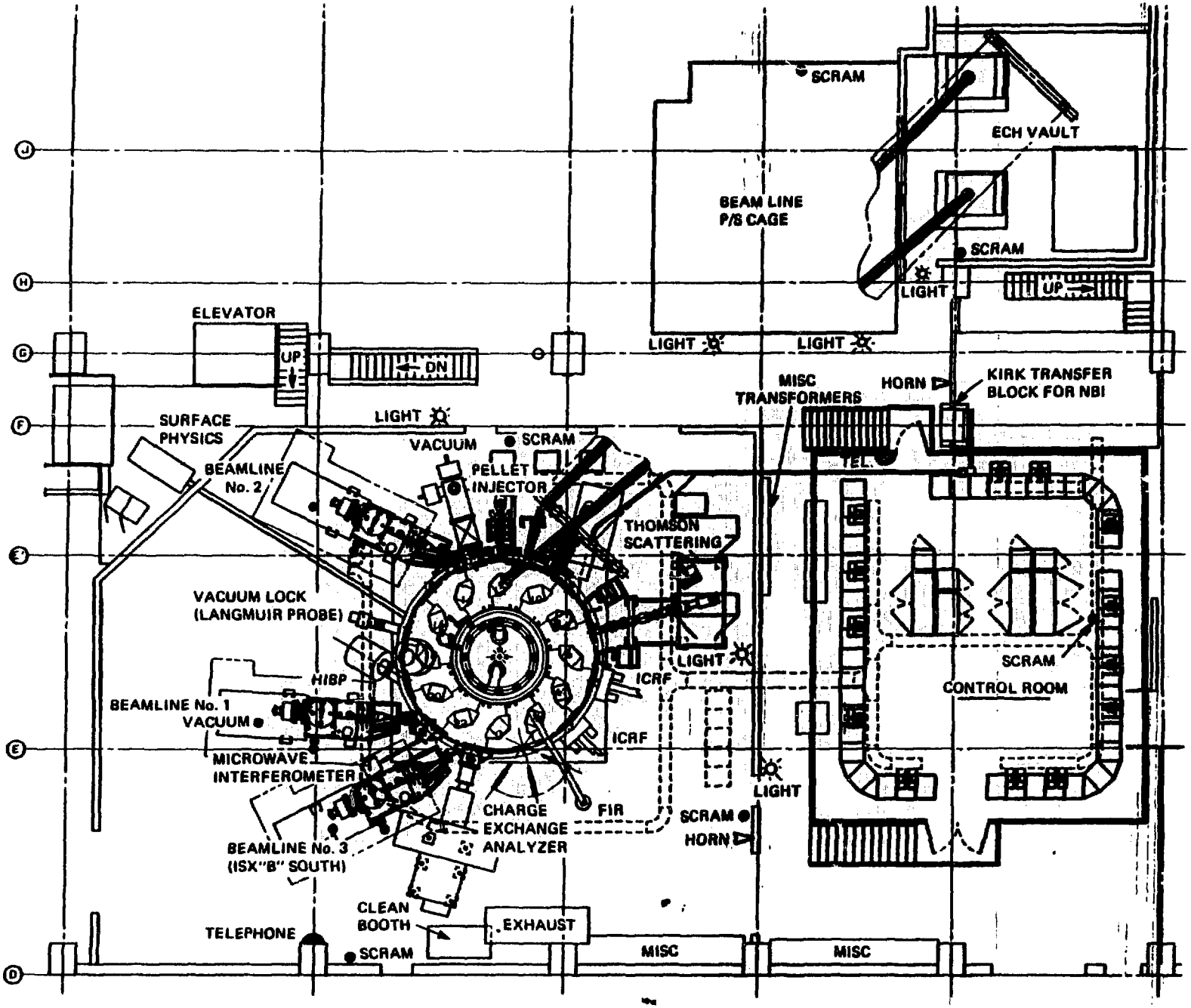
SCRAM
ECH VAULT
BEAM LINE
P/S CAGE
SCRAM
LIGHT
UP
ELEVATOR
UP
DN
LIGHT
LIGHT
MISC
TRANSFORMERS
HORN
KIRK TRANSFER
BLOCK FOR NBI
SURFACE
PHYSICS
LIGHT
VACUUM
SCRAM
BEAMLINE
No. 2
PELLET
INJECTOR
TEL.
THOMSON
SCATTERING
VACUUM LOCK
(LANGMUIR PROBE)
LIGHT
SCRAM
CONTROL ROOM
HIBP
ICRF
BEAMLINE No. 1
VACUUM
ICRF
MICROWAVE
INTERFEROMETER
LIGHT
CHARGE
EXCHANGE
ANALYZER
FIR
SCRAM
HORN
BEAMLINE No. 3
(ISX"B" SOUTH)
CLEAN
BOOTH
EXHAUST
TELEPHONE
SCRAM
MISC
MISC

JULY 30, 1987

AEDC-TR-87-9

AEF FACILITY MAP
EXPERIMENTAL PLAN

Basic Facility Systems

- HF power supply– 125 kA, 1250 V, 5 s.
- VF power supplies (3)– 15 kA, 625 V, 5 s.
- Vacuum pumping– $3 \times 2,200\ \ell/s$.
- Gas puff– $2 \times \sim 100\ torr - \ell/s$.
- X-ray suppression:
  - Rotary probe– $\leq$ 0.5-second stroke.
  - Fast Argon discharge– $\Delta p = 10^{-2}$ torr in 10 ms.
- Control system– 4 programmable logic controllers (PLC).
- Data acquisition– VAX 8700 computer with CAMAC.
- Discharge cleaning:
  - Glow discharge– 1 kV, 2.5 A.
  - ECR– 6 kW @2.45 GHz.
- Chromium/titanium gettering.
- Vacuum vessel baking (delayed):
  - Induction heating via HF coils– 50 kW @60 Hz.
  - Tape heating for flanges, ducts, etc.– 30 kW.

Heating and Particle Control Systems

- Electron cyclotron heating:
  - 0.4 MW @53 GHz (1987-88).
  - + ~0.2 MW @28 GHz (1989).
- Neutral beam injection heating:
  - 1 MW Co– + 1 MW Ctr– @40-50 keV (1988).
  - +1 MW @40-50 keV (1989).
- Ion cyclotron heating:
  Power:
  - 0.1 MW @5-30 MHz +0.2 MW @5-15 MHz (1988).
  - +2 MW @5-30 MHz (1989).

  Antennas: Fast wave (1988); Ion Bernstein wave (1989).
- Pellet injector– 8-shot cluster gun type; 1.0–2.5 mm diameters, $v \geq 1.2\ km/s$.
- Limiters (graphite, instrumented, movable):
  - 2 horizontal top and bottom rail limiters with 12 graphite tiles.
  - 1 vertical outboard plate.

Commissioning Plan

1. Complete ATF construction (Nov. 1987).
2. Commission HF sytem to B_0=1 T (I_{HF}=62.5 kA) and commission X-ray suppression systems.
3. Apply ECH to obtain "Zero-th" plasma with minimum diagnostic set.
4. Conduct radiation surveys and evaluate (for safety).
5. Install remaining Phase I diagnostics.
6. Obtain "First" plasma (with diagnostics) and document target plasma (January 1988).
7. Begin NBI experiments (January 1988).
8. Make initial magnetic surface measurements with e-beam system (March 1988).
9. Install Phase II diagnostics (May 1988).
10. Install fast wave antenna ($\sim$July 1988).

ATF MILESTONE SCHEDULE (Rev: 3-Sep-1987)

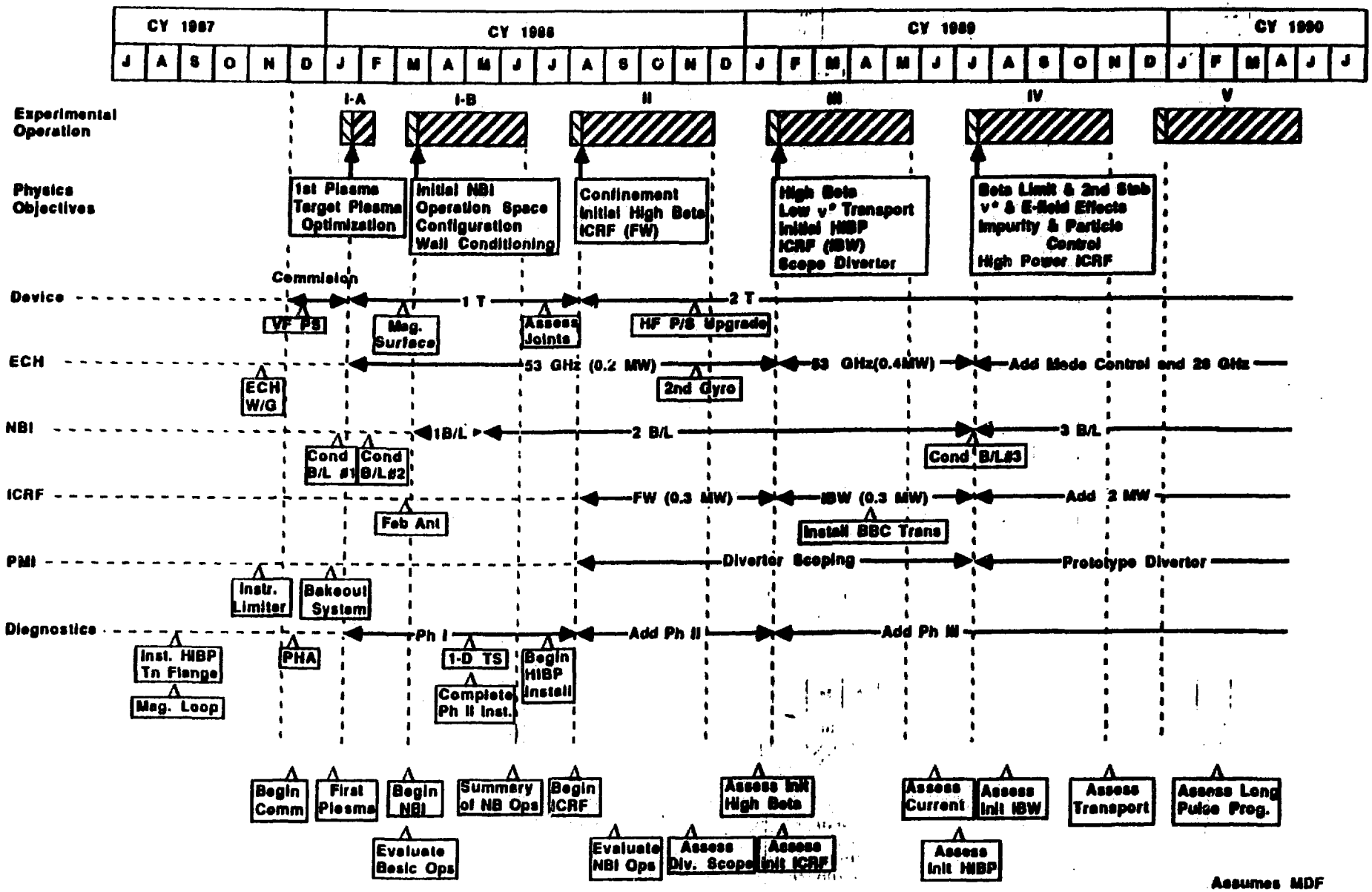

Assumes MDF Completion 12/1/87

Summary

- ATF construction project is now proceeding extremely well.
- Power supplies, vacuum, and ECH system have been tested.
- Construction will be completed November 25, 1987; about 1 year late due to delay in vacuum vessel fabrication.
- Commissioning will start December 1.
- "Zero-th" plasma in December.
- "First" plasma in January.

US-JAPAN
STELLARATOR/HELIOTRON WORKSHOP
Oak Ridge, November 9-13, 1987

STATUS OF THE WENDELSTEIN W7AS STELLARATOR.

H. RENNER
MPI-Plasmaphysik, EURATOM-Ass.
8046 GARCHING, W.GERMANY

The "Advanced Stellarator" W 7AS (major radius 2m, minor radius 0.2 m, main field <3T) , which is being realized according to an optimization of the magnetic configuration for equilibrium and transport, will be operational at spring 1988. At 4 November the 5 modules were assembled on the supporting structure. The final vacuum test and the completion of the magnet system has been started.

ECF 70 Ghz

The ECF-system has been successfully tested in collaboration with the IPF Stuttgart at simultaneous operation of up to 3 VARIAN gyrotrons (the application of 4 gyrotrons is planned). The full power during the full pulse duration of 3 sec could be transferred successfully with small losses (<10%) over a distance of ca. 50m close to the device W 7AS by an advanced waveguide system (in- cluding bends, mode convertors, k-spectrometer etc.).
VALVO, the developer of the fourth gyrotron, informed about technical problems running out of control and offered to cancel the contract. VARIAN will supply the missing gyrotron within 9 months. At the start of W 7AS only a restricted power of 3 gyrotrons (600 kW, 3 sec), but with sufficient power for the first operation of plasma will be available.
To explore the possibilities of ECRH at even higher frequences with a favourable extension of the density range first experiments at 140 GHz are proposed. An installation of a 140 GHz-gyrotron, which is under development at KFK Karlsruhe, is pursued for the end of 1988.

NBI

The first beamline is installed at the experimental hall. The control system is under test.The second beamline will follow at the end of this year and will be ready at the beginning of the experiment.

ICF

The first experimental antenna system ($P_{IN} < 1.5$ MW, $\Delta t < 0.5$ sec) is completed and is being adapted inside the vessel. The transmission line has to be modified for W 7AS. The control units, which have been already used at W 7A, are replaced.

DIAGNOSTICS

All the instrumentation, which has to be installed before the different modules can be assembled at the final position, is ready and is being fixed inside the vessel: Coils for electric, magnetic measurements (diamagnetism, current, current distribution, equilibrium by pressure effects, fluctuations etc.), limiter and secondary limiters, ECF-probes, antenna and reflector, receiving horns.
The diagnostic for the first phase of the experiment is under test. The hardware for the data acquisition is being installed. The local network for the connection of the μVAX-subsystems and the central VAX 750 unit is in operation.

The first experimental activity at W 7AS concentrates on magnetic field mapping. Two different methods will be used (1) to determine the magnetic twist, to compare the experimental results with the data of calculations based on geometry and currents of the magnets, (2) to localize the magnetic axis, (3) to describe error fields, which lead to island formation and ergodization at the boundary. The measurements will be carried out at paticular values of the magnetic twist, including rational ones, e.g. 1/3, 1/2.

JOK 744

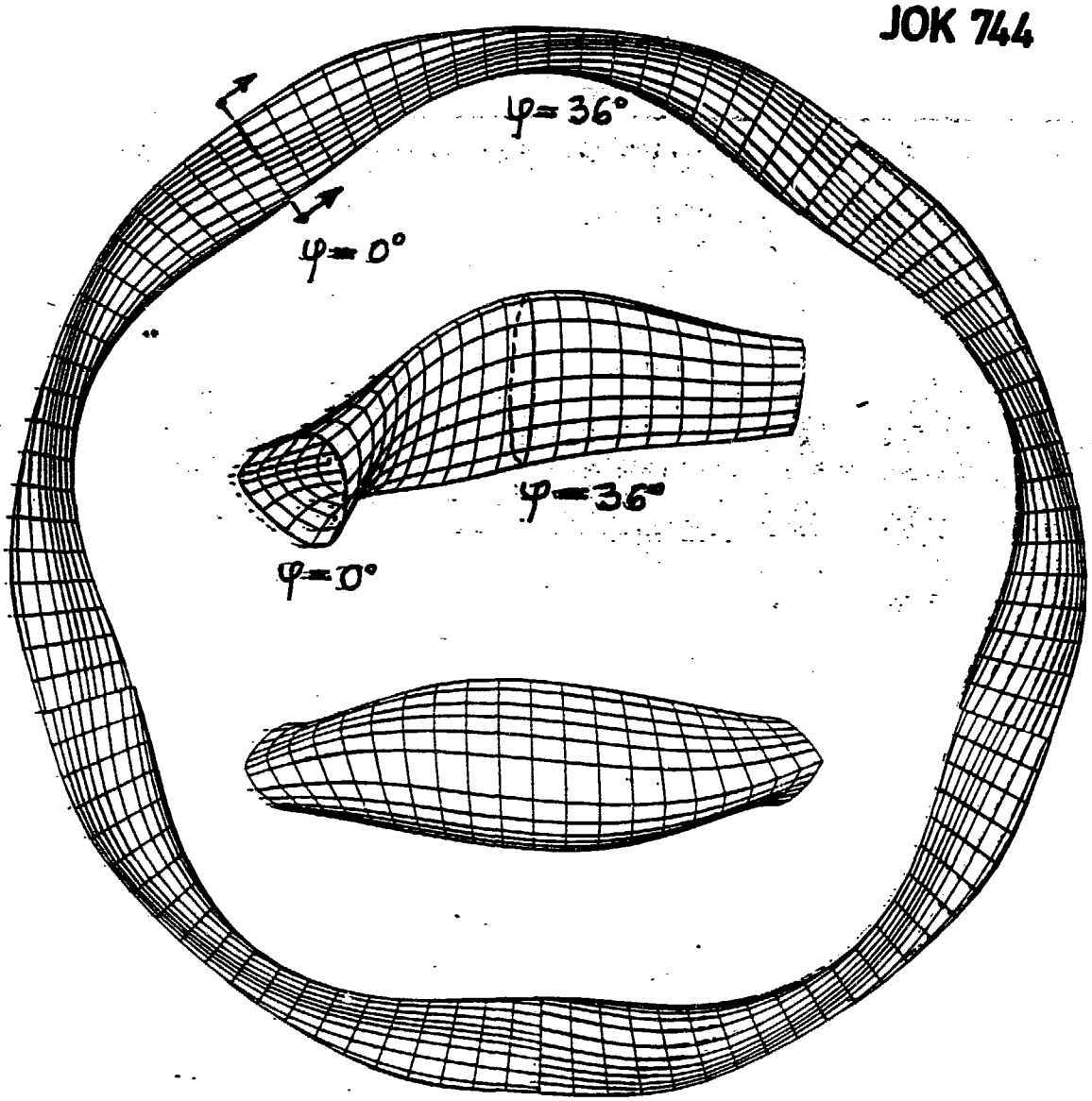

W VII-AS

Plasma Column

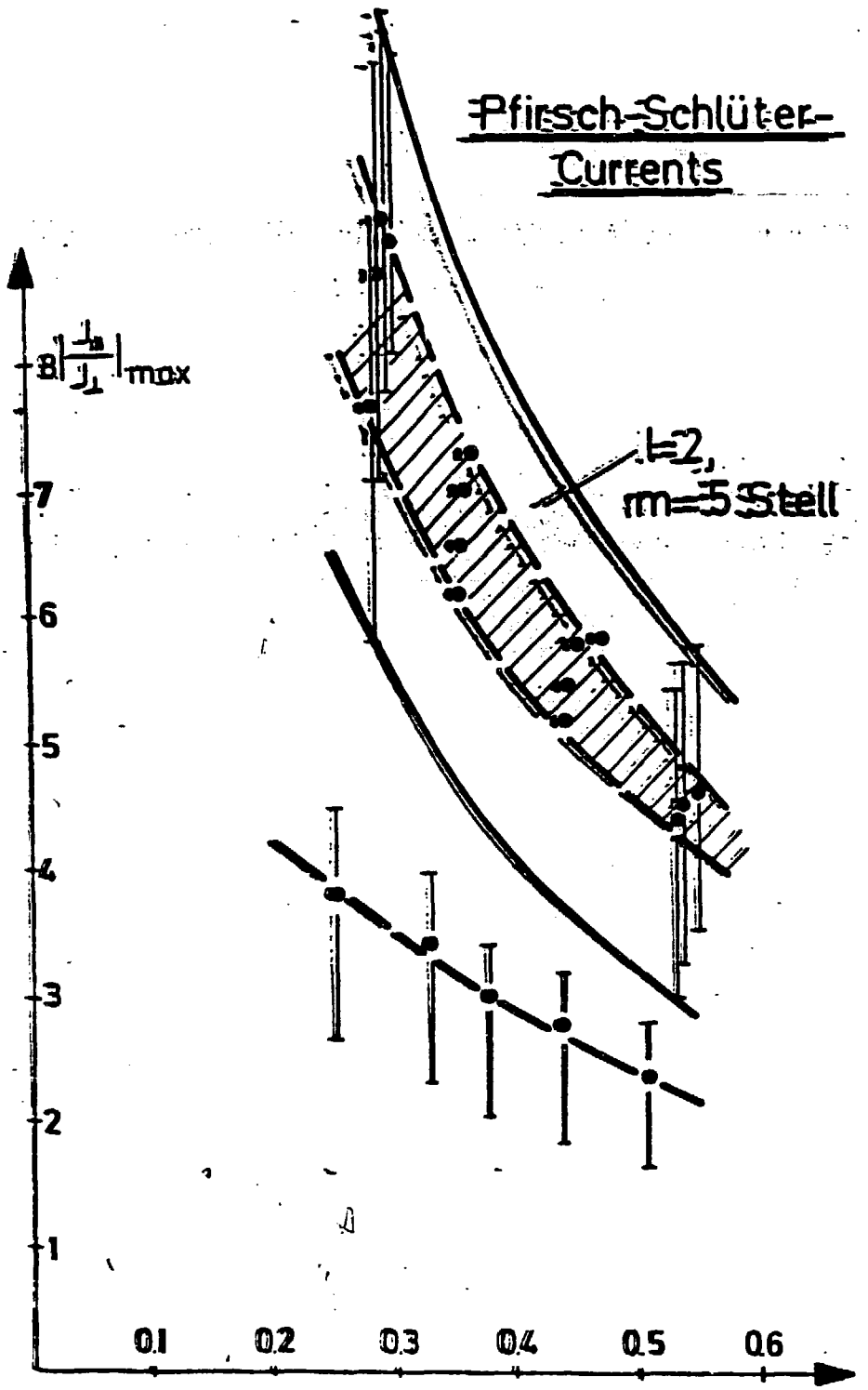
Pfirsch-Schlüter-
Currents
$B\left|\frac{j_\parallel}{j_\perp}\right|_{max}$
l=2,
m=5 Stell
7
6
5
4
3
2
1
0.1
0.2
0.3
0.4
0.5
0.6

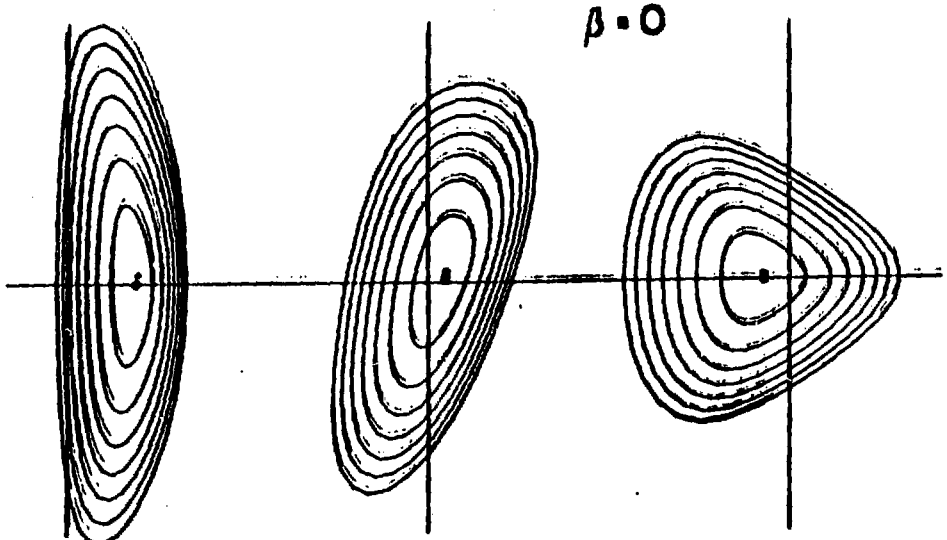
β = 0

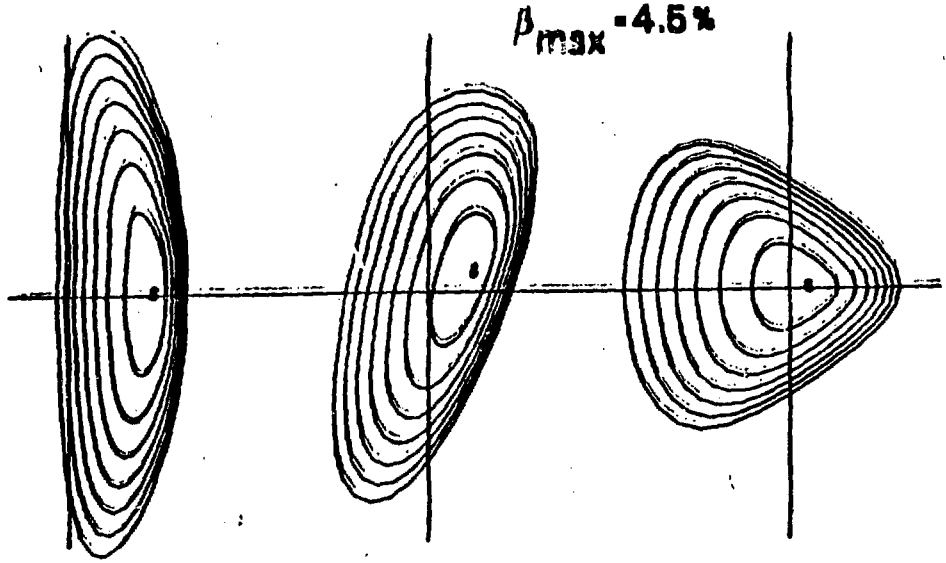
β_{max} = 4.5%

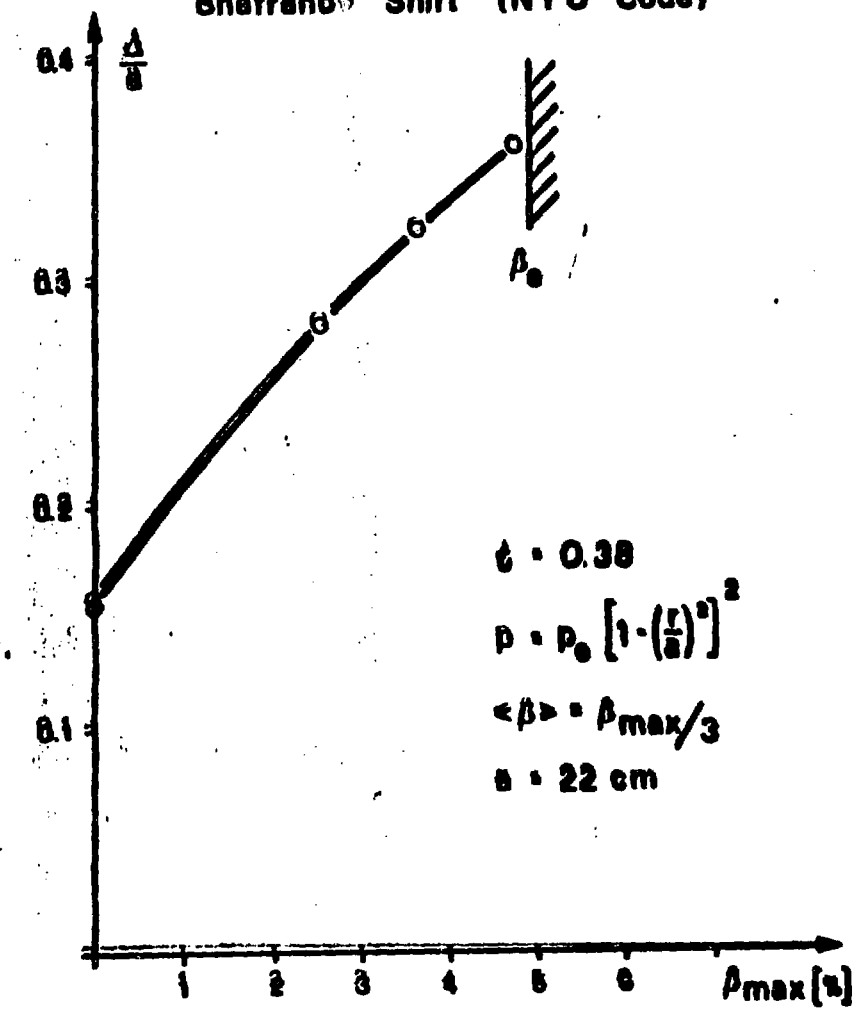
Shafranov Shift (NYU Code)
Δ/a
0.4
0.3
0.2
0.1
β_0
t = 0.38
$p = p_0\left[1-\left(\frac{r}{a}\right)^2\right]^2$
$\langle\beta\rangle = \beta_{max}/3$
a = 22 cm
1
2
3
4
5
6
β_{max} [%]

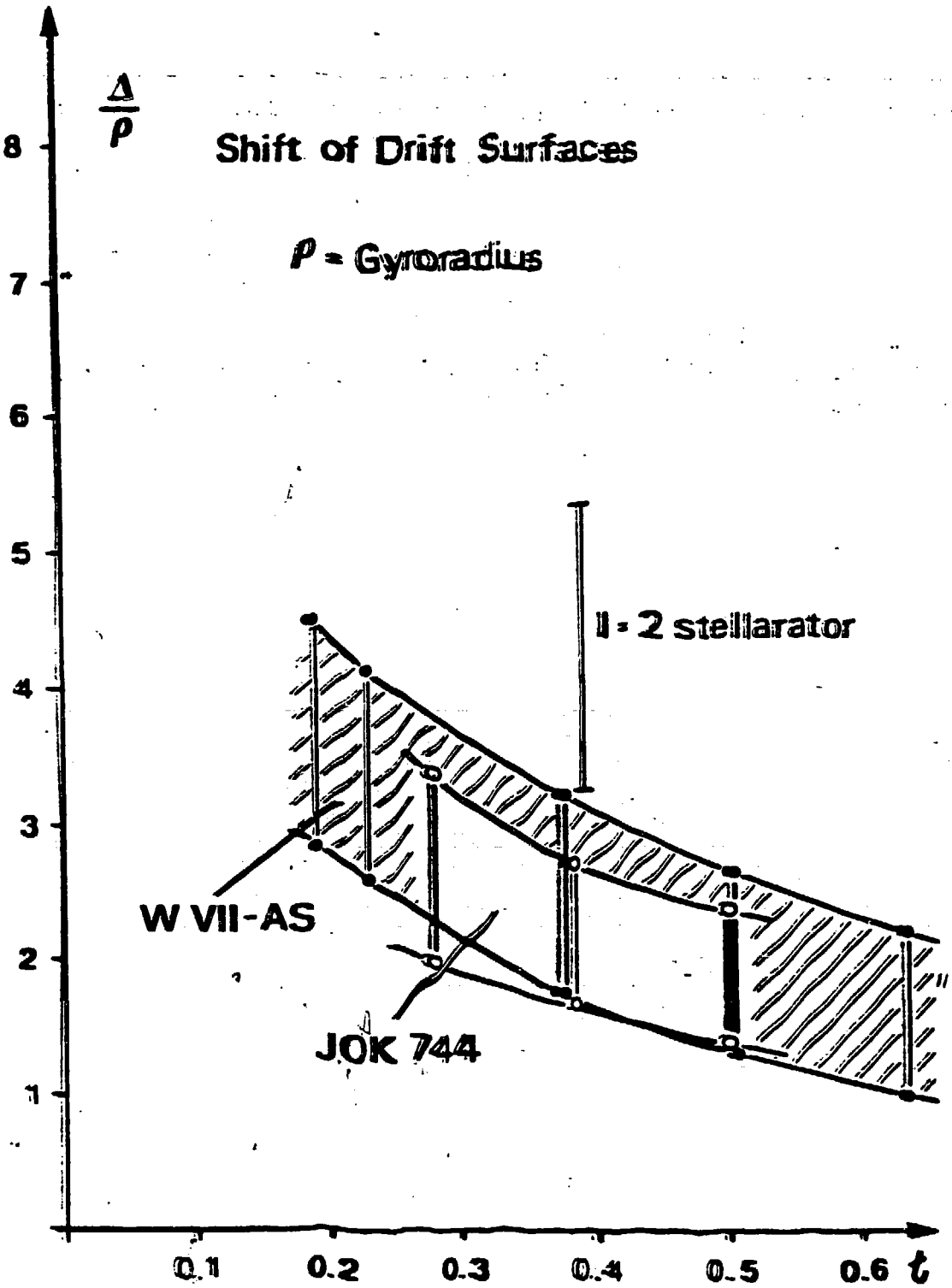
Δ/ρ
Shift of Drift Surfaces
ρ = Gyroradius
8
7
6
5
4
3
2
1
l = 2 stellarator
W VII-AS
JOK 744
0.1
0.2
0.3
0.4
0.5
0.6
t

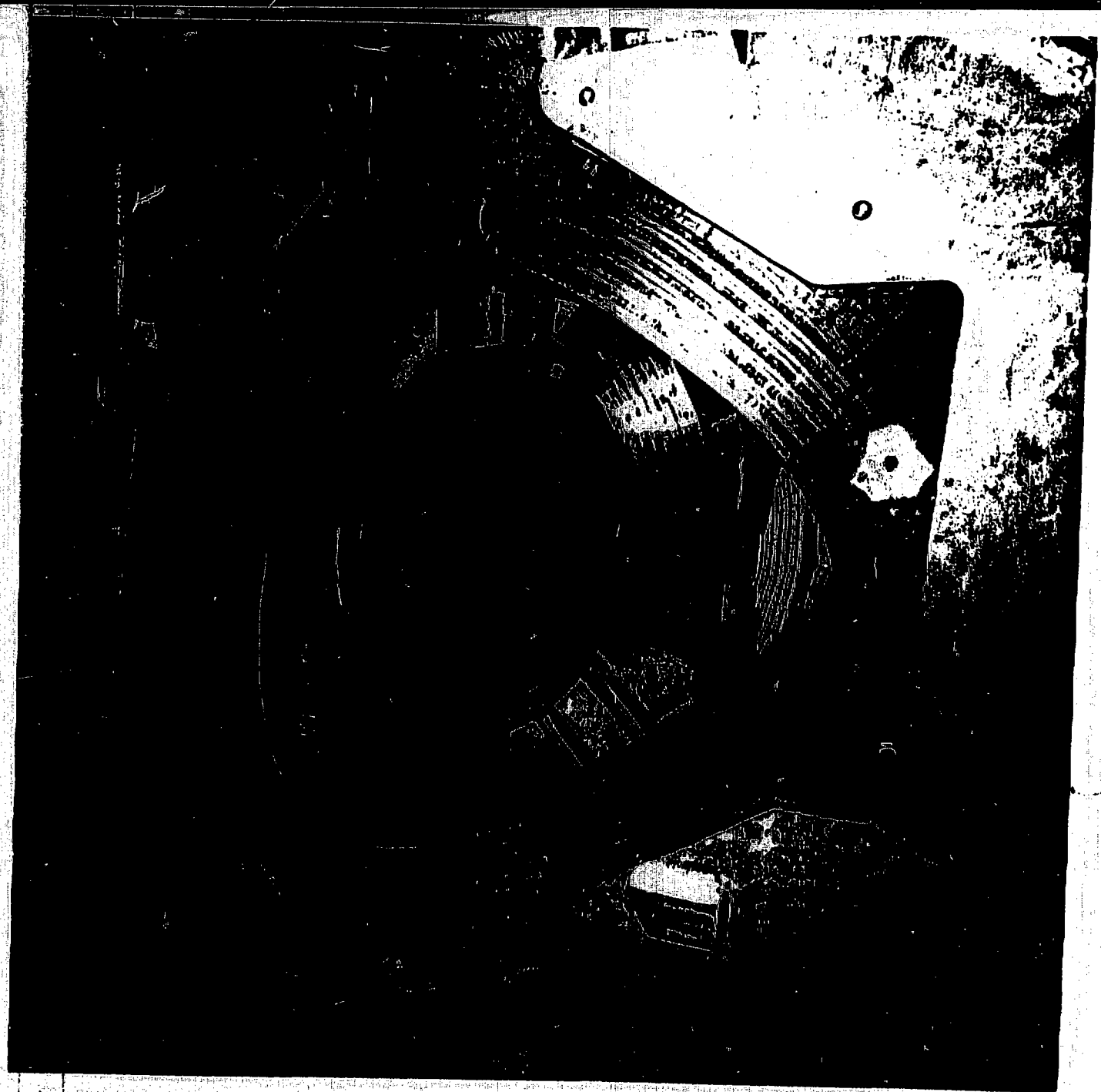

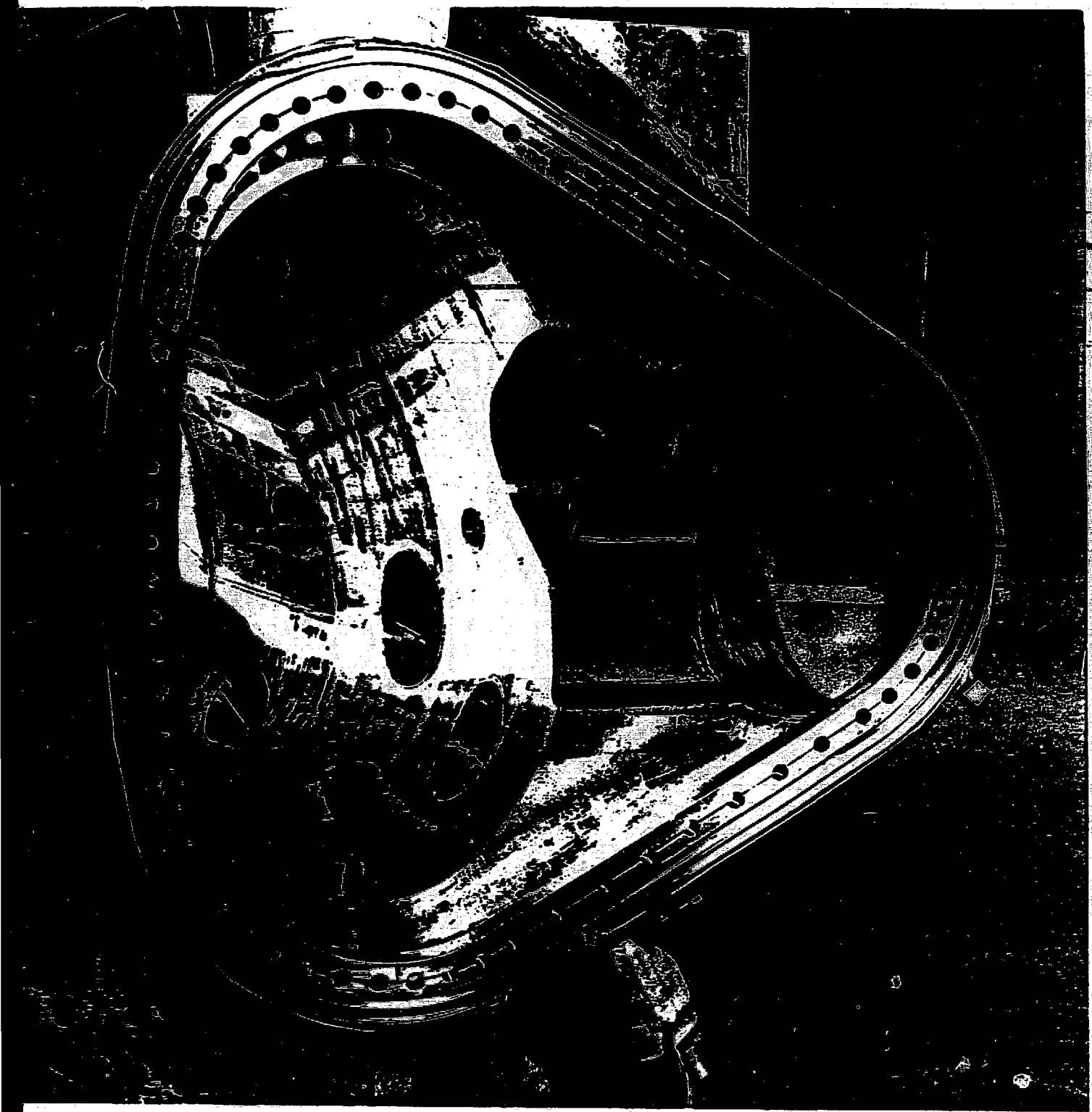

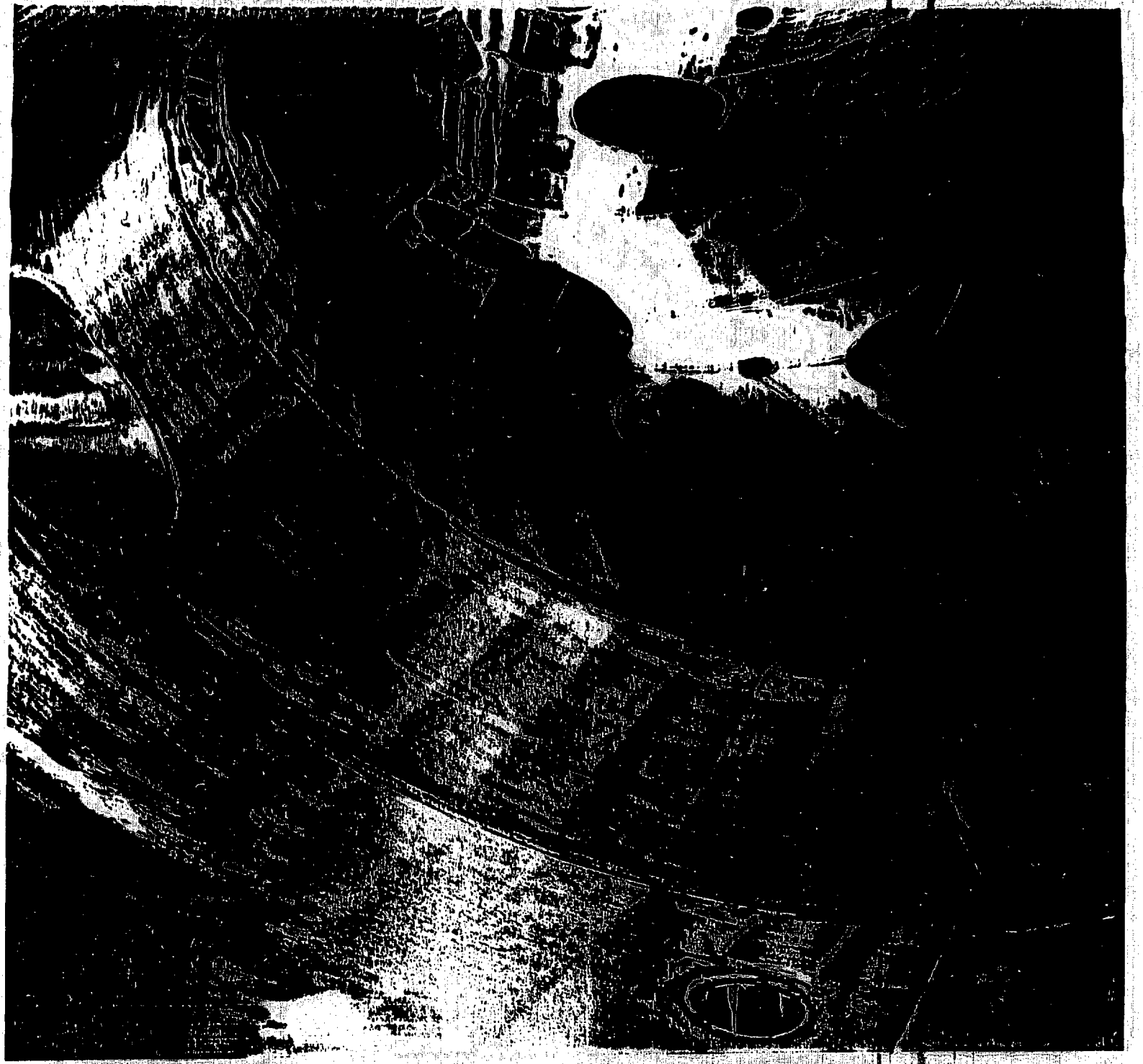

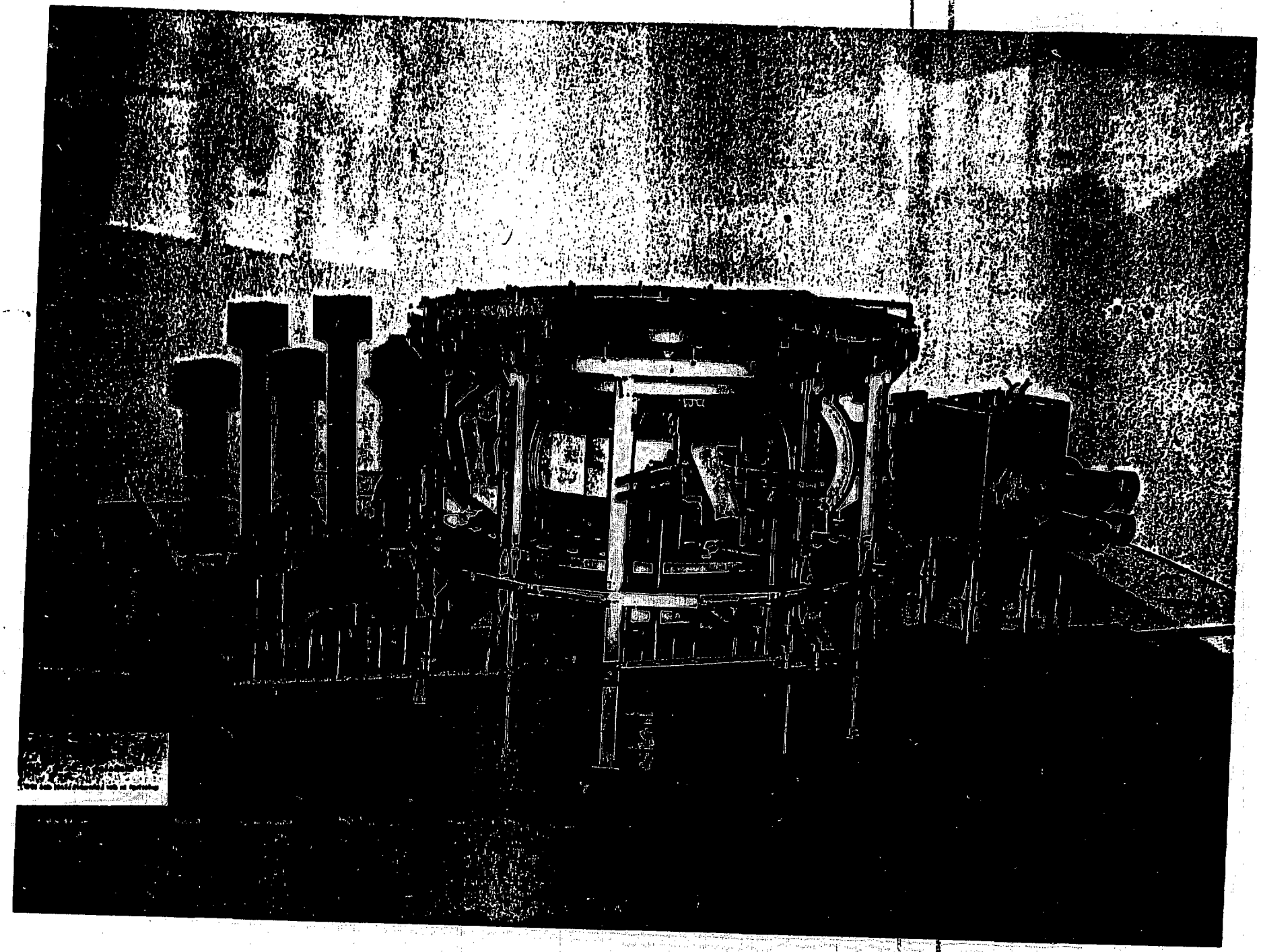

W 7A 1975 -1985	W 7 AS 1987
R = 2.0 m	R = 2.0 m
a = 0.1 m	a = 0.2 m
STELLARATOR	OPTIMIZED MODULAR COIL STELLARATOR
l=2 m=5	m=5
B_{TOR} = 3.5 T	3.0 T
$.1 < \iota < .5$	.39
	.2 – .6 VARIED BY ADDITIONAL $B_{TOR} = \pm 1$ T
$\Delta W_\perp / W_\perp(0) = -3\%$	VARIABEL + 1% – 1.5%
" TOROIDAL RIPPLE $\delta_{B/B} < 10^{-4}$	AXIS $\delta_{B/B} \leq 9 \cdot 10^{-2}$
	LAST SURFACE $\delta_{B/B} \leq 3 \cdot 10^{-1}$
HELICAL RIPPLE $\delta_{B/B} < 3\ 10^{-2}$	

$\beta_{EQU} \sim$	$2\ \beta_{EQU}$
4.5%	2%
$\Delta/R \sim$	$1/2\ \Delta/R$
W 7 AS	W 7A

DH

ECF 28 GHz 1 T 200 kW
70 GHz 2.5 T ω_{ICE}
1.25 T $2\omega_{ICE}$

70 GHz 1 MW , 3 s
140 GHz .2 MW , .1 s

NI 30 kV „ 1 MW „ .2s
60° $\perp B_{TOR}$

45 kV „ 1.5 MW „ 3s
TANGENTIAL „ BALANCED

ICF 30 -- 110 MHz 500 kW

30 – 110 MHz 3 MW 3s

WENDELSTEIN W 7AS
ADVANCED STELLARATOR

MAIN GOALS

DEMONSTRATION OF THE OPTIMIZATION PRINCIPLE FOR A MAGNETIC CONFIGURATION GENERATED BY A SYTEM OF MODULAR COILS.

OPTIMIZATION OF DIFFERENT HEATING SCHEMAS.

ANALYSIS OF TRANSPORT INFLUENCED BY MAGNETIC RIPPLE, RADIAL ELECTRIC FIELDS AND PLASMA CURRENT (bootstrap current).

IMPURITY TRANSPORT AND SOURCES AT LONG PULSE OPERATION.

EQUILIBRIUM AND MHD STABILITY DEPENDING ON THE MAGNETIC CONFIGURATION.

DATA BASE FOR FURTHER DEVELOPMENT OF THE ADVANCED STELLARATOR CONCEPT (W 7X).

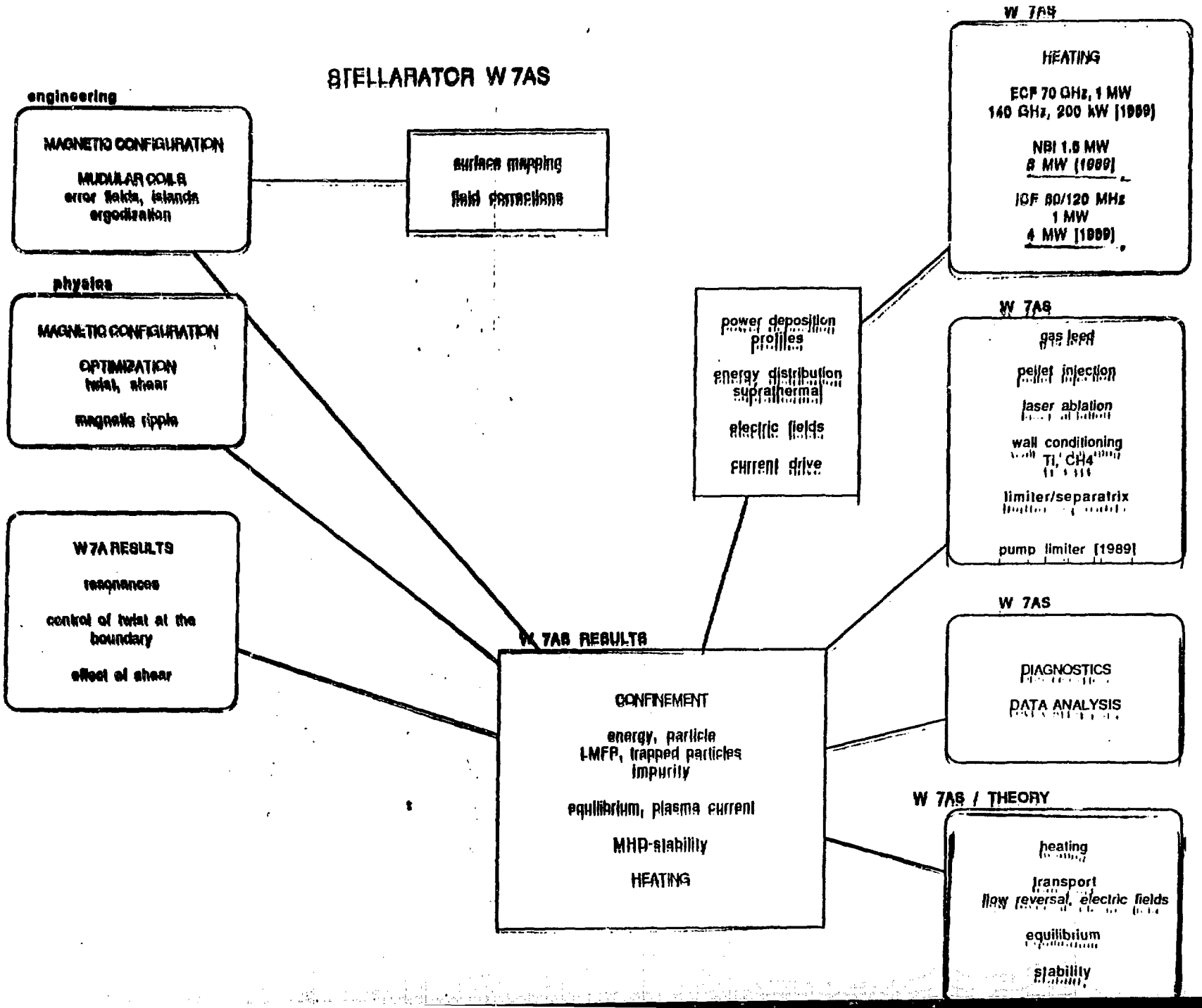
STELLARATOR W 7AS
engineering
MAGNETIC CONFIGURATION
MODULAR COILS
error fields, islands
ergodization
surface mapping
field corrections
physics
MAGNETIC CONFIGURATION
OPTIMIZATION
twist, shear
magnetic ripple
W7A RESULTS
resonances
control of twist at the boundary
effect of shear
power deposition profiles
energy distribution suprathermal
electric fields
current drive
W 7AS
HEATING
ECF 70 GHz, 1 MW
140 GHz, 200 kW [1989]
NBI 1.5 MW
8 MW [1989]
ICF 80/120 MHz
1 MW
4 MW [1989]
W 7AS
gas feed
pellet injection
laser ablation
wall conditioning
Ti, CH4
limiter/separatrix
pump limiter [1989]
W 7AS RESULTS
CONFINEMENT
energy, particle
LMFP, trapped particles
impurity
equilibrium, plasma current
MHD-stability
HEATING
W 7AS
DIAGNOSTICS
DATA ANALYSIS
W 7AS / THEORY
heating
transport
flow reversal, electric fields
equilibrium
stability

W7AS Programme (Heating)

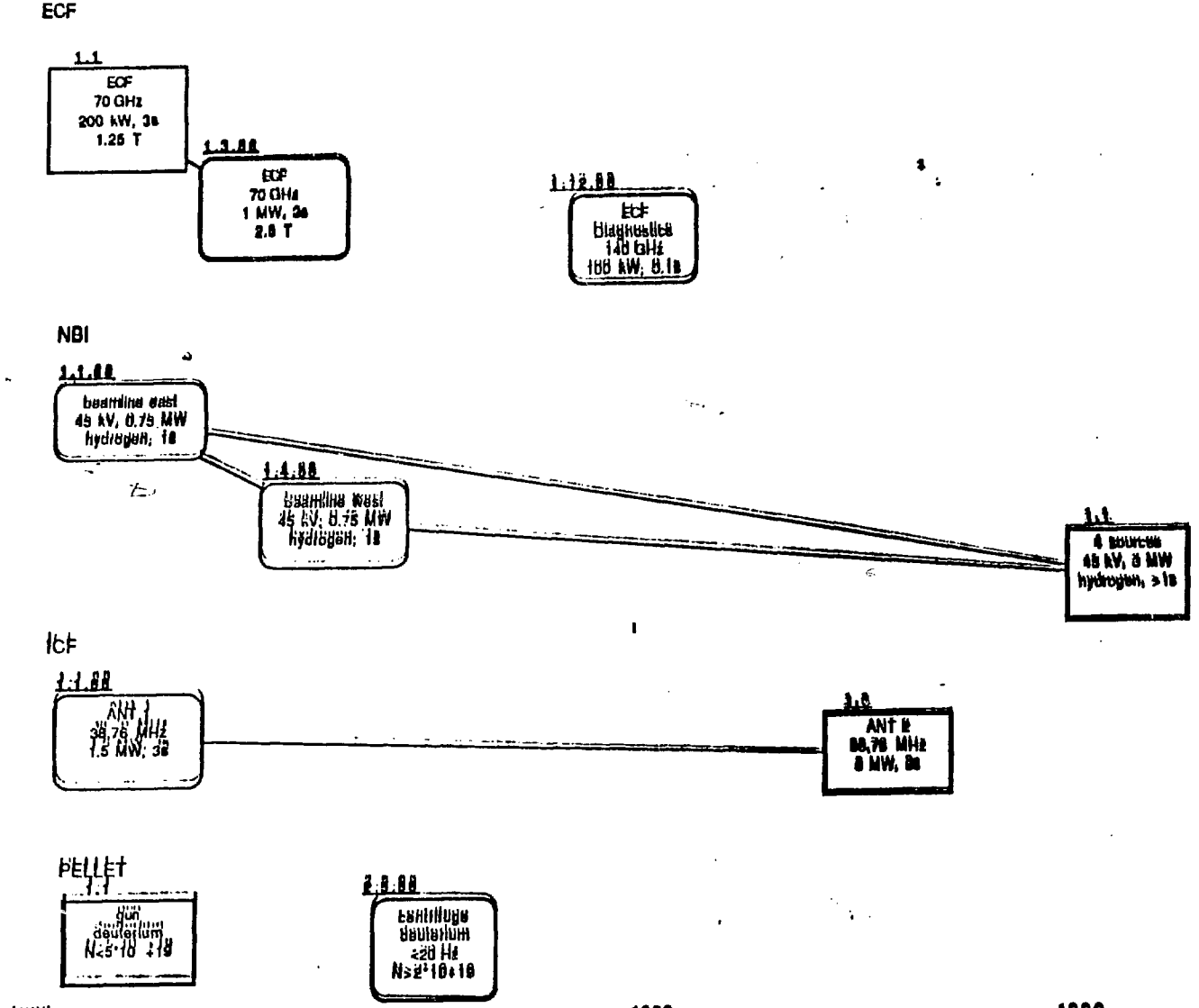

SCHEMATIC OF THE TRANSMISSION LINES

DETAILS MAY BE FOUND E.G. IN
M. THUMM ET AL, PROC. 4TH INT. SYMP. ON HEATING IN TOROIDAL PLASMAS
ROME 1984, VOL. II, P. 1461

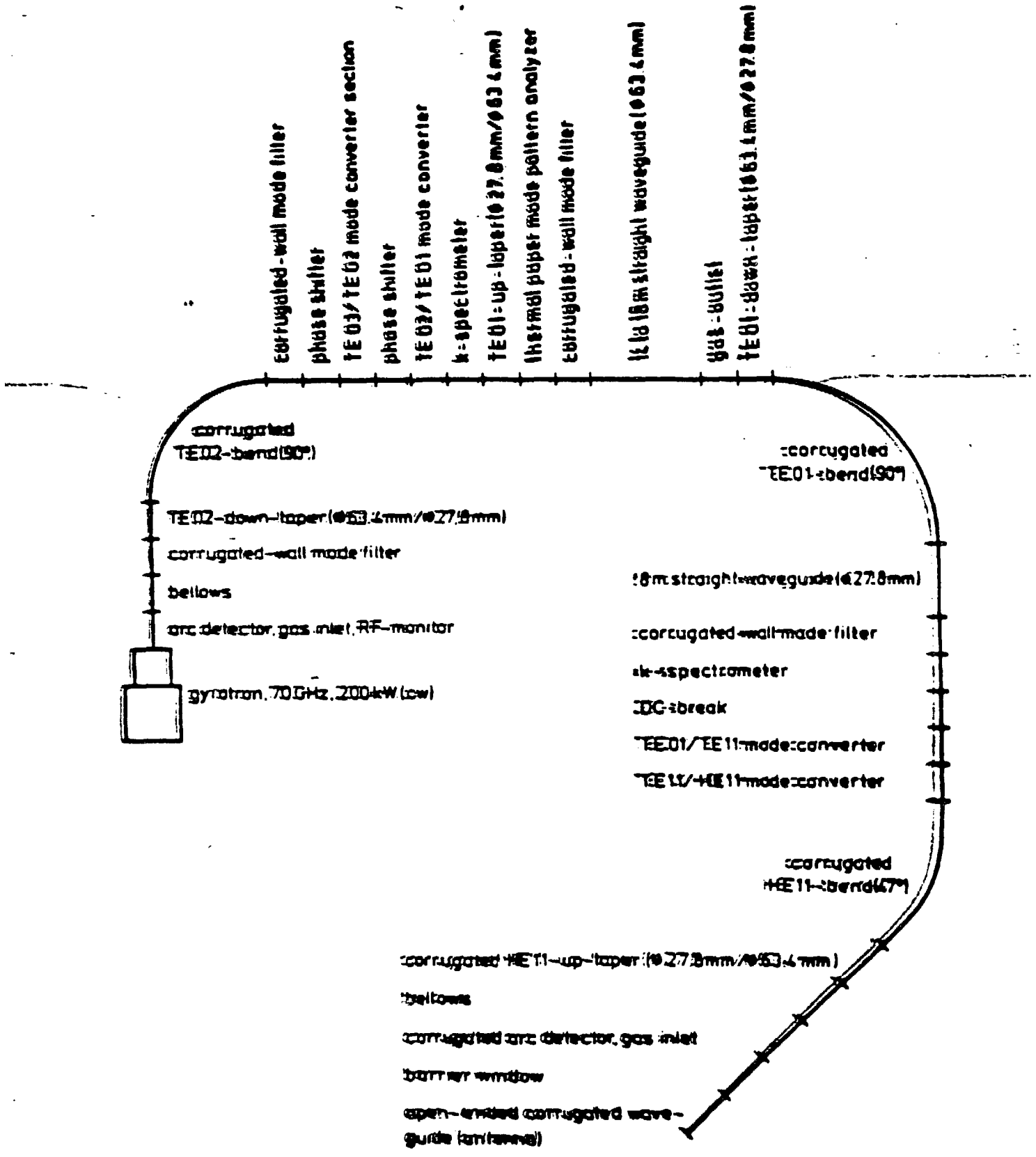

W VII-AS

ECRH launching system

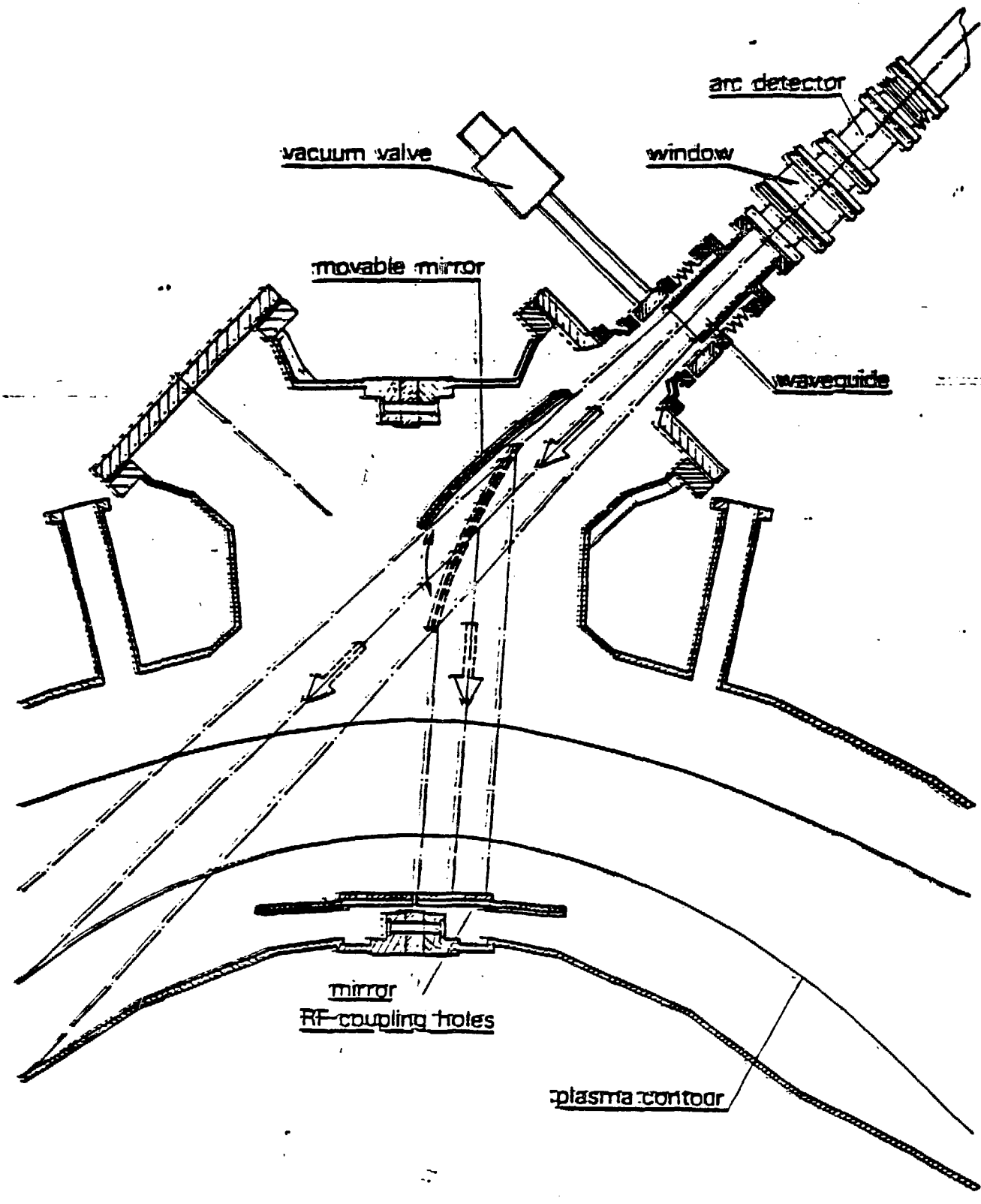

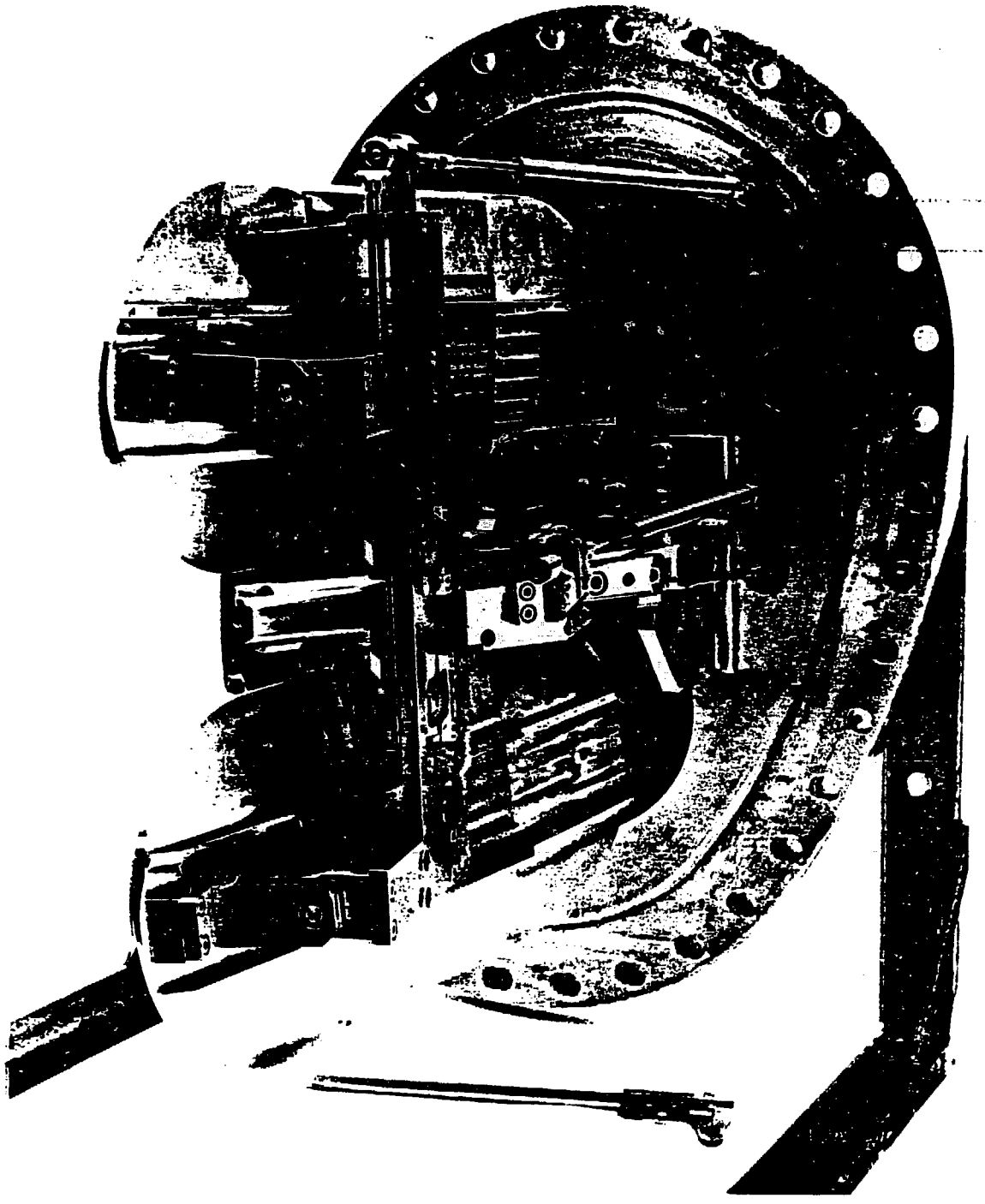

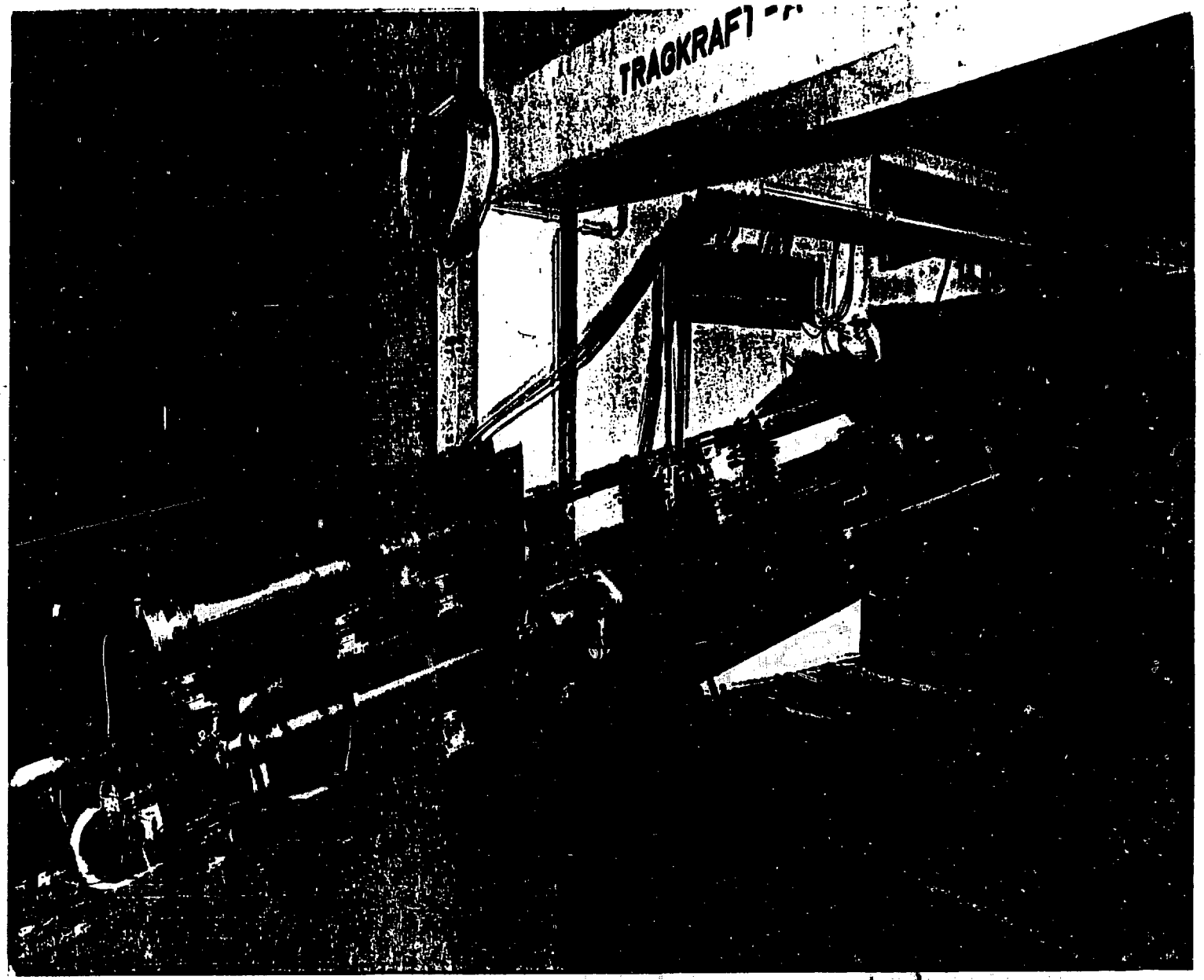
TRAGKRAFT

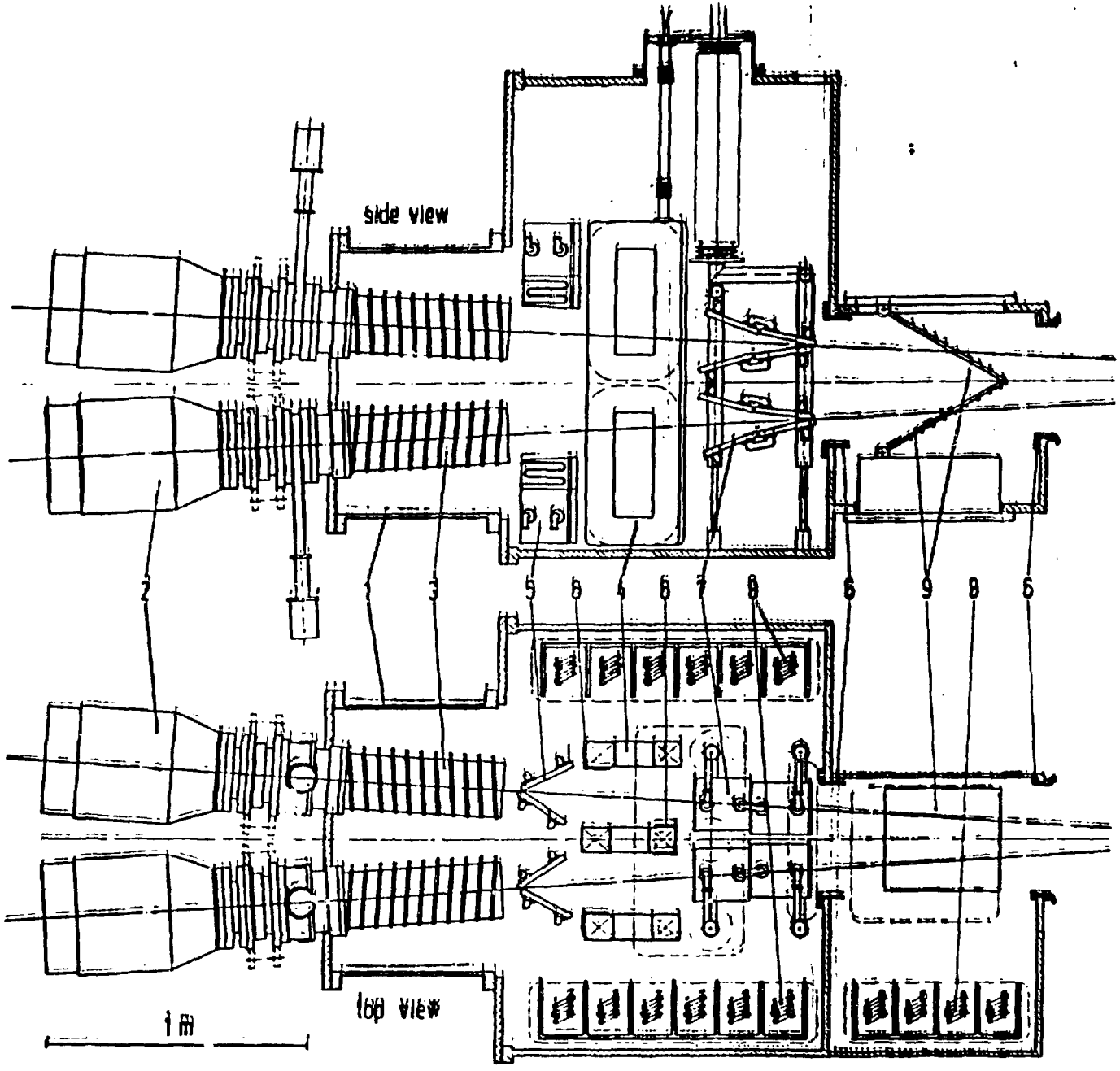

1 Vacuum box
2 Ion source
3 Neutralizer
4 Reflecting magnet
5 Ion dump
6 Scraper
7 Calorimeter
8 Titanium pump
9 Adiabatic calorimeter

up to 4 sources per box

ASDEX / W VII AS
LPNI - BEAMLINE
(3 S)

Injection geometry indicating the projections of the beam paths for the inner and outer sources on the toroidal plane ;
plasma cross sections with the profiles of the penetrating beams of the inner sources (L and L) are given also for five positions .

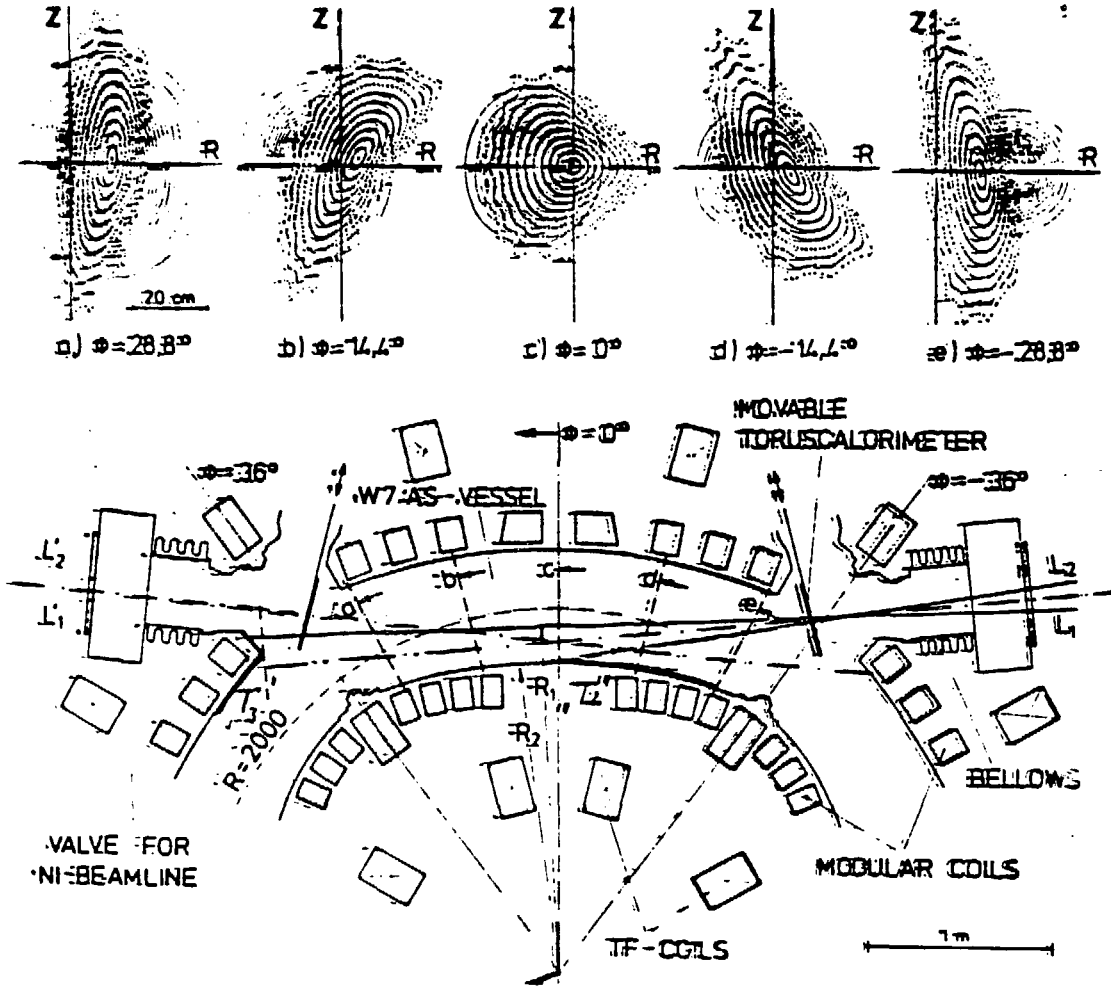

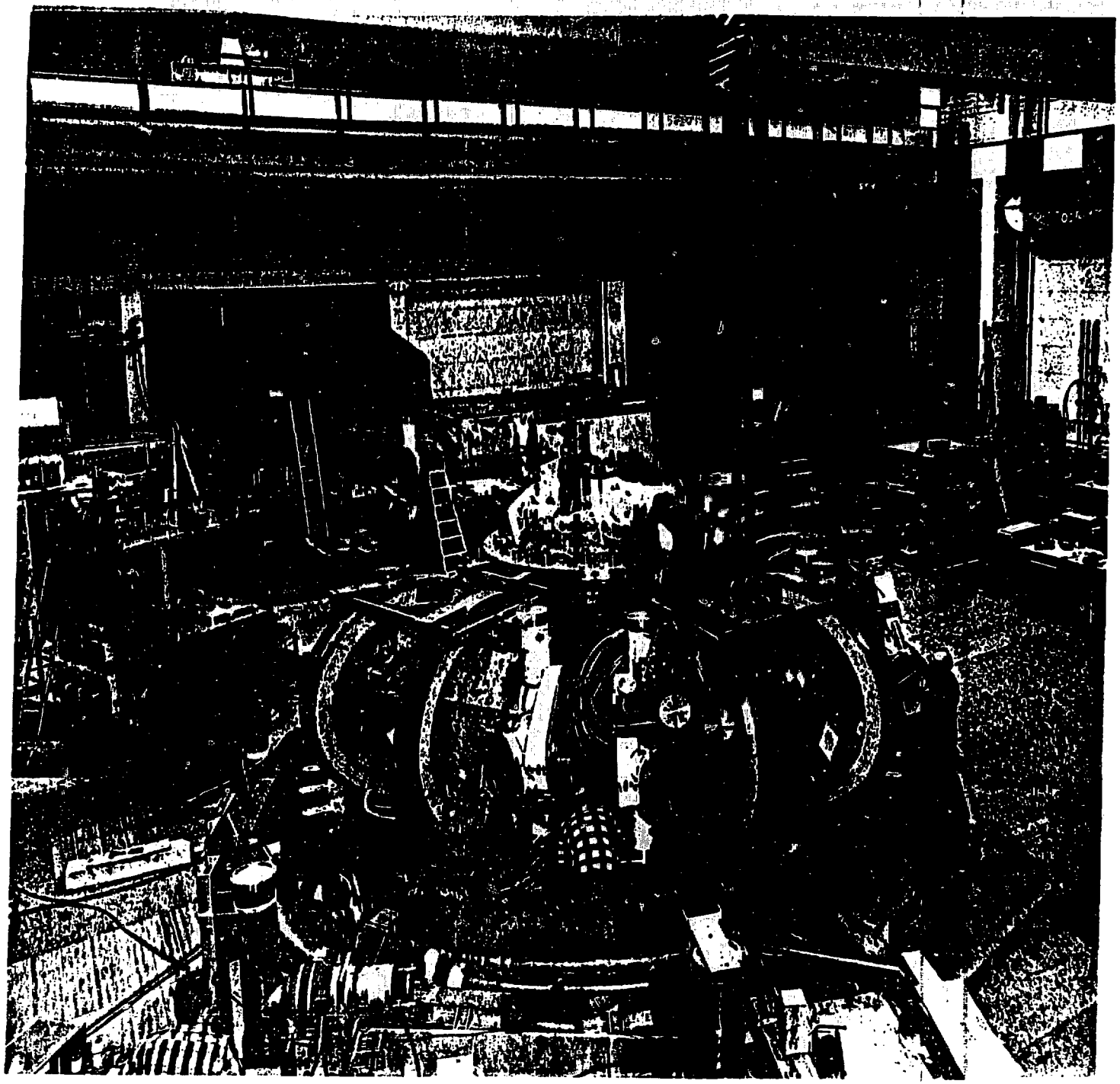

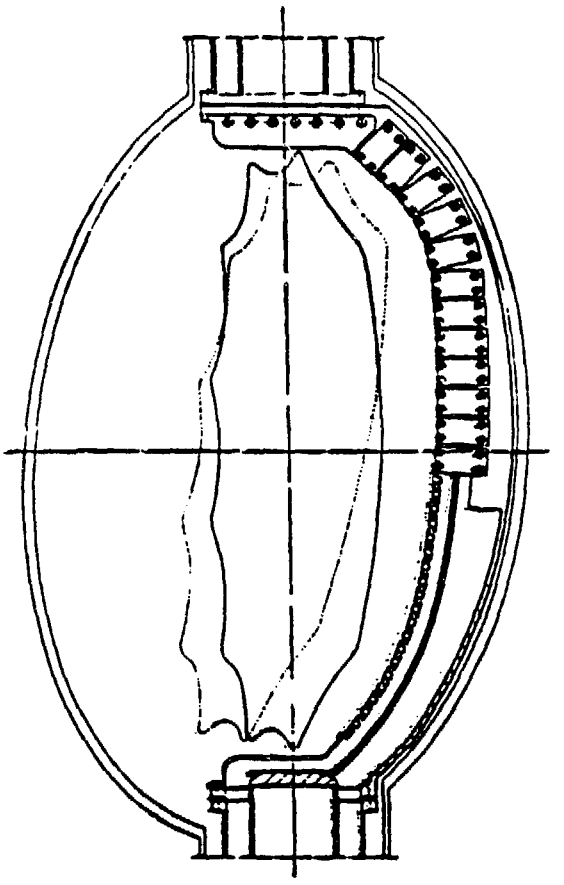

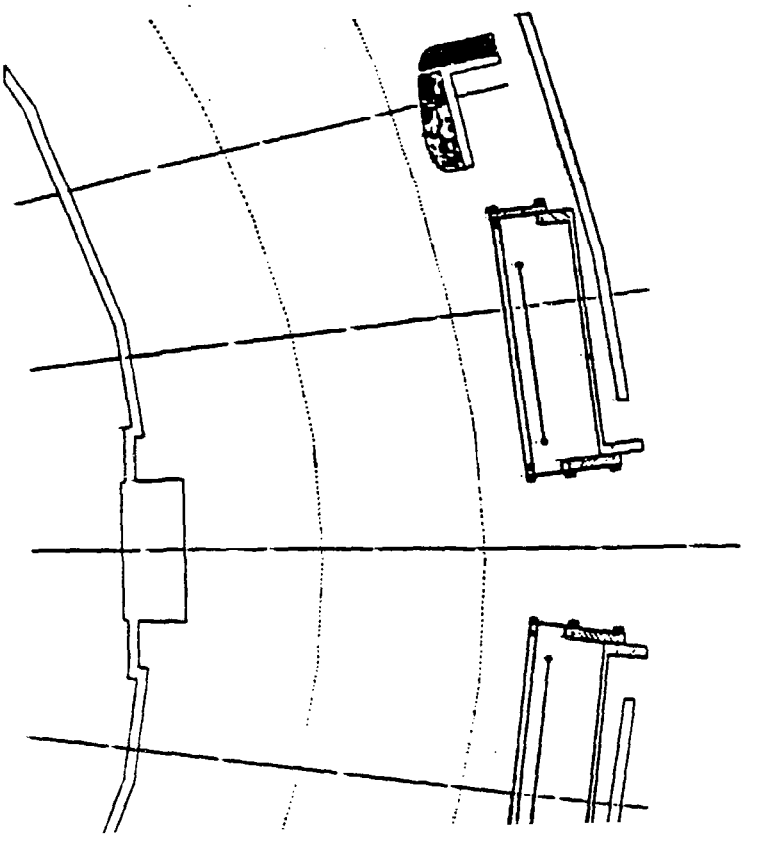

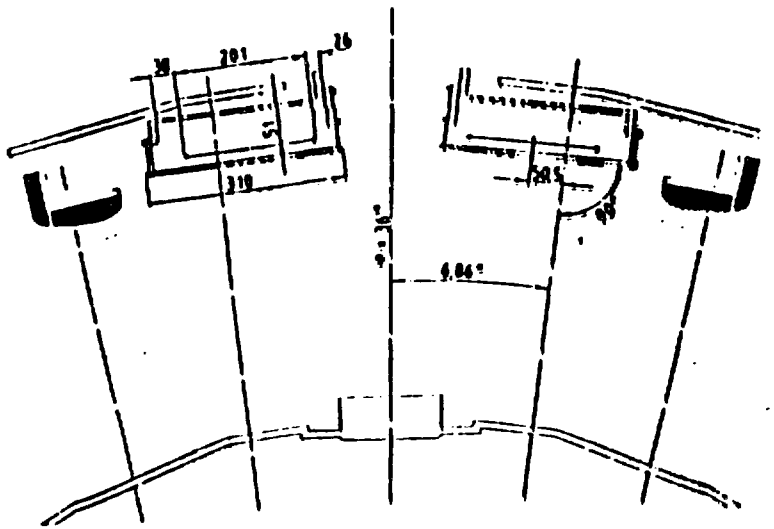

Cut in the z=0 plane
(all dimensions in mm)

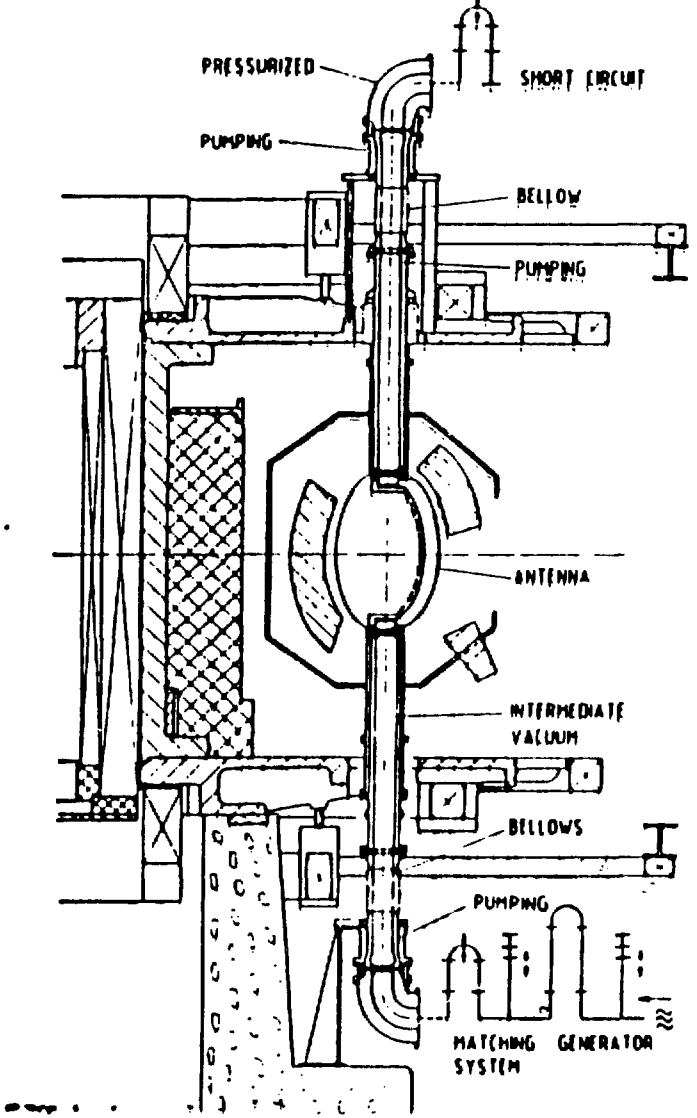

Antenna and interface

WENDELSTEIN VII-AS STELLARATOR

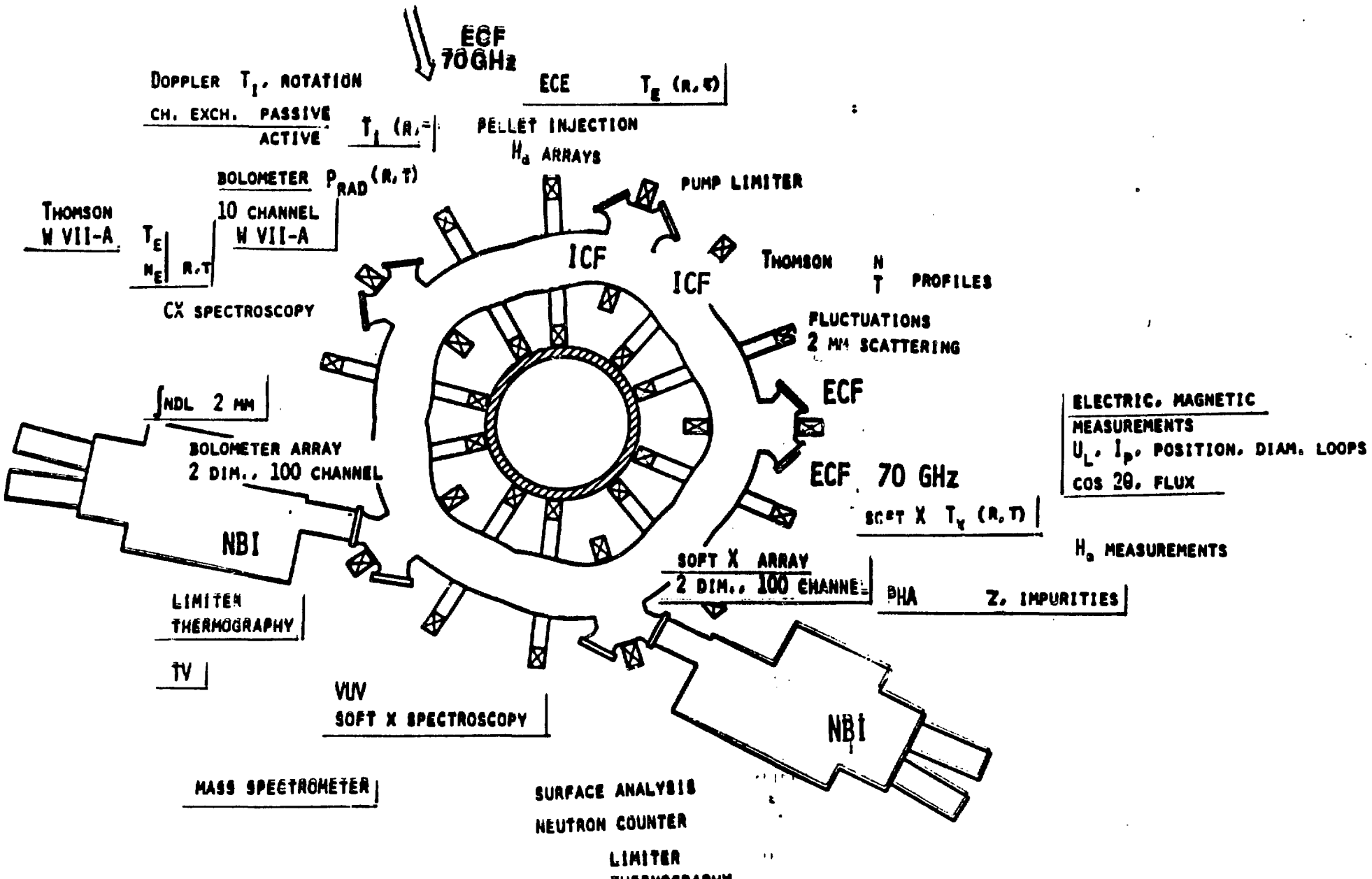

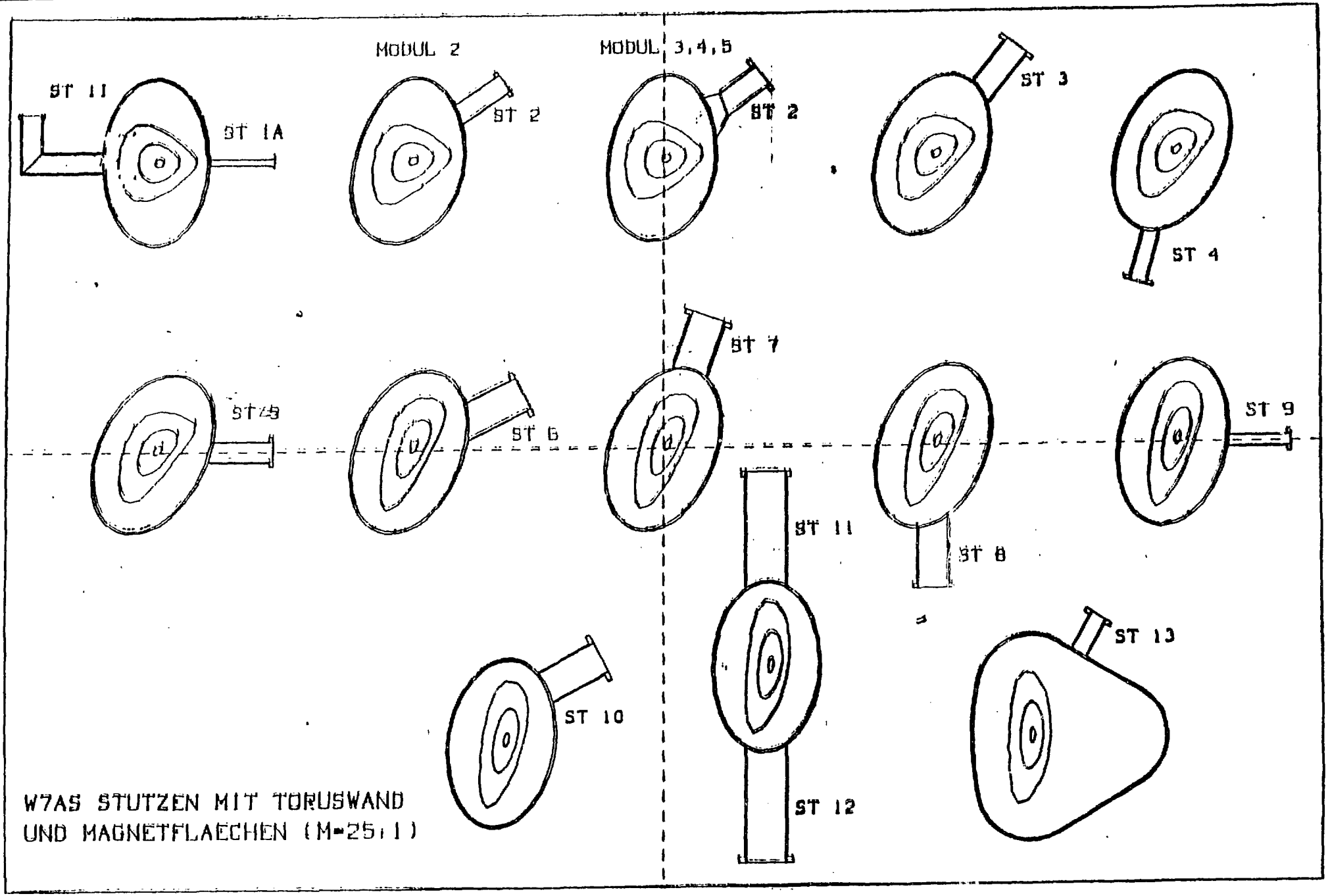

W7AS STUTZEN MIT TORUSWAND
UND MAGNETFLAECHEN (M=25,1)

W 7AS
MEASUREMENTS ON MAGNETIC SURFACES

W7AS-Team, IPF Stuttgart
(Jänicke)

"CLASSICAL METHOD"
movable electron gun
movable probe

FLUORESCENT METHOD
movable electron gun
swinging fluorescent rod

~ CCD camera with light amplifier ($< 10^{-4}$ Lux)

video tape recorder

image prozessor/screen

(expected time needed for measurement 10 sec)

MAIN GOALS

*measurements of rotational transform
with varied currents of the magnets for comparison with code calculations
B_0= 0.2-0.3 T (operational field B_0= 2.5-3T)

vertical field
OH stray field

**magnetic axis

**island formation at transform = 1/3, 1/2, 2/5.
ergodization at the boundary

**field corrections by superimposed fields or alignment of magnets

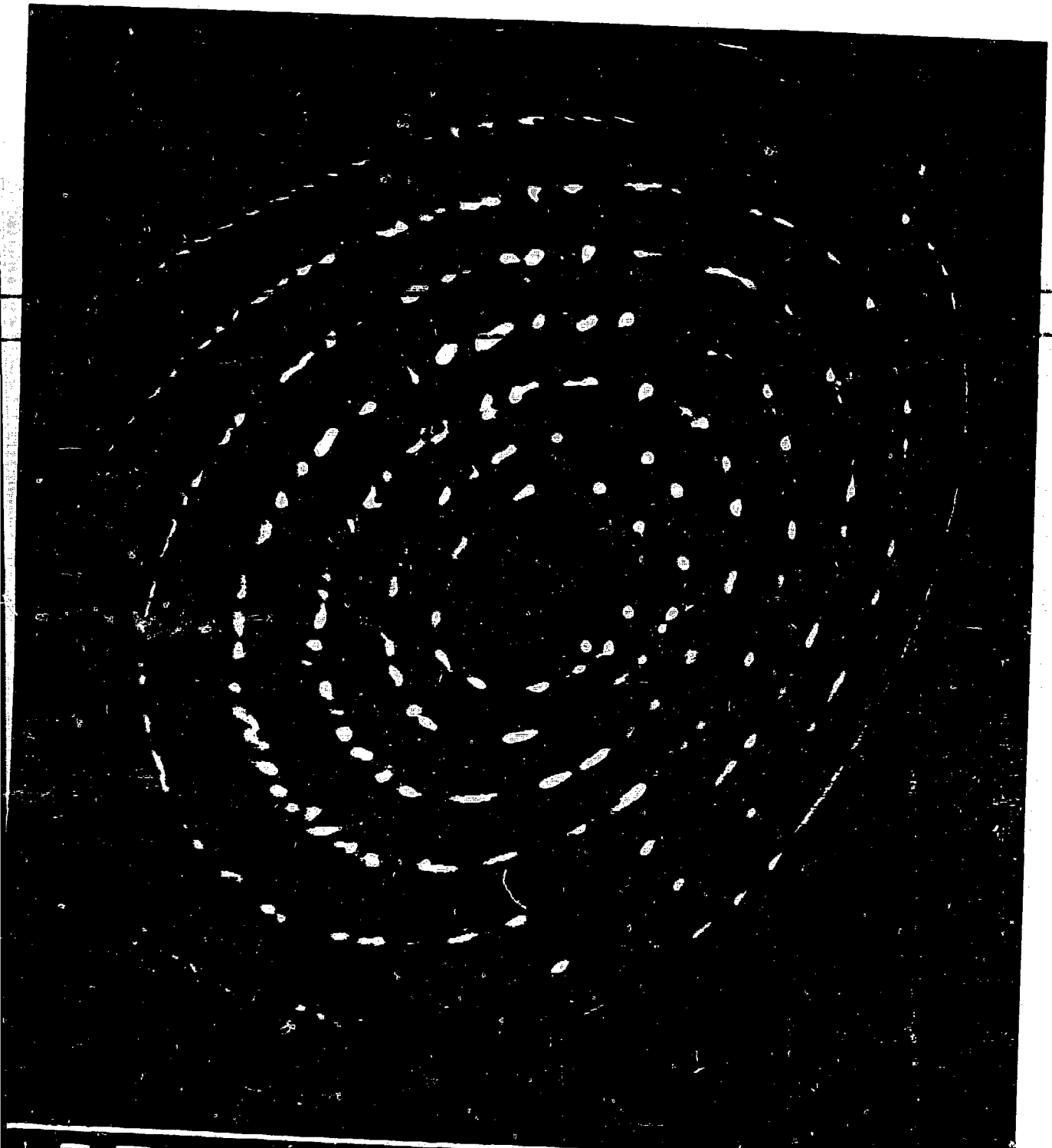

IPF

Institut für Plasmaforschung Stuttgart

WEGA

Electron Drift Surfaces

I_t = 401,7 A, I_h = 459,1A, U = 60V

Date: 4. 3. 87 , Pict. No.: 7.3

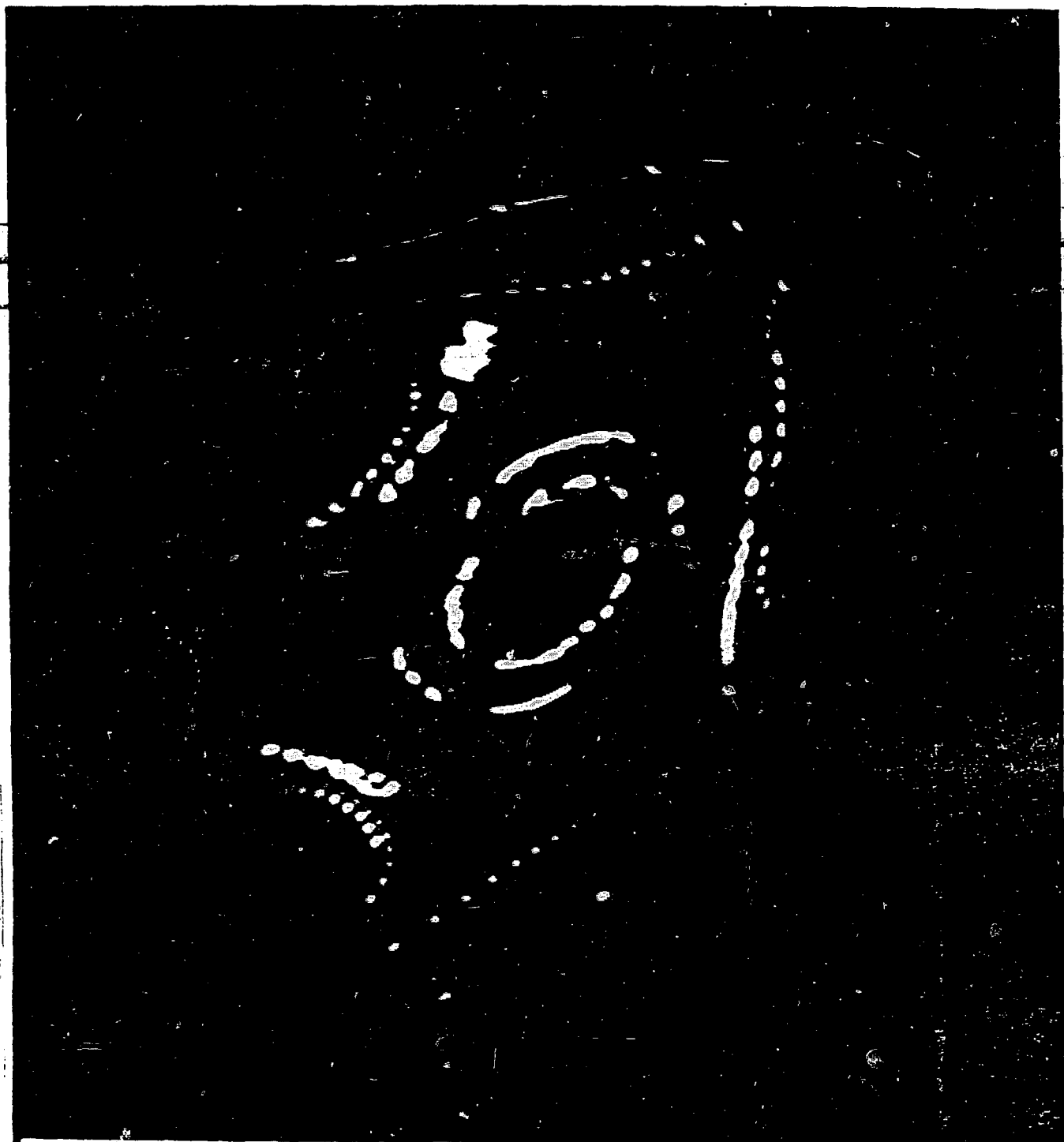

IPF
Institut für
Plasmaforschung
Stuttgart

WEGA
Electron Drift Surfaces
I_v = 245,1A, I_h = 459,1A, U=60V
Date: 6.3.87, Pict. No.: F 6.1

displacement

$\Delta r \approx 1.5$ mm
toroidal field/
vertical field system

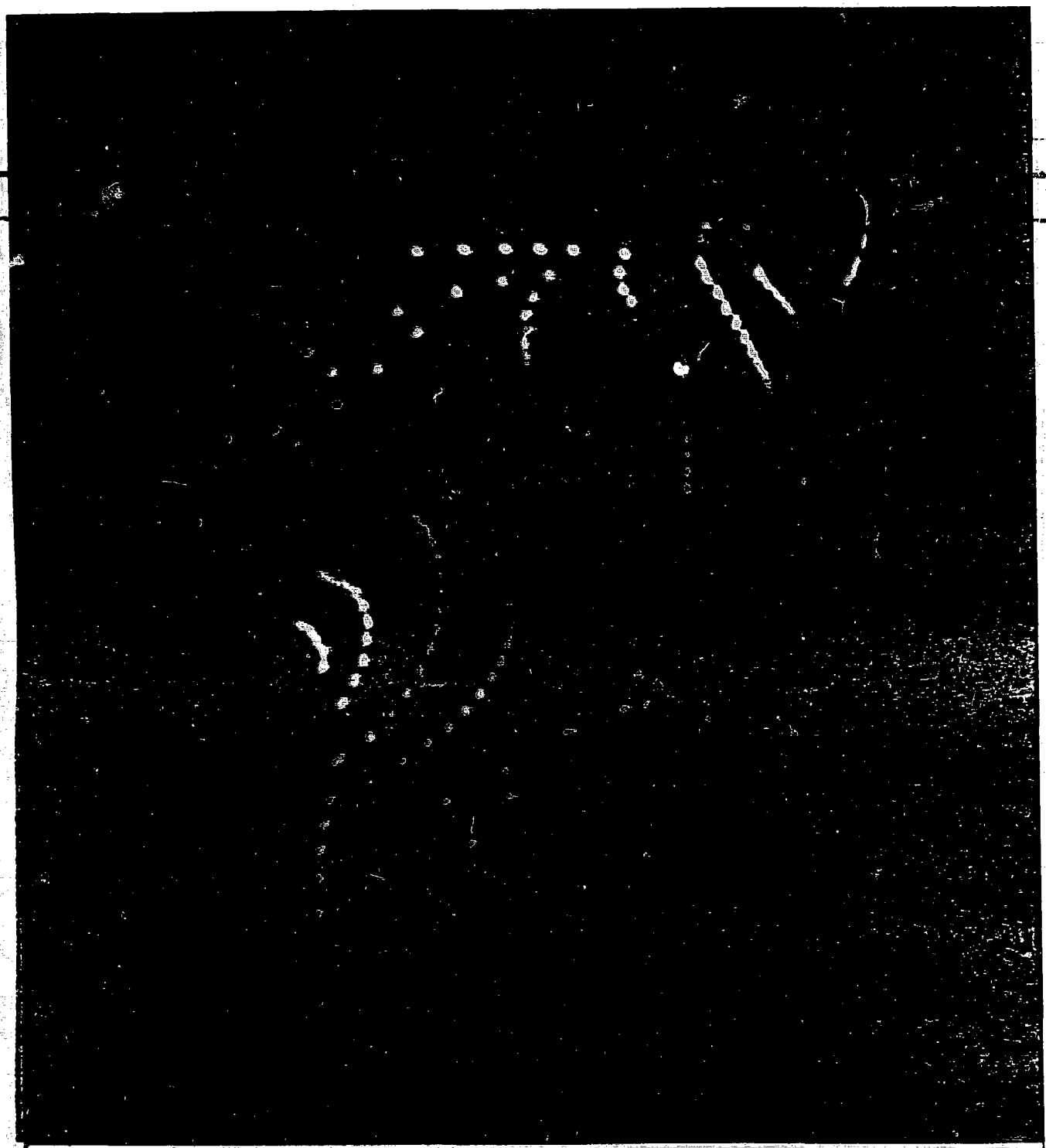

W E G A

Institut für Plasmaforschung Stuttgart

Electron Drift Surfaces
$\varepsilon = 1/2$, $I_v = 404.5$ A, $I_h = 919.0$ A, $U = 60$ V
Date: 30.3.87 Pict. No.: 107

W7AS Programme (Physics)

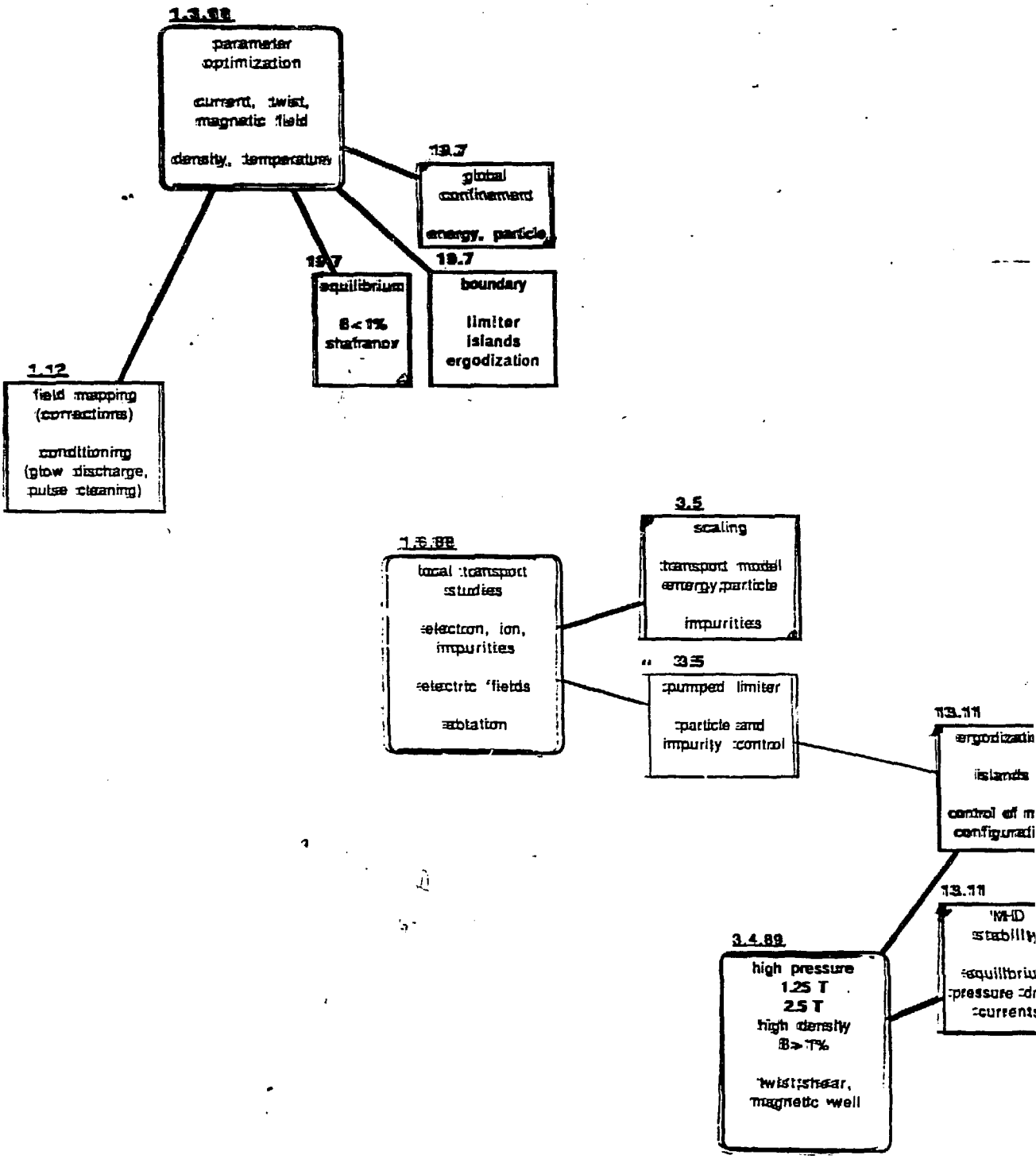

TJ-II PROGRAM

STATUS

A. P. NAVARRO
Asociación EURATOM/CIEMAT para FUSION
28040 Madrid, SPAIN

U.S.-JAPAN STELLARATOR/HELIOTRON WORKSHOP

OAK RIDGE, NOVEMBER 1987

TJ-II PROGRAM STATUS

INDEX

CONTRIBUTIONS

- **ASOCIACION EURATOM/CIEMAT**

  - **THEORY SECTION**

    C. ALEJALDRE
    F. CASTEJON
    J. GUASP
    A. L. FRAGUAS
    A. VARIAS

  - **EXPERIMENTAL SECTION**

    E. ANABITARTE
    E. ASCASIBAR
    S. CLEMENT
    B. GARCIA
    C. HIDALGO
    F. S. MOMPEAN
    M. A. OCHANDO
    C. PARDO
    M. A. PEDROSA
    A. P. NAVARRO
    L. RODRIGUEZ
    J. SANCHEZ
    F. L. TABARES
    J. VEGA
    B. ZURRO

  - **ENGINEERING SECTION**

    J. ALONSO
    J. BOTIJA
    J. R. CEPERO
    R. MARTIN
    A. PEREA
    M. SOROLLA

- ATF DESIGN TEAM

- WVII-A GROUP

TJ-II EXPERIMENT

TJ-II IS A MODERATE SIZE FLEXIBLE HELIAC DEVICE, PLANNED TO BE THE FOCAL POINT OF SPAIN FUSION RESEARCH PROGRAMME.

GOAL

STUDY HELICAL AXIS STELLARATOR PROPERTIES IN A WIDE RANGE OF CONFIGURATIONS.

TASKS

- ACCESS TO THE DIFFERENT EQUILIBRIUM ι WINDOWS.
- EFFECTS ON STABILITY FROM MAGNETIC WELLS AND (MODERATE) SHEAR.
- ELECTRON HEAT CONDUCTION AND IMPURITY BEHAVIOUR IN THE LONG MEAN FREE PATH.
- EFFECTS DUE TO FINITE β AND β LIMITS.

TJ-II PARAMETERS

NUMBER OF FIELD PERIODS	$M = 4$
MAJOR RADIUS	$R_0 = 1.5$ m
TOROIDAL FIELD	$B_T = 1$ T
TF COIL RADIUS	$r_c = 0.4$ m
TF COIL SWING	$r_{sw} = 0.28$ m
NUMBER OF TF COILS	$N = 32$
MAXIMUM TF CURRENT	$I_T = 260$ kA
l = 1 HELICAL COIL SWING	$r_{hc} = 0.07$ m
MAXIMUM HARD CORE CURRENTS	I_c , $I_{hc} = 300$ kA
MAXIMUM VT CURRENT	$I_v = 100$ kA
$\iota(0)$	0.64 →2.5
$< a_p >$	0.10 → .23 m
MAGNETIC WELL	2 % → 6 %
SHEAR	- 1 % → + 15 %

TJ-II COIL STRUCTURE

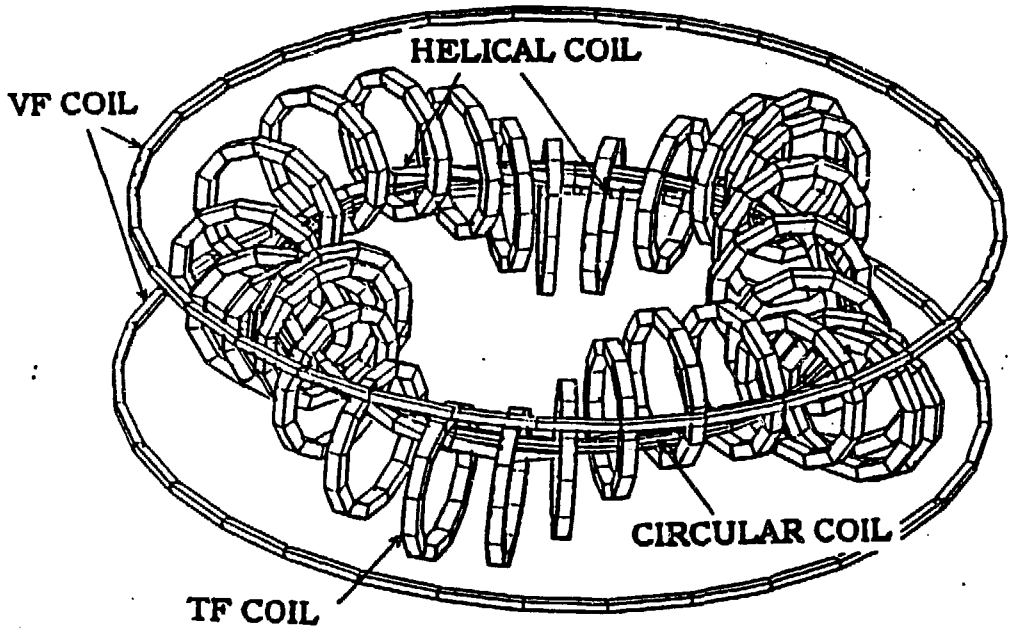

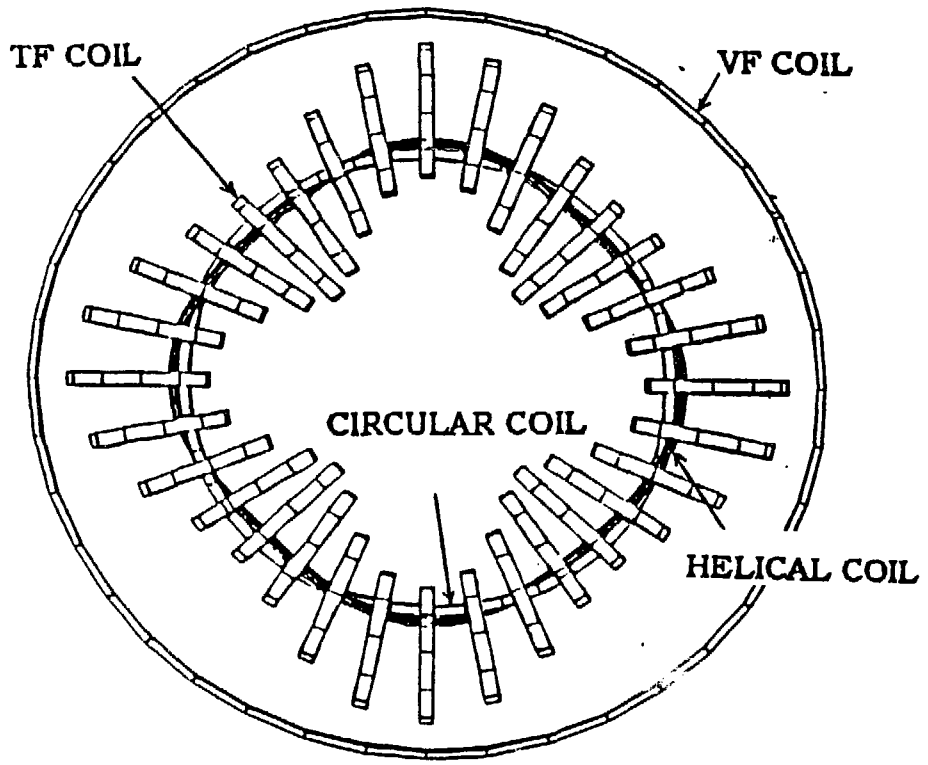

(UPPER VIEW)

MAGNETIC SURFACE SHAPE

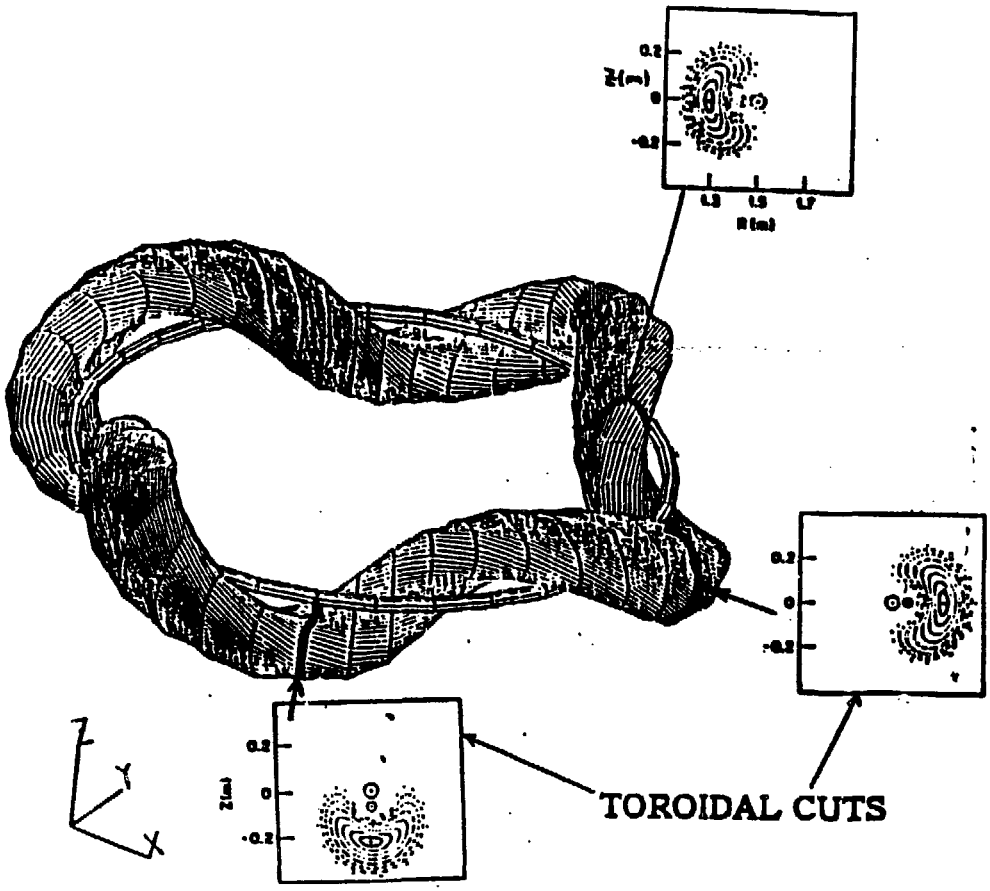

MAGNETIC SURFACE SHAPE

(TOP VIEW)

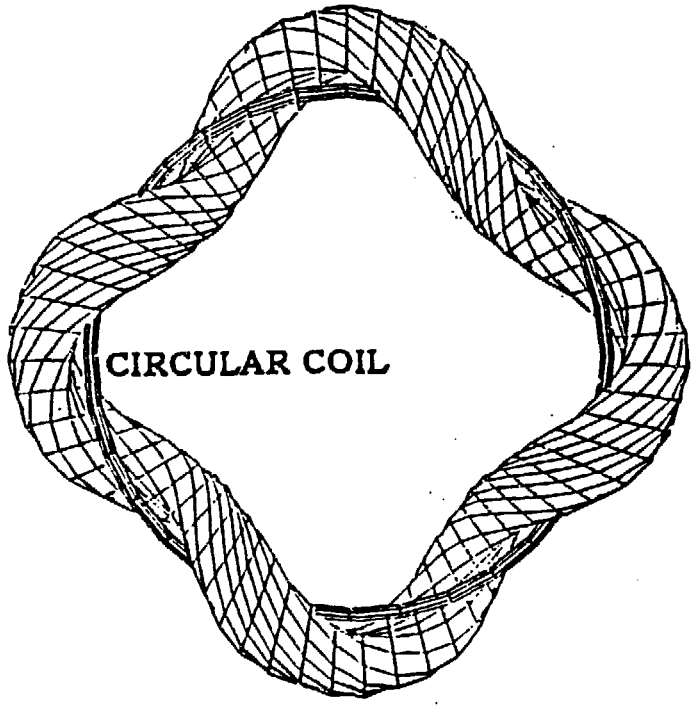

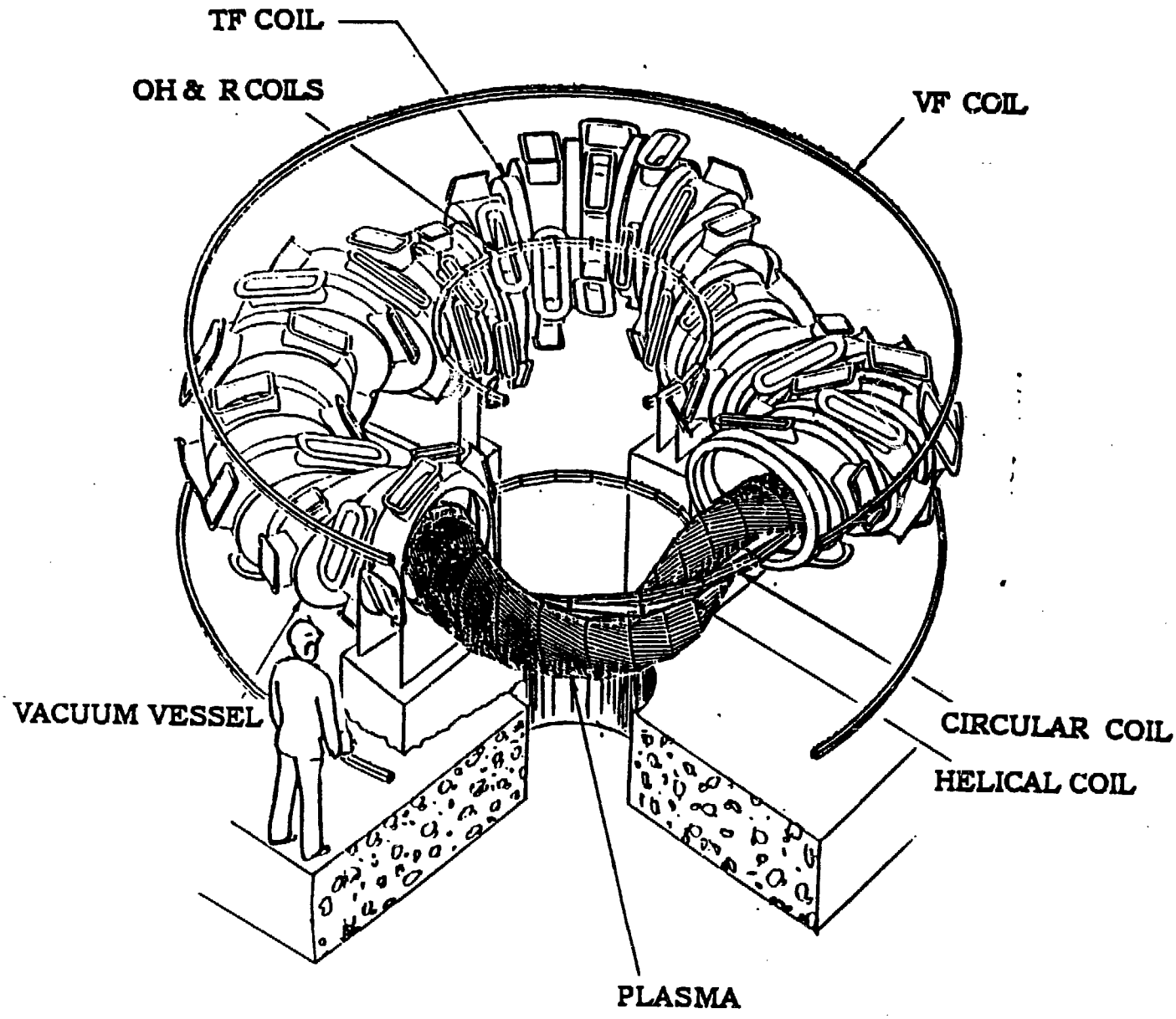

TJ-II EXPERIMENT

• TJ-II CHARACTERISTICS ARE IN THE RANGE OF THE PRINCIPAL NEAR-TERM STELLARATORS

Name	Hel-E	W7AS	ATF	L-2M	U-2M	CHS	H-1	TJ-II
Location	Kyoto	Garching	Oak Ridge	Moscow	Kharkov	Nagoya	Canberra	Madrid
Type	$\ell = 2$ tors.	mod. stell.	$\ell = 2$ tors.	$\ell = 2$ tors.	$\ell = 2$ tors.	$\ell = 2$ tors.	heliac	heliac
R(m)	2.2	2.0	2.1	1.1	1.7	1.0	1.0	1.5
$\tilde{a}$(m)	0.2	0.2	0.3	0.19	0.22	0.2	0.2	0.22
B(T)	2.0	3.0	2.0	2.5	2.4	1.5	1.0	1.0
W_m(MJ)	2.8	5.7	5.9	2.0	3.7	0.71	0.31	0.57
Pulse(s)	<1	3	5-∞	1			1	0.5
Power(MW)	8	5.5	4.5	3.3	7	2	0.2	0.4
Operate	1980	1987	1987	1989	1989	1988	1988	1990

Equilibrium and Stability

- HERA MHD Code
  - Modified for TJ-II
  - Straight (Helically symmetric) Model (✓)
  - Toroidal effects (Under development)

- Stability of local modes
  - Configuration studies(✓)
  - Precise determination of plasma boundary (Magnetic surface inside but close to plasma boundary)(✓)
  - Improvement for the very indented case
  - Equilibrium for chosen configurations (UD)

- Development of a 2-D MHD code
  - Based on Hender & Carreras,*Phys.Fluids* **27** (1984), 2101
  - Invert directly Grad-Shafranov equation

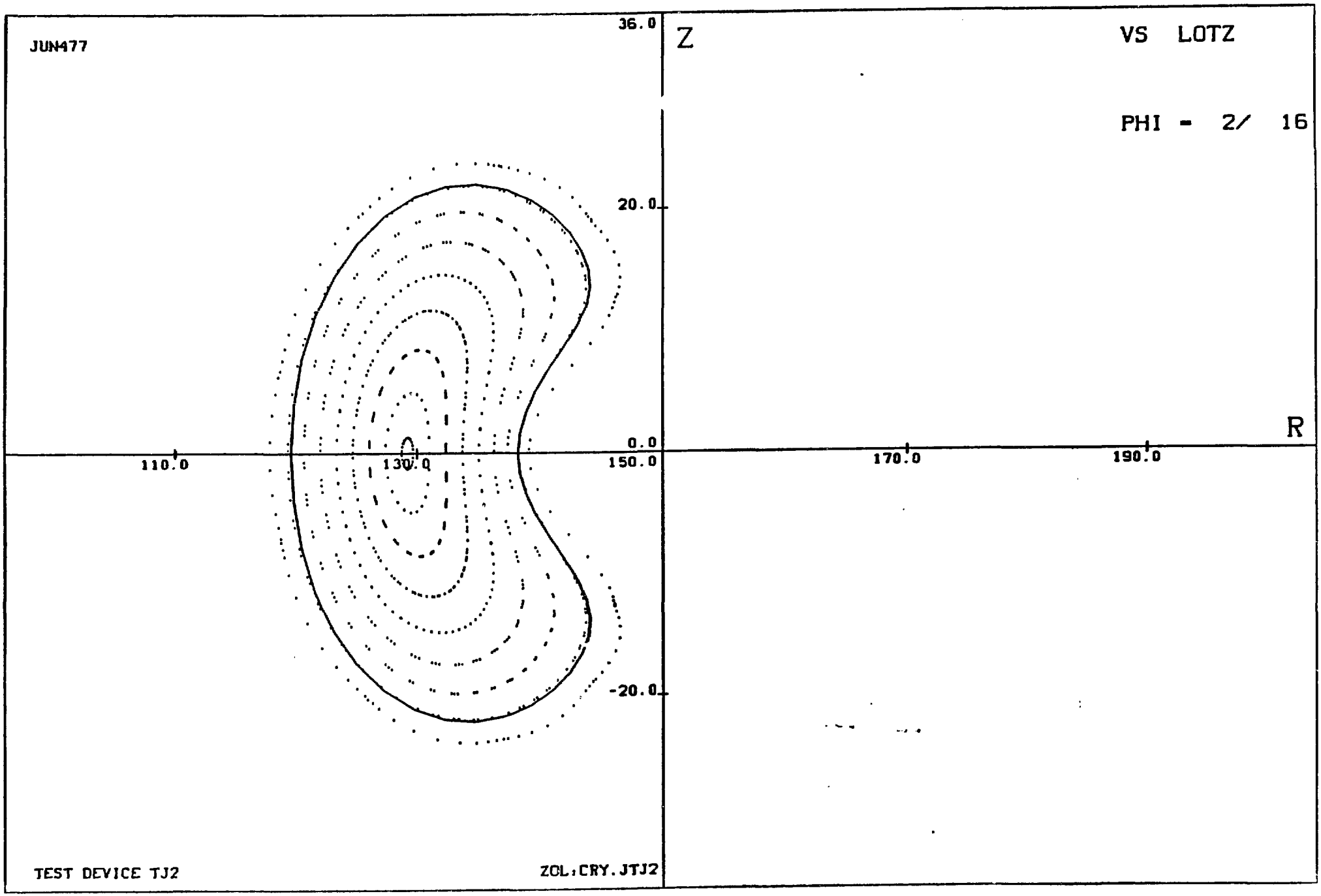
JUN477
36.0
Z
VS LOTZ
PHI = 2/ 16
20.0
0.0
R
110.0
130.0
150.0
170.0
190.0
-20.0
TEST DEVICE TJ2
ZOL:CRY.JTJ2

IPP-CRAY JUN477 2 N2-07 05.05.87 15:32:23

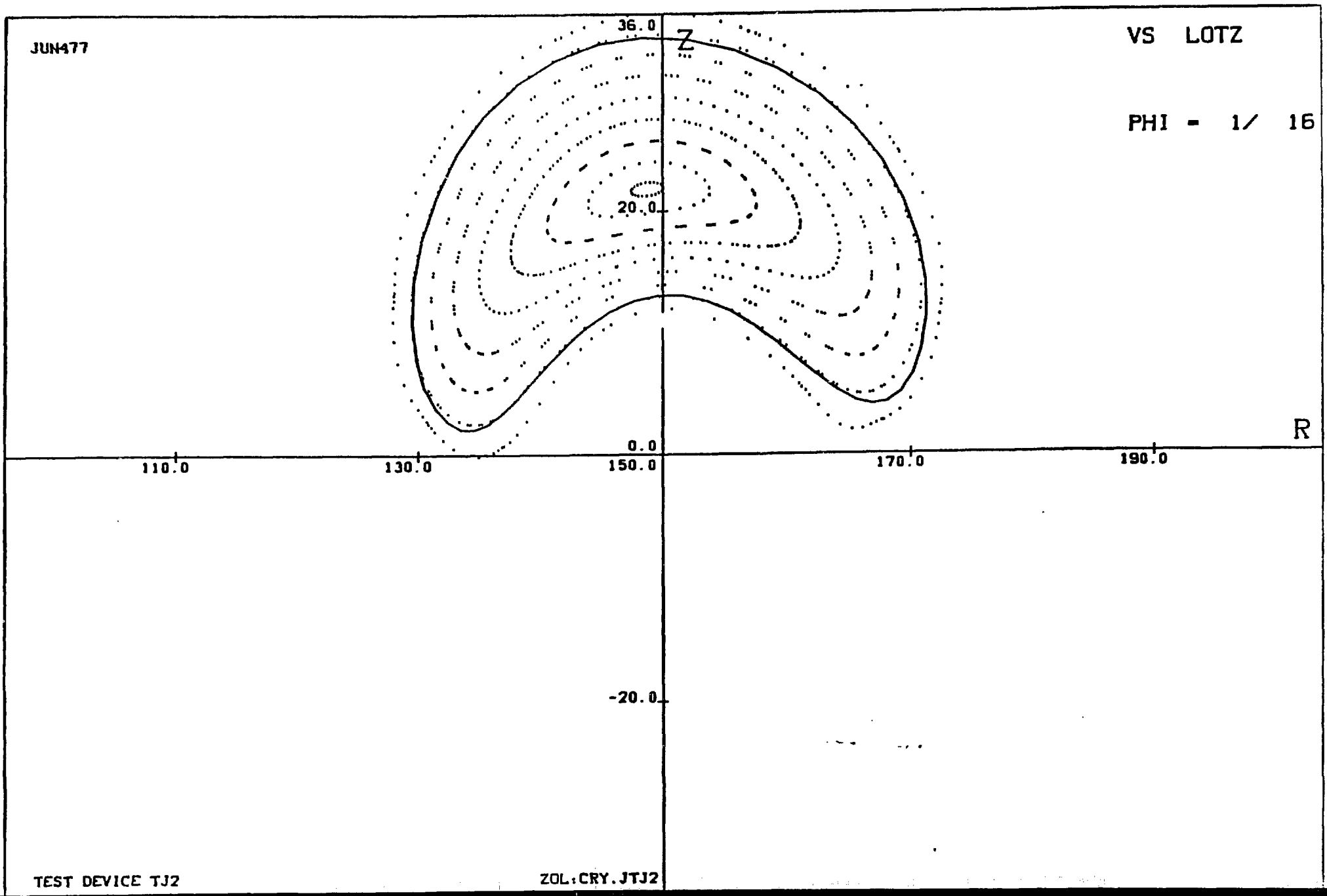

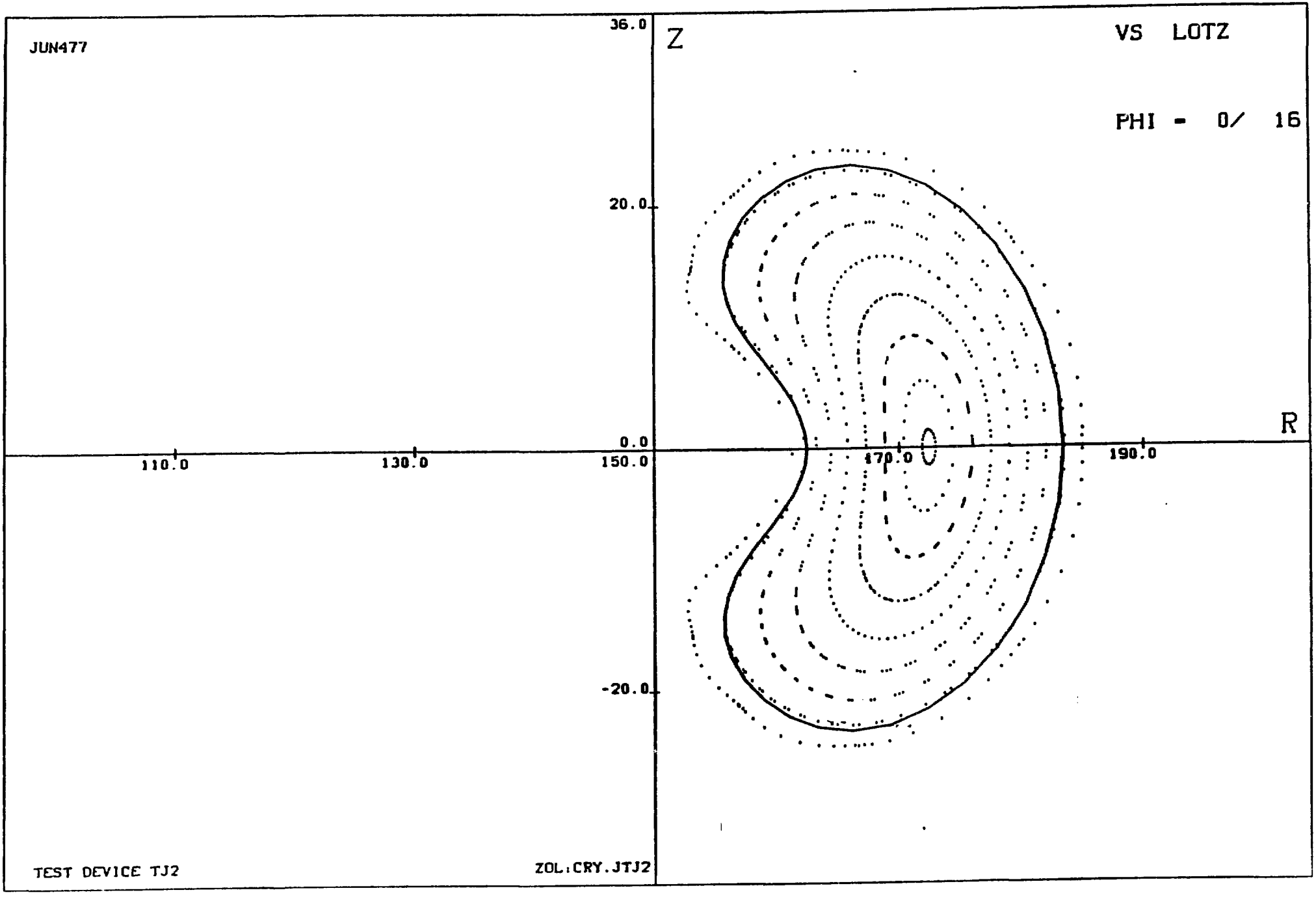
JUN477
Z
VS LOTZ
PHI = 0/ 16
R
36.0
20.0
0.0
-20.0
110.0
130.0
150.0
170.0
190.0
TEST DEVICE TJ2
ZOL:CRY.JTJ2

MHD Stability for a Topological TJ–II

- The equilibria are calculated with the MOMCON fixed–boundary 3D code, taking a large number of helical periods. From vacuum field calculations aproximating TJ–II configurations we get the plasma boundary.

- For high-($\simeq 0.40$) and low-($\simeq 0.02$) β a sequence of equilibria with rotational transform per period ι_p in the range $0.15 < \iota_p < 0.40$ is generated. This corresponds to a curvature κ of the magnetic axis between $\kappa = 0$ and $\kappa = 0.17$.

- The $(m = 1, n = 1)$ mode is stable for high–β for $\kappa > 0.16$. Figure I shows the $\kappa = 0.17$ case with ι_0 (at the magnetix axis) $= 0.36$ and ι_E (at the boundary) $= 0.40$. For low–β the marginal point is $\kappa = 0.14$. Figure II shows $\kappa = 0.127$ with $\iota_0 = 0.24$ and $\iota_E = 0.26$.

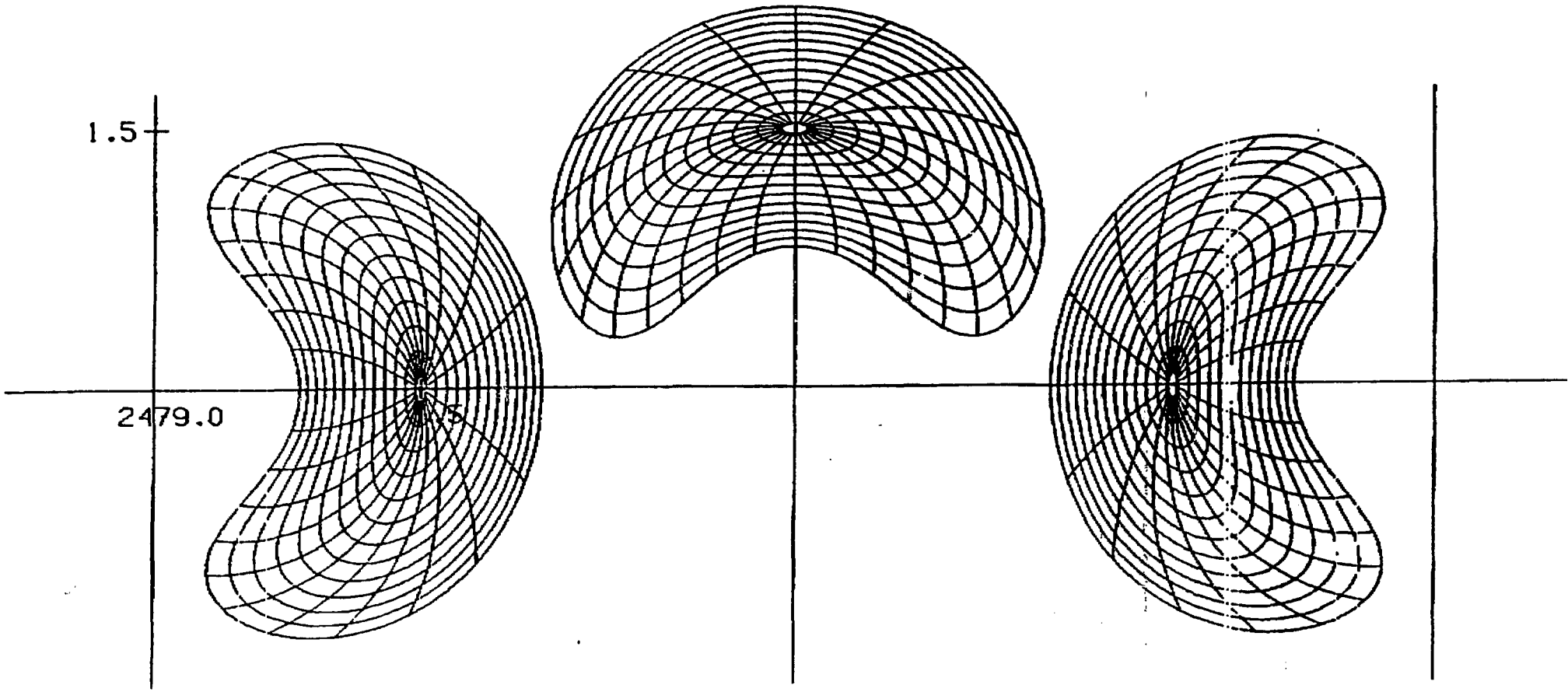

Figure I

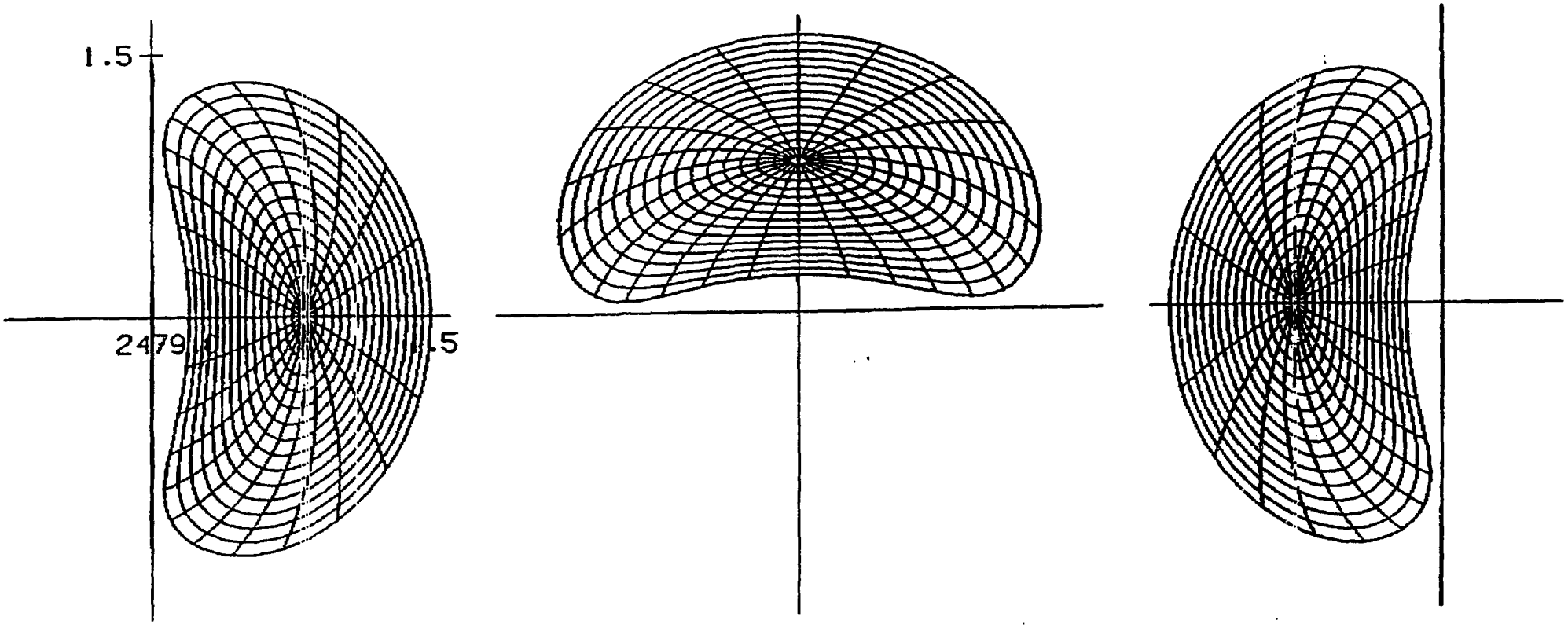

Figure II

Transport

- Drift Kinetic Equation
  - Transport coefficients for TJ-II (✓)
  - Particle and energy fluxes (✓)
- Magnetic surface dysimmetry Pfirsch-Schlüter currents(✓)
- Monte-Carlo transport calculations
- Adaptation of PLASMATOR code to TJ-II

Data Adquisition

- D.A.S. software
  - Textor
  - ORNL
- VAX/785
- CAMAC /VME

ECRH

- Cold Plasma(✓)
  - Cut-offs
  - Resonances
- Warm Plasma(✓)
  - Slab geometry
  - Absorption Profiles
    - No Relativistic model
    - Relativistic model
- Superthermal Tail(✓)
  - No Relativistic model
  - Relativistic model
- Ray-tracing code
- Fockker-Planck code

MICROWAVE INJECTION

Plasma cross-section showing resonances and X-mode cut-off for different toroidal angles

$\overline{n}_e = 1.5 \times 10^{13}\ cm^{-3}$ $f = 56$ GHz

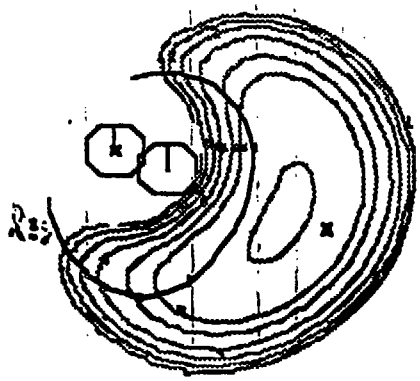

$\phi = 5.6°$

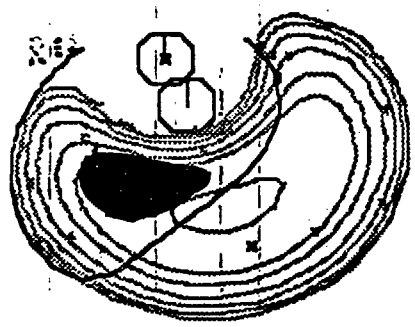

$\phi = 16°$

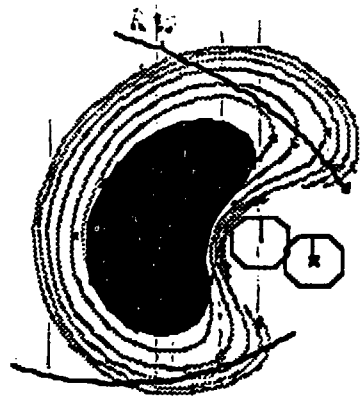

$\phi = 51°$

Cut-offs and resonances for several densities

$f = 54$ GHz $\qquad \phi = 5°$

$\bar{n}_e = 1.5 \times 10^{13}$ cm^{-3}

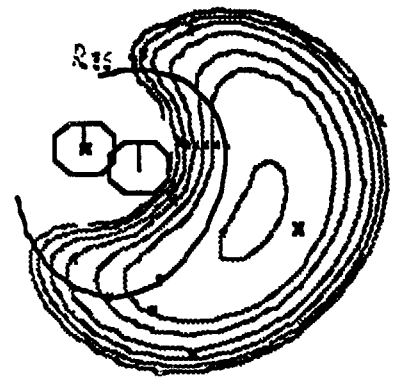

$\bar{n}_e = 1.6 \times 10^{13}$ cm^{-3}

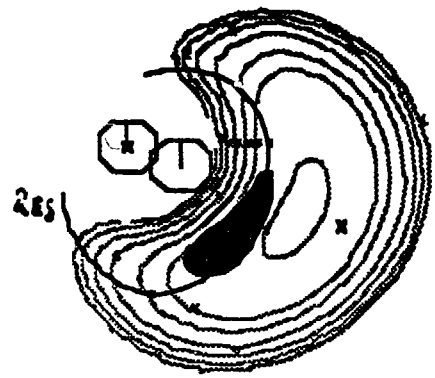

$\bar{n}_e = 2.3 \times 10^{13}$ cm^{-3}

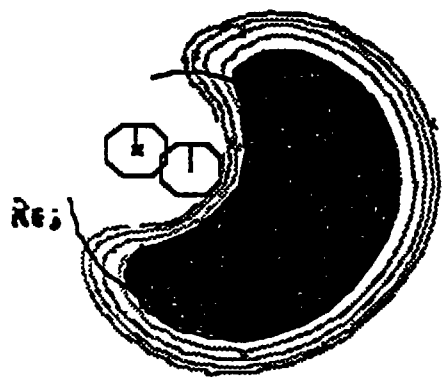

No RELATIVISTIC CASE

CIEMAT 10/20/87 8:[illegible]

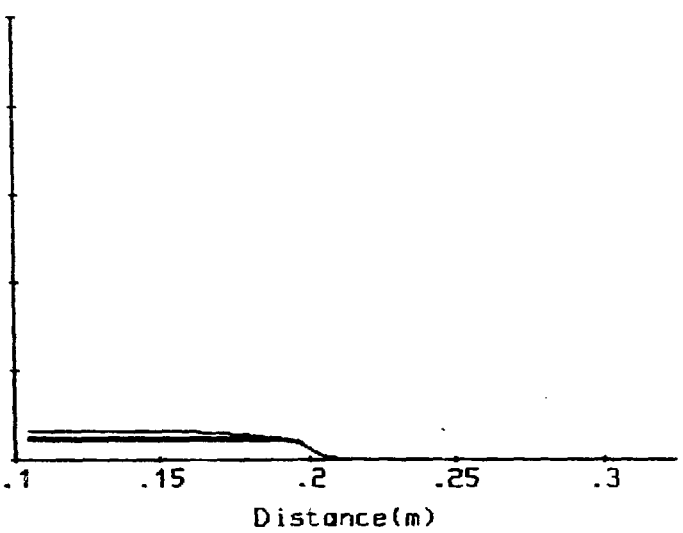

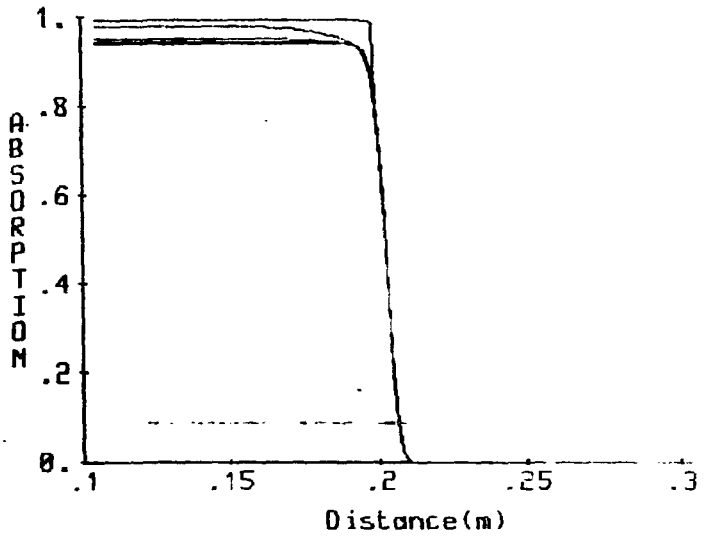

Ordinary Wave

Coeff.=0005
Density=1.5x10^{13} cm^{-3}
Frequency=53.2GHz
Angle=80. deg.
Drift Veloc.=1.5V$_{te}$
Temperature=.7keV

Extraordinary Wave

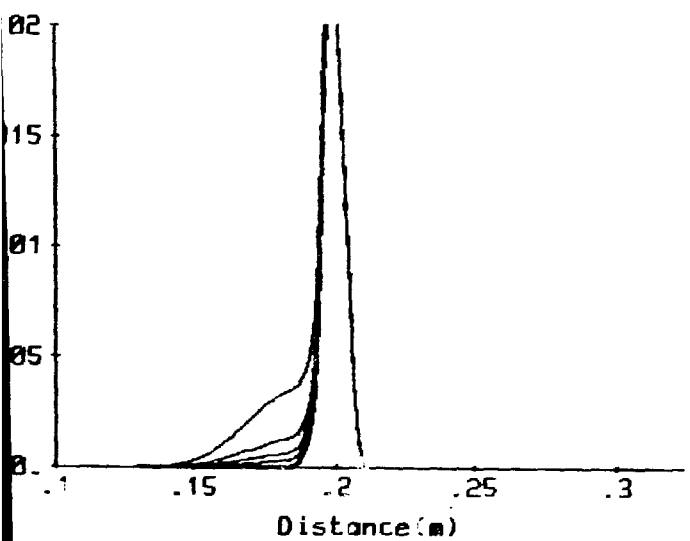

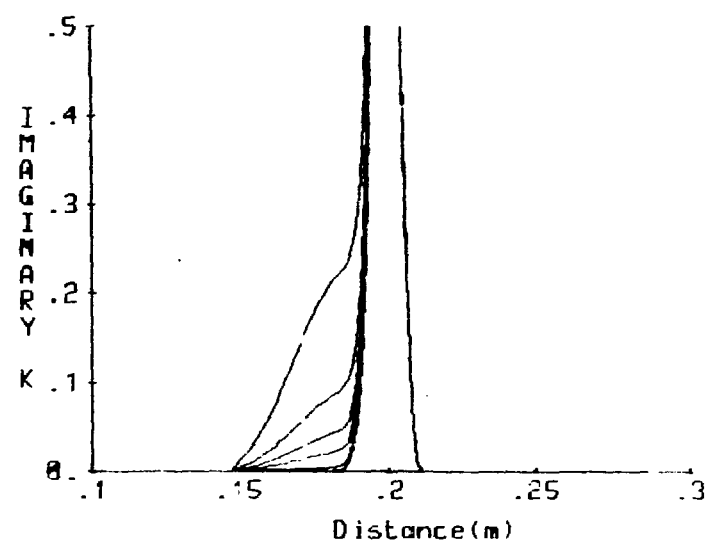

RELATIVISTIC CASE

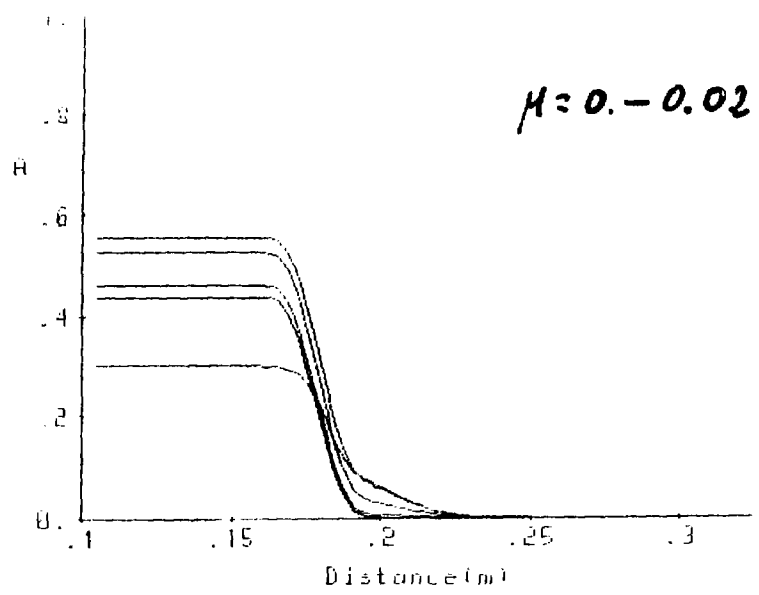

$\mu = 0. - 0.02$

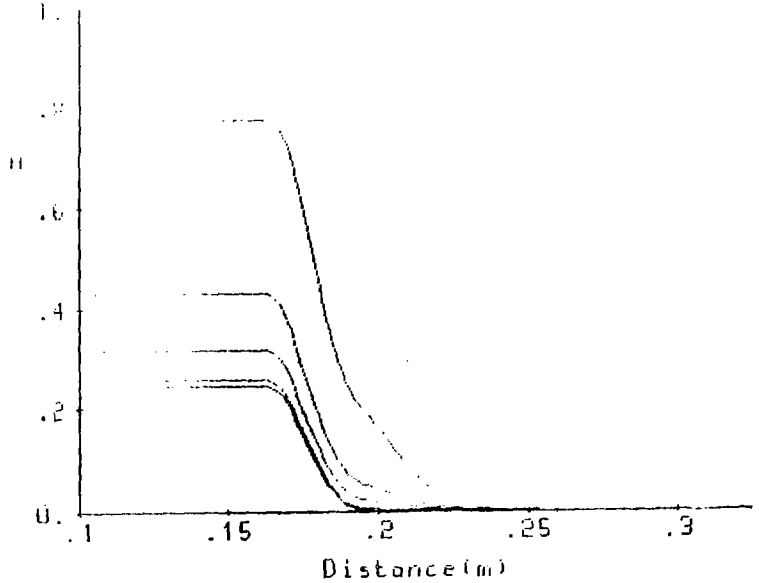

Coeff.=0.01
Density=.64×10^{13} cm^{-3}
Frequency=28.6GHz
Angle=30. deg.
Drift Veloc.=1.5v_{te}
Temperature=1.8keV

Ordinary Wave

Extraordinary Wave

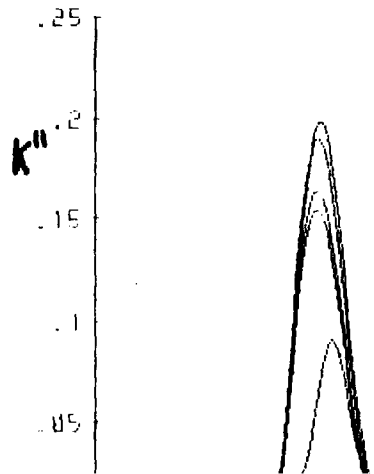

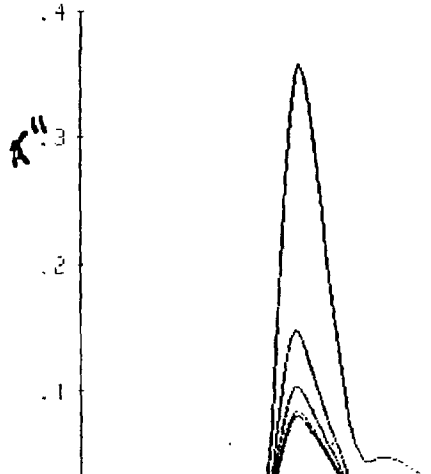

TJ-II EXPERIMENTAL PROGRAMME

- **THREE CONSECUTIVES STEPS :**

  (related to the increase in heating power)

  - **STUDY OF LOW β PLASMAS**

    (USING 400 KW ECH ,53.2 GHZ)

  - **FINITE β EFFECTS**

    (ADDITIONAL HEATING : 1 MW NBI, ICH?)

  - **β LIMITS**

    (ADDITIONAL HEATING : 5 MW NBI, ICH?)

I.- STUDY OF TJ-II PLASMAS AT LOW ß

USING ECH, FOR PLASMA BREAKDOWN AND HEATING, THE PREDICTED PARAMETERS ARE :

$n_e = 1.6\ 10^{19}\ m^{-3}$, $T_e = 700$ eV , $T_i = 200$ eV

$\tau_E \approx 4$ ms , $\beta_O \approx 0.7$ %

MAIN TASK IN THIS PHASE IS TO GET ACCESS TO THE DIFFERENT ι EQUILIBRIUM WINDOWS :

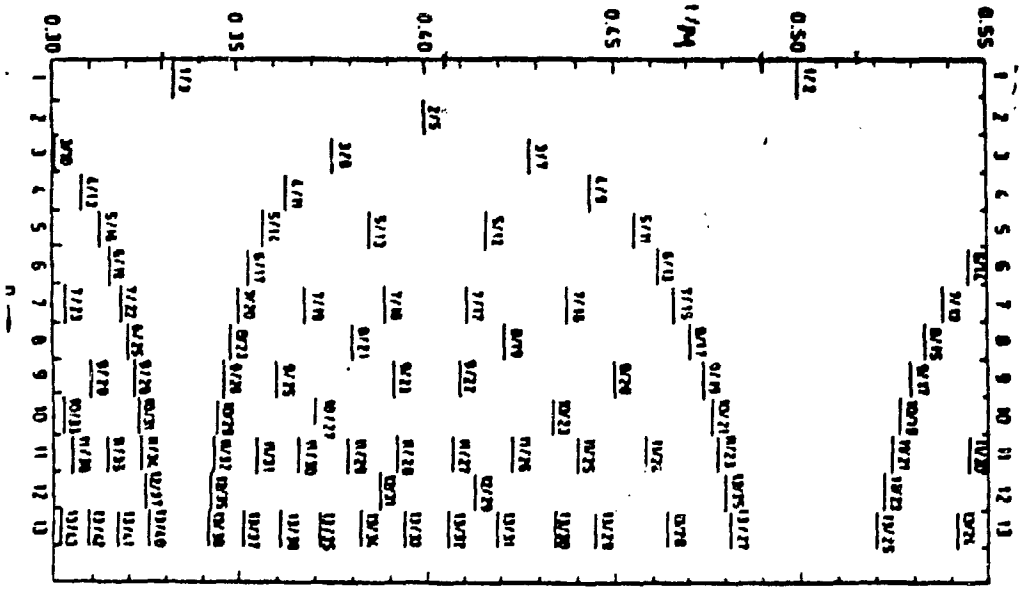

STUDYING FOR EACH POSSIBLE CONFIGURATION :

- <u>TRANSPORT</u> :
  - SCALING OF PARTICLE AND ENERGY CONFINEMENT TIMES
  - ELECTRON HEAT CONDUCTION AND IMPURITY BEHAVIOUR IN THE LONG-MEAN-FREE-PATH.
  - TURBULENCE
- <u>EQUILIBRIUM</u> :
  - DEPENDENCE ON CONFIGURATION
  - SHEAR EFFECTS
- <u>STABILITY</u> :
  - DEGREE OF INSTABILITY FOR LOW AND HIGH ORDER RESONANCES
  - EFFECTS FROM MAGNETIC WELLS AND SHEAR

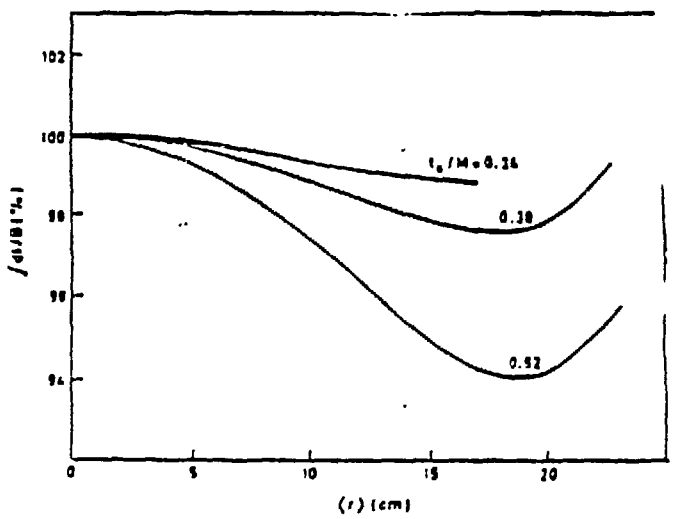

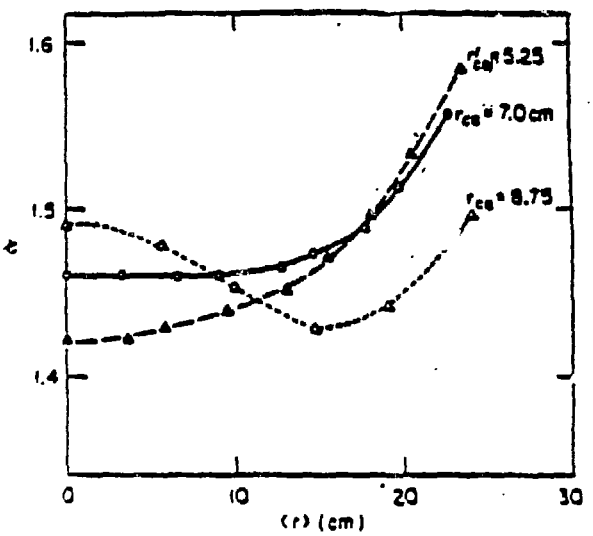

II.- FINITE β EFFECTS

(NBI AS AUXILIARY HEATING, 1MW)

PREDICTED VALUES :

$n_e = 2.4\ 10^{19}\ m^{-3}$

$T_e = 700$ eV

$T_i = 1500$ eV

$\beta_0 = 2.5\ \%$

STUDY IN ADDITION TO THE PREVIOUS TOPICS, THE FOLLOWING EFFECTS :

- LOW SHAFRANOV SHIFT

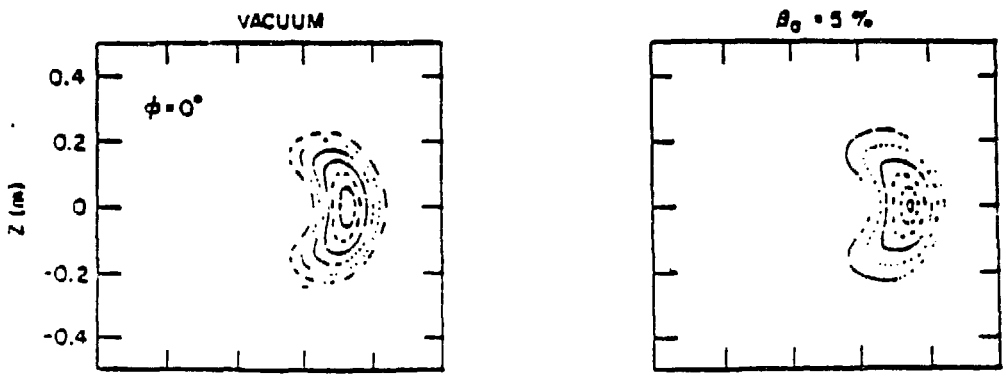

- CONFINEMENT OF HIGH ENERGY IONS

- EFFECTS OF β ON THE EQUILIBRIUM WINDOWS.

III.- β LIMITS

(ADDITIONAL HEATING UPGRADE UP TO 5 MW)

EXPECTED VALUE: $\beta_{0,max} \approx 9\ \%$

STUDY DEPENDENCE ON CONFIGURATION

TJ-II DIAGNOSTICS

THREE PHASES TO CONSIDER FOR DIAGNOSTICS PLANNING:

I.- PREOPERATION

II.- START-UP

III.- DETAILED DOCUMENTATION

PHASE I : PREOPERATION

* E-BEAM
* POWER SUPPLY MONITORS
* RESIDUAL GAS ANALISER
* MAGNETIC LOOPS
* ERROR FIELD MONITORS

PHASE II : START-UP

* LOOPS (DIAMAGNETIC, ROG.., V_p ...)
* 2 MM. INTERFEROMETER
* THOMSON SCATTERING (MONOCHAN.)
* VIS. MONOCHROMATOR
* VUV MONOCHROMATOR
* XPHA
* BOLOMETER ARRAY
* PLASMA TV

PHASE III : DETAILED DOCUMENTATION

* THOMSON SCATTERING (PROFILES CAPAB.)
* CX (PERPENDICULAR AND TANGENTIAL)
* X-RAY ARRAYS
* ECE RADIOMETER
* H_α MONITORS
* LASER BLOW-OFF
* PROBES (LANGMUIR, ELECTR., MAGN.)
* BIASSED LIMITERS
* μ-WAVE REFLECTROMETRY (??)

ACCESS

TJ-II HAS A REMARKABLE DEGREE OF ACCESS TO THE PLASMA.

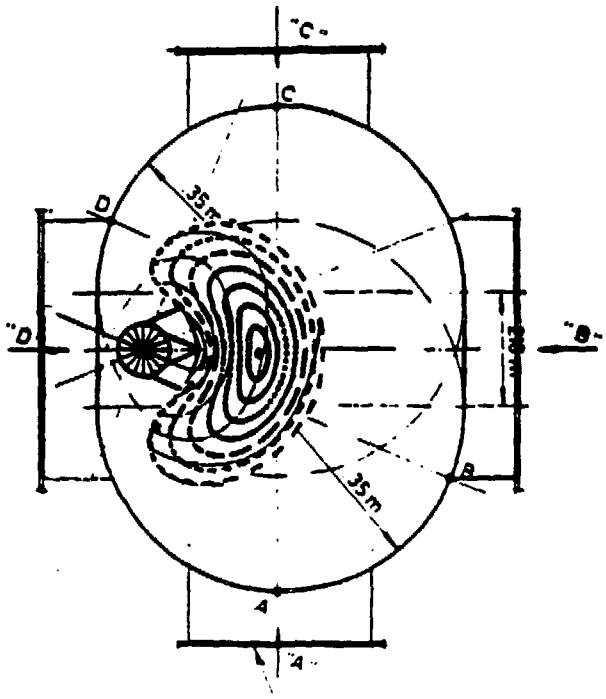

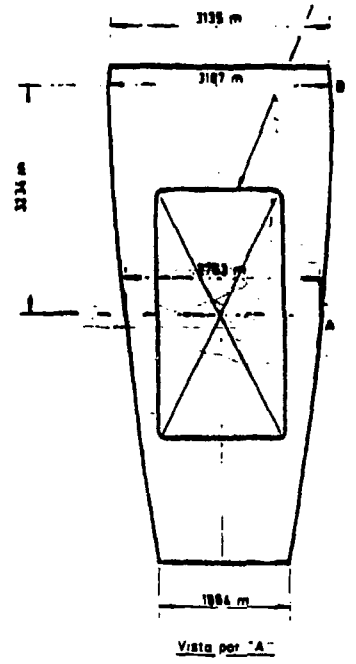

TYPICAL OBSERVATION PORTS FOR TJ-II
(PRELIMINARY DESIGN)

PORT SIZE	NUMBER
50 X 24 CM	8
50 X 12	32
50 X 5	16
35 X 18	24
35 X 12	12
35 X 6	20
18 X 13	8
Ø 10 (NBI)	4
TOTAL	124

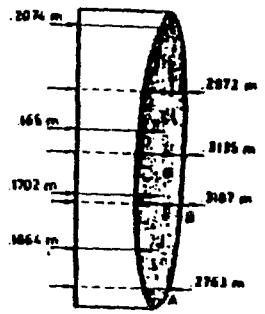

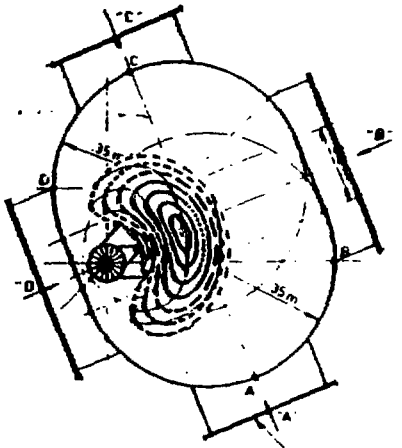

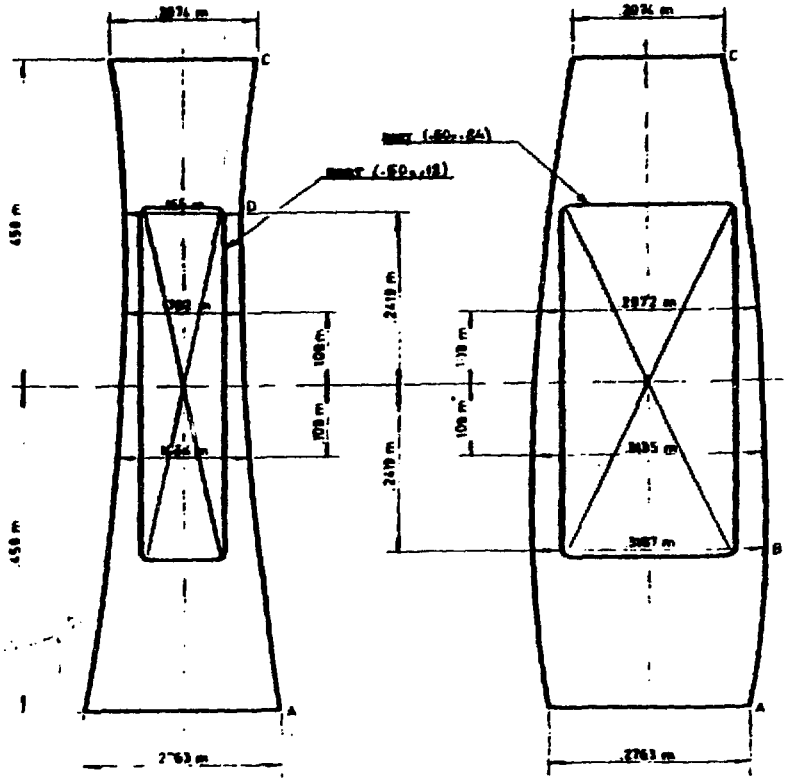

Vista por "D"
E 1/5

Vista por "B"
E : 1/5

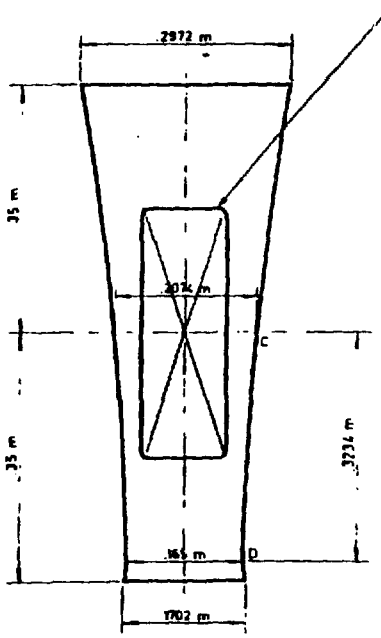

Vista por "C"

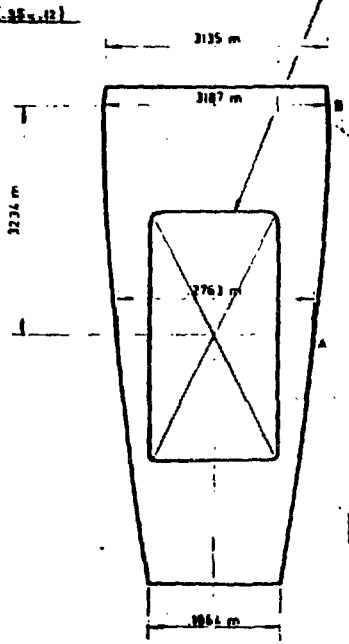

Vista por "A"

MODULOS A0 , B0 , C0 y D0

APPLICATION TJ-I TOKAMAK TO THE TJ-II PROGRAMME

- THE MAIN PART OF THE EXPERIMENTAL PROGRAMME DEVELOPED AT THE TJ-I TOKAMAK, NOW IN OPERATION AT CIEMAT, IS DEDICATED TO PREPARE DIAGNOSTICS AND ANALYSIS TECHNIQUES FOR THE TJ-II DEVICE.

- SO FAR, THE FOLLOWING AREAS HAVE BEEN ADDRESSED

  - IMPURITY STUDIES
  - TURBULENCE
  - CONVENTIONAL AND NEW DIAGNOSTICS.

IMPURITY STUDIES IN TJ-I

- A LASER BLOW-OFF SYSTEM HAS BEEN DEVELOPED TO STUDY IRON AND SILICON CONFINEMENT AT LOW B_T IN TJ-I.

- VISIBLE AND V.U.V. SPECTROSCOPY ARE USED FOR IMPURITY BEHAVIOUR STUDIES.

- LASER FLUORESCENCE IS UNDER DEVELOPMENT. TO BE IN OPERATION AT BEGINNING 89
  (Collaboration with Univ. Dusseldorf, FRG)

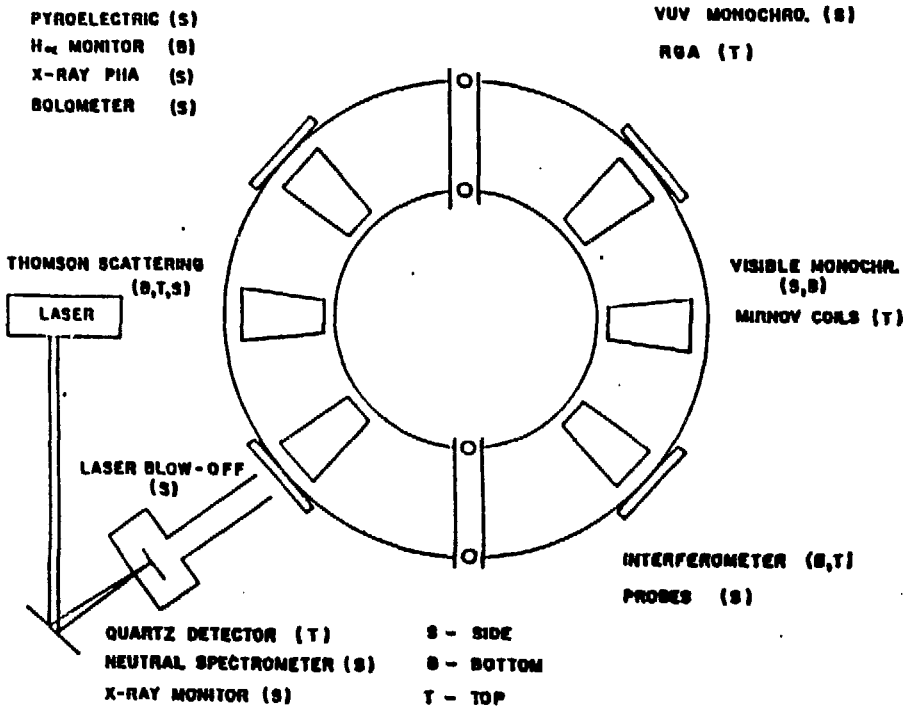

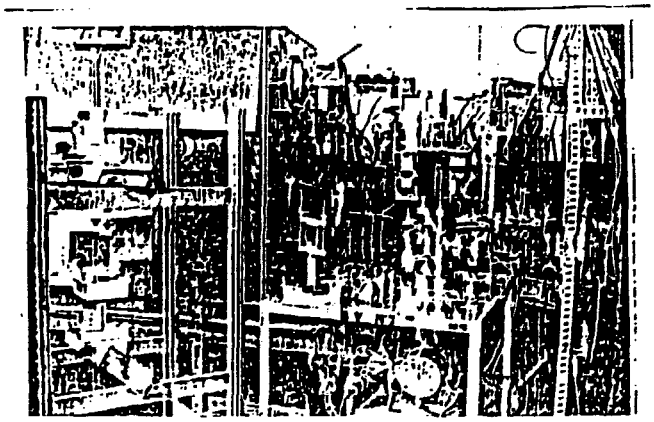

PHOTO OF THE EXPERIMENTAL SET UP

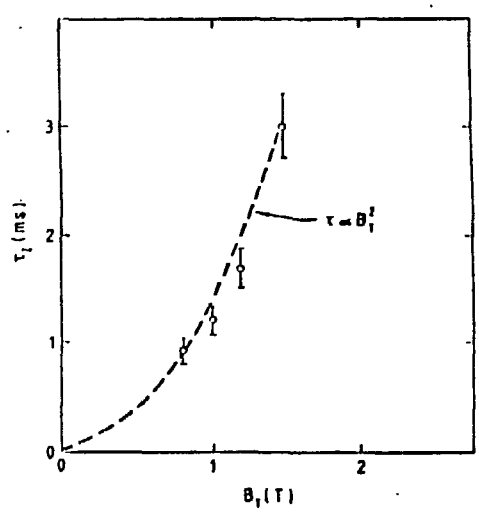

FIGURE 2

VARIATION OF THE IRON CONFINEMENT TIME WITH TOROIDAL FIELD FOR $\bar{N}_e$ =2.5 E13 CM-3.

TURBULENCE STUDIES AT TJ-I

- STUDY OF PLASMA FLUCTUATIONS ($\tilde{n}_e$, $\tilde{\phi}$, $\tilde{T}_e$, $\tilde{B}_\Theta$) IN PLASMAS WITH TOROIDAL OR POLOIDAL LIMITERS IN THE TJ-I IS PLANNED. MAIN DIAGNOSTICS DEVELOPED FOR THESE STUDIES :

  - PROBES (LANGMUIR, EMISSIVE,MAGNETIC)
  - INa(Tl) IN CURRENT AND PHA MODES
  - MICROWAVE REFLECTOMETER

TURBULENCE STUDIES IN TJ-I TOKAMAK

MICRO WAVE REFLECTOMETRY

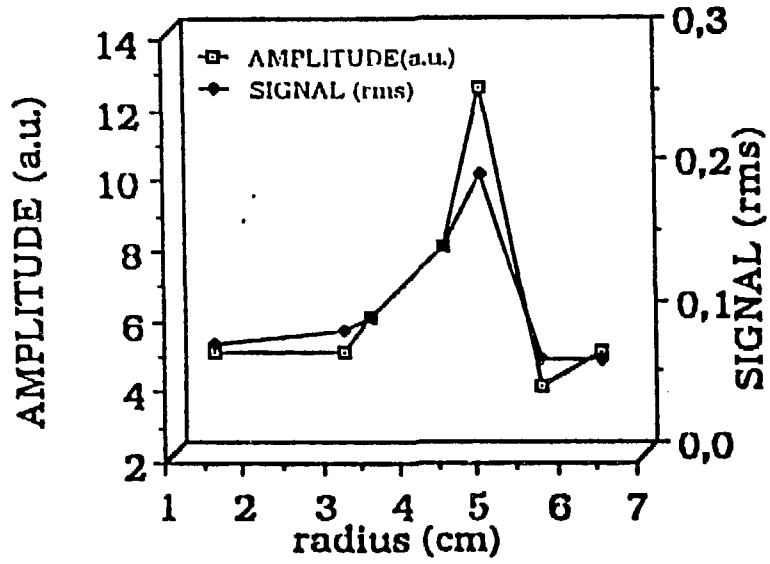

HARD-X-RAY ANALYSIS

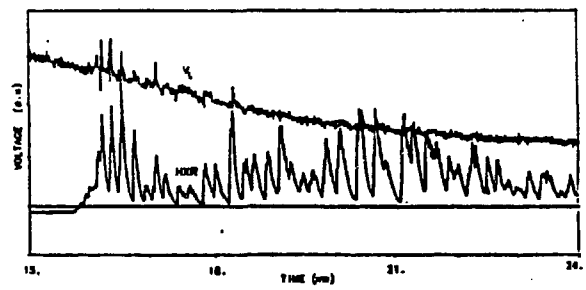

1-T_e = 300 ev. $\bar{n}_e = 10^{19}$ m^{-3}, V_L = 4.V

2-T_e = 600 ev. $\bar{n}_e = 1.5 \times 10^{19}$ m^{-3}, V_L = 4.V

3-T_e = 300 ev. $\bar{n}_e = 10^{19}$ m^{-3}, V_L = 2.V

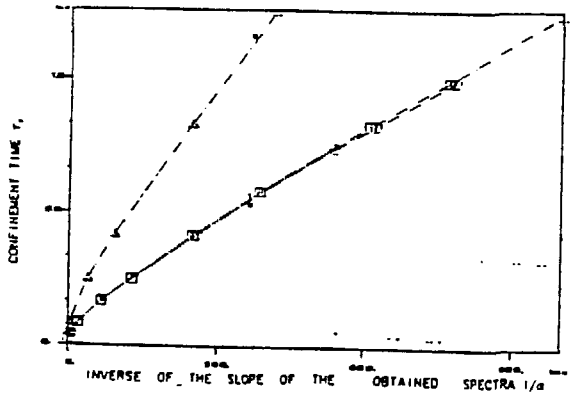

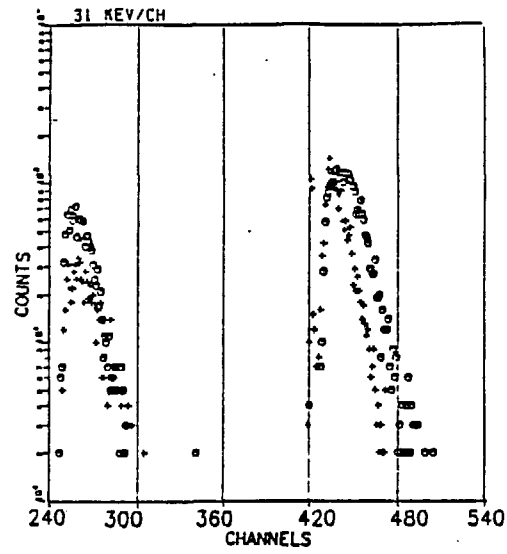

THEORETICAL MODEL

HARD-X-RAY SPECTRA

CONVENTIONAL AND NEW DIAGNOSTICS

- **SEVERAL DIAGNOSTIC SYSTEMS DEVELOPED FOR TJ-I HAVE BEEN REDESIGNED FOR APPLICATION TO TJ-II:**
  - **2 mm MICROWAVE INTERFEROMETER (1 channel)**
  - **C X ANALYSER (no mass separation)**
  - **THOMSON SCATTERING (1 channel)**
  - **VISIBLE and ULTRAVIOLET MONOCHROMATORS**
- **TEST OF NEW DIAGNOSTICS AND TECHNIQUES ARE ALSO IN PROGRESS:**
  - POSITRON INJECTION FOR TRANSPORT STUDIES
  - BOLOMETRY FOR LOW POWER DENSITIES
  - SUPRATHERMAL ELECTRON CONFINEMENT FROM HARD-X-RAY SPECTRA.
  - USE OF MOVABLE DETECTOR FOR TOMOGRAPHIC RECONSTRUCTIONS.

ENGINEERING ASPECTS

THE MAIN TASKS FOR TJ-II ENGINNERING ARE RELATED TO THE ELEMENTS IN THIS DESIGN PARAMETERS TABLE :

General

Major radius	1.5 m
Mean field on axis	1 T
Duty cycle	0.5 s/300 s

Circular Central Winding

Major radius	1.5 m
Current density	10 kA/cm^2
Total current	300 kA
Power at 1 T	5.5 MW
Copper weight	250 kg

1=1 Helical Central Winding

Major radius	1.5 m
Swing radius HX1	5.7 cm
Swing radius HX2	8.5 cm
Current density	10 kA/cm^2
Total current (both coils)	300 kA
Power at 1 T	6 MW
Copper weight	250 kg

Toroidal Field Coils

Number of coils	32
Coil radius	0.4 m
Swing radius of centers	0.28 m
Current density	5 kA/cm^2
Total current per coil	240 kA/cm^2
Power at 1 T (total)	19 MW
Copper weight	3400 kg

Vertical Field Coils

Number of Coils	2
Major radius	2.25 m
Vertical location	±0.562 m
Current density	5 kA/cm^2
Total current per coil	80 kA
Power at 1 T (total)	2.25 MW
Copper weight	400 kg

HARD CORE

- A POSSIBLE FABRICATION SQUEME HAS BEEN DETERMINED :

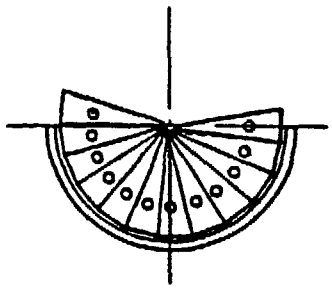

1) WIND CIRCULAR CORE COIL INTO BOTTOM HALF OF STAINLESS STEEL TUBE

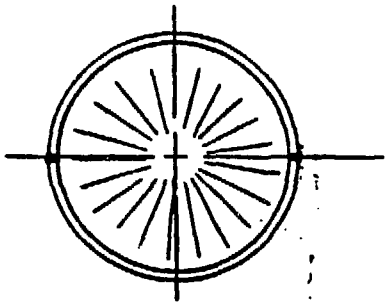

2) WELD TOP HALF OF TUBE TO BOTTOM HALF

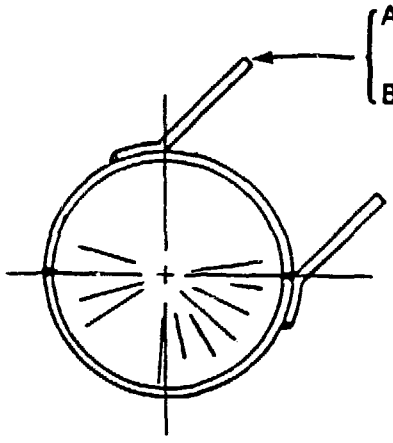

3) LOCATE SIDE SUPPORTS FOR HELICAL WINDING PIN AND WELD

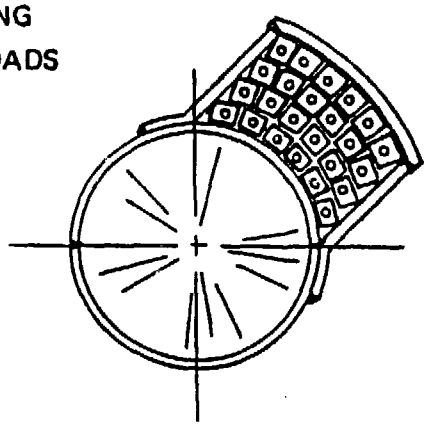

4) WIND HELICAL COIL AND WELD ON CLOSURE COVER

- TWO INDEPENDENT FEEDS FOR THE HELICAL COIL ENABLE SOME SHEAR CONTROL

VACUUM CHAMBER

- AN INSIDE VACUUM CHAMBER WAS SELECTED FOR TJ-II

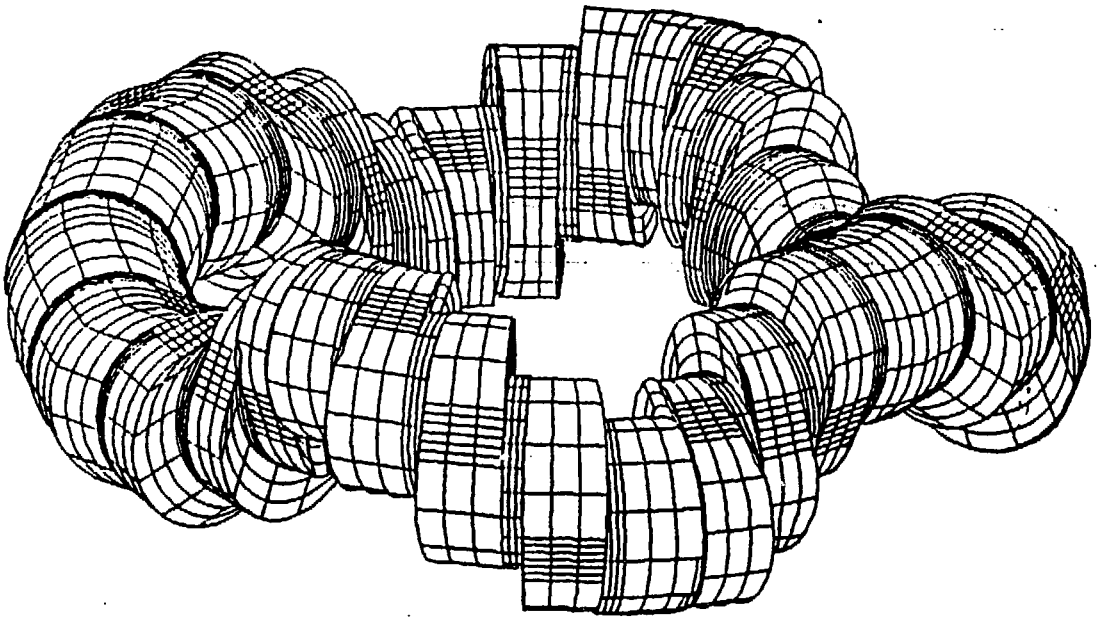

- THIS CHAMBER IS FEASIBLE BY COMBINING FLAT PLATES AND CIRCULAR RINGS.

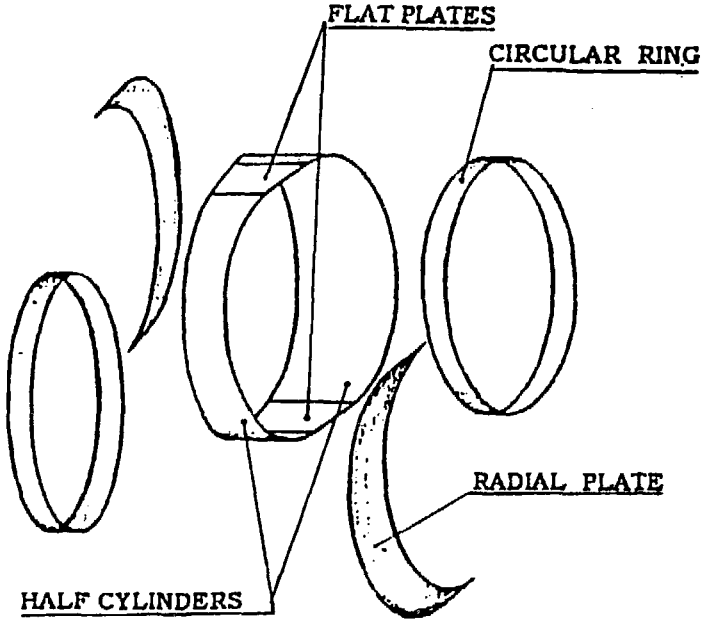

TJ-II VACUUM VESSEL SEGMENTS

ECH

- A CONCEPTUAL DESIGN FOR A 53.2 GHz TRANSMISION LINE HAS BEEN COMPLETED.

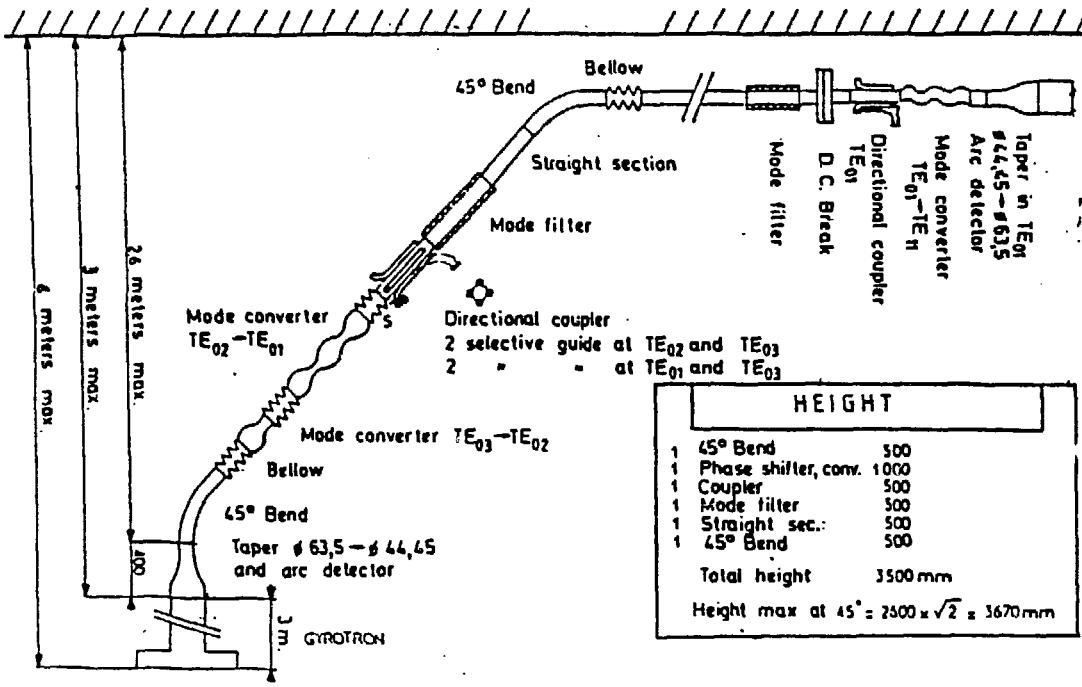

- WORK ON DEVICES TO MEASURE THE FAR FIELD STRUCTURE OF MICROWAVE LAUNCHING ARE IN PROGRESS.

CURRENT STATUS

- Phase I Euratom Preferential Support approved.
- Engineering design to start in Dec/87.

SCHEDULE

• Dec/87 to July/88	Engin. Design
• July/88 to Oct/88	Binding for const.
• Oct/88 to Oct/90	Construction
• Nov/90 to Jun/91	Assembly and com.
• Jul/91	Operation

ATF EXPERIMENTAL PLANS

Masanori Murakami

The ATF Group

Presented at

U.S.-Japan Stellarator/Heliotron Workshop

Oak Ridge, Tennessee

November 10, 1987

87-140

Masanori Murakami
Oak Ridge National Laboratory

The ATF Experimental Plans

The ATF Experimental Program focuses on better understanding and improvement of toroidal confinement through studies of (1) scaling of beta limits with magnetic configuration properties and plasma behavior in the second stability region; (2) low collisionality transport and the role of electric field; (3) effects of magnetic configurations (externally controllable) on beta and transport; and (4) issues critical to steady state operation (such as, energy and particle handling and ICRF). The first year program will emphasize implementation of hardware and physics capabilities. This will be followed by individual physics studies consisting of configuration studies, high beta/MHD stability studies, transport/rate of E-Field studies, edge and particle control studies, and RF heating studies. Objectives, issues, and schedules of these studies are discussed. The highlights presented include confinement scaling, prospects of currentless operation, and second stability region.

THE ATF EXPERIMENTAL PROGRAM

- **The Program is directed at <u>better understanding and improvement</u> of toroidal confinement through studies of:**
  - **β limit; 2nd stability region**
  - **Low ν^* transport; role of E-field**
  - **Effects of magnetic configurations (externally controlled) on β and transport**
  - **Issues critical to steady state operation (energy and particle handling, ICRF)**

OUTLINES

1. **First-year Experimental Plans :**
   - **Capabilities Available and Upgrades**
   - **General Confinement Studies** Conf. scaling
2. **Goals and Issues of Individual Physics Studies :**
   - **Confuguration Studies** Current-free ops.
   - **High Beta / MHD Stability Studies** 2nd Stab. region
   - **Transport / Role of Electric Field Studies**
   - **Edge and Particle Control Studies**
   - **RF Heating Studies**

OTHER ATF PRESENTATIONS IN THIS WORKSHOP

Monday Morning

Status of ATF Project – G. H. Neilson

Tuesday Morning

ATF Diagnostics – R. C. Isler

Tuesday Afternoon

Transport Scaling in the Collisionless–Detrapping Regime – E. C. Crume

Transport Analysis for ATF – H. C. Howe

Wednesday Morning

Benchmarks of NBI Codes for Stellarators – R. H. Fowler

ECH Commissioning and Plans for ATF – T. L. White

ECH and ICH Startup Analysis – M. D. Carter

Wednesday Afternoon

ICH Program for ATF – F. W. Baity

ICRF Wave Propagation – D. B. Batchelor

Thursday Morning

Compact Torsatron Studies – B. A. Carreras

Configuration Studies for ATF – J. H. Harris

Thursday Afternoon

Currents in ATF – B. A. Carreras

Friday Morning

PMI Program and Wall Conditioning for ATF – P. K. Mioduszewski

Hard X-ray Suppression on ATF – D. A. Rasmussen

Status of Heavy Ion Beam Probe for ATF – A. Carnevali (RPI)

The first-year program emphasizes implementation of basic hardware and physics capabilities in preparation for physics program

Phase I-A	**First Experimental Plasmas**
	[H. Neilson's talk]
Phase I-B	**Initial NBI**
Phase II	**NB Confinement**

Expected Capabilities at the End of the Phase I-A : Commissioning and First Plasma Operation (Dec 87 - Jan 88)

- Magnetic field (HF to B_0=1 T; Inner and Trim VF).
- Runaway suppression systems (interceptor probe, Ar dump) in operation and hard X-ray survey completed
- ECH target plasma with P_{ECH} = 0.2 MW, 2^{nd} harm. at 53 GHz
- Wall conditioning (GDC and ECR-DC)
- Phase I diagnostic and limited analysis capabilities (magnetics, 2mm, PHA , etc.)
- First NBI (if possible)
- Magnetic surface verified with e-beam technique after Phase I-A (and later after Phase I-B)

ATF EXPERIMENTAL PROGRAM (Rev: 8-Oct-1987)

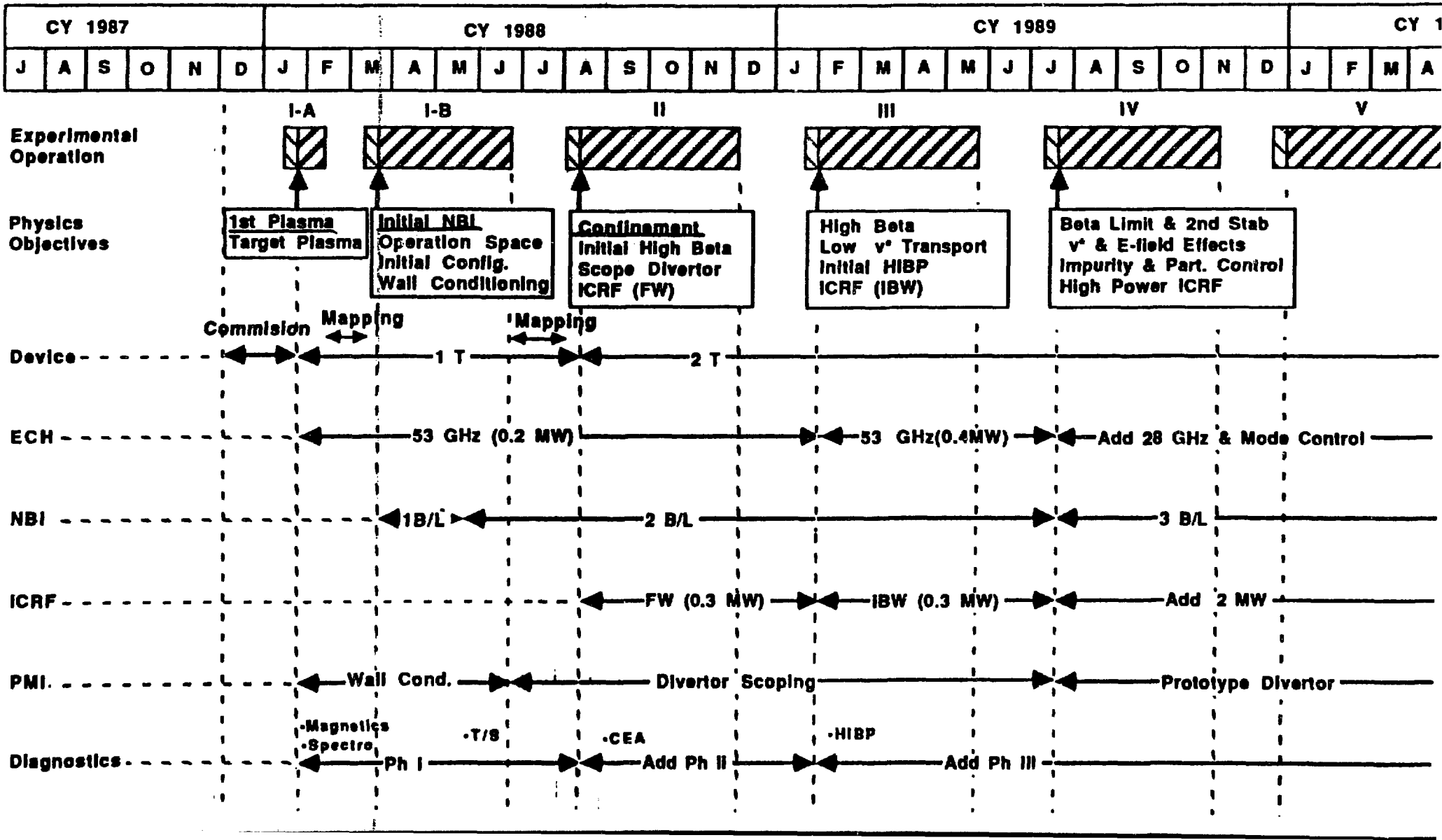

Basic Hardware Capabilities in the First Year and Their Upgrades

- **Magnetic Field :**
  - HF - B_0=1 → 2T (Ph II)
  - VF - Inner and Trim VF, Mid VF (Ph. II)
- **ECH :**
  - 53GHz - P_{ECH} =0.2MW → 0.4Mw (Ph. III)
    Open waveguide launch
    → mode controlled launch (Ph. IV)
  - 28GHz - P_{ECH} ~ 0.2Mw (Ph. IV)
- **NBI :**
  - # 1 (CO), # 2 (CN) } P_{NB}=2MW at 40keV
  - # 3 P_{NB}=3MW (Ph. IV)
- **ICRF :**
  - FW antenna (Ph. II), IBW antenna (Ph. III) } P_{ICRF} = 0.3 → 2 MW (Ph. IV)
- **Wall Conditioning :**

  GDC, ECR-DC, Baking at 150°C, RF-assist.-DC, Ti or Cr Getter
- **Diagnostics :**

  Phase I (global), Phase II (profile)

  Phase III (HIBP)

[R. Isler's Talk]

General Confinement Studies in Phase I-B and II

1. Establish Basic Mode of Operation
   - "Baseline" Conditions:
     NBI (CO+CN), B_0=0.95T with I_p=0,
     Clean, Reproducible
   - Bringing up new diagnostics

2. Survey Operating Space for <u>General</u> Purposes
   - Test "knobs":
     - Beam Power and Beam Directivity
     - Density (gas puffing)
     - Configuration (ΔQ_1, ΔQ_2)
   - Look for:
     - Operating limits [$(\bar{n}_e)_{max}$, β_{max}]
     - τ_E^* and scaling
     - Current
     - Profile changes [e.g., $\bar{n}_e(R)$ from FIR]
     - Any gross change in impurity and edge behavior, etc.

3. Systemetic (Single) Parameter Scans with Detailed Documentation

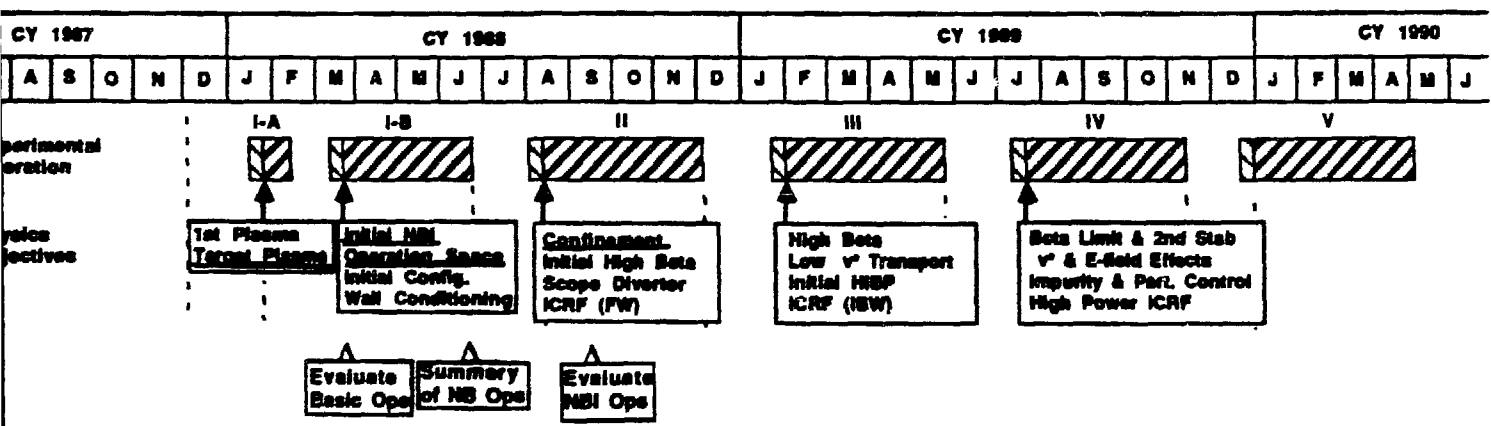

Confinement Scaling

- **PROCTR Analysis with He-E NB data**
  - **Finite-β equilibria (VMEC)** [H. Howe; J. Harris]
  - **Beam calc. benchmarked with MC** [R. Fowler]

  } **No substantial changes in global τ_E**

  - $\tau_E^{HE} = 11 \cdot P^{-0.66} n^{0.45} B^{0.51}$ [ms; Mw, $10^{20} m^{-3}$, T]

- **A τ_E scaling used in the Next Large Device Design Studies in Japan:**

$$\tau_E^{emp1} = 170 \cdot P^{-0.58} n^{0.69} B^{0.84} a^{2.0} R^{0.75}$$

fits reasonably well with data from Heliotron-E and other devices.

- **These scalings show that τE values expected in ATF with 2MW injection at B=0.95 T are of the order of 20 - 30 ms, corresponding to $\langle \beta \rangle$ values of the order of 2 - 3 %:**

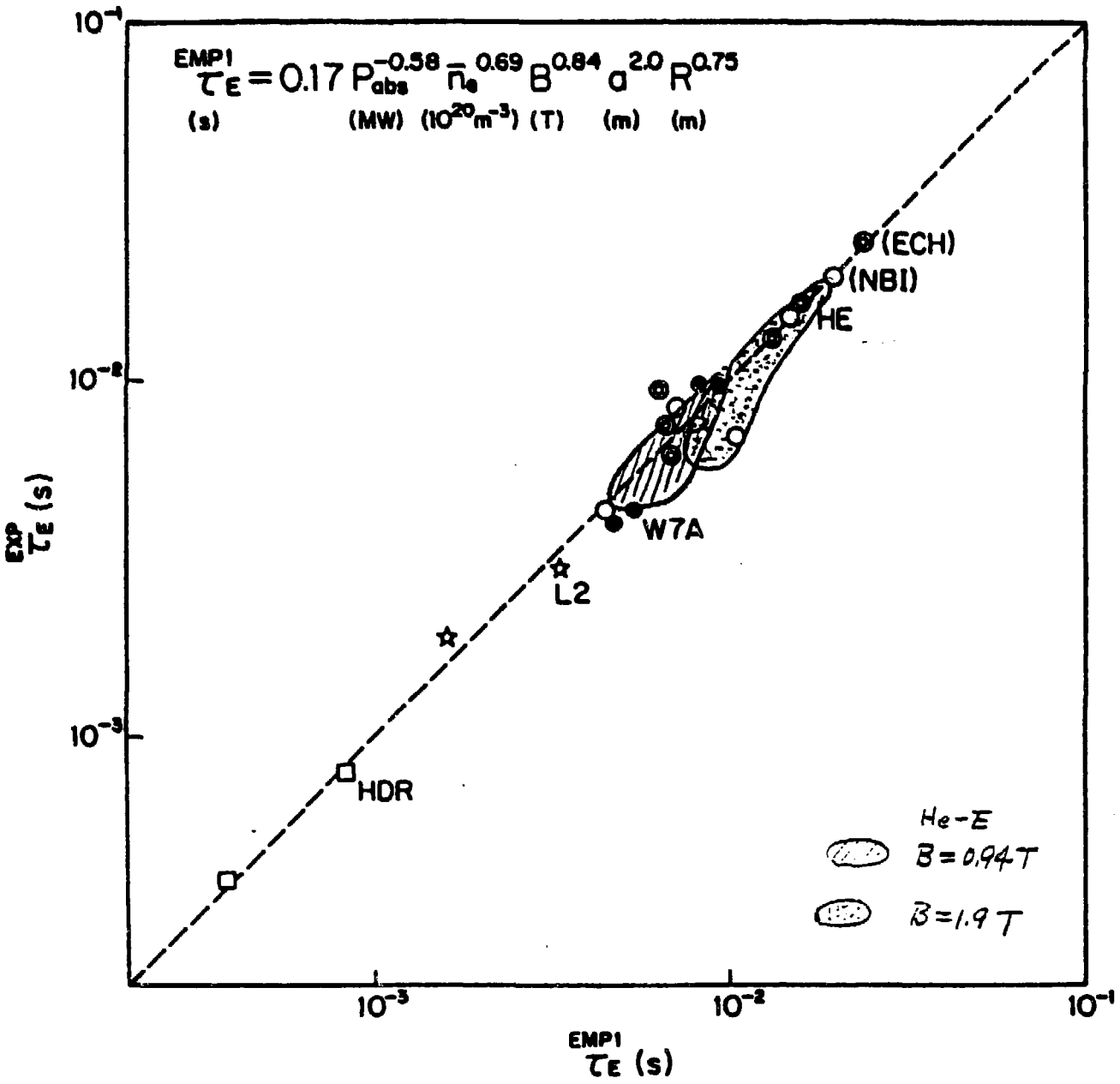

図３－１－２　ヘリカルシステムのスケーリング

Individual "Physics" Studies Branch out from the Initial General Confinement Studies.

- Configuration Studies
- High Beta / MHD Stability Studies
- Transport / Role of E-Field Studies
- Edge and Particle Control Studies
- RF Studies

MAGNETIC CONGIGURATION CONTROL STUDIES

- **Ability of varying the magnetic configuration provides a powerful experimental tool that will enable us to:**

  - **Vary MHD stability properties (e.g., second stability operation)**
  - → **Control net currents**
  - **Control the geometry (e.g., for plasma wall-interaction)**

[J. Harris' talk]

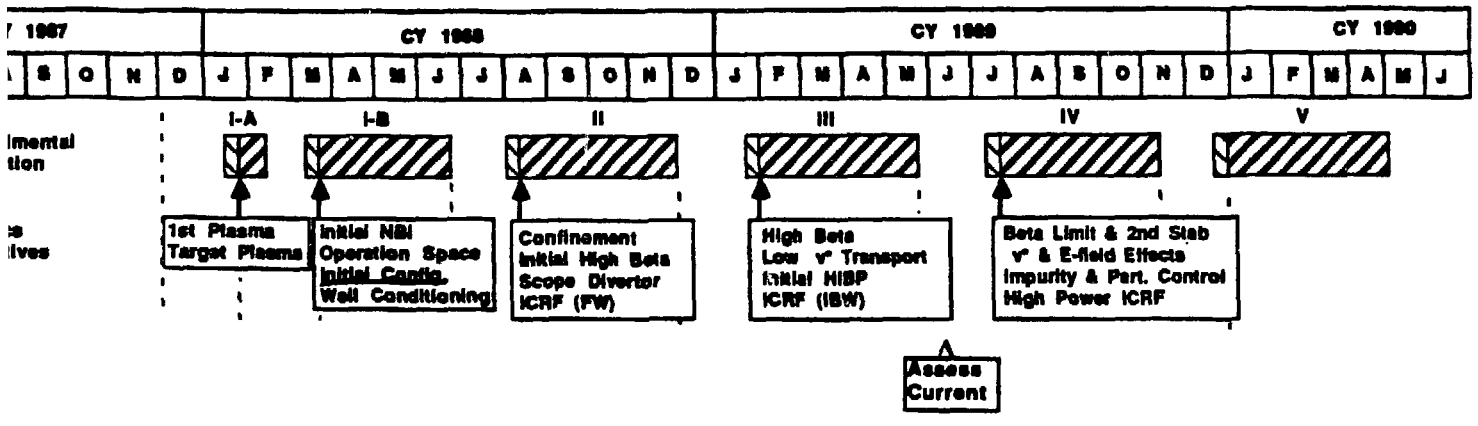

Control of Magnetic Configuration

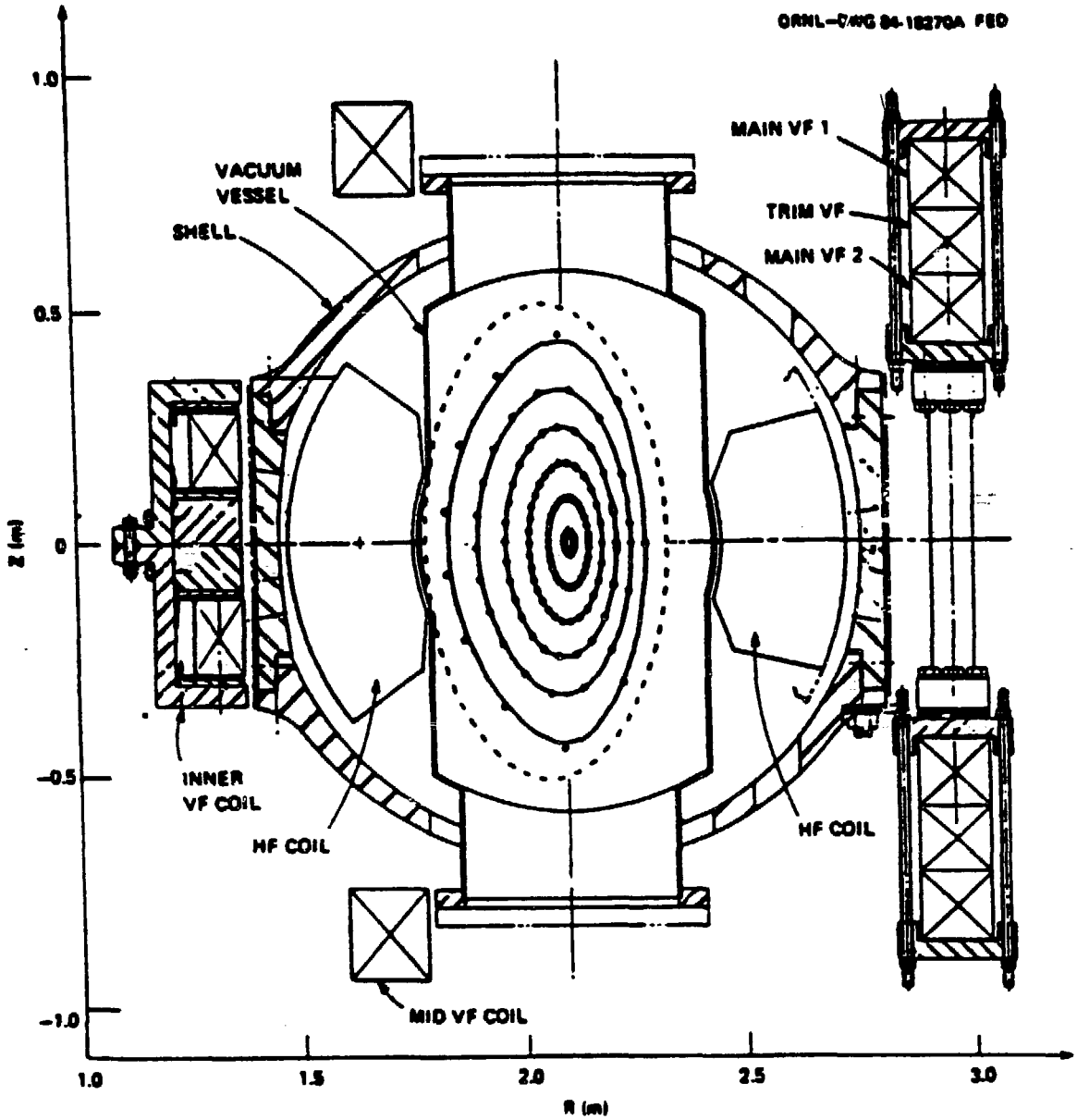

- 3 independent VF coils provide 3 control "knobs":

multipole fields
- Q_0(pol.flux) → I_p
- Q_1(dipole) → horiz. shift → well / hill
- Q_2(quadrupole) → elongation → $\iota(0)$,

harmonic contents in B_t

ATF VF COIL SYSTEM OPERATIONAL RANGE

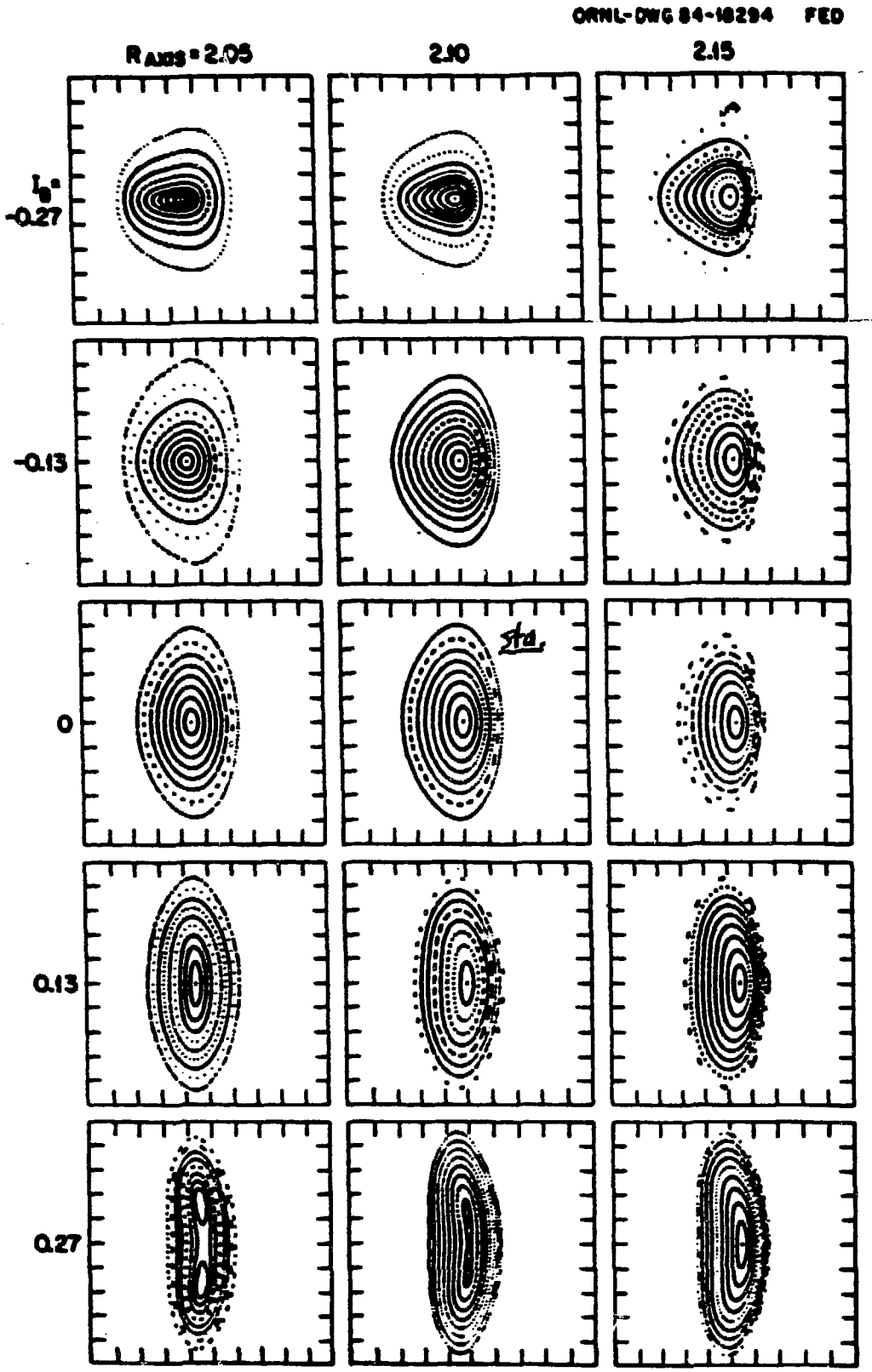

⇑ Bootstrap current studies

ΔQ_2

High β operation ⇓

⇐ Stability studies ⇒

ΔQ_1

CURRENTLESS OPERATION

- Possible causes of net toroidal current
  - "Flux conserving" current

    $I_{fc} \sim 4 \cdot \beta_0(\%)$ [kA]
  - Beam-driven current

    $I_{bd} \sim -4 \cdot \bar{n}_e(10^{20} m^{-3})^{-1.5} \cdot (P_{CO}(MW) - P_{CN}(MW))$
  - Bootstrap current

    $I_b \sim 52 \cdot G_b \cdot \beta_0(\%) \cdot B_T(T) \cdot f(\upsilon^*)$

    $\sim 5 \beta_0(\%) \cdot f(\upsilon^*)$ [kA] [G_b=0.1 for high β]
  - External source (VF)

    $I_{ext} \sim \pm 200 \cdot (\Delta I_{VF} / I_{VF})$ [kA]

- The ATF VF coil system has been designed to handle
  - large change in $\iota(r)$ with ΔQ_2
  - residual net current by Q_0

- The bootstrap current can be maximized
  - G_b = 0.5 by adjusting the VF quadrupole components
  - I_b as high as ~ 90 kA

[B.Carreras' talk]

High Beta / MHD Stability Studies

- Objectives are to study MHD stability and β limits, with emphasis on :
  - Maximum $\langle\beta\rangle$ values
  - → Second Stability region (i.e., "β self-stabilization")
  - Configuration effects (ι_0, V', I_p)
  - Flux conserving effects
- τ_E scalings based on He-E NBI data analysis predict $\langle\beta\rangle$ values of 2 - 3 %. Achievement of $\langle\beta\rangle$ higher than these values may require :
  - Low field operation (28GHz gyrotron → B_0=0.5T in FY89)
  - More heating power, requiring
    - -- Third beamlines (1.0-1.5Mw) late FY89-FY90
    - -- BBC transmitter (2Mw) for ICRF in FY90.

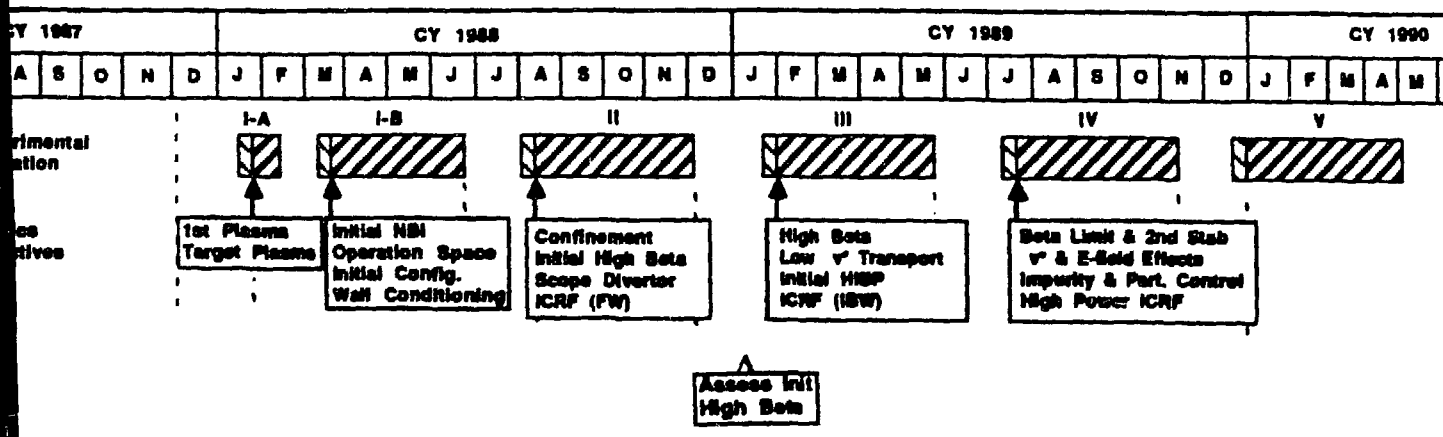

STABILITY BOUNDARIES (2nd stability region) CAN BE TESTED AT RELATIVELY LOW BETA BY SHIFTING THE MAGNETIC AXIS

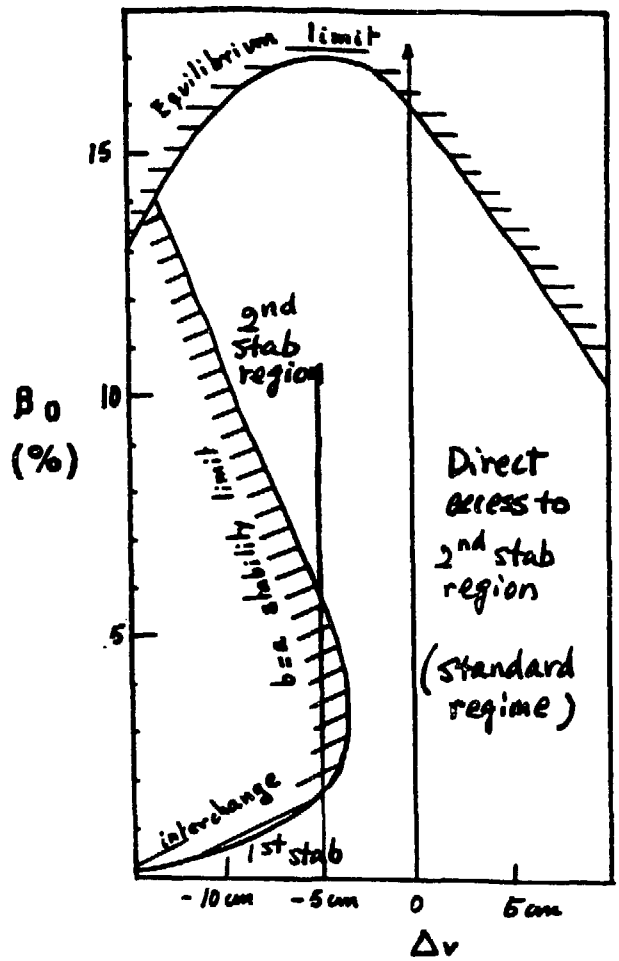

- $p \propto \psi^2$
- Equilibrium limit → $\Delta_p \sim \frac{a}{2}$

[B. Carreras]

- Global modes (m, n ≈ 1 - 3) can be studied:
  - variation of configuration (shift (V"), shaping (ι), I_p)
  - diagnostics:
    - magnetic loop array (external $\tilde{B}$)
    - FIR interferometer (chordal $\tilde{n}$)
    - soft x-ray array (internal $\tilde{n}T$)

[R. Isler]

THE BETA SELF-STABILIZATION IS PREDICTED TO REDUCE TURBULENT FLUCTUATIONS

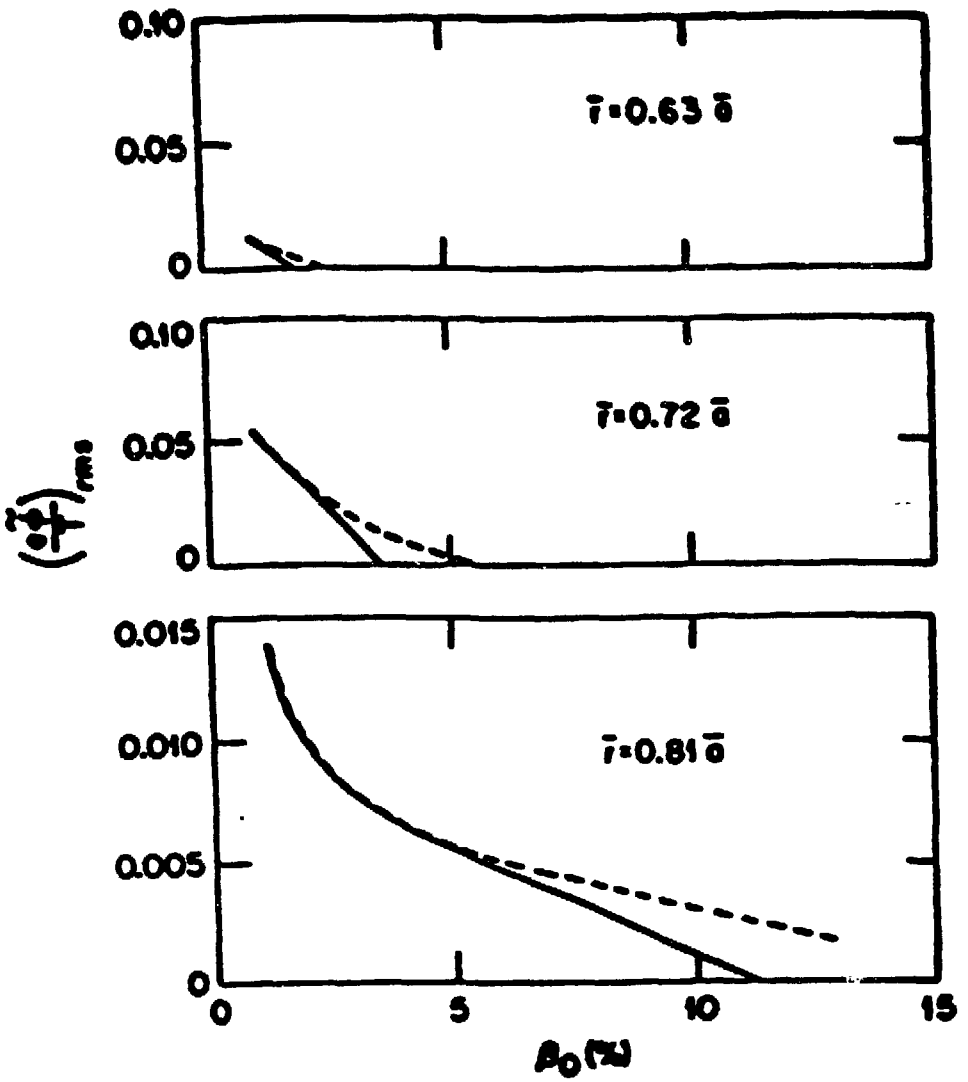

[B.A.Carreras et al IAEA / Kyoto,1986]

- The nonlinear model for resistive ∇p - driven instabilities (higher m,n) predicts flucuation levels.

- Variations of the turbulent fluctuations can be observed by:
  - Microwave reflectometry (with CIEMAT, Madrid)
  - Heavy ion beam probe (with RPI)
  - FIR Scattering
  - Edge Langmuir Probes

ANOMALOUS DIFFUSIVITY DUE TO SATURATED ∇ p - DRIVEN FLUCTUATIONS

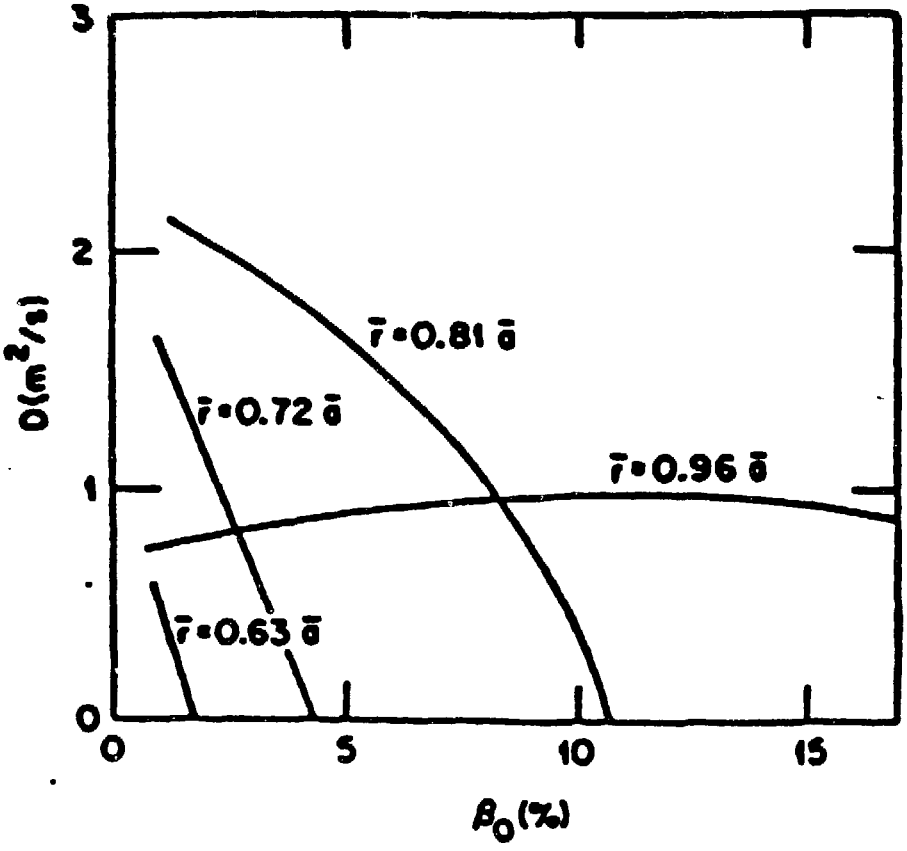

[B.A.Carreras e

IAEA / Kyoto,1

- Similar behavior predicted for electron heat conductivity
- The β self-stabilization improves confinement with increasing β in ATF.
- Turbulent spectra can be correlated with confinement.

Transport / Role of E-field Studies

- Objectives are to study stellarator transport with emphasis on :
  - Transport in low collisionality regime
  - Fast ion ripple losses
  - → Role of electric field

- Early information will come from :
  - τ_E scaling with B_0, $\bar{n}_e$, P_{NB}, etc.
  - PROCTR analysis → neoclasical anomaly [H. Howe]
  - T_i, v_ϕ, v_θ measurements from spectroscopy
  - T_i and fast ion measurements from NPA

- Comprehensive studies require :
  - High temperature at low $\bar{n}_e$ (B_0=2T, higher power, particle control)
  - Profile diagnostics
  - HIBP

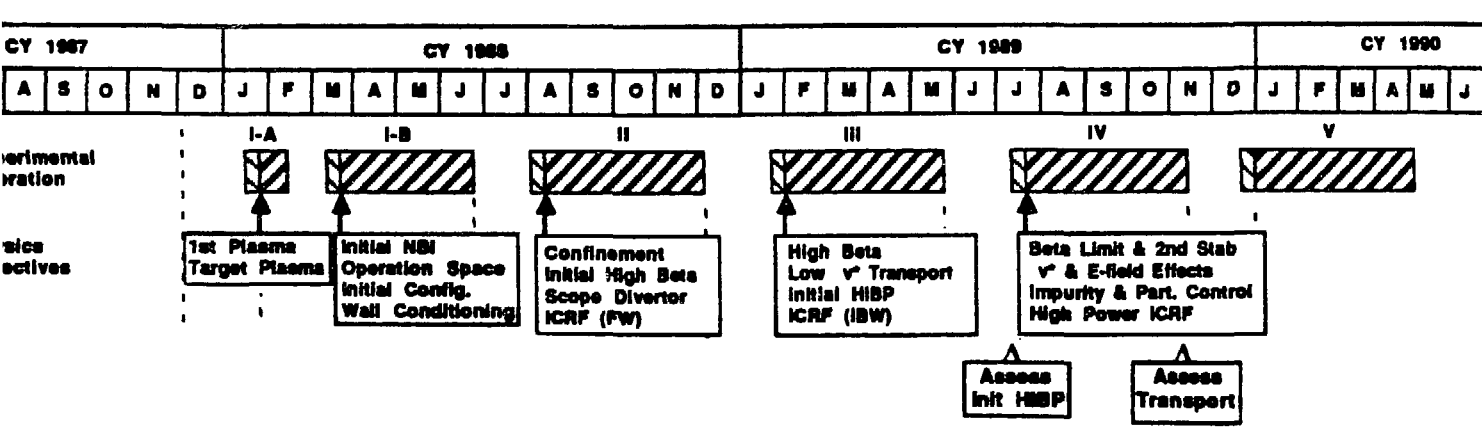

NEOCLASSICAL THEORY PREDICTS THAT RADIAL ELECTRIC FIELDS OF EITHER POLARITY REDUCE HELICAL RIPPLE LOSS, THEREBY IMPROVE CONFINEMENT

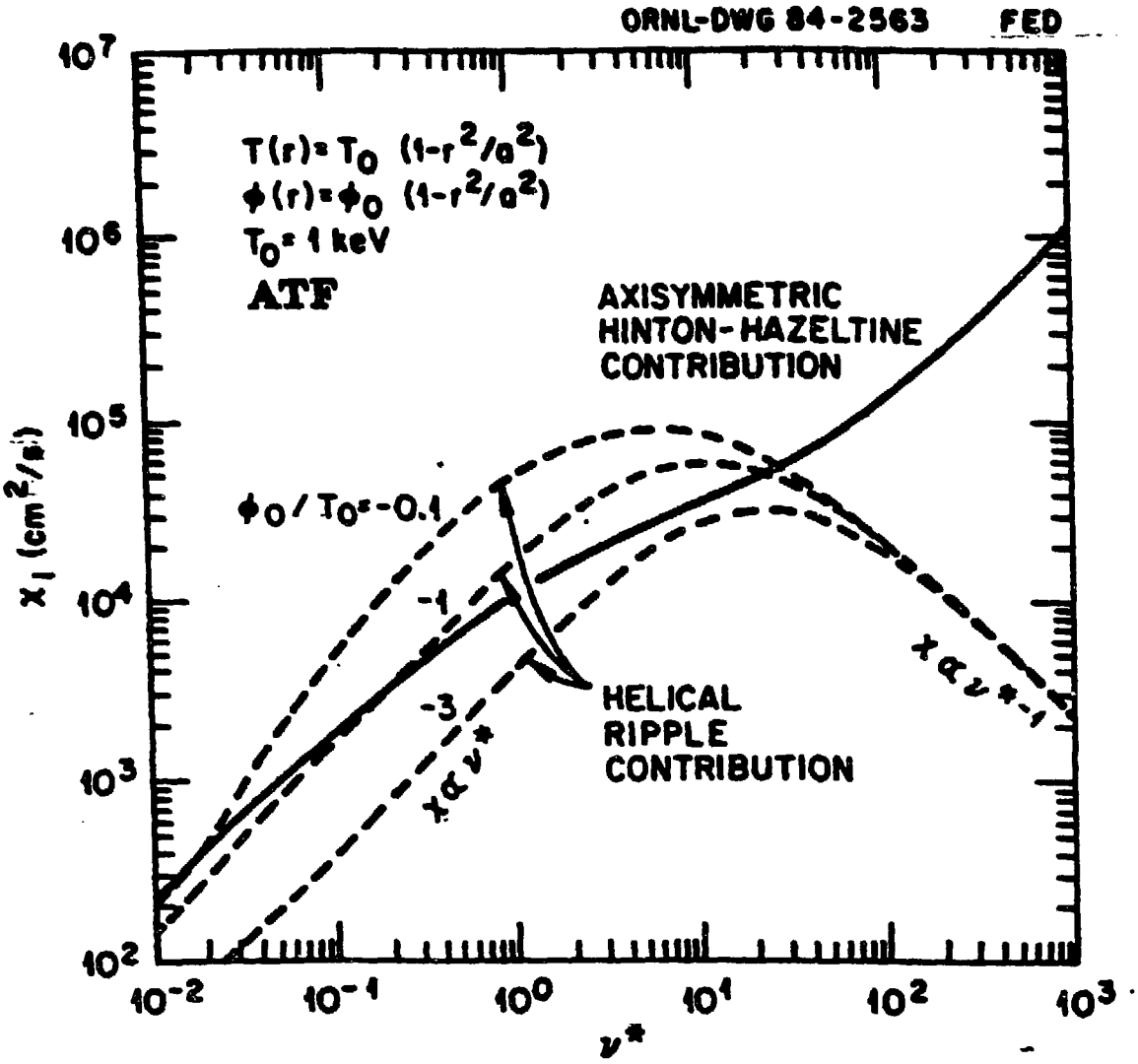

- Electric potential measured with HIBP (*with RPI*) [A. Carneval:]
- Control of potential with:
  - Momentum inputs from opposing tangential beams (as in ISX-B)
  - Overlapping ECH and NBI (?) (as in H-E and W7A)

Edge and Particle Control Studies

- **Investigate optimal procedures for reducing impurity sources and removing impurities**
  - **Additional wall conditioning : RF-assisted glow, Cr or Ti getter**

- **Investigate particle and energy flows in the plasma edge region to provide a database for the design of divertors and cooled panels.**

[P. Mioduszewski]

  - **Divertor scoping studies with a graphite target to determine edge parameters and connection lengths of divertor "stripes"**
  - **Prototype divertor and cooled panel modules**
  - **Pellet injector**

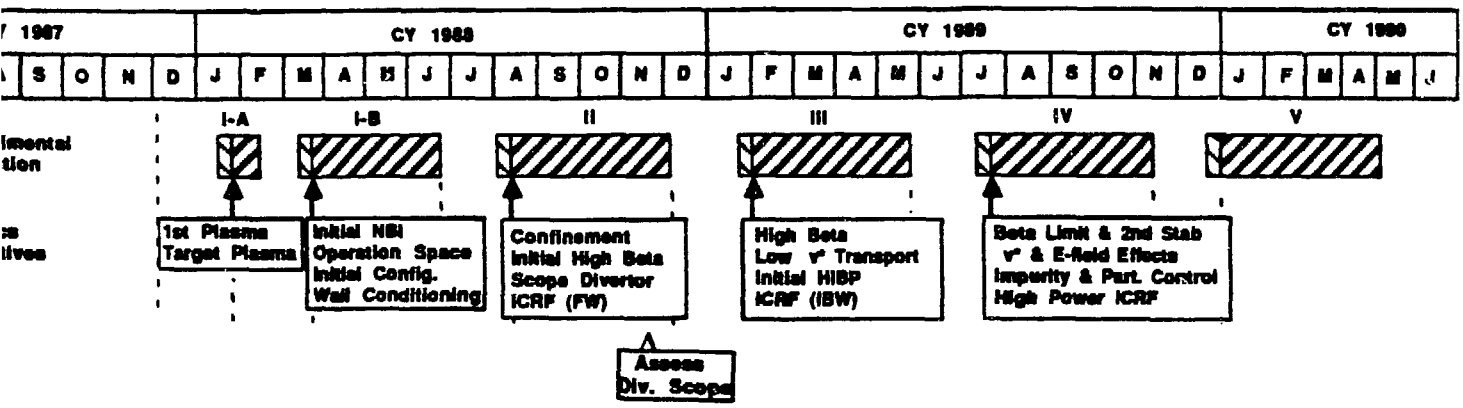

PARTICLE AND IMPURITY CONTROL

- Divertor action should occur in ATF
- Experimental observations of helical stripe patterns in stellarators are consistent with modeling

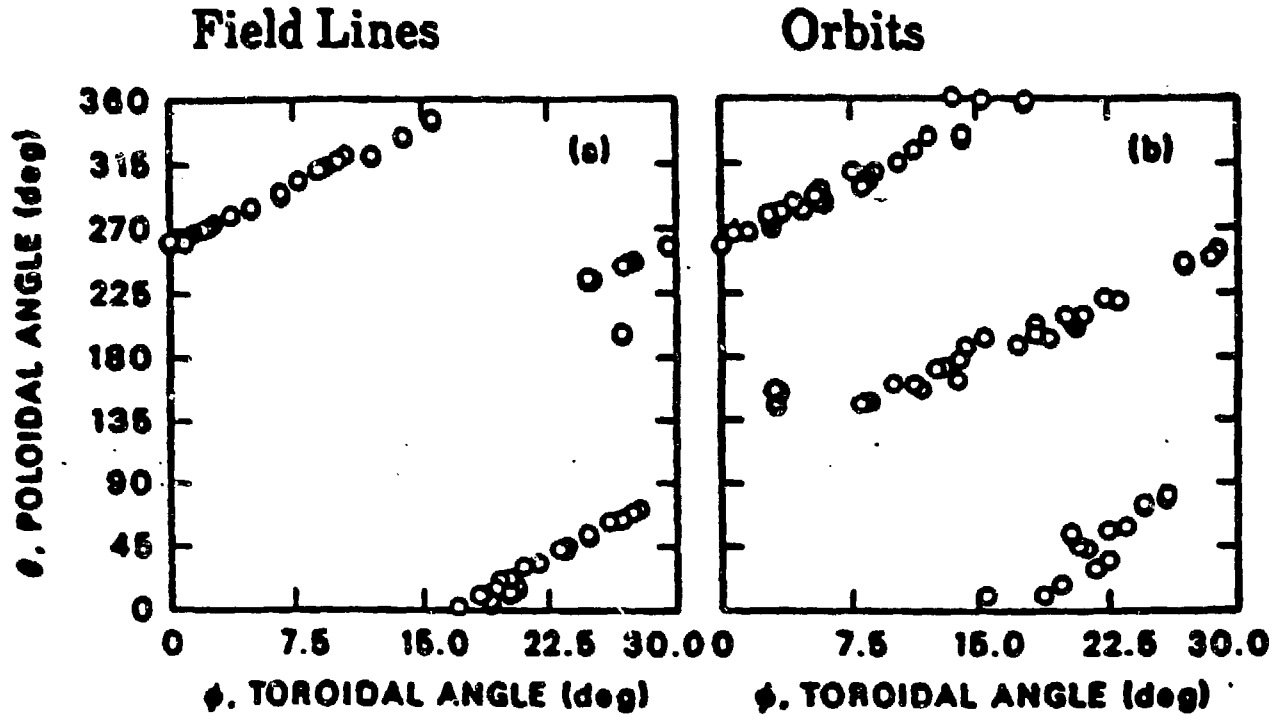

RF Heating Studies

- **Objectives are to develop long pulse (to steady state?) high-power heating**

- **Initial low-power (<0.3MW) experiments will determine optimum approach by comparing :**

  - **Fast wave (minority, 2nd harm.) launcher**
  - **Ion Bernstein wave (3/2, 2nd, 3rd, 4th harm.) launcher**

- **High power ICRF :** [W. Baity ; D. Bachelar]

  - **BBC transmitters (2MW @ 5-20MHz; upgraded to 30MHz) in FY90**

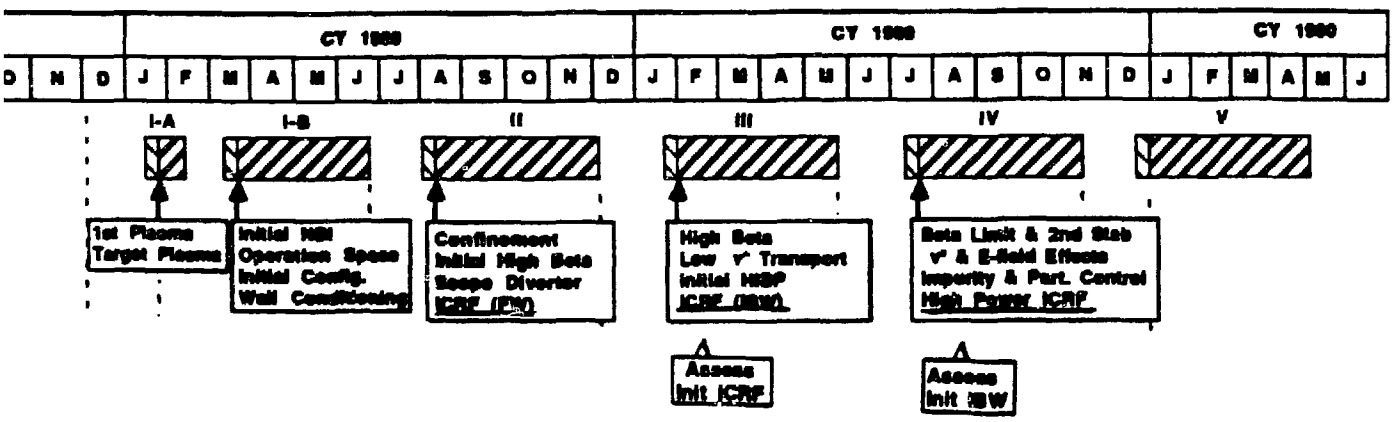

ATF ICRF Antenna

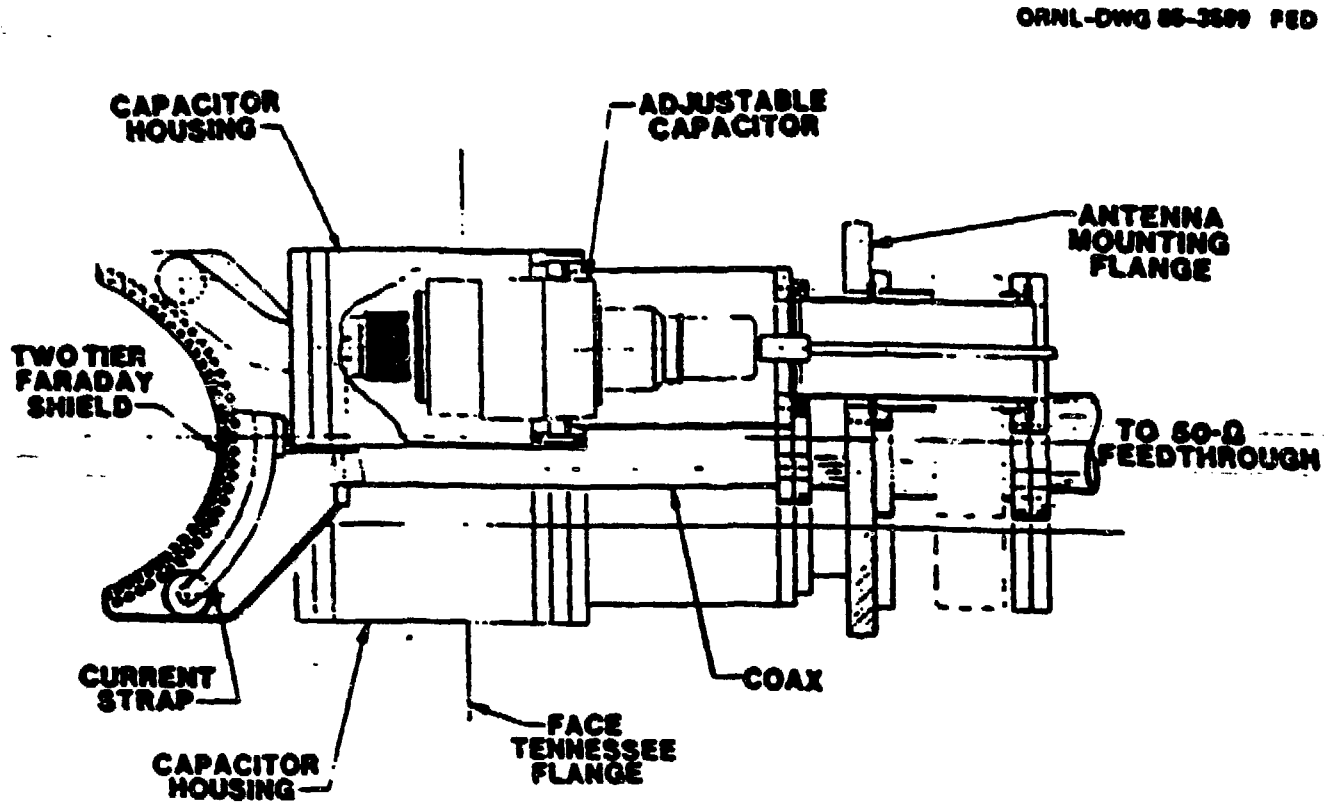

- Uses ORNL compact loop design as on D-III-D, Tore Supra, TFTR.
- Tuned by adjustable vacuum capacitors.
- Radially movable over 15 cm range.
- Uses two-tier graphite-coated Faraday shield, and graphite armor on sides of housing.

ATF MILESTONE SCHEDULE (Rev: 9-Oct-1987)

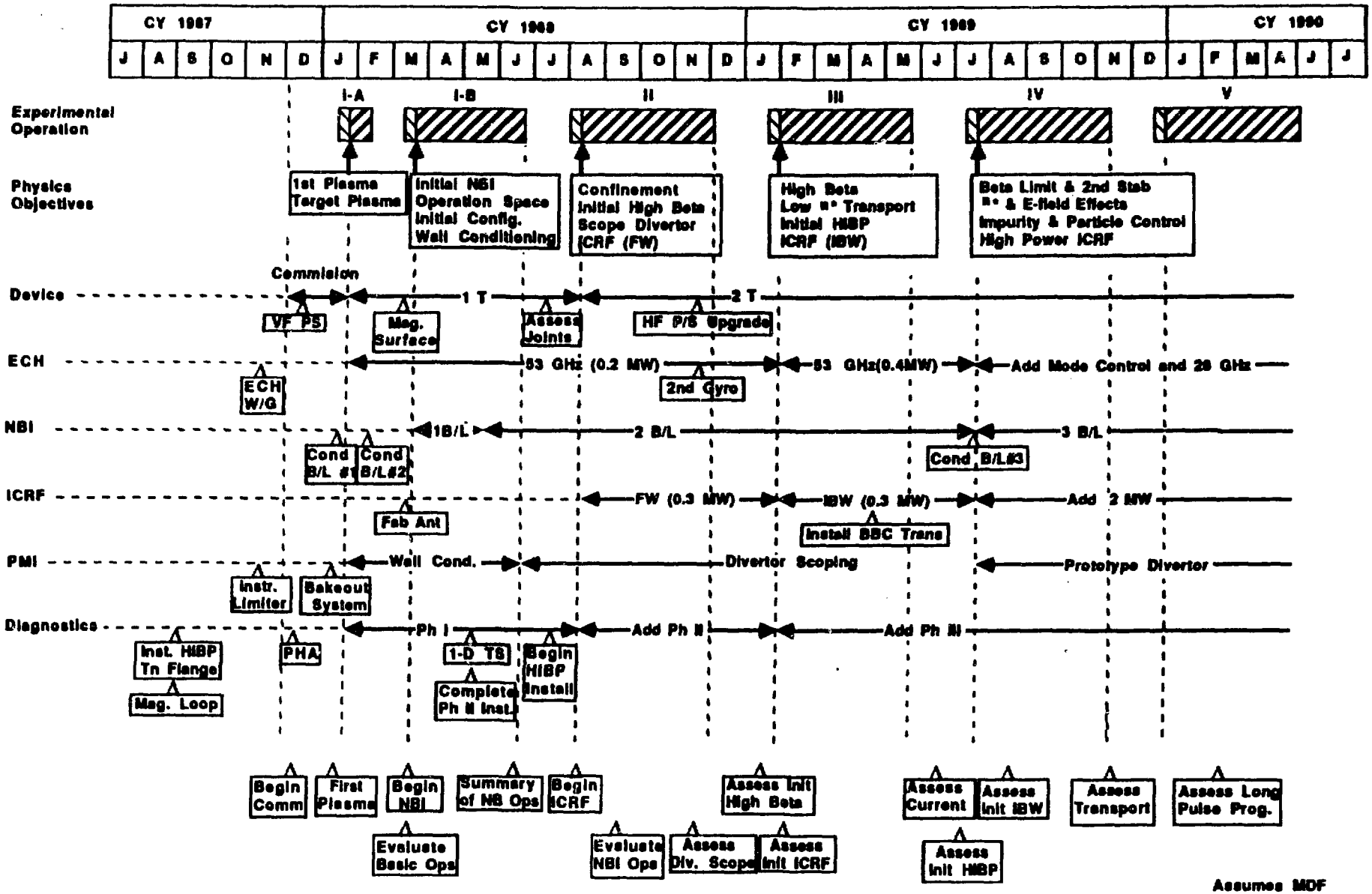

Assumes MDF Completion 12/1/87

SUMMARY

- The ATF Experimental Program is directed at better understanding and improvement of toroidal confinement through
  - Configuration Studies
  - High Beta and MHD Stability Studies
  - Transport / Role of E-field Studies
  - Edge and Particle Control Studies
  - RF Heating Studies
- The first-year program will increase hardware and physics capabilities and provide early indications for these studies.
- Collaboration with Heliotron-E and other groups has been very beneficial in formulating the ATF Program.

DIAGNOSTICS FOR ATF

Ralph C. Isler
Fusion Energy Division
ORNL

Presented at the US-Japan
Stellarator/Heliotron Workshop
Oak Ridge , 9-13 November, 1987

Phase IA Dec., 1987 – March, 1988

- Residual Gas Analyzer
- Vessel Thermocouples
- Coil Alignment Apparatus
- Electron Beam for Flux Surface Mapping
- Hard X-ray Monitor
- Neutron Monitors
- Instrumented Limter
- CCD Camera
- Magnetic Loops
  - Diamagnetic Loop
  - Full Rogowski Coil
  - Segmented Rogowski Coil
  - Rogowski Coils for Buss Bars
  - Voltage Loops
- 2 mm Interferometer
- H_α Detectors
  - Horizontal View
  - Vertical View
  - Limiter View
  - Gas Puff
  - Neutral Beam View
- Bolometers

Phase IB March, 1988 – July, 1988

- Spectrometers
  - Grazing Incidence
  - Vacuum Ultraviolet Czerny-Turner
  - Visible Czerny-Turner

- Pulse Height Analysis System

Phase II July, 1988 – Dec., 1988

- Far Infrared Interferometer
- Thomson Scattering
- Neutral Particle Analyzer
- Visible Bremsstrahlung
- Langmuir Probe
- Infrared Camera
- Soft X-ray Array
- Mirnov Loops
- Laser Ablation
- Electron Cyclotron Emission Apparatus
- Limiter/Probe-Viewing Spectrometer

Phase III After Dec., 1988

- Bolometer Array
- Surface Analysis Station
- Heavy Ion Beam Probe

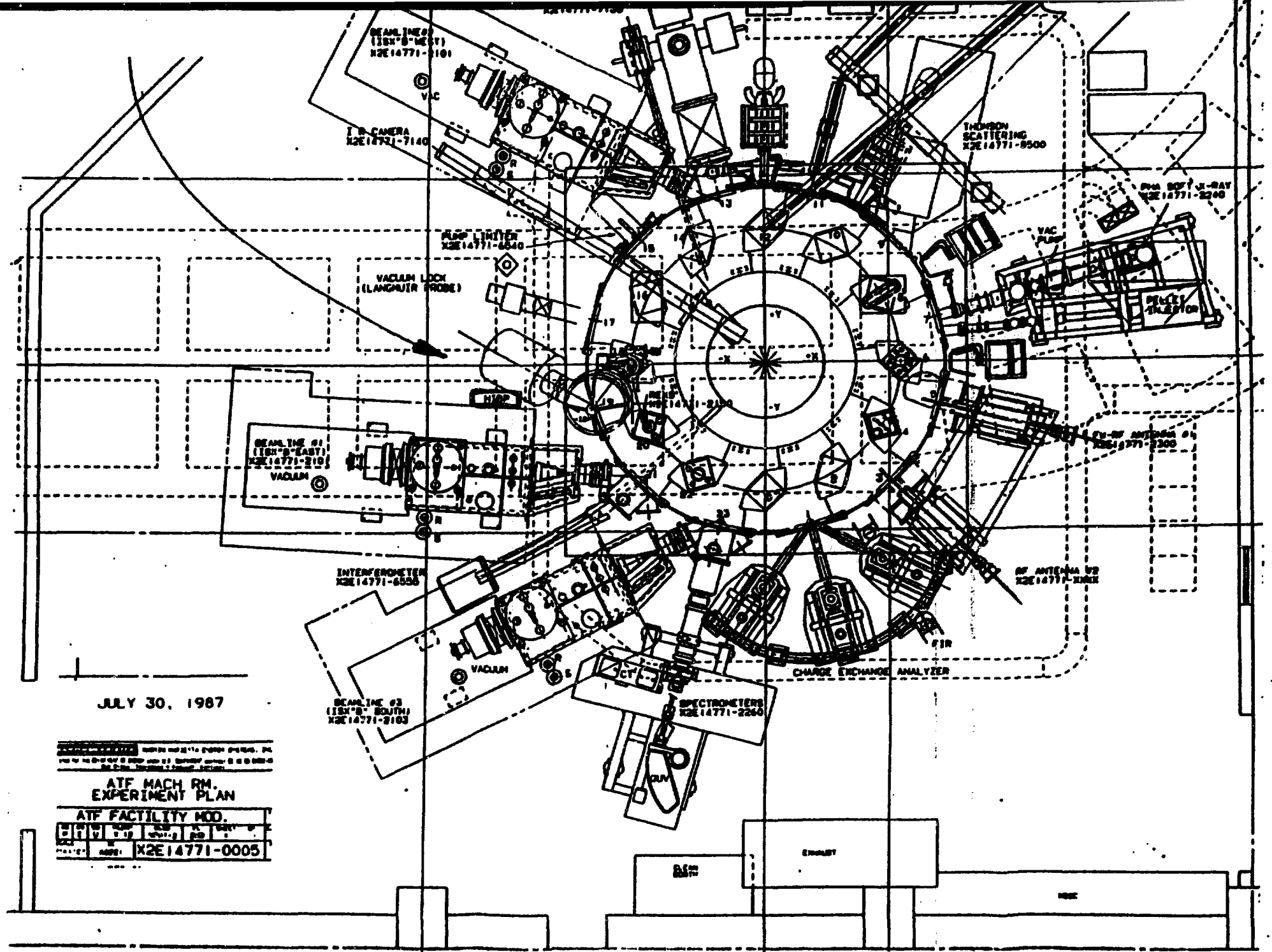
BEAMLINE #2
(18X"B"WEST)
X2E14771-3101
VAC
I.B. CAMERA
X2E14771-7140
THOMSON
SCATTERING
X2E14771-8500
PHA SOFT X-RAY
X2E14771-3240
VAC
PUMP
PELLET
INJECTION
PUMP LIMITER
X2E14771-6540
VACUUM LOCK
(LANGMUIR PROBE)
HIBP
BEAMLINE #1
(18X"B"EAST)
X2E14771-210
VACUUM
INTERFEROMETER
X2E14771-6550
RF ANTENNA #2
X2E14771-3300
FIR
VACUUM
CHARGE EXCHANGE ANALYZER
BEAMLINE #3
(18X"B" SOUTH)
X2E14771-2103
SPECTROMETERS
X2E14771-2260
DUMP
JULY 30, 1987
ATF MACH RM.
EXPERIMENT PLAN
ATF FACILITY MOD.
X2E14771-0005

THE ROGOWSKI COILS AND DIAMAGNETIC LOOP ARE FITTED INTO TUBES WHICH CONFORM TO THE VACUUM VESSEL WALLS. THESES TUBE CAN ALSO ACCOMODATE OPTICAL FIBERS SO THAT FARADY ROTATION OF A LASER LIGHT SOURCE CAN BE EXPLORED AS A TECHNIQUE FOR MEASURING MAGNETIC FIELDS.

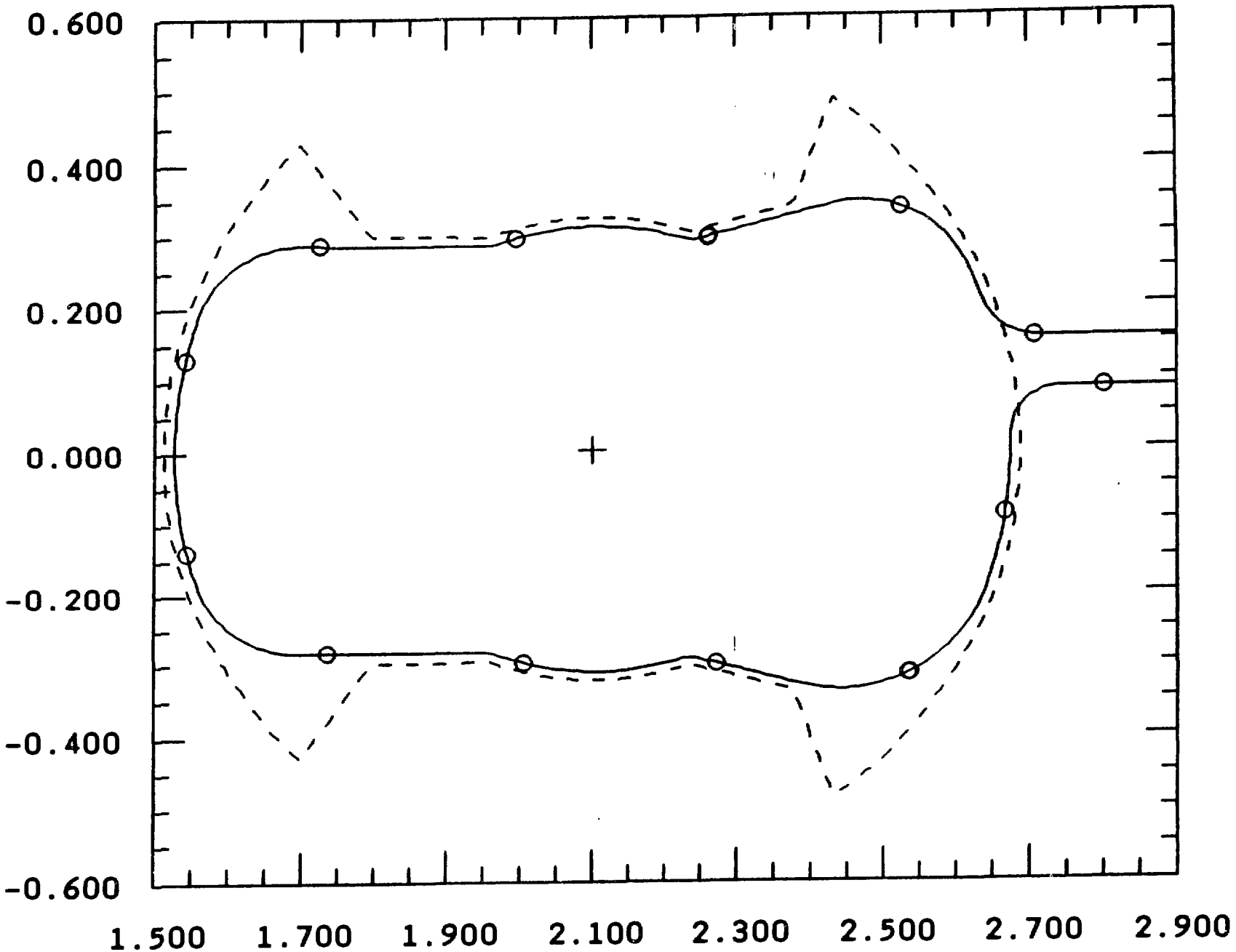
0.600
0.400
0.200
0.000
-0.200
-0.400
-0.600
1.500
1.700
1.900
2.100
2.300
2.500
2.700
2.900

BOLOMETERS INSTALLED AT 7 LOCATIONS AROUND ATF INCORPORATE 3 DETECTORS EACH. THE DETECTORS ARE MASKED TO MEASURE RADIATION FROM EITHER BROAD OR NARROW ANGULAR REGIONS.

ATF Bolometer Monitor
Sector 20, $\phi = 5°$ section
10/22/86, 4:30 PM

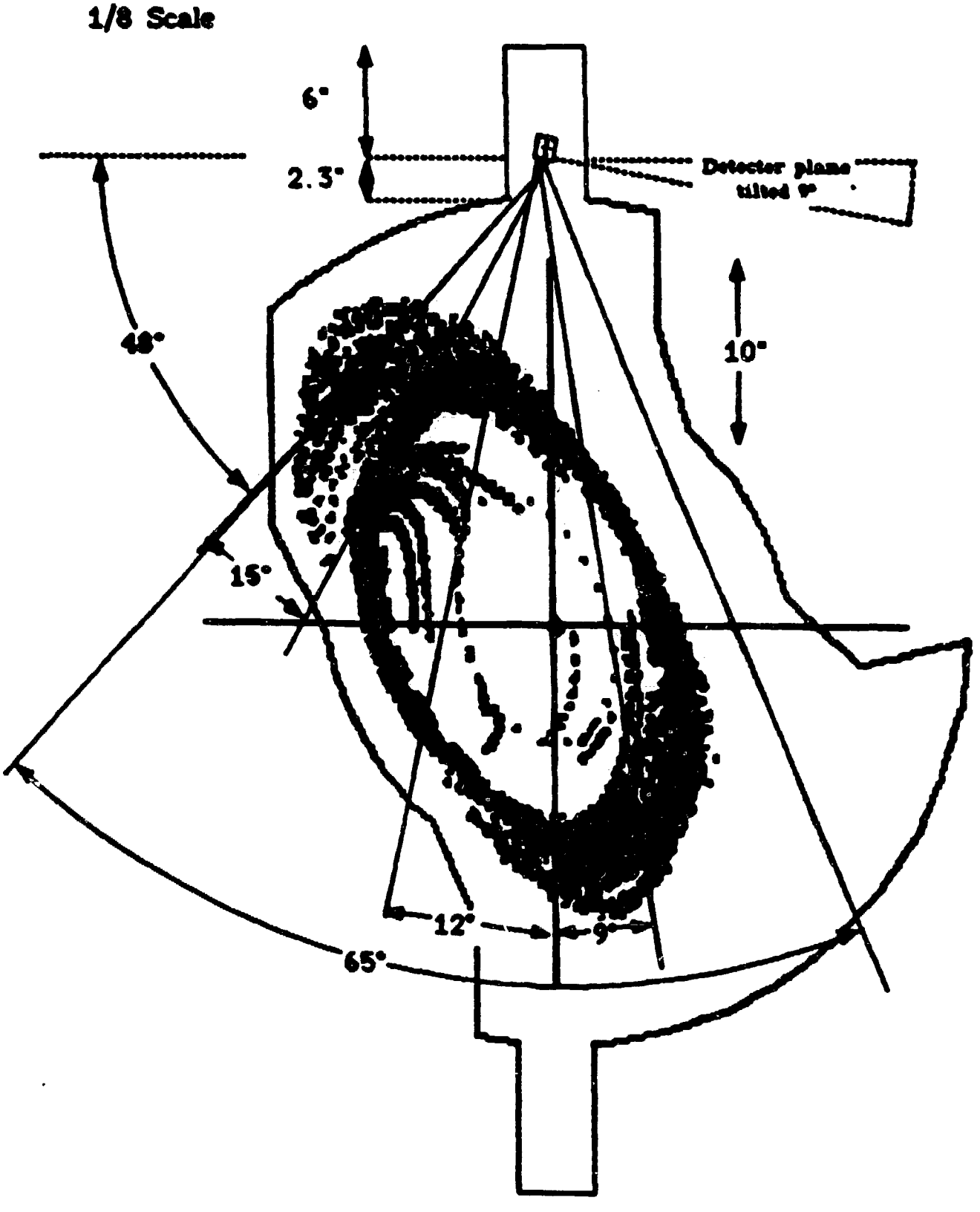

PLASMA EDGE PARAMETERS AND PLASMA MATERIAL INTERACTIONS ARE INVESTIGATED WITH LANGMUIR PROBES, CCD CAMERAS, IR CAMERAS, AND SPECTROMETERS. A MOVEABLE, INSTRUMENTED GRAPHITE PLATE IN AN OUTER RADIAL LOCATION IS EMPLOYED TO STUDY POWER LOSSES TO THE WALLS. WE WILL CONCENTRATE ON TRYING TO DETERMINE WHETHER ENERGY IS PREFERENTIALLY TRANSPORTED THROUGH THE "STRIPES".

IR Camera View of ATF Instrumented Limiter

Sector #14

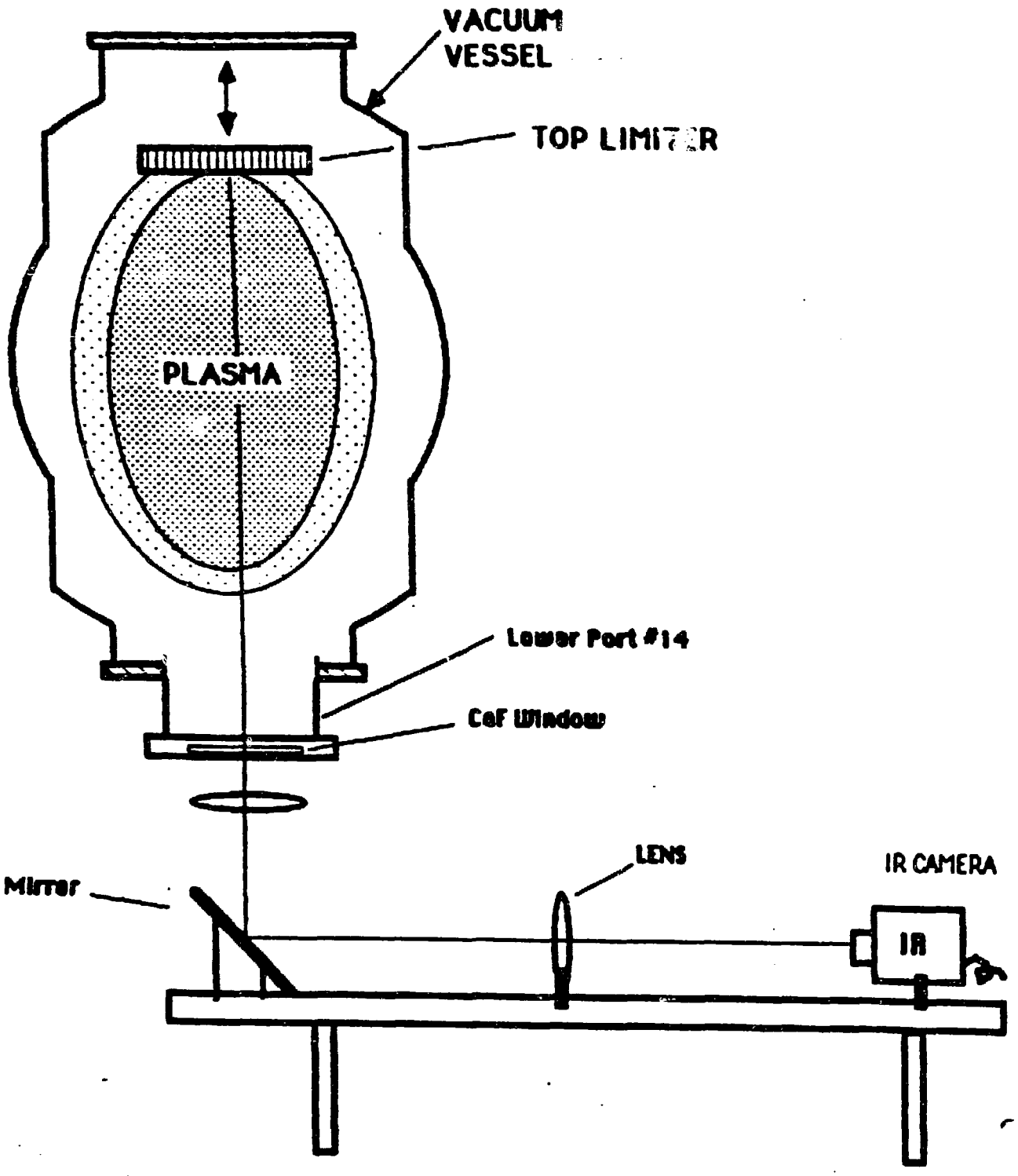

DLH 3/19/87

DIVERTOR CONFIGURATION EXPERIMENT ON ATF

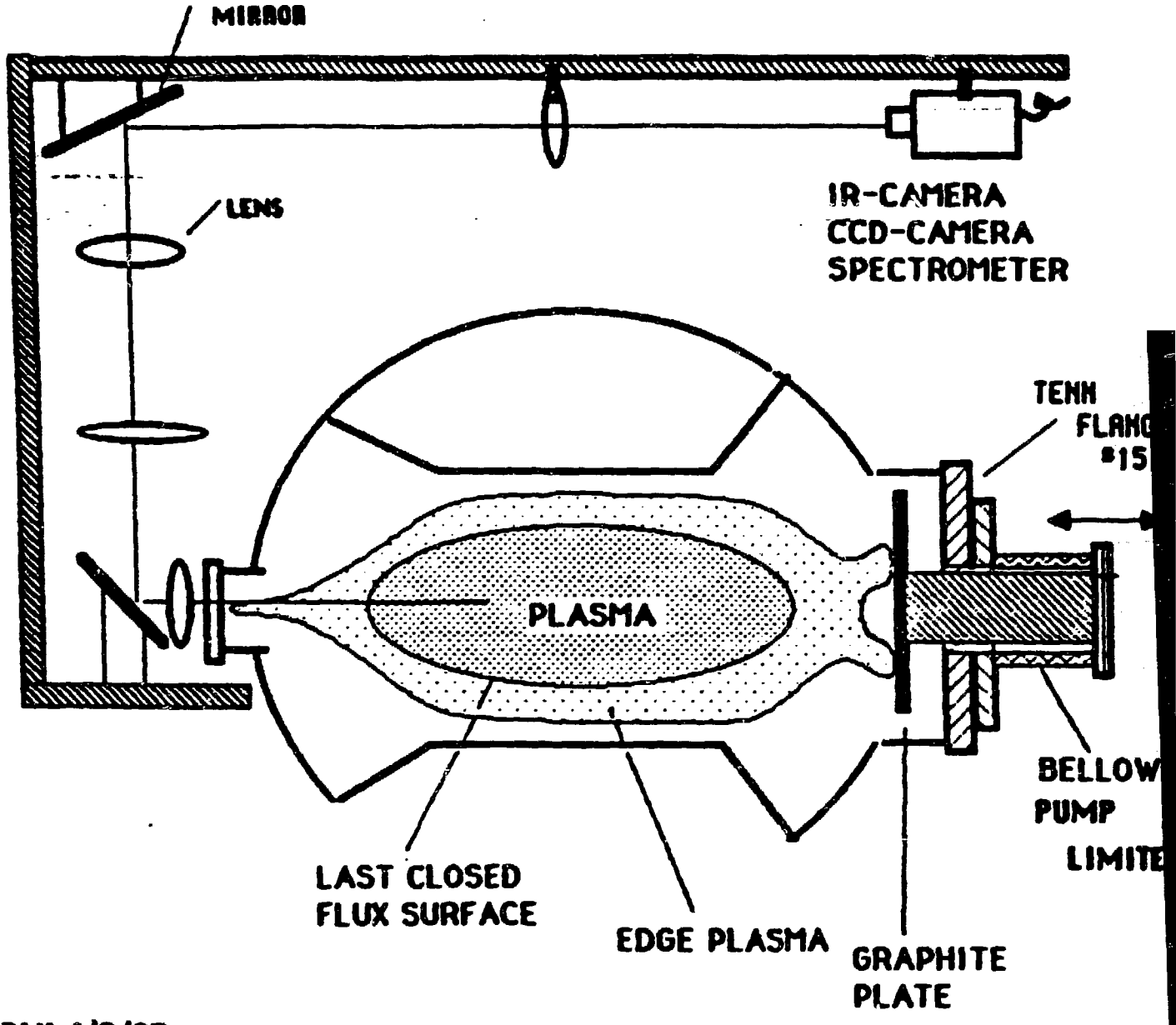

DLH 4/9/87

TENN PORT #15

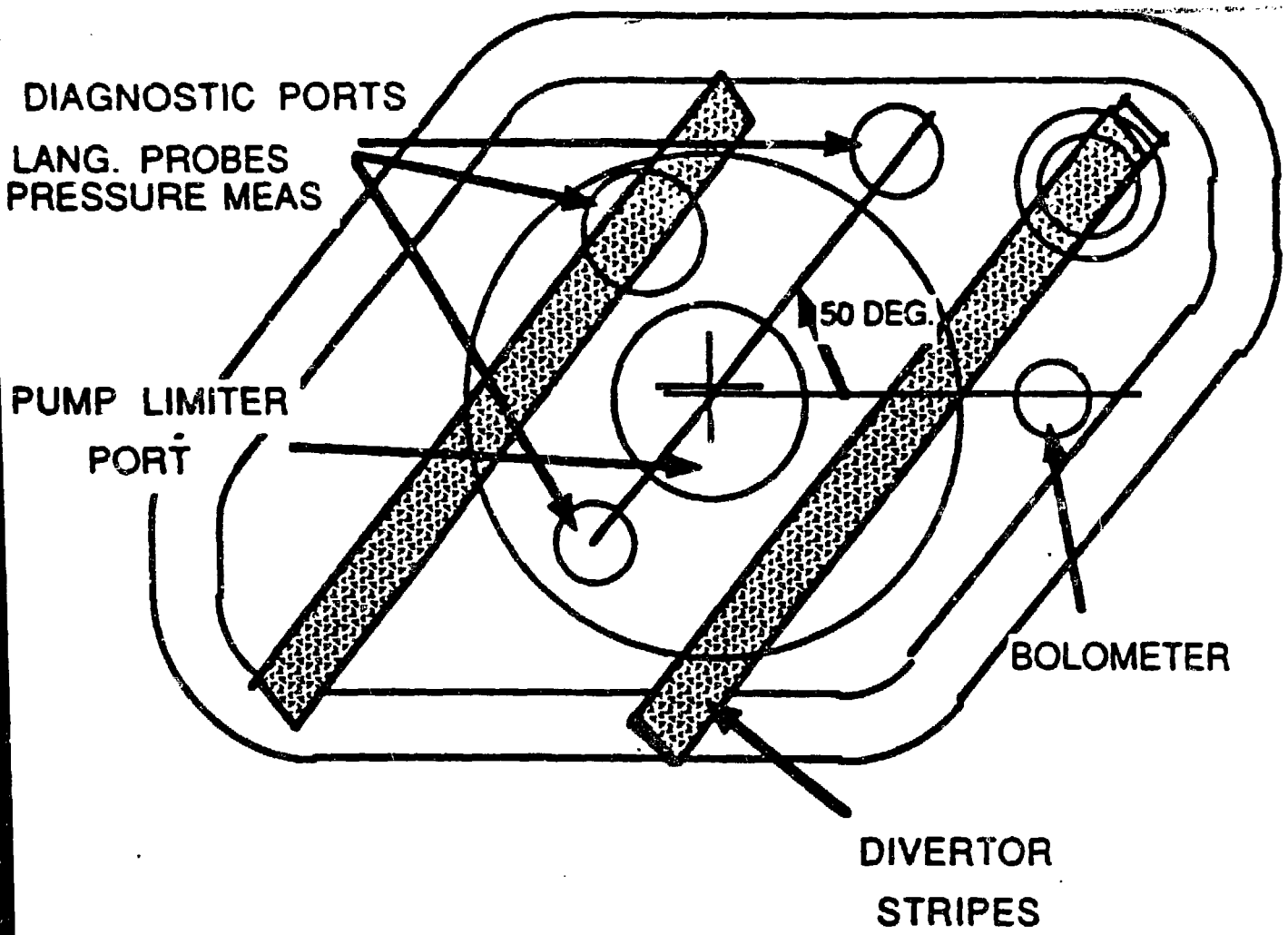

EDGE DIAGNOSTICS AND PUMP LIMITER

FOUR SPECTROMETERS ARE PLANNED FOR ATF. THE SPECTRAL REGION FROM 20 Å TO 8000 Å CAN BE UTILIZED FOR INVESTIGATING IMPURITY PRODUCTION AND CONFINEMENT. IN ADDITION, TWO OF THE INSTRUMENTS ARE ALSO SUITABLE FOR MEASURING ION TEMPERATURES AND PLASMA ROTATION FROM DOPPLER WIDTHS AND SHIFTS.

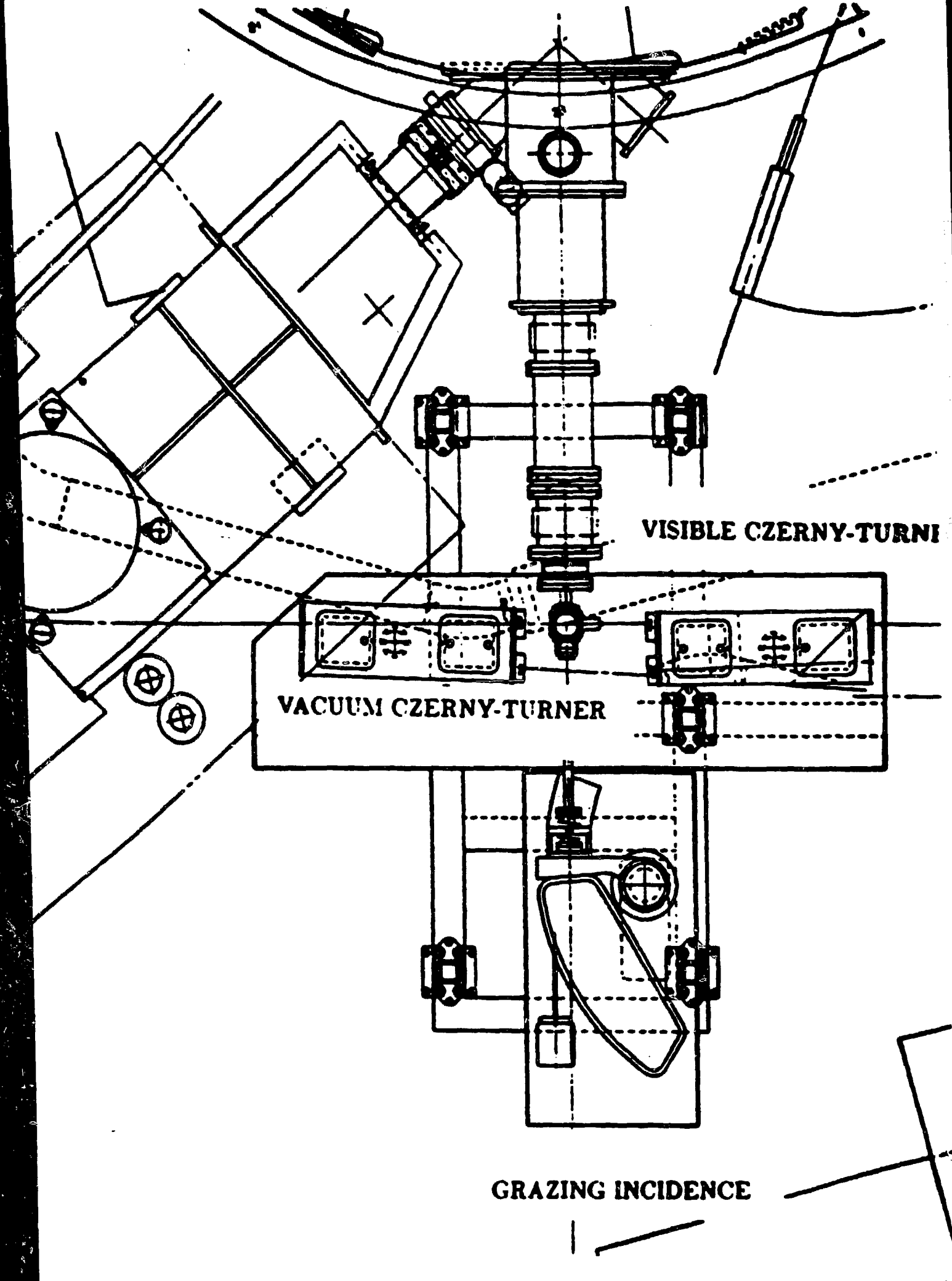
VISIBLE CZERNY-TURNI
VACUUM CZERNY-TURNER
GRAZING INCIDENCE

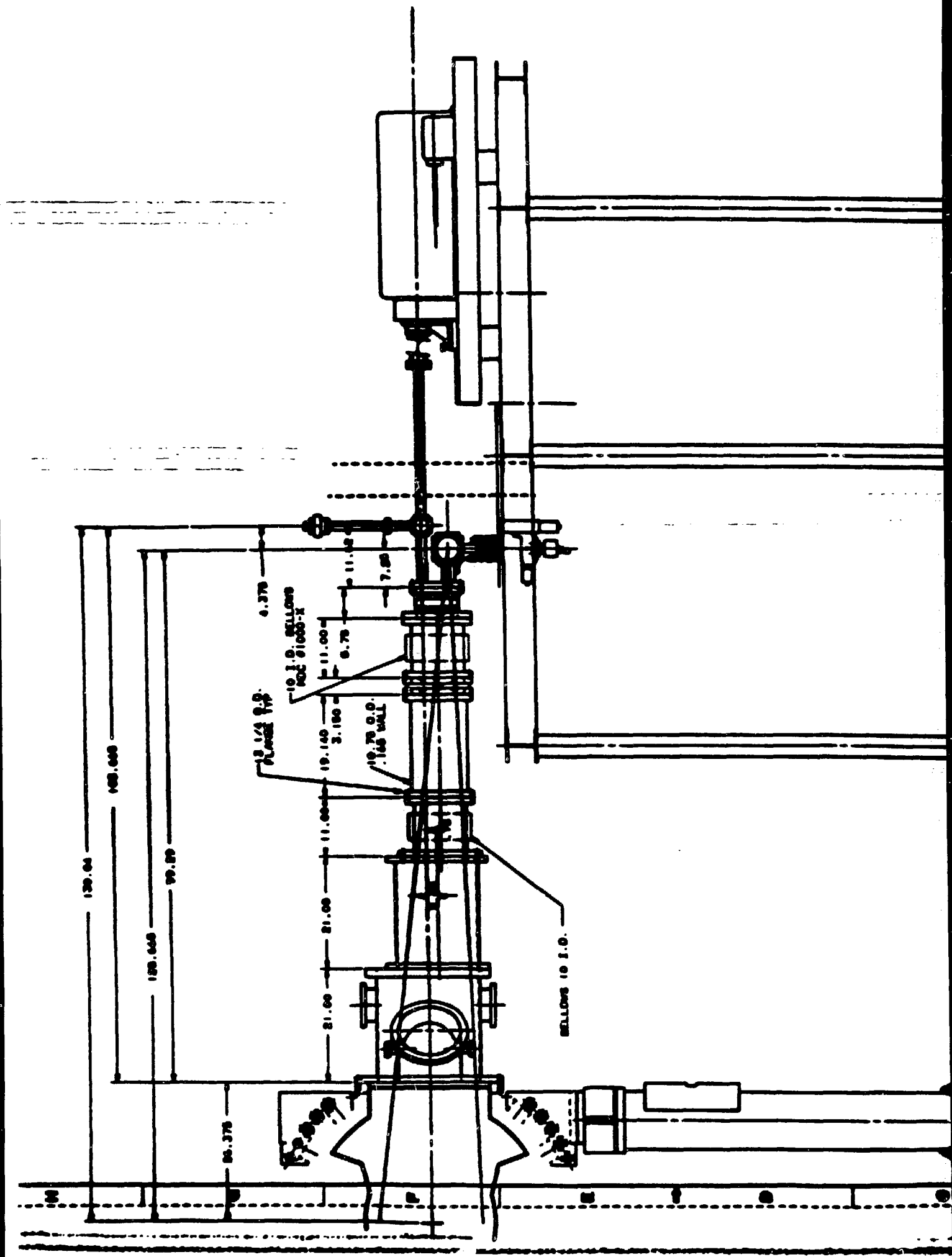

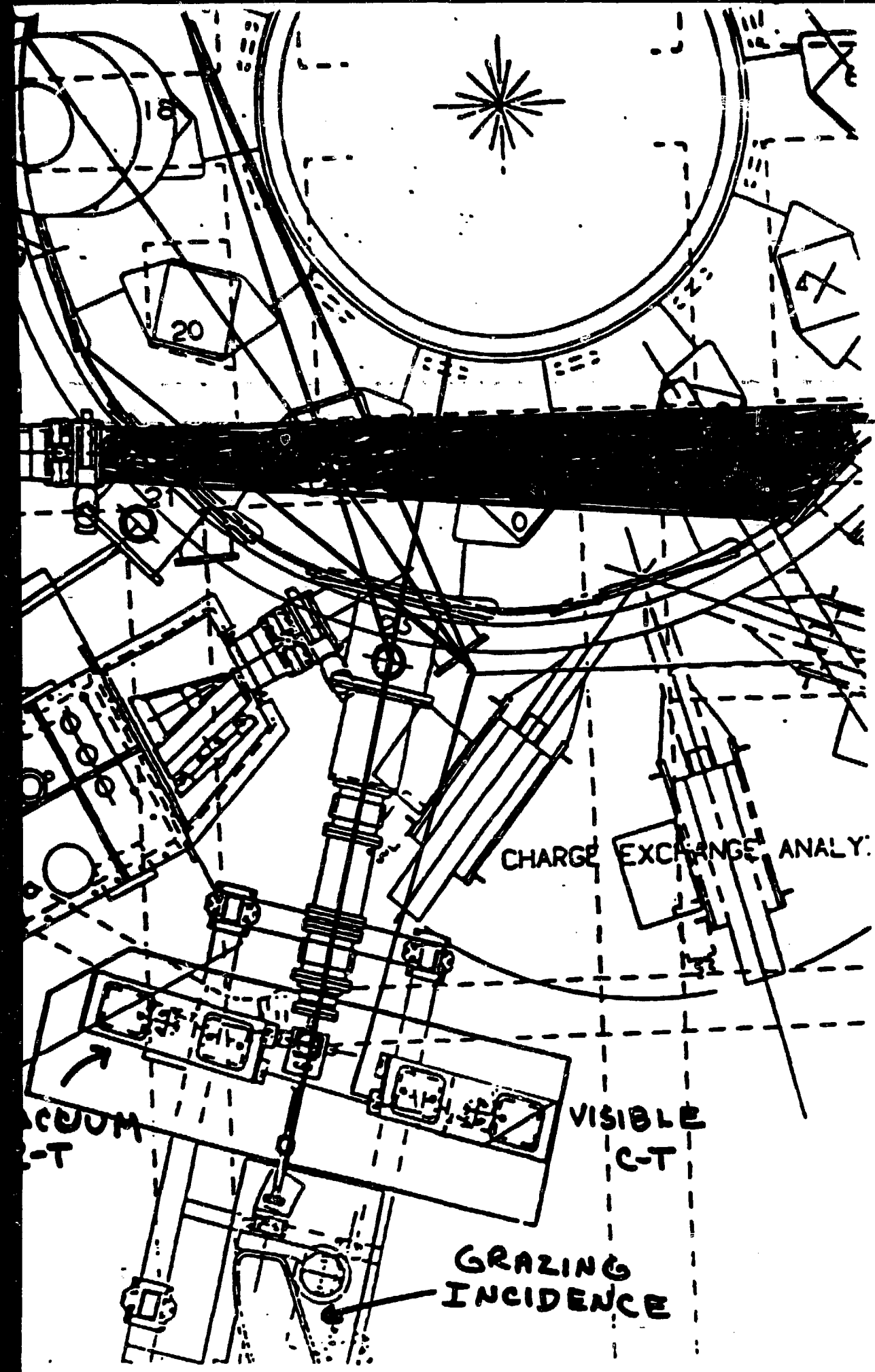
20
CHARGE EXCHANGE ANALY
VISIBLE
C-T
GRAZING
INCIDENCE

Puncture Plots Showing Spatial Resolution of the Czerny-Turner System in a Vertical Plane at R_0.

Spherical Mirror Only

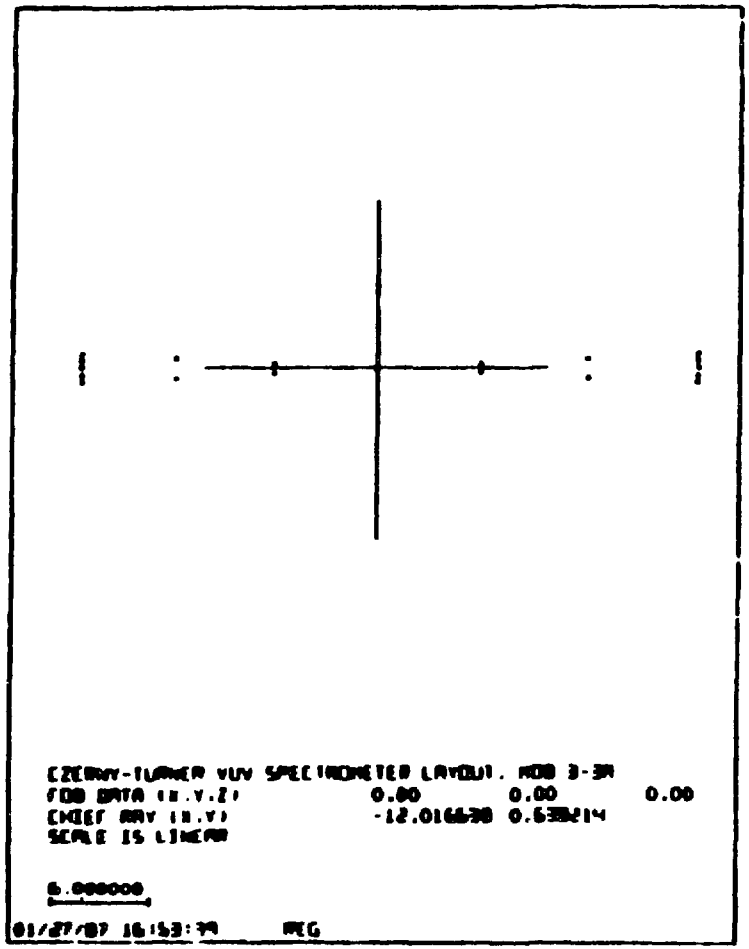

Spherical Mirror + Cylindrical Mirror

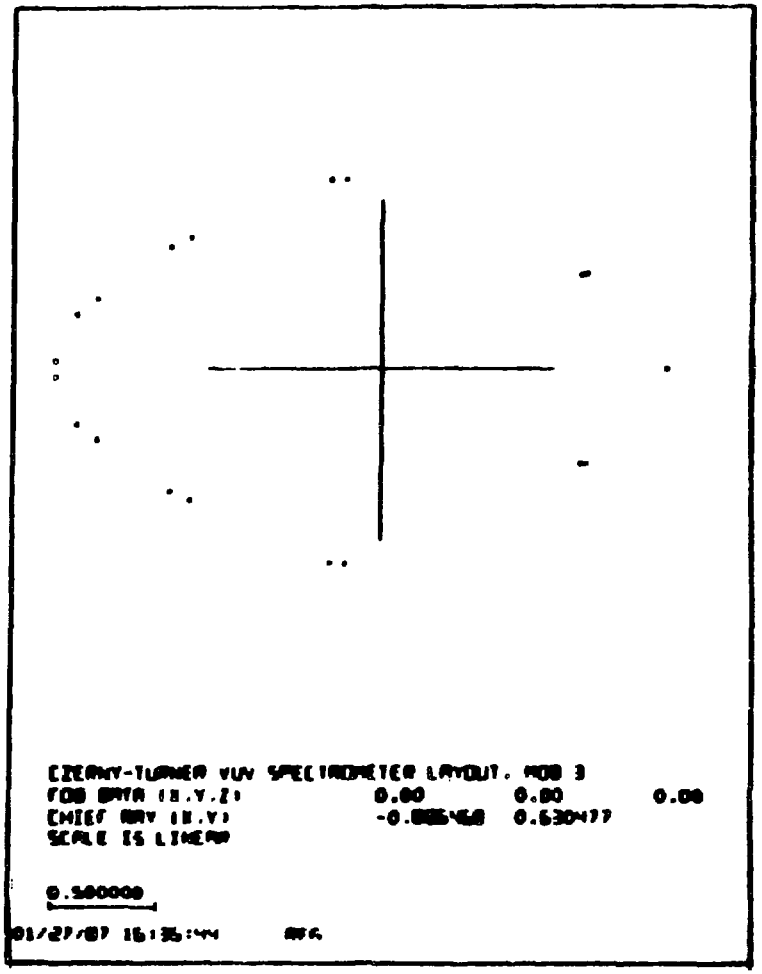

THE NEUTRAL PARTICLE ANALYZER WILL INITIALLY BE INSTALLED WITH A FIXED RADIAL VIEW. LATER, IT WILL BE MOUNTED ON A MOVEABLE STAND WHICH WILL ALLOW BOTH POLOIDAL AND TOROIDAL SCANNING OF APPROXIMATELY $\pm 45°$.

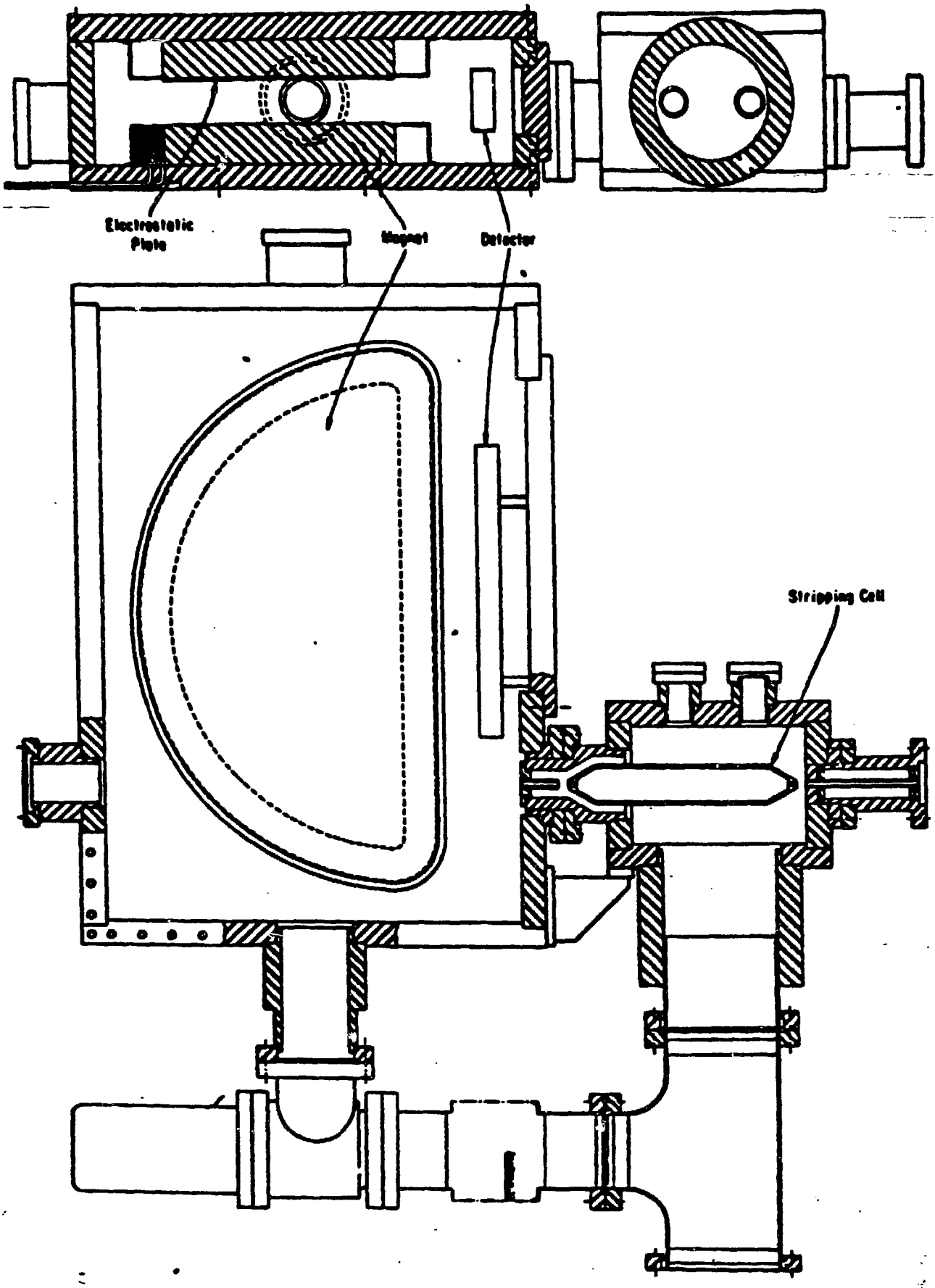
Electrostatic Plate
Magnet
Detector
Stripping Cell

A 15 CHANNEL METHYL ALCOHOL LASER OPERATING AT 119 μm with 1W STEADY STATE OUTPUT IS USED FOR ELECTRON DENSITY MEASUREMENTS. THIS DEVICE INCORPORATES A NOVEL MIRROR SYSTEM TO EXPAND THE LASER BEAM SO THAT FULL PLASMA COVERAGE IS OBTAINED.

ATF Multichannel FIR Inteferometer

15 channels, radial resolution = 3 cm

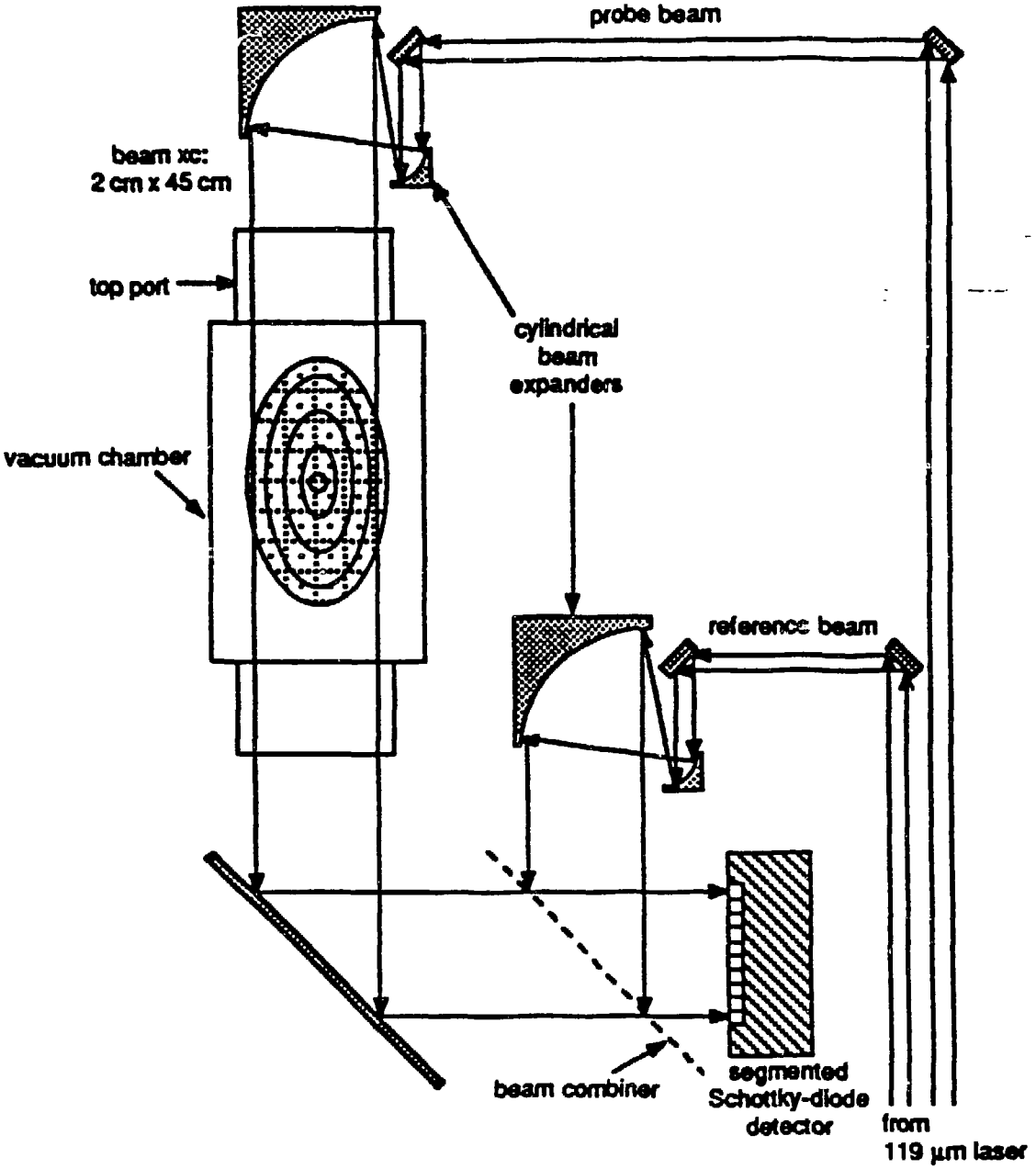

FLUCTUATIONS ARE STUDIED BY SOFT X-RAY ARRAYS AND BY HIGH AND LOW FREQUENCY MIRNOV COILS. LANGMUIR PROBE DATA AT THE PLASMA EDGE AND HEAVY-ION BEAM PROBE SIGNALS FROM THE CENTER ARE ALSO EXPECTED TO PROVIDE INFORMATION ABOUT FLUCTUATIONS OF DENSITY AND ELECTRIC FIELDS.

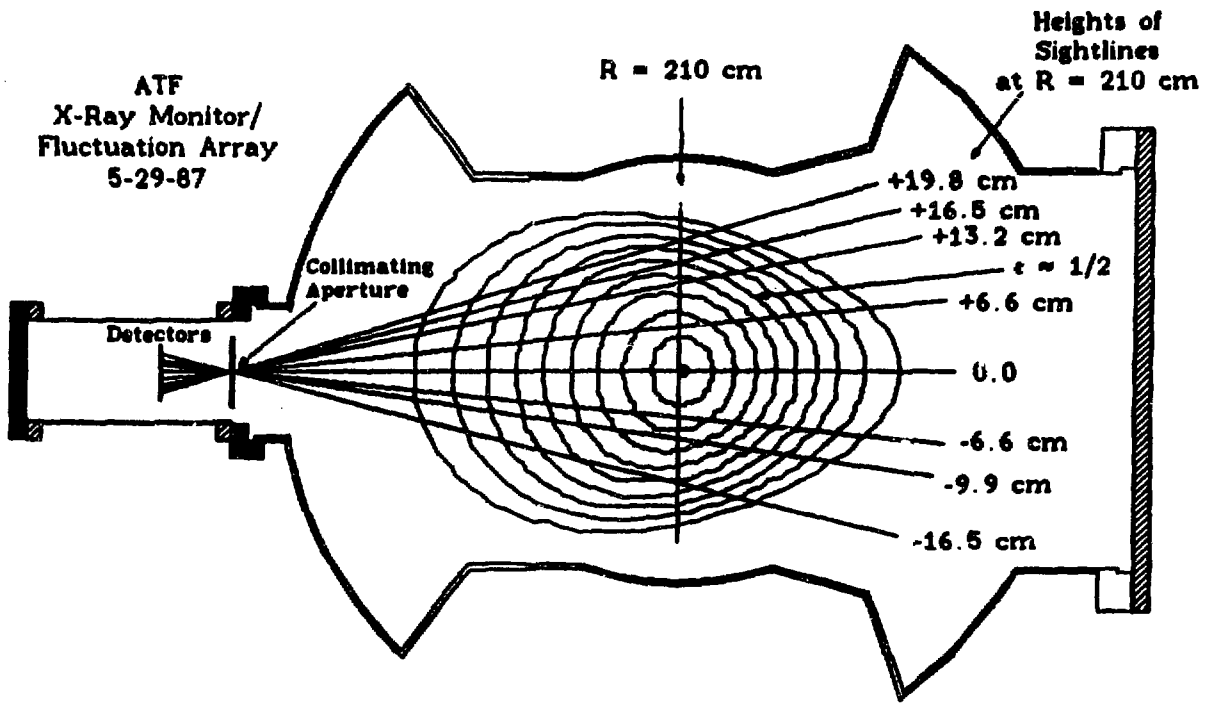
ATF
X-Ray Monitor/
Fluctuation Array
5-29-87
R = 210 cm
Heights of
Sightlines
at R = 210 cm
Collimating
Aperture
Detectors
+19.8 cm
+16.5 cm
+13.2 cm
ε ≈ 1/2
+6.6 cm
0.0
-6.6 cm
-9.9 cm
-16.5 cm

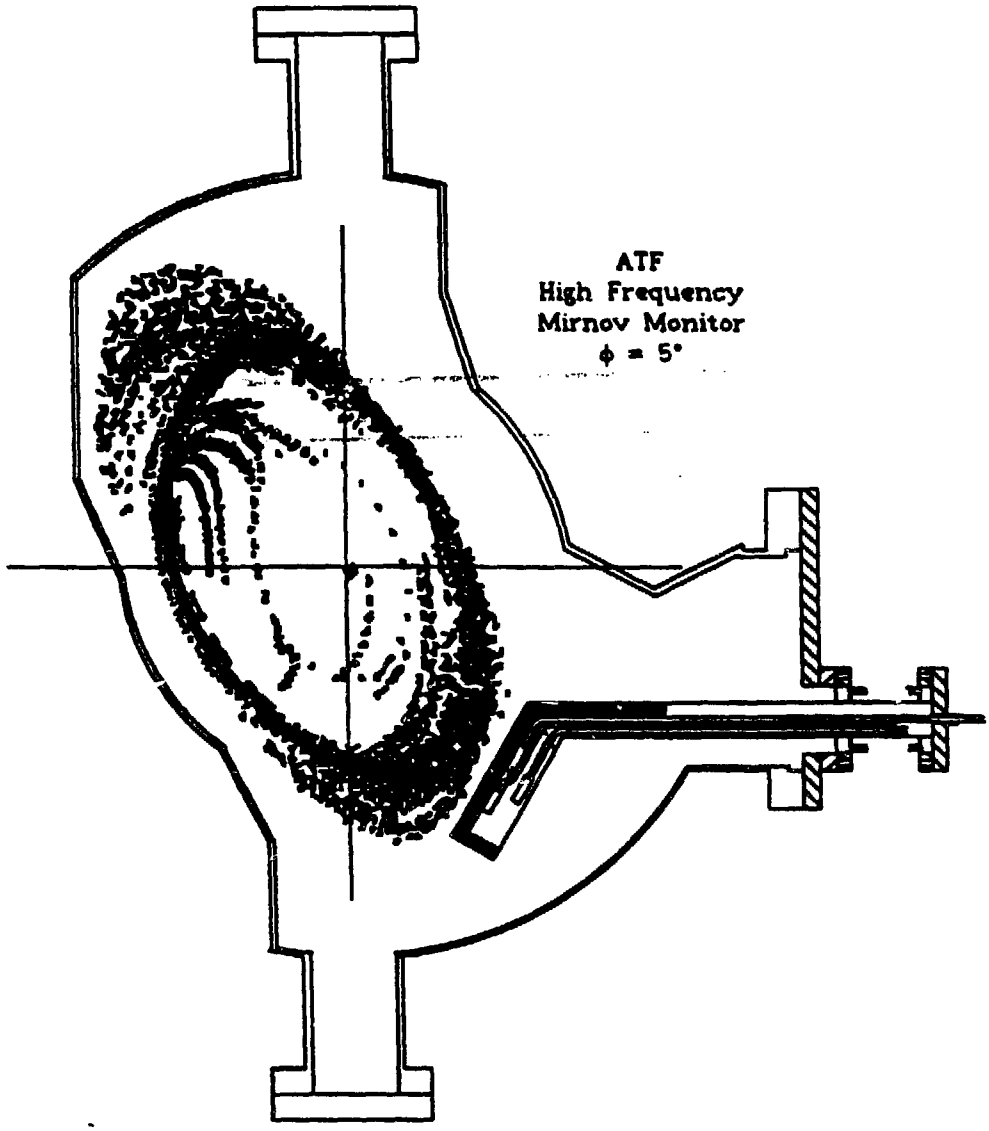
ATF
High Frequency
Mirnov Monitor
ϕ = 5°

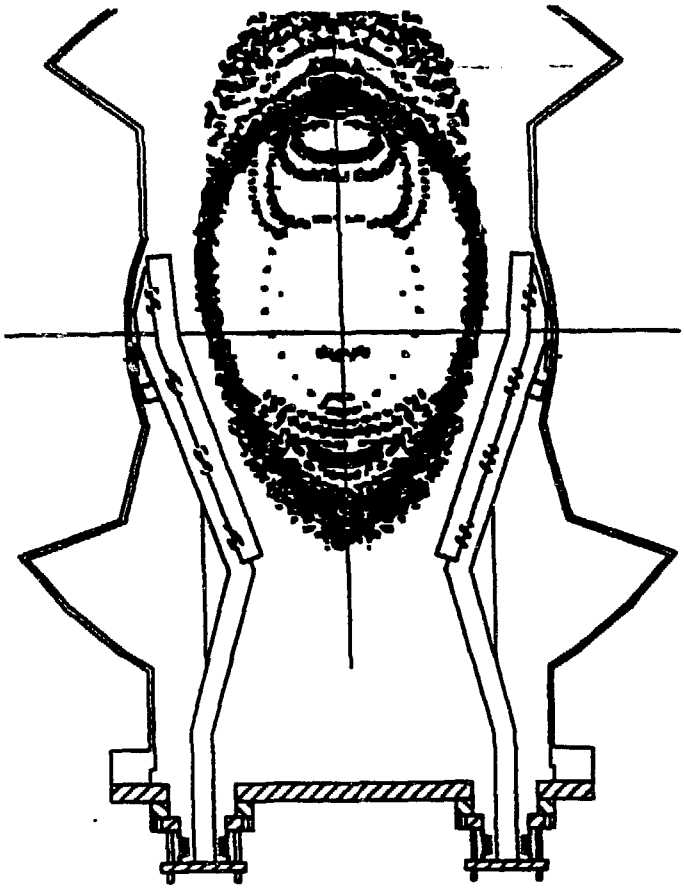

THE THOMSON SCATTERING SYSTEM USES A 20 JOULE Q-SWITCHED RUBY LASER AND IS CAPABLE OF MAKING MEASURMENTS AT 15 SPATIAL POINTS AT ONE TIME DURING A DISCHARGE. THE BEAM CAN BE SCANNED RADIALLY TO GIVE 2-DIMENSIONAL INFORMATION. AN UPGRADE TO A YAG LASER IS POSSIBLE SO THAT SEVERAL PROFILES MAY BE OBTAINED DURING A SHOT.

ATF SYSTEM OUTLINE

ORNL-DWG 88-2000R FED

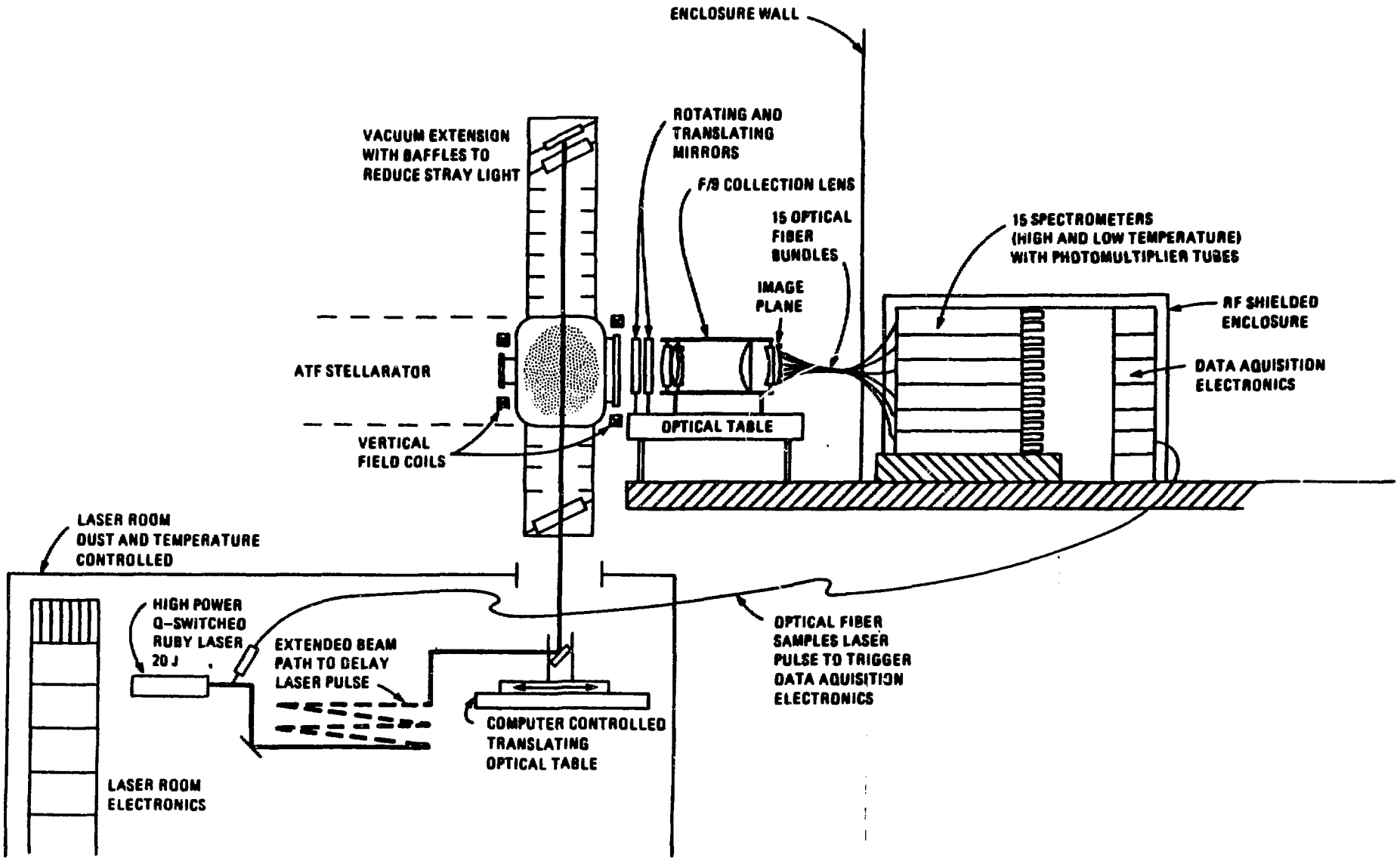

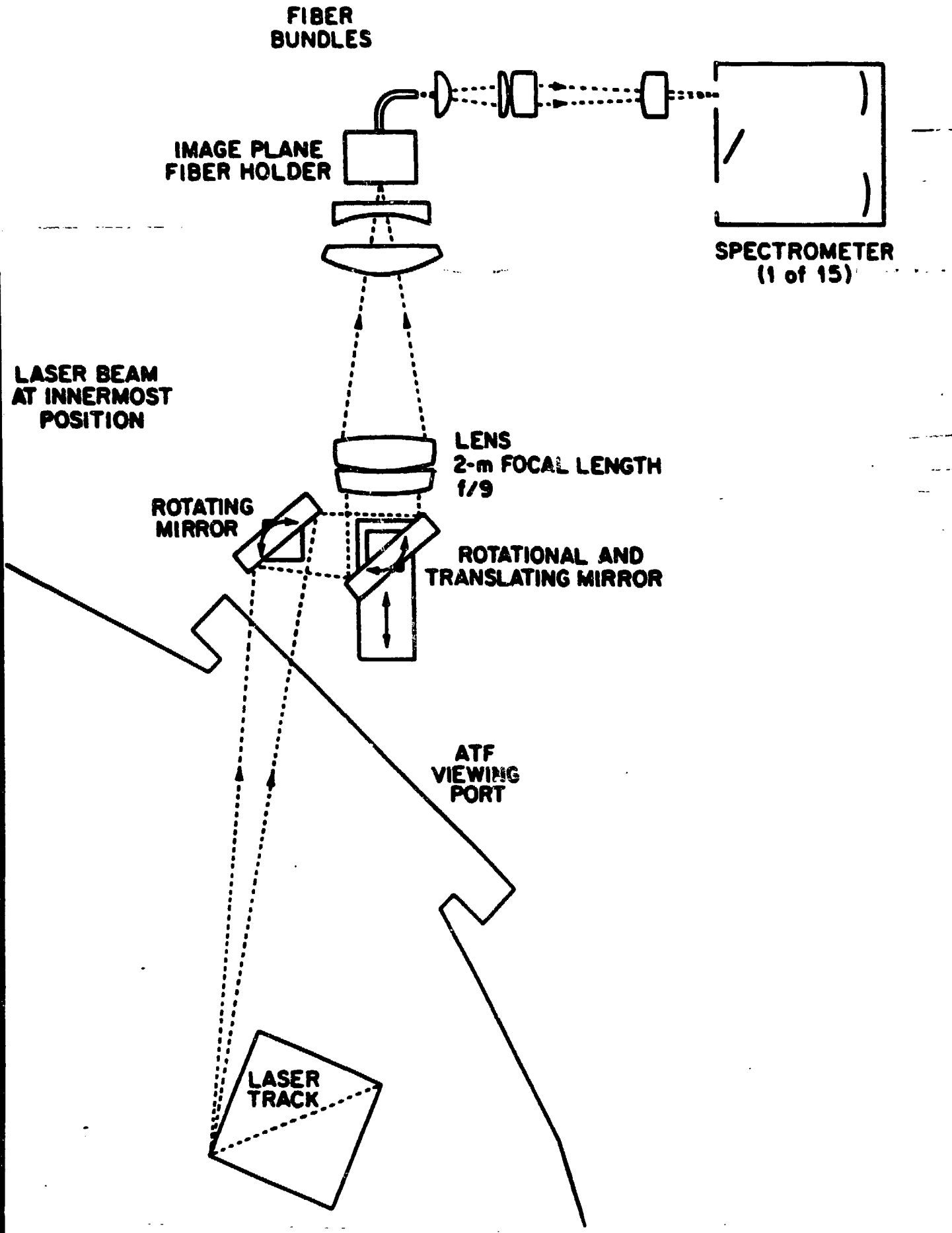
FIBER
BUNDLES
IMAGE PLANE
FIBER HOLDER
SPECTROMETER
(1 of 15)
LASER BEAM
AT INNERMOST
POSITION
LENS
2-m FOCAL LENGTH
f/9
ROTATING
MIRROR
ROTATIONAL AND
TRANSLATING MIRROR
ATF
VIEWING
PORT
LASER
TRACK

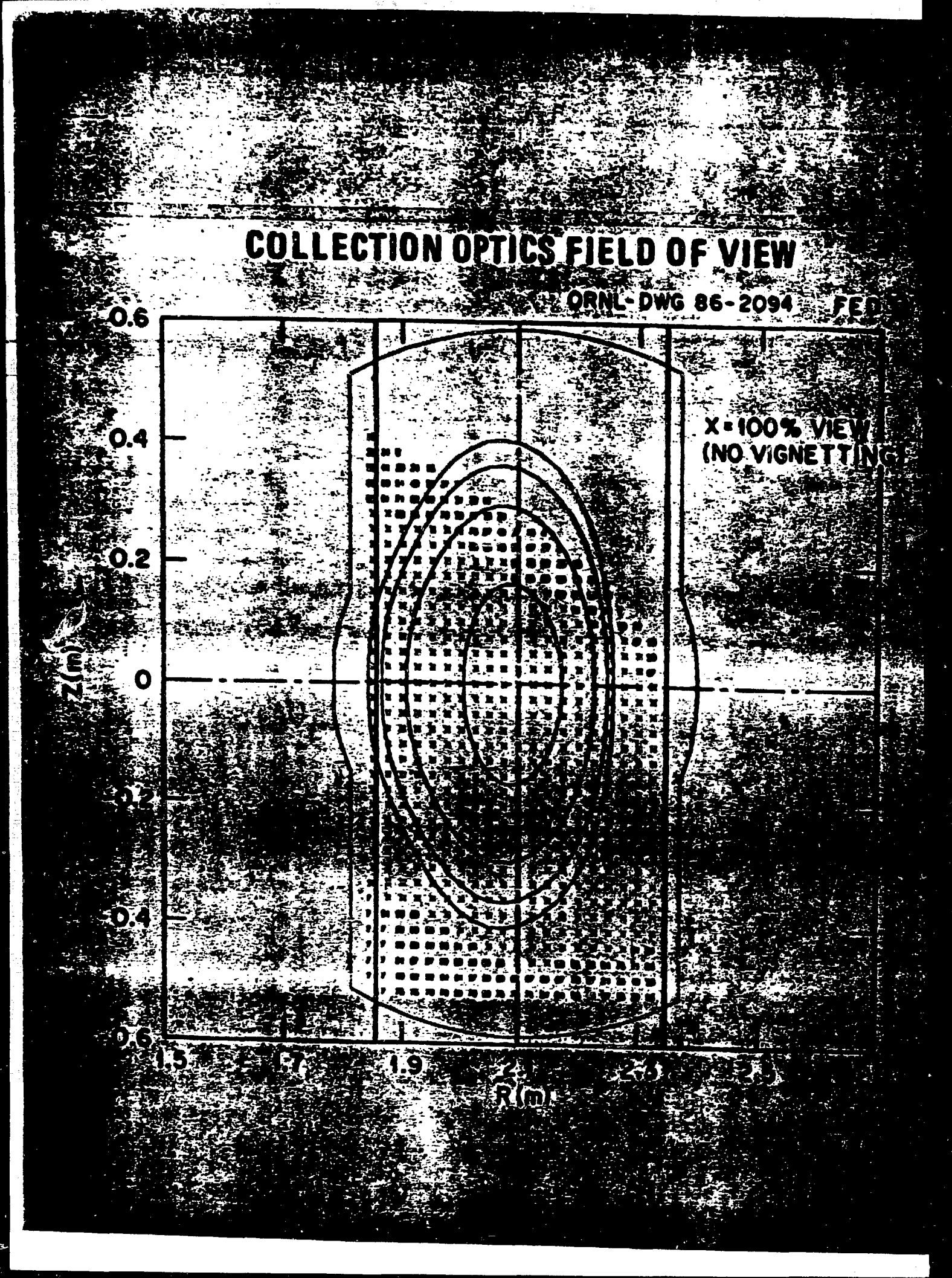
COLLECTION OPTICS FIELD OF VIEW
ORNL-DWG 86-2094
X = 100% VIEW
(NO VIGNETTING
0.6
0.4
0.2
0
0.2
0.4
0.6
Z(m)
1.5
1.9
2
R(m)

ECE Measurements

The frequency range of 67-114 GHz is covered by the combination of three recievers, with 1 GHz resolution.

The focused viewing beam is directed vertically and has a width of 6-7 cm in center of the plasma. In this view, mod-B contours are symmetric with respect to flux surfaces.

For B=.95 T,

Second harmonic is severely restricted by cutoff density.

Instead, use third harmonic, X-mode:

Cutoff censity = 5.2×10^{13} cm-3
Optically thick only near center, where dB/dz => 0, which corresponds to 79.5 GHz.
16 channel receiver covers 67-83 GHz.

Expect to get Te(0) versus time from the emission peak near 79 GHz.

For B = 1.9 T

Second harmonic, X-mode.

Cutoff density = 7.0×10^{13} cm-3
Optically thick over much of profile, covered by two recievers, 82-98 and 98-114 GHz.

Expect to get some Te(r) profile information.

Initially, only the 67-83 and 98-114 GHz recievers will be available.

16 CHANNEL FILTER BANK

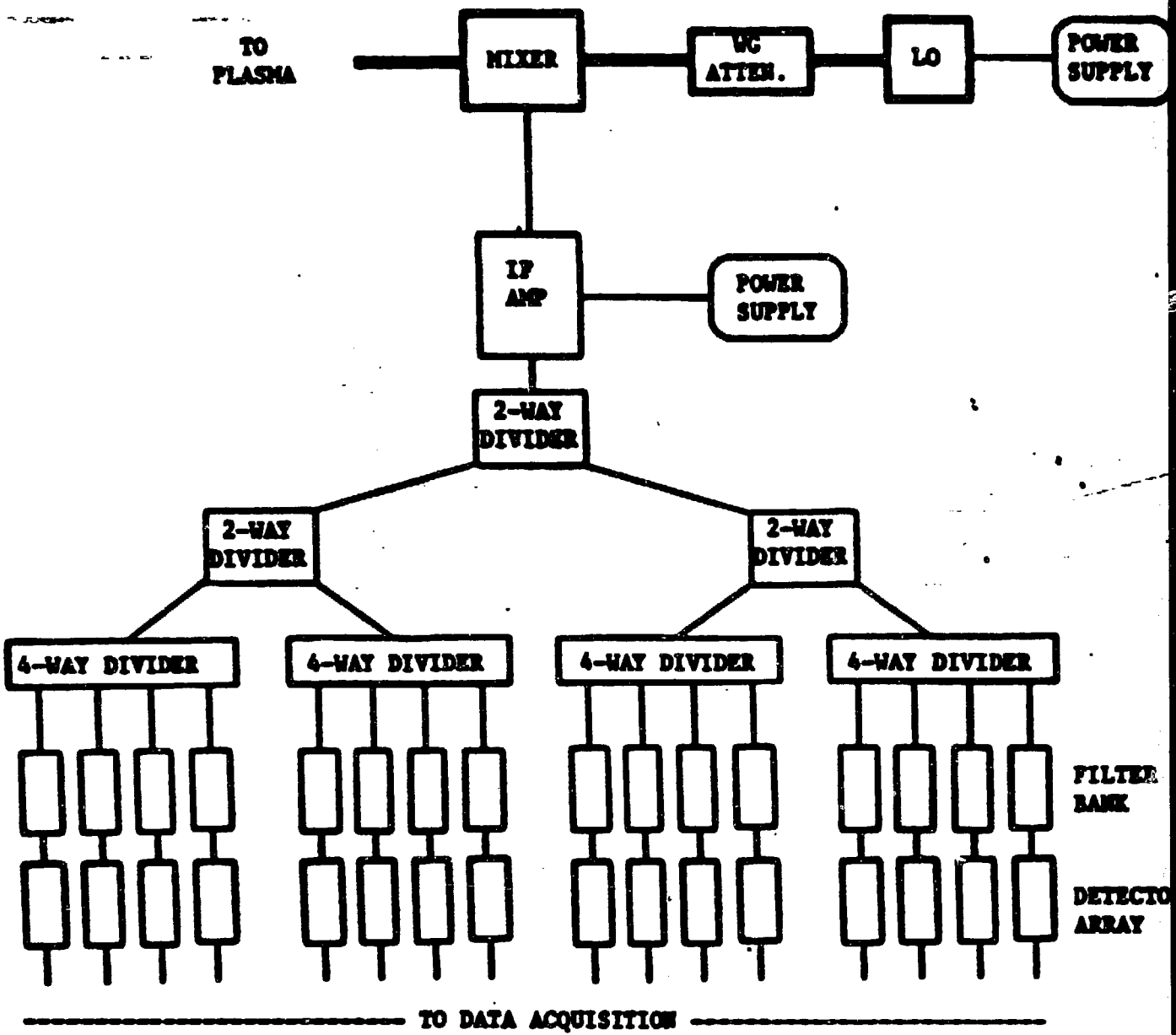

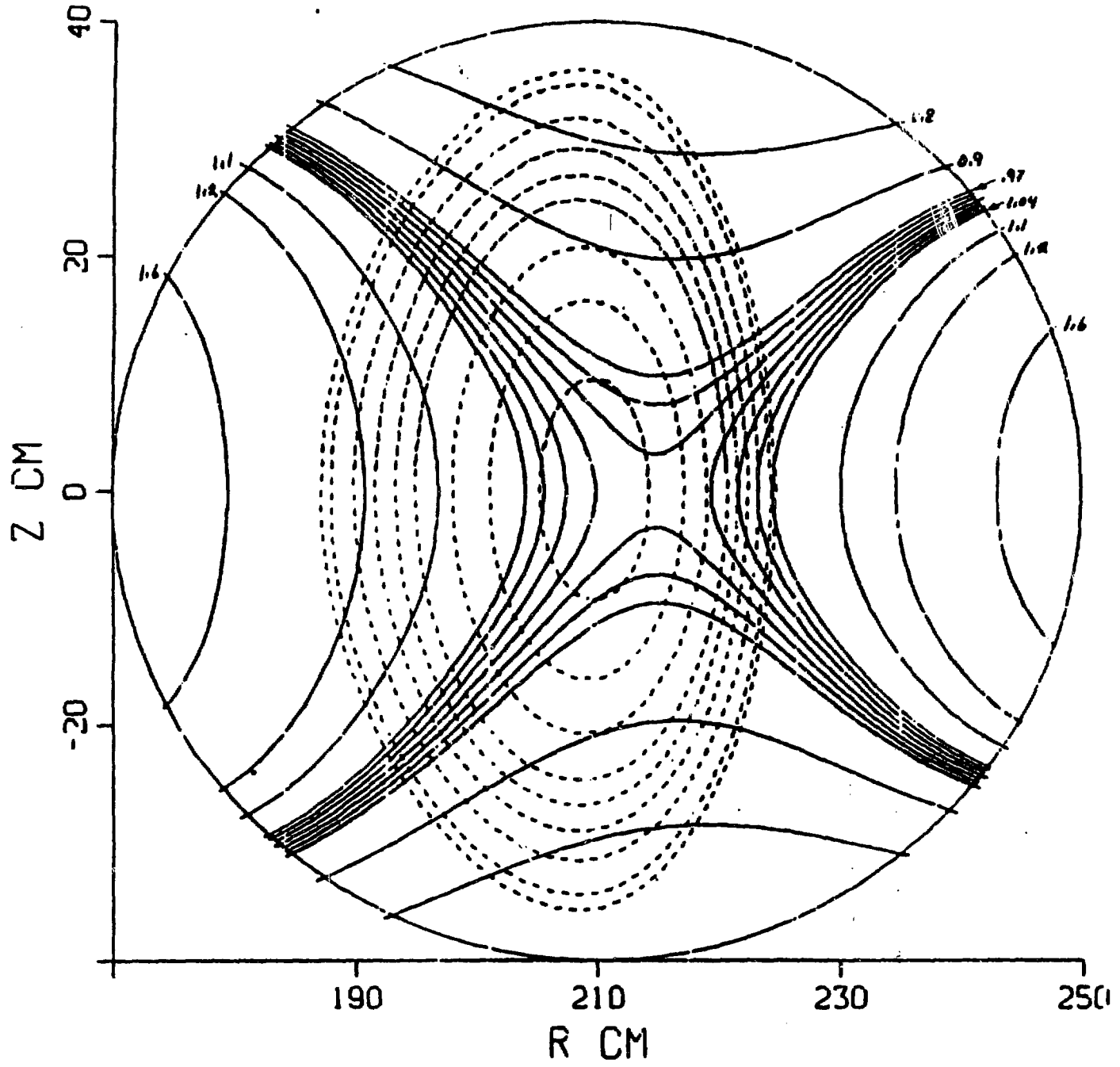
40
20
0
-20
Z CM
190
210
230
250
R CM
1.2
0.9
.97
1.04
1.1
1.14
1.6
1.1
1.2
1.6

PHYSICAL PRINCIPLE OF THE DIAGNOSTIC TECHNIQUE

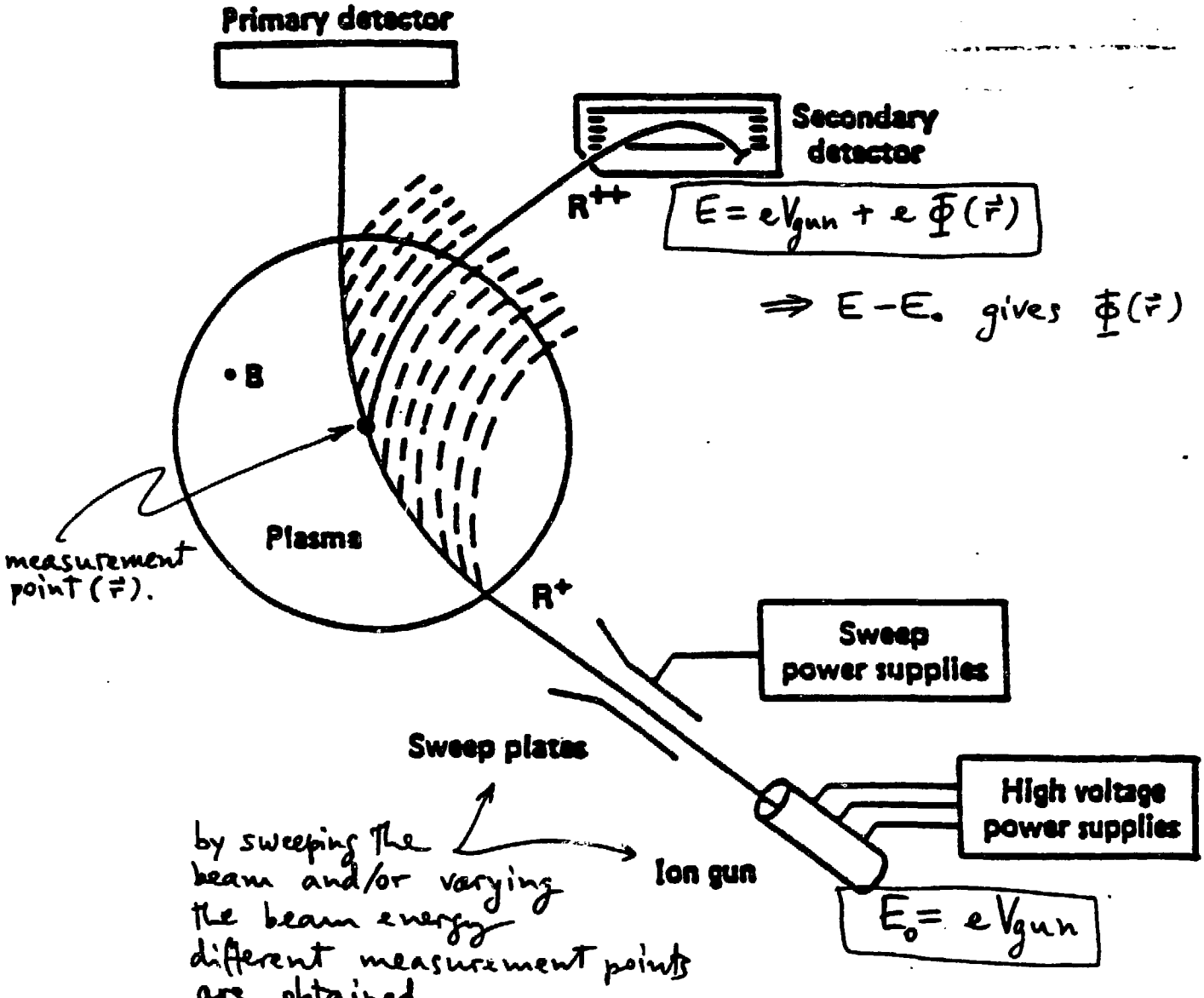

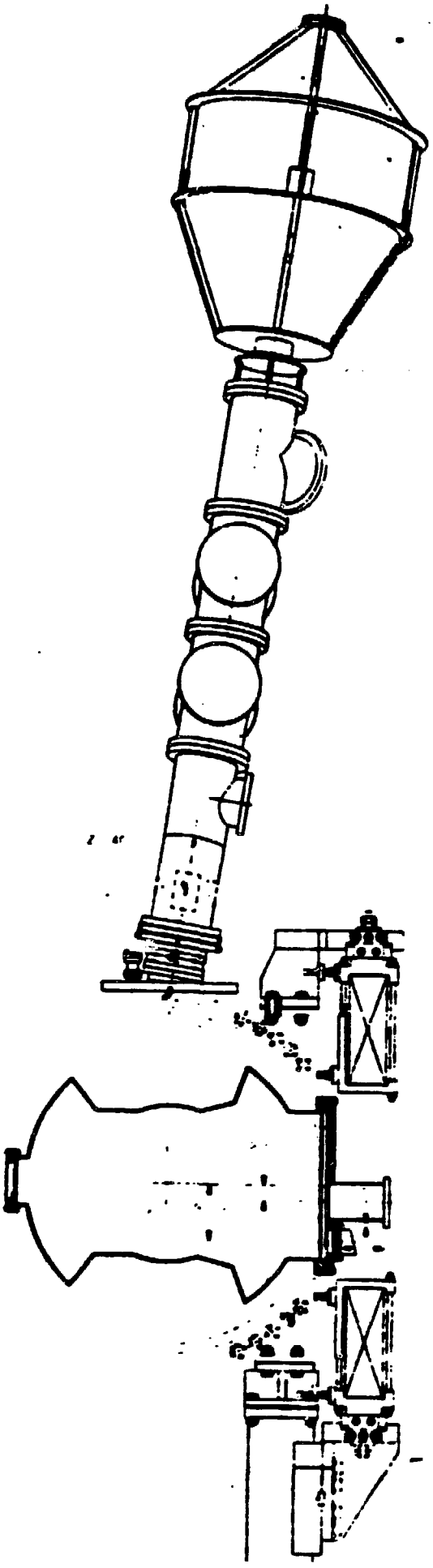

ATF/HIBP Layout

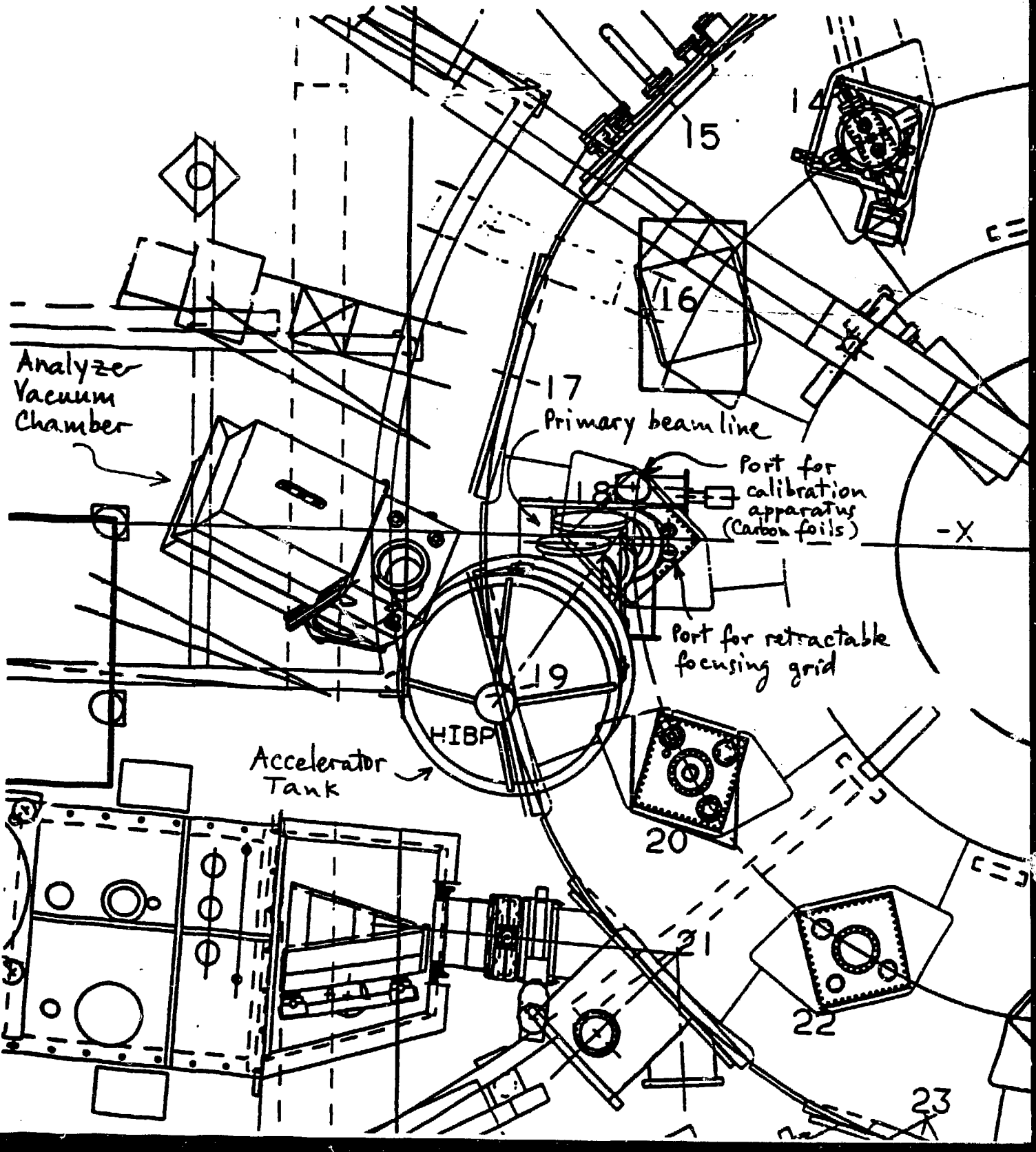

EXPECTATIONS FOR MEASUREMENT CAPABILITIES

Phase IA (ECH only)

- Flux Surface Integrity
- $\overline{n}_e$

  $\left.\right\} \tau_p^*, \tau_p$
- Hydrogen Influx
- Radiated Power (global)
- Plasma Currents
- Plasma Configuration
- Power to Limiters
- Edge parameters from Probes in Limiters

EXPECTATIONS FOR MEASUREMENT CAPABILITIES

Phase IB (ECH + NBI)

- β (diamagnetic)
- T_e (PHA) } τ_E^*
- Beam power into plasma
- T_e (PHA) } τ_E
- T_i (NPA, spectroscopy) } E_r
- Poloidal, toroidal rotation
- Impurity composition

EXPECTATIONS FOR MEASUREMENT CAPABILITIES

Phase II (ECH + NBI +ICRH)

- T_e profiles (TS)
- n_e profiles (TS, FIR)

} χ_e, χ_i, β **(kinetic)**

- Power Accountability
- T_e(t) (ECE)
- Fluctuation information (Mirnov loops, SXR, etc.)
- Impurity confinement times
- Details of impurity production
- Z_{eff}

Phase III

- fast ion distributions (NPA)
- E_r (HIBP)
- Local fluctuations (HIBP)
- P_{rad}(r)

US-Japan Stellarator/Heliotron
Workshop (Nov.9-13,1987)

Machine of Compact Helical System

CHS group (presented by K.Matsuoka)
Institute of Plasma Physics
Nagoya Univ., Nagoya, Japan

1. Status
2. HF & PF coils
3. Vacuum Vessel
4. Estimate of Error Field

MACHINE OF COMPACT HELICAL SYSTEM

CHS group (presented by K.Matsuoka)

Institute of Plasma Physics, Nagoya University, Nagoya 464, Japan

Compact helical machine characterized by small aspect ratio (Ap~5) is now under construction after detailed design in IPP, Nagoya University. To elucidate plasma transports and MHD phenomena in the low Ap regime, we are going to suppress error fields caused by several engineering reasons to the level of $\delta B/B \sim 10^{-4}$ which gives vacuum magnetic surfaces almost no perturbation. We need to pay careful attention to alignment of poloidal field coils in the final stage of construction.

HF coil conductor winding with small cross section and a lot of turn numbers has been selected. This type of winding has a relatively low packing factor(~0.6) and it is not so easy to keep a long pulse length. However, this type has several merits in ensuring the coil accuracy. No connection in the conductor eliminates the mechanically weak point and makes the coil accuracy more established. The positions of crossovers between two pies(in the direction of width) and between turn numbers(in the direction of height) are different, hence this winding configuration makes the error field extremely small.

The vacuum vessel is manufactured from forged stainless steel block by a numerically controlled machine, hence it can serve as a very accurate winding guide for HF coil. The vessel is to be completed by welding of 8 sectors(4 toroidal and 2 poloidal). Since the skew due to welding is unavoidable, we have machined the vacuum vessel again after welding. The insulator inside the guide is also machined numerically in the final stage and we are going to get the accuracy of +/- 0.5mm for HF coil guide. Nitrogen added stainless steel and electron beam welding have been used not to raise magnetic permeability in welding(μ<1.05). One turn resistance should be more than 1 mΩ for HF coil current to build up. The resistance is to be by use of Inconel 625 bellows with thickness of 0.48 mm. Protection plate against plasma bombardment is prepared.

An error field is caused by the following reasons: 1) design of feeder and crossover of coils, 2) alignment error of coils, 3) deformation of coils due to electromagnetic and thermal forces, 4) increment in magnetic permeability of vacuum vessel by welding and 5) presence of ferromagnetic materials near the machine. The error field resulting from the design of feeder and crossover of HF and PF coils is 1~2 gauss at the plasma boundary when the field strength is 1.5 Tesla. These error fields do not have any influence on vacuum magnetic surfaces, because they are not resonant with dangerous modes in addition to the small absolute value. The most dangerous error field is the horizontal field resonant with m/n=1/1 mode. This kind of field could happen by alignment error of coils. It is almost impossible to know the alignment error of HF coil conductor, so we give random displacements whose maximum value is +/- 0.5 mm to current filaments when we calculate magnetic surfaces using the Biot-Savart law. We can hardly see any disturbance on the magnetic surface when these random displacements are given. When we assume displacement or tilt of 3 mm for OVF/TVF coil whose major radii are 1.5 m (normalized accuracy is 0.2%), the resulting dipole moment δm is about $5\times10^{3}A.m^{2}$, hence this gievs the horizontal field of several x 10^{-4} Tesla whose normalized value $\delta B/B$ is about 5×10^{-4}. This field results in disturbances on magnetic surfaces. The alignment accuracy of PF coils can be improved in constructing them because we can estimate the accuracy through magnetic field measurements(horizontal and vertical components) around the major axis and can compensate the positions if there is any misalignment. Hence the final accuracy is expected to be within 1mm/1.5m, and in this case we can not see any legible disturbance on the magnetic surface.

<< Compact Helical System >> 87-03-07 <17:34:23>

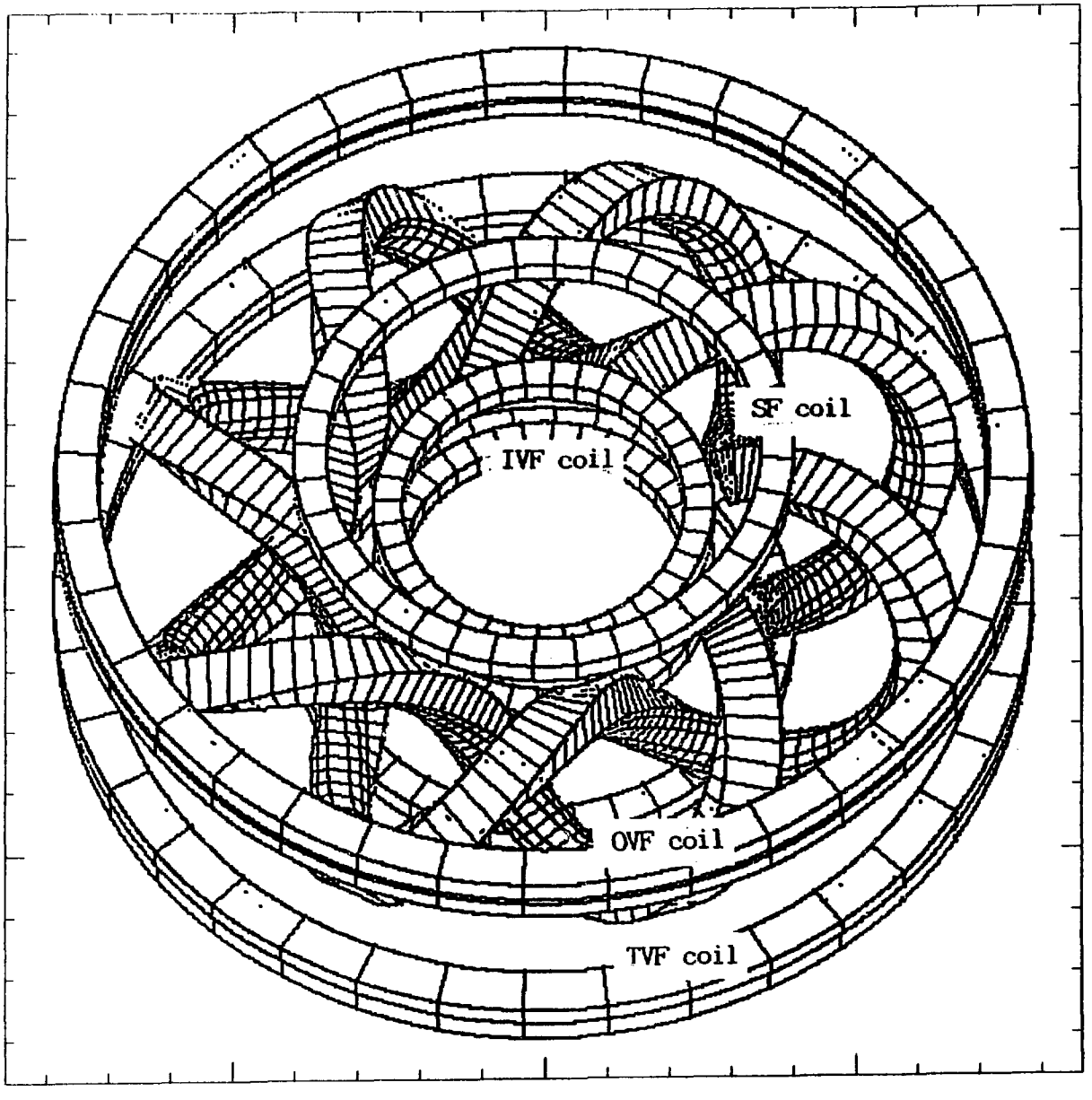

Helical coil parameter

Rc = 100.00 (cm)
Ac = 31.30 (cm)
M = 8
L = 2
alfa* = 0.30

HCw(cm)	HCh(cm)
9.20	7.01
9.20	-5.39
7.00	-7.29
3.40	-9.07

PR/PZ	PCW/PCH
150.00	7.25
35.00	3.95
150.00	6.55
45.00	4.80
75.00	5.30
55.00	4.60
50.00	4.60
20.00	4.60

Theta 1. = 22.50 (deg.)
Theta 2. = 30.00 (deg.)

CPU = 174.934 (sec.)

Table 1.Major parameters of CHS

Parameter	Value
Major radius R	1.0 m
Helical coil radius a_c	0.313m
Average plasma radius a_p	0.2m
Plasma aspect ratio A_p	5
Multipolarity l	2
Number of field period m	8
Pitch parameter γ_c	1.25
Pitch modulation α^*	0.3
Field strength on axis B	1.5T-2.0T
Plasma current	0
Central transform ι_0	0.33
Edge transform ι_s	0.8~1.0
Pulse length	2 sec at 1.5T
Access port size	30cm$^\phi$,63cmx38cm,...
Number of ports	68

Table 3. HF coil parameters

Coil width	164.0 mm
Coil height	155.8 mm
Current center	313 mm
Conductor size(net)	7.40x7.40-4$^\phi$
(gross)	8.20x8.20
Packing factor	59.9 %
Turn number	342/4=85.5
Coil current	2.74 kA
Current density(net)	68.09 A/mm^2
(gross)	40.77 A/mm^2
2 sec/5 min operation(square equivalent)	
Coil current(rms)	223.8 A
Current density(rms)	5.56 A/mm^2
Temperature rise	54.7°C
Water temp.rise	41.5°C
Max.coil temperature	136.2°C
Water flow rate	4.2 ton/hr

Table 2. PF coil parameters

	IVF	SF	TVF	OVF
Major radius (m)	0.5	0.75	1.5	1.5
Height (m)	±0.2	±0.55	±0.45	±0.35
Coil width (cm)	9.2	10.6	11.3	12.6
Coil height (cm)	9.2	9.2	11.3	8.2
Ampere-turn (kAT)	120x2	-200x2	-200x2	-219.3x2
Turn number/coil	60	39	33	20
Maximum current (kA)	2.0	5.0	6.06	10.965
Resistance (mΩ)	166	75	82	34
Self inductance (mH)	13.3	9.6	16.5	6.4
Magnetic energy(MJ)	0.027	0.12	0.303	0.385
Time constant (sec)	0.08	0.13	0.2	0.19
Conductor size (mm^2)	50.8	115.8	175.5	281.0
	(9x9 -6°)	(12.5x12.5 -7°)	(16x16 -10°)	(18x22 -12°)
2 sec/5 min operation (square equivalent)				
Current density (A/mm^2)				
(peak)	39.4	43.2	34.5	39.5
(rms)	3.22	3.53	2.82	3.18
Heat/pulse (MJ)	1.33	3.75	6.02	8.18
Temperature rise (°C)	17.2	21.6	13.9	18.0
Water temp.rise (°C)	14.2	29.2	27.7	14.9
Max.coil temp.(°C)	71.4	91.0	81.6	73.0
Water flow rate (ton/hr)	0.27	0.37	0.62	1.57

Machining of Forged Stainless Steel Block

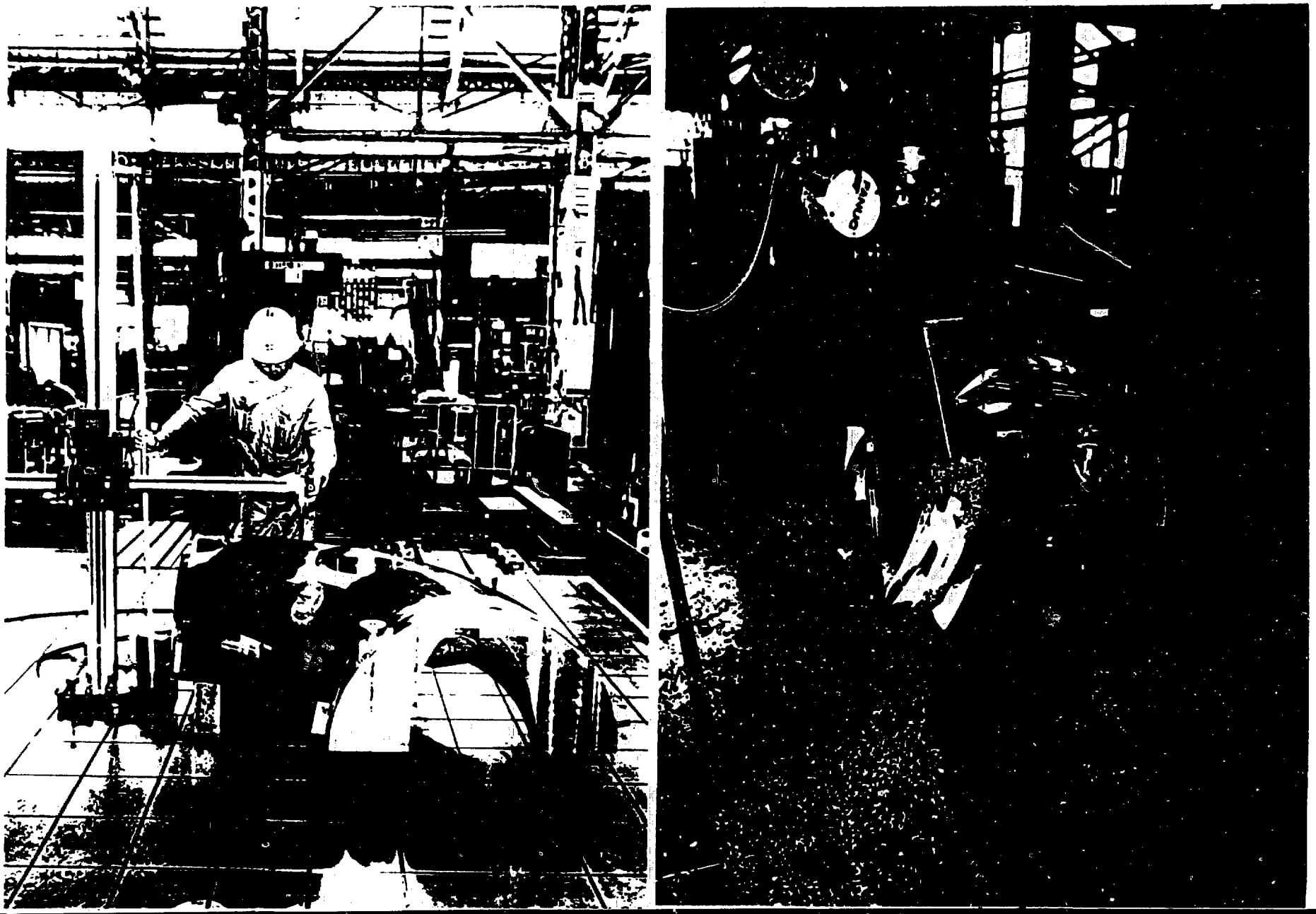

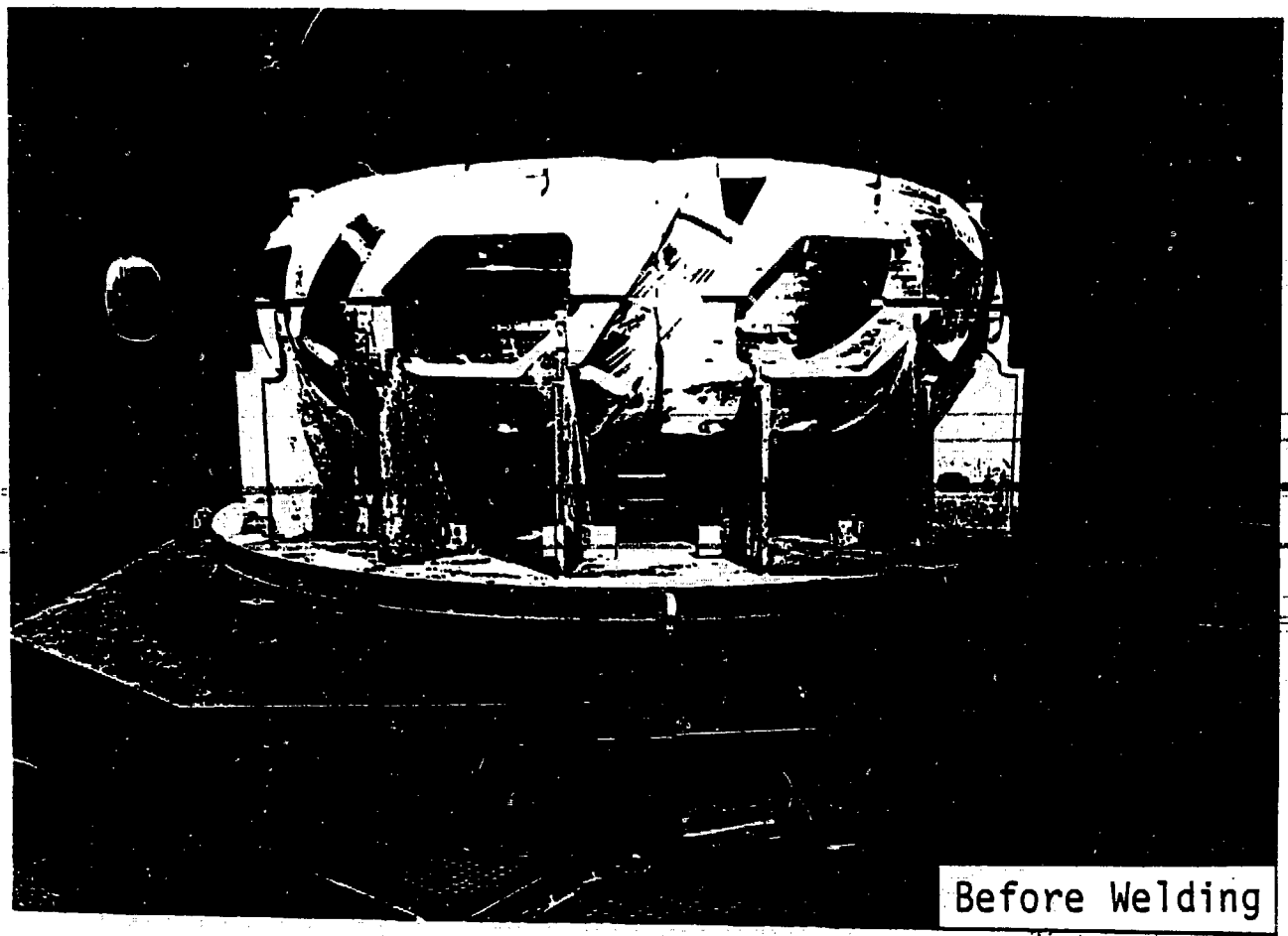

Before Welding

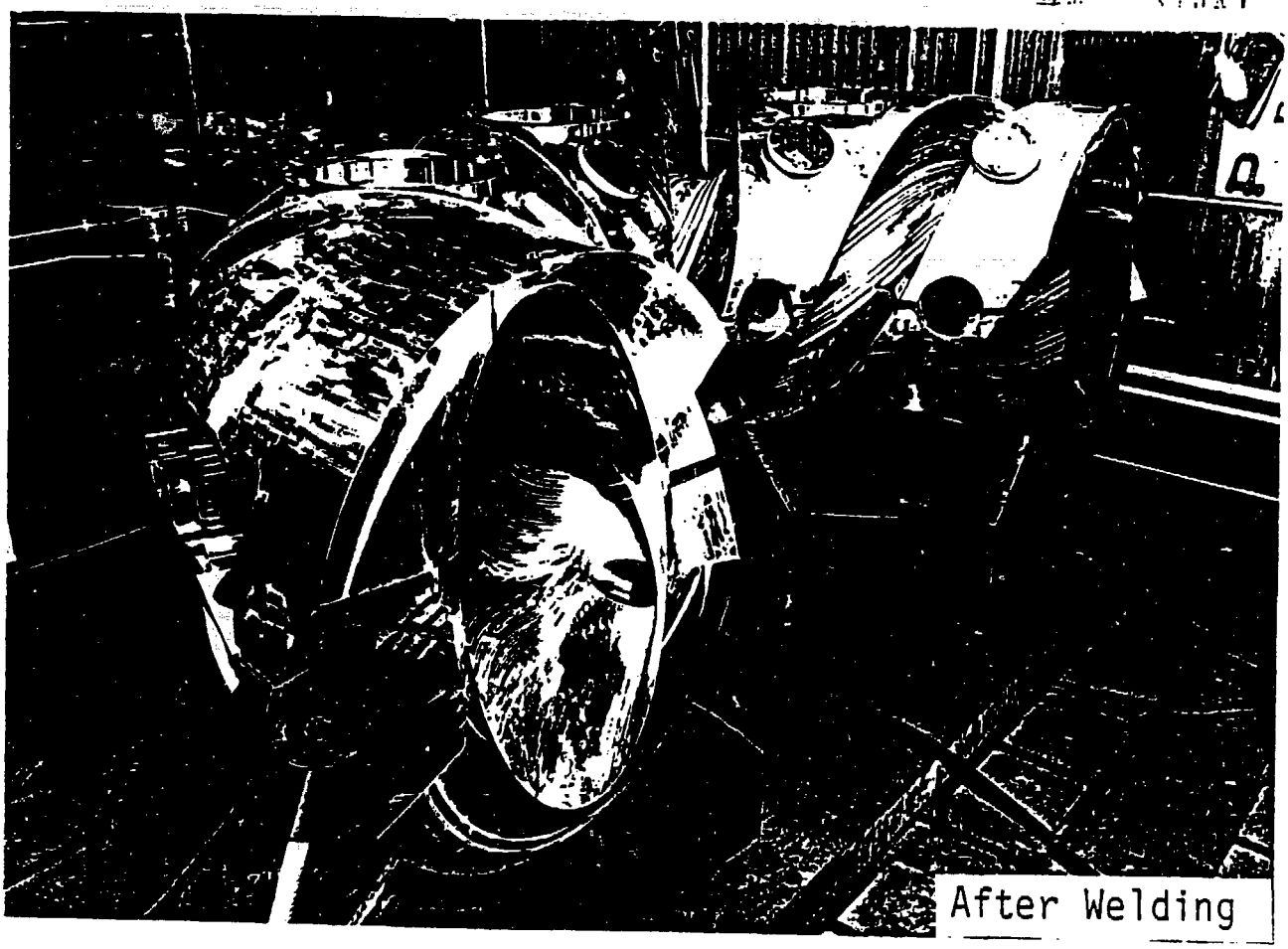

After Welding

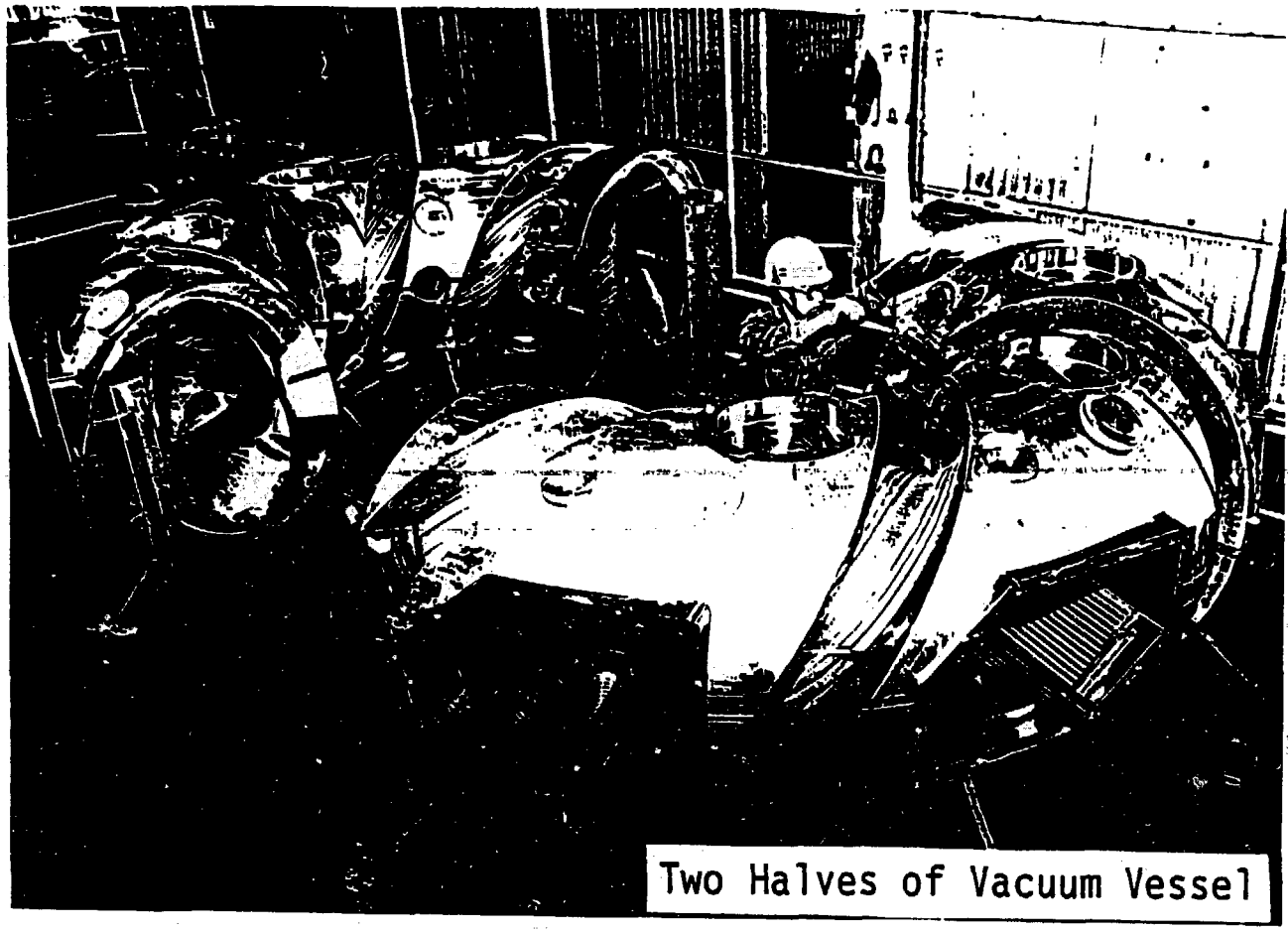

Two Halves of Vacuum Vessel

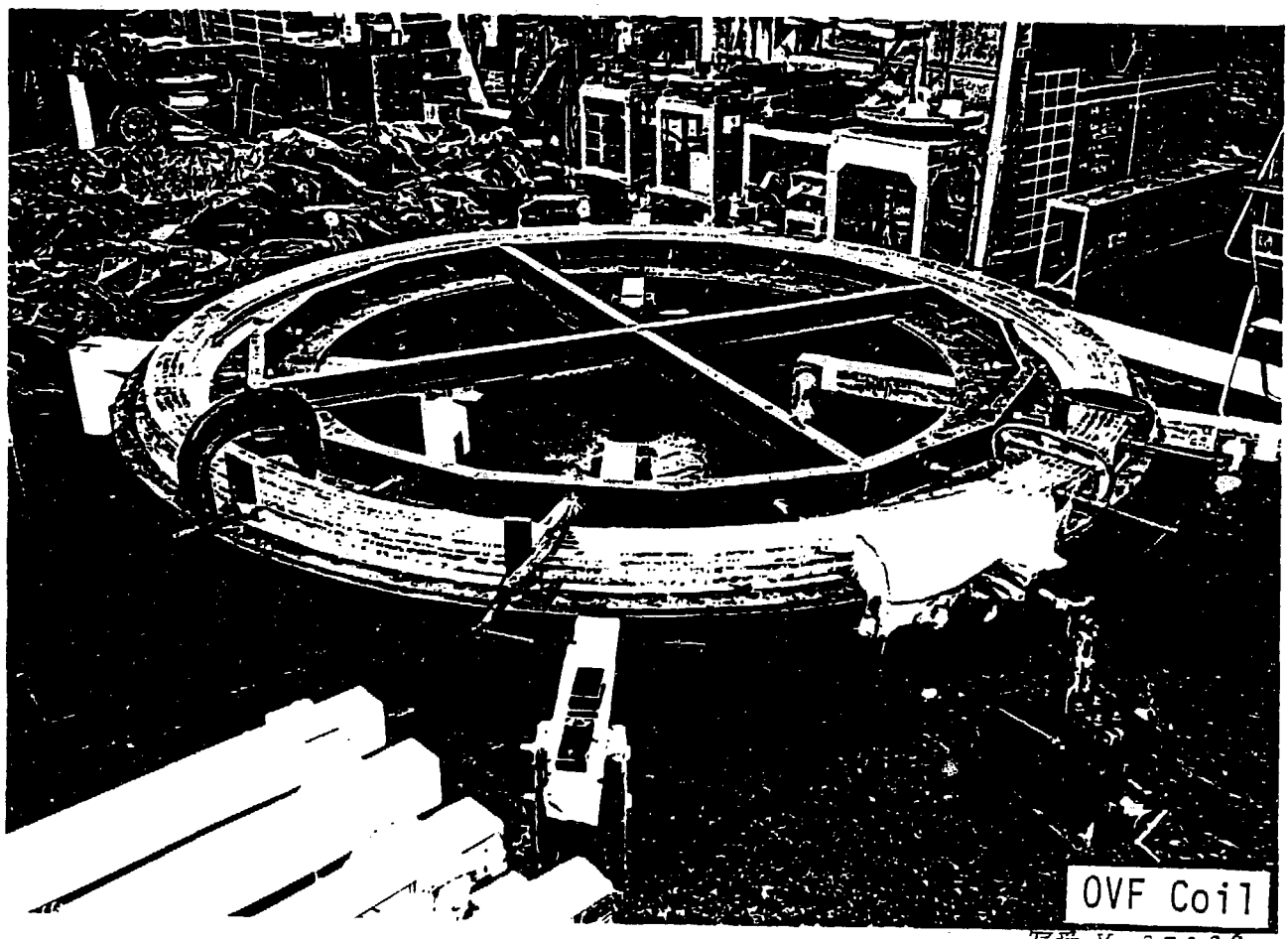

OVF Coil

写番 K-87066

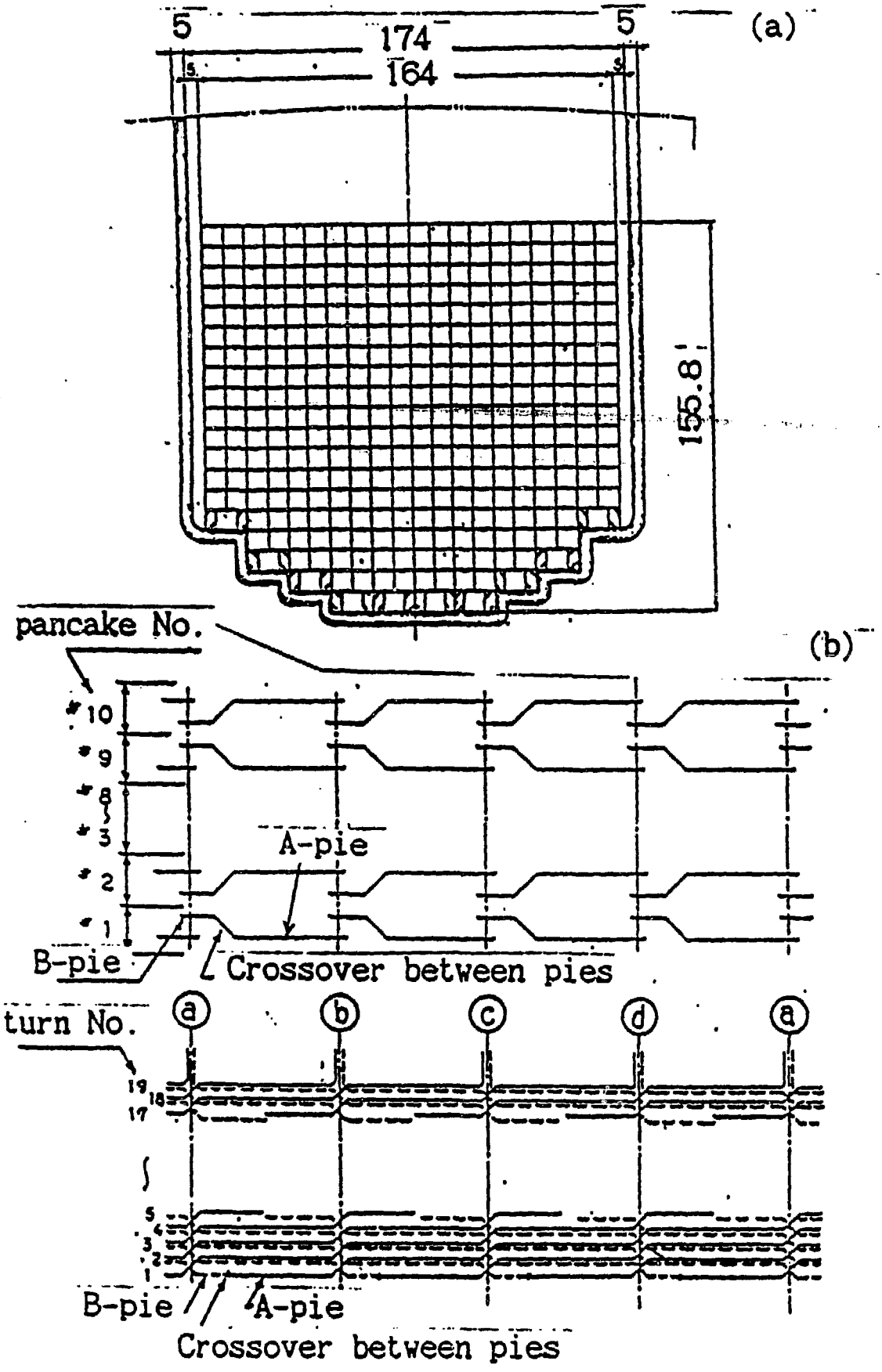

Fig.3 Details of HF coil winding. (a) Cross section (b) Winding process. Pancake number and turn number are lined in the direction of width and height respectively. The signs ⓐ~ⓓ designate toroidal angles every $\pi/2$ for one coil(z=0, toroidal angle $\phi=0, \pi/2, \pi, 3\pi/2$).

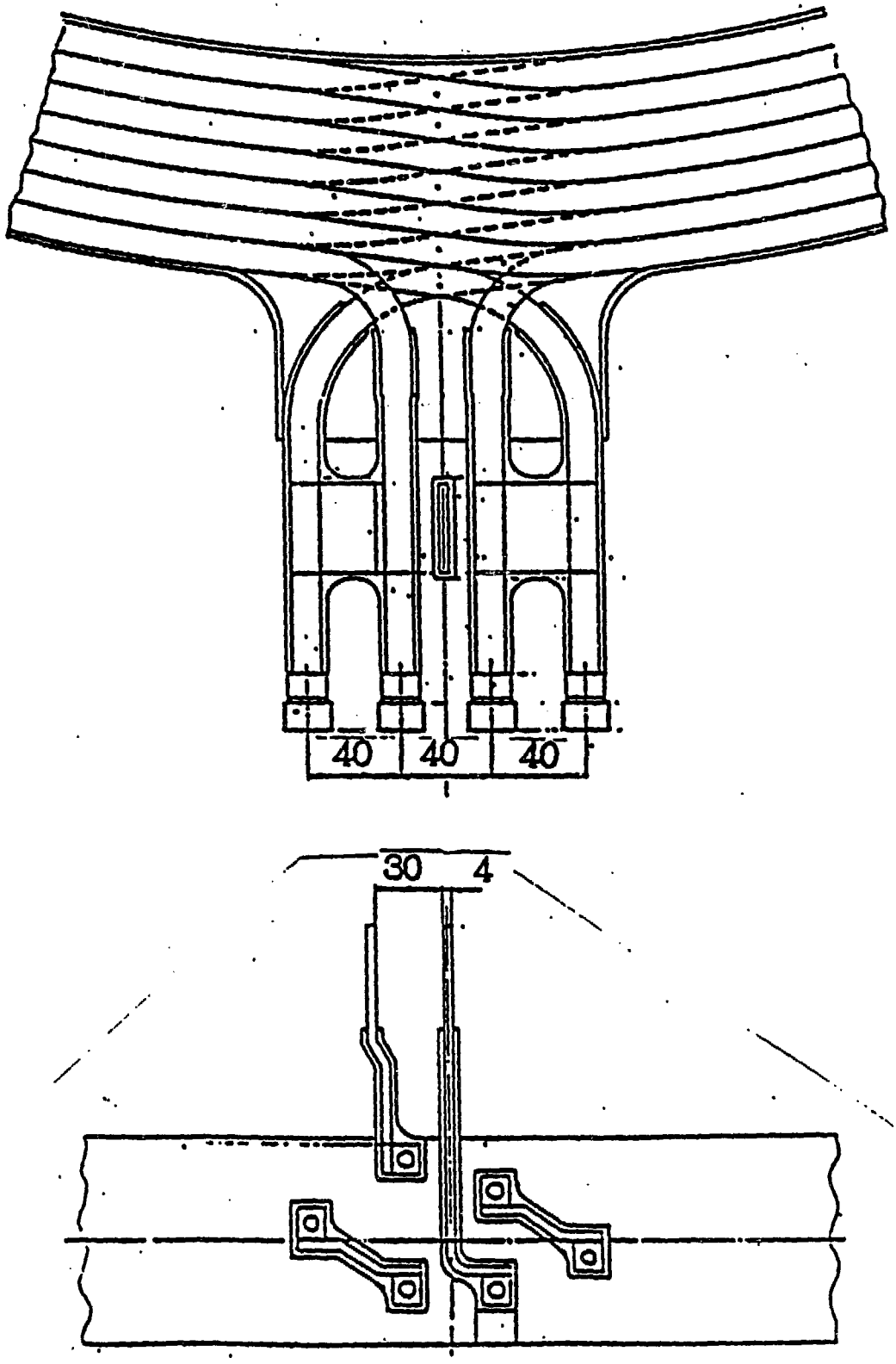

Fig.4 Feeder and crossover of SF coil.

Estimate of error field

1. Design	
HFC --- crossover, feeder	
PFC --- crossover, feeder	magnetic dipoles, 10-100 $A.m^2$
2. Alignment	
HFC	random error (max.$\pm$ 0.5mm)
PFC	displacement & tilt
3. Deformation	
Electromagnetic force	Δa_c = 0.3 mm x $\sin\theta$
Thermal force	ΔR = 0.5 mm, Δa_c = 0.5 mm
4. Increase in permeability	
Weld of vacuum vessel	$\mu \sim 1.03$
5. Ferromagnetic material	volume $\gtrsim 10^{-2}$ m^3

Error Field

under the location of crossover between two pies

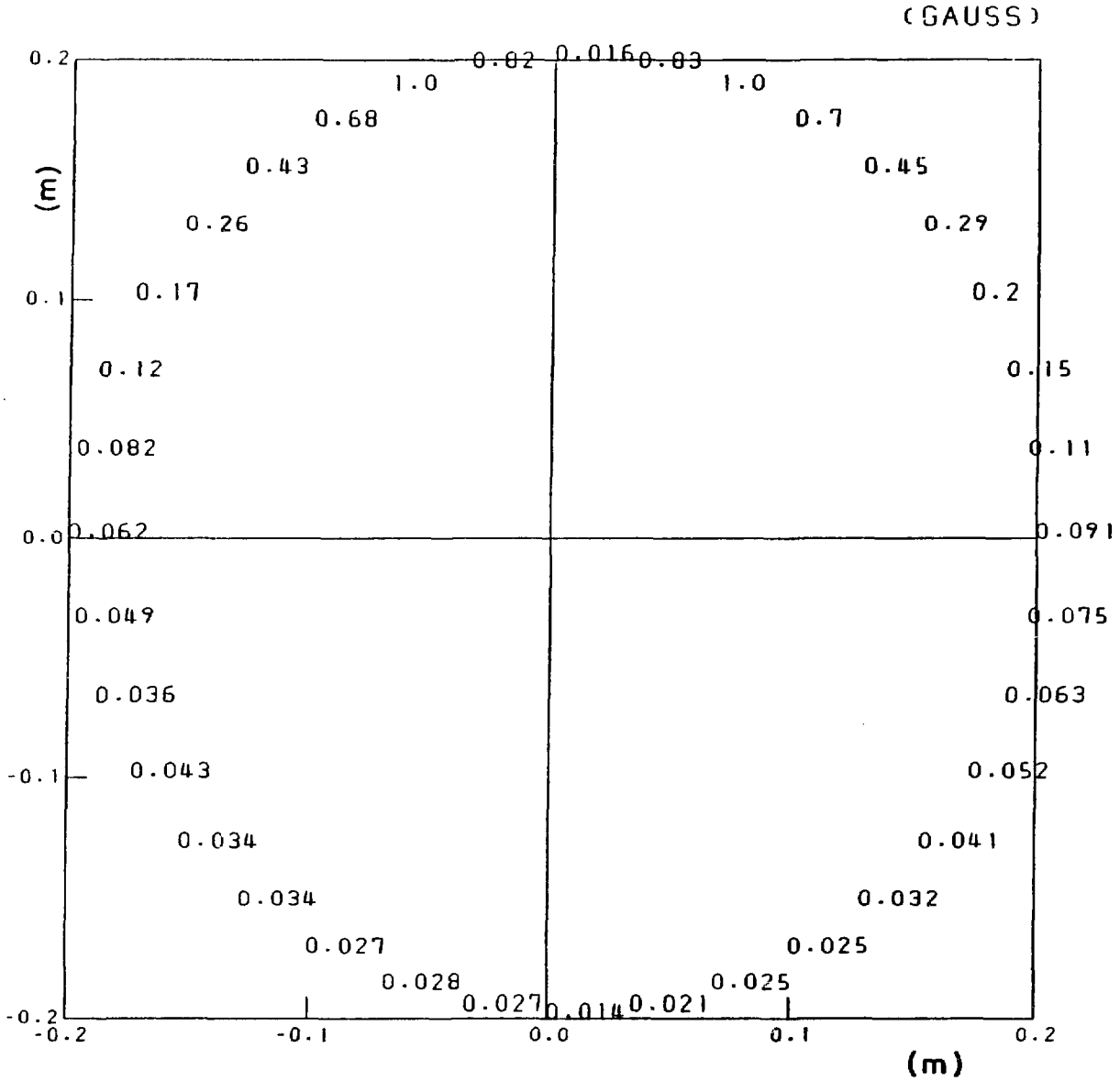

Alignment of HF & PF coils

1. HF coil

   specification : ± 0.5 mm / 1 m

   - supported by vacuum vessel

     N.C. machining of v.v. ---> weld -$\frac{1}{1}$-> N.C. machining --->
     (max. 2mm)

     insulation ---> N.C. machining of insulator

   - to estimate the accuracy effect by giving random errors

2. PF coil

   specification : ± 0.2 % (± 3 mm / 1.5 m)

   - supported by supporting structures

     vacuum vessel ↔ supporting structure ↔ PF coil

   - misalignment produces long pitch error field

Random error field of HF coil

setting error $\pm$ 0.5 mm/ 1m

Biot - Savart law
27 filaments / conductor

$x \to x + d\cos\theta_1$ $\quad X \to X + d\cos\theta_2$

$y \to y + d\cos\theta_1$ $\quad Y \to Y + d\cos\theta_2$

$z \to z + d\cos\theta_1$ $\quad Z \to Z + d\cos\theta_2$

θ_1, θ_2 ... random number

$d = 5 \times 10^{-4}$ m

Random error
of HF coil
(27 filaments)

$d = 10^{-4}$ m

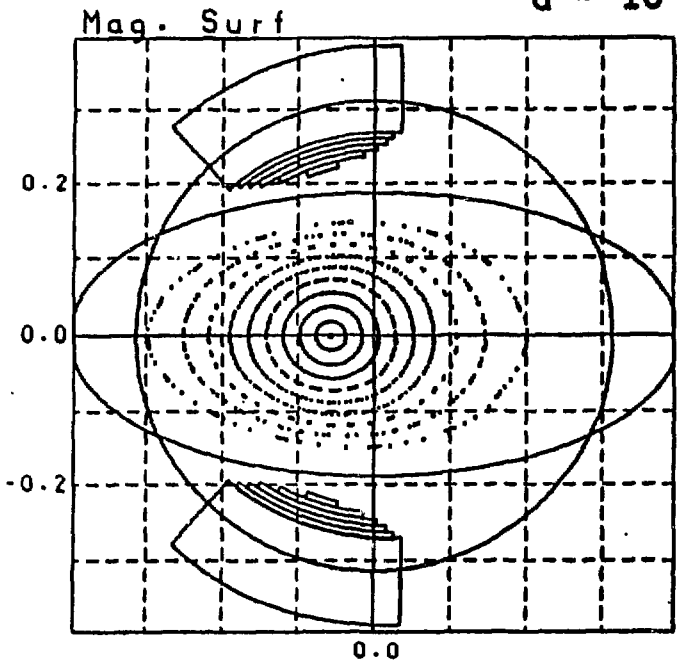

$d = 5 \times 10^{-4}$ m

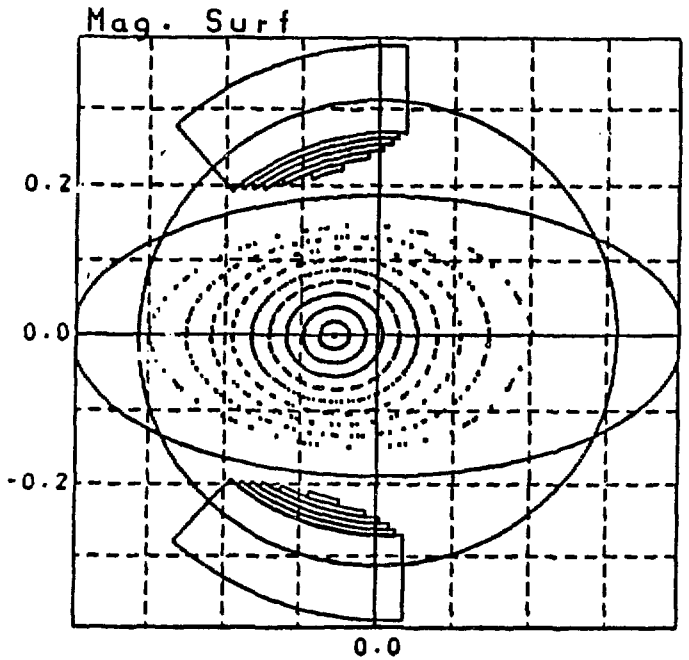

$d = 10^{-3}$ m

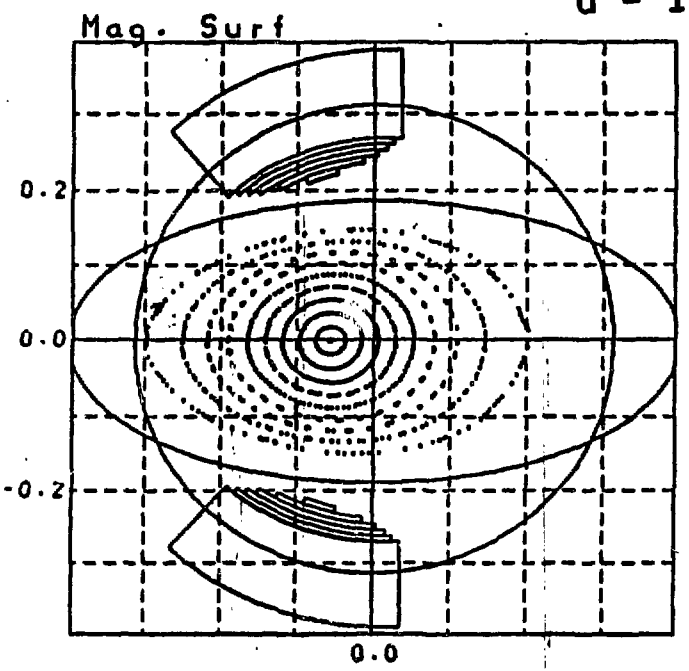

Effect of Horizontal Field on Vacuum Magnetic Surface

$B_R/B = 0$

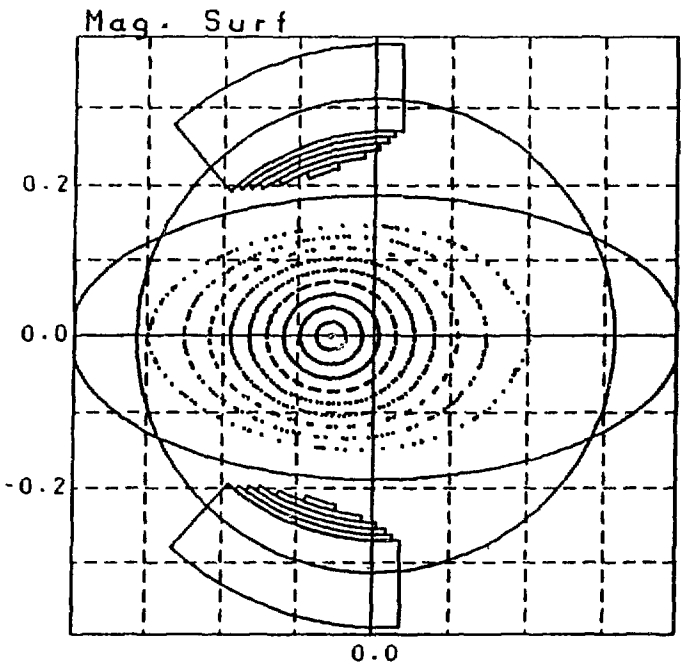

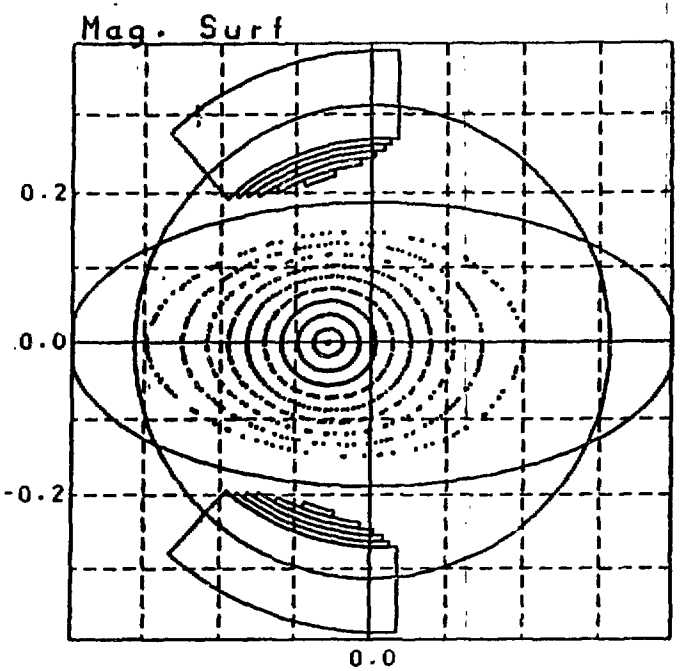

10^{-4}

5×10^{-4}

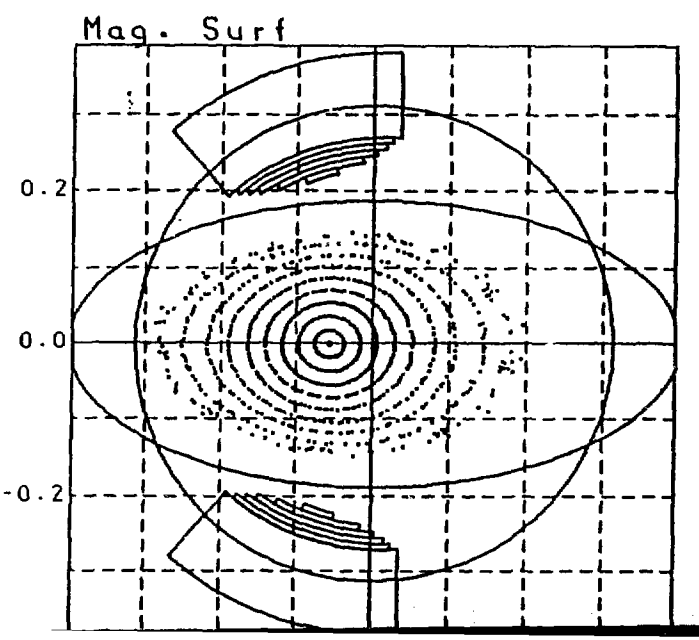

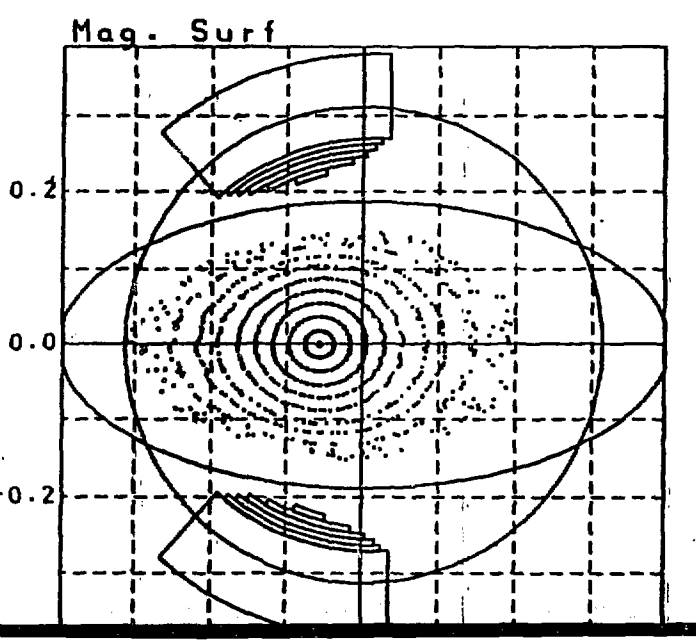

10^{-3}

HORIZONTAL FIELD

setting error in PFcoil

1. Displacement

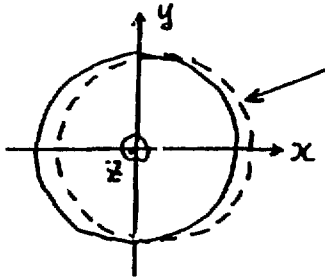

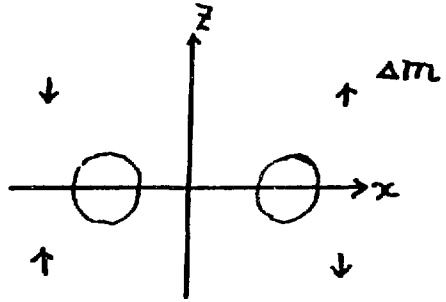

$\Delta m = I \cdot S$, $S = 2 R \cdot d$, $I = 350kA$, $R = 1.5m$, $d = 3mm$

$B_R = 3 \times 10^{-4}$ T, 2 magnetic dipole moments

$B_R/B = 4 \times 10^{-4}$

2. Tilt

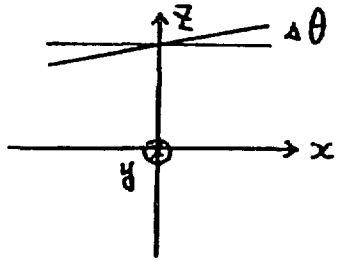

$\Delta m = m \cdot \Delta\theta$, $m = \pi R^2 \cdot I$, $\Delta\theta = d/R$

$\Delta m = 5 \times 10^3$ A·m^2

$B_R = 5 \times 10^{-4}$T, 2 magnetic dipole moments

$B_R / B = 6 \times 10^{-4}$

Effect of Several Misalignments in OVF/TVF Coils

displacement

3 mm

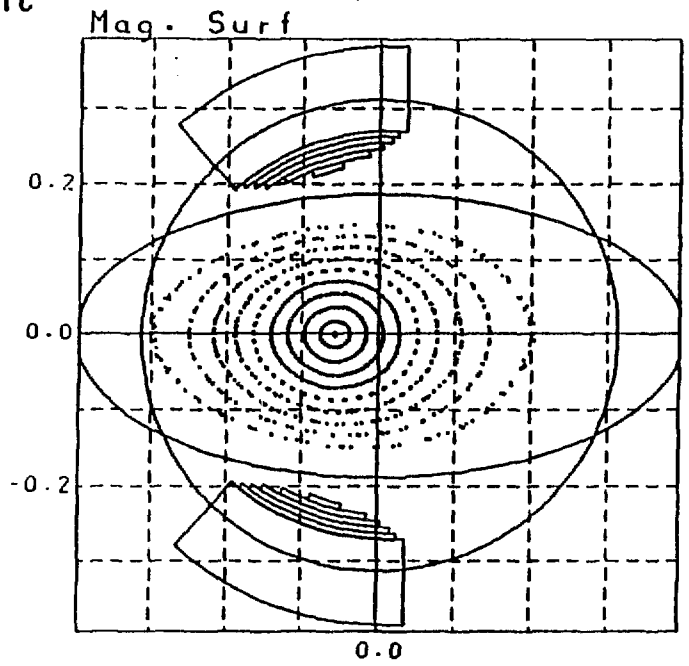

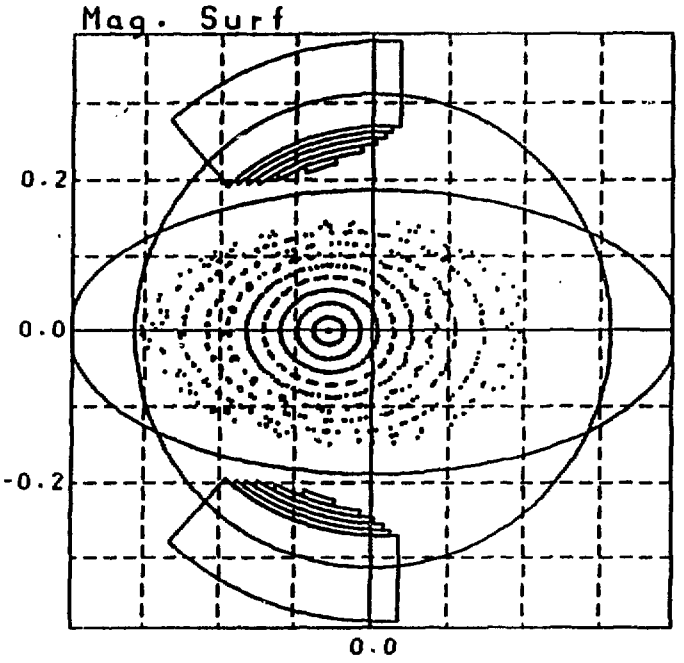

tilt

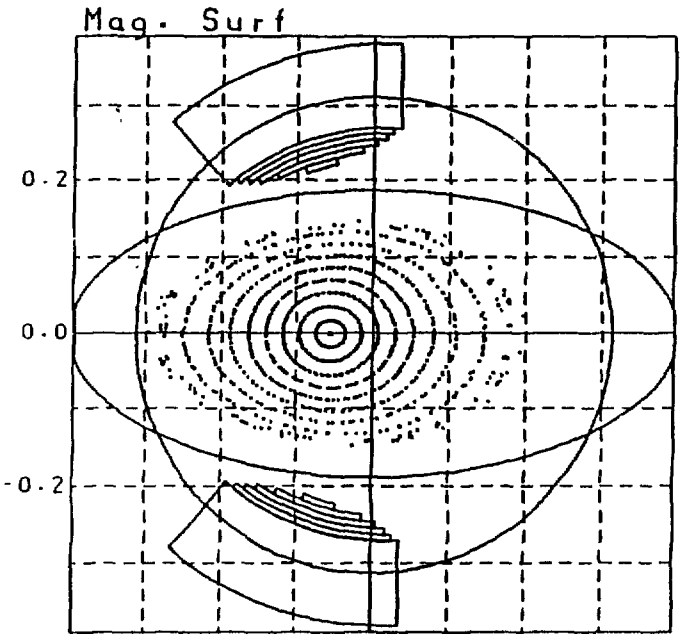

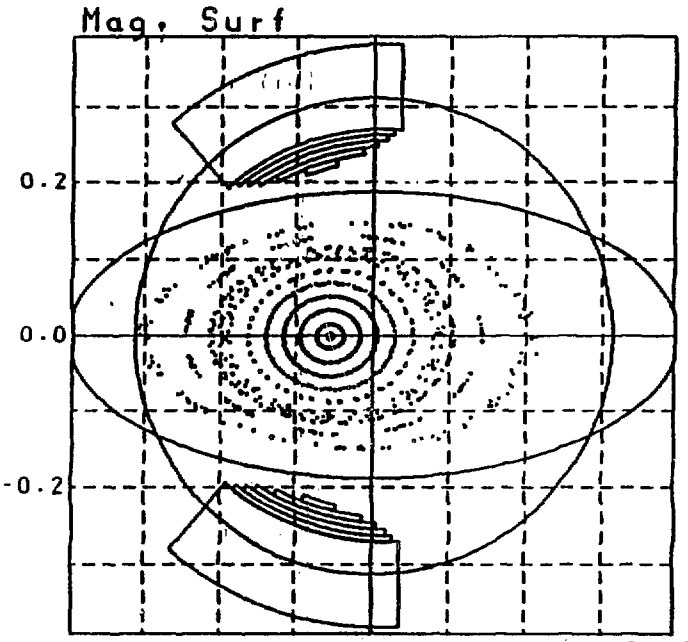

Deformation of HF coil

1. Electromagnetic force
   - most pessimistic case when B_0= 2T and no current in PF coils except OVF coil
   - boundary condition is given by vacuum vessel
   - maximum deformation
     0.35 mm (conductors with independent rigidity)
     0.11 mm (single)

2. Thermal force
   - adiabatic temperature rise $\Delta T = 60^{\circ}C$
   - same boundary codition as above
   - deformation looks like the winding law with ΔR = 0.5 mm and Δa_c = 0.5 mm

LIGHT DIR
X= 0.0
Y= 1.00
Z= 0.0

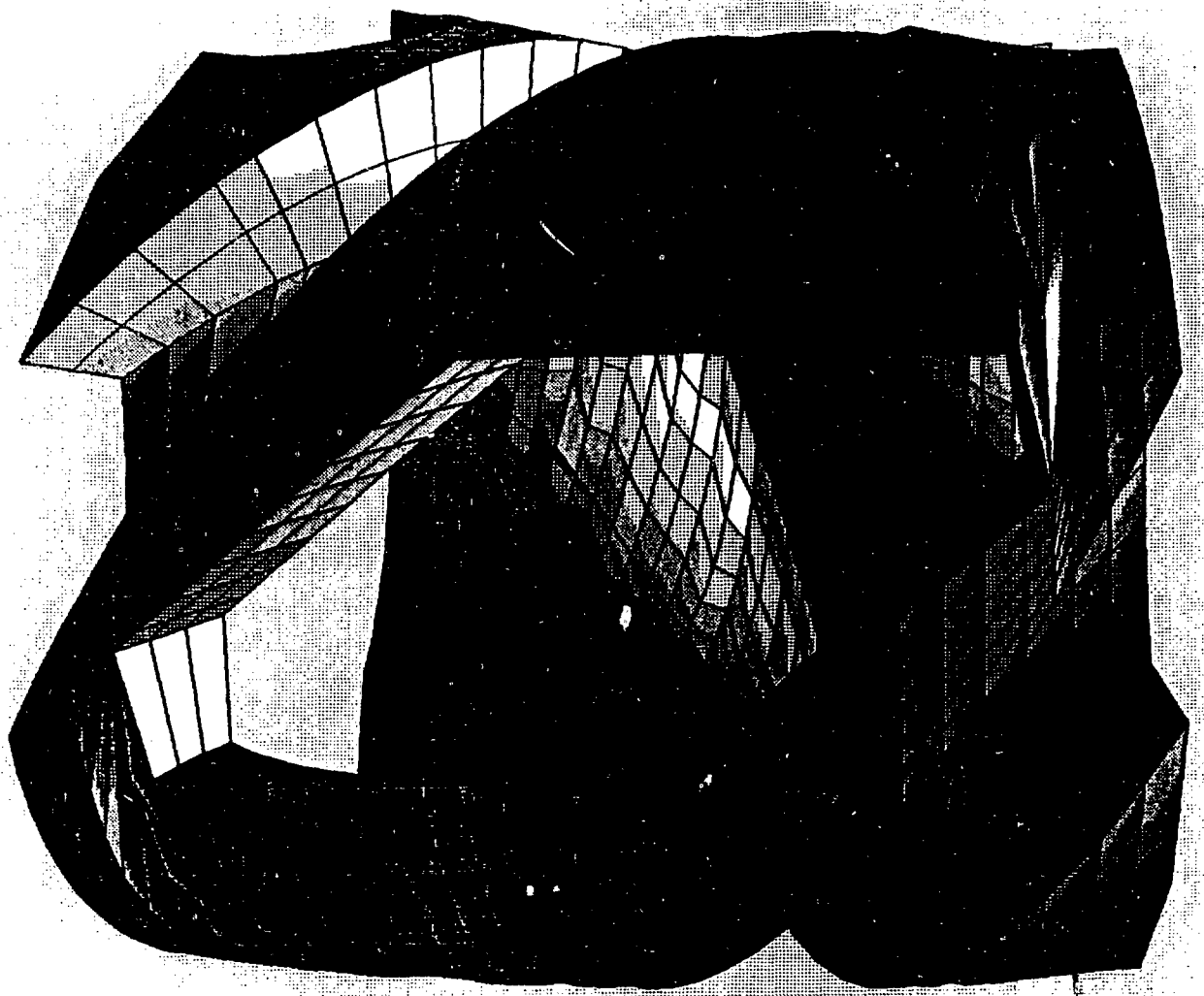

Z

Increased μ of vacuum vessel

$M = \chi_m H$, $\quad B = \mu_0 (1 + \chi_m) H$

$\chi_m = 0.03$ when $\mu = 1.03$

$H = B / \mu_0$ ($B = 1.5$ T)

$I = M\, dz \sim 0.4$ kA ($dz = 1$ cm)

$B = (\mu_0 I / 2a)\, dr / a$

($dr \sim 1$ cm, $a = 20$ cm)

$= 0.6$ gauss

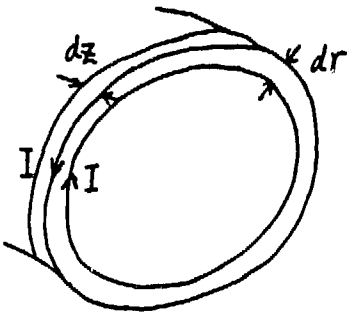

Ferromagnetic material

- stray field < several gauss
- ferromagnetic

saturation $\Rightarrow$ $M = 1.5\ T / \mu_0$

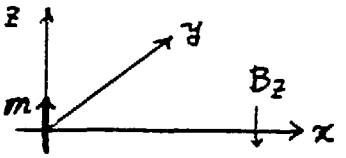

$B_z(X,0,0) = (-\mu_0/4\pi)\, m/X^3$, $\quad X \sim 3$ m

$m = M\, dV$

$|B_z| < 1$ gauss $\longrightarrow$ $dV = 2.3 \times 10^{-2}\ m^3$

shielding box

height = 1 m, $\quad d = 5$ mm, ----- $l \gtrsim 1$ m

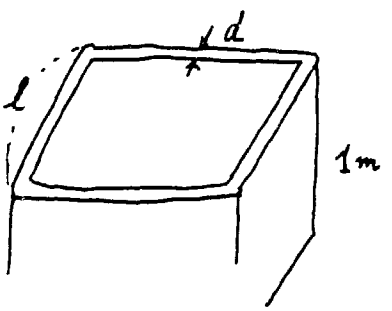

Effect of Whole Error Fields

o misalignment
n PFC

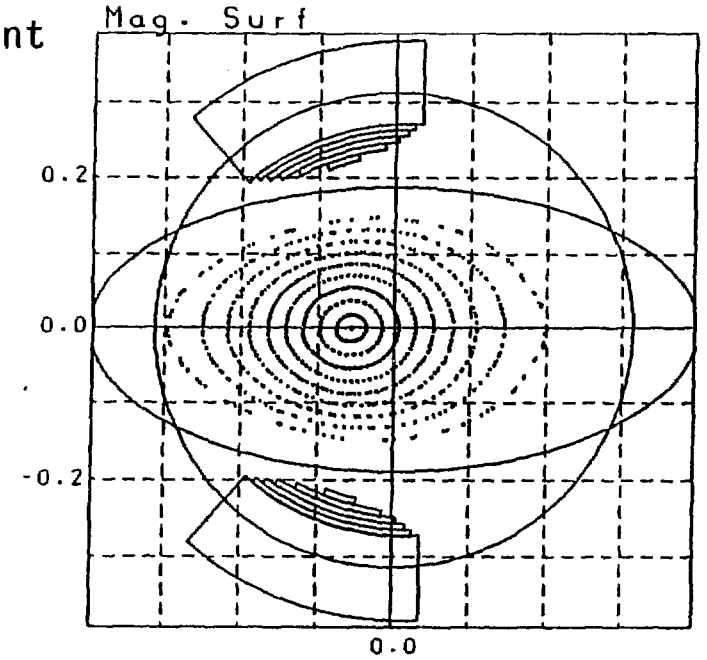

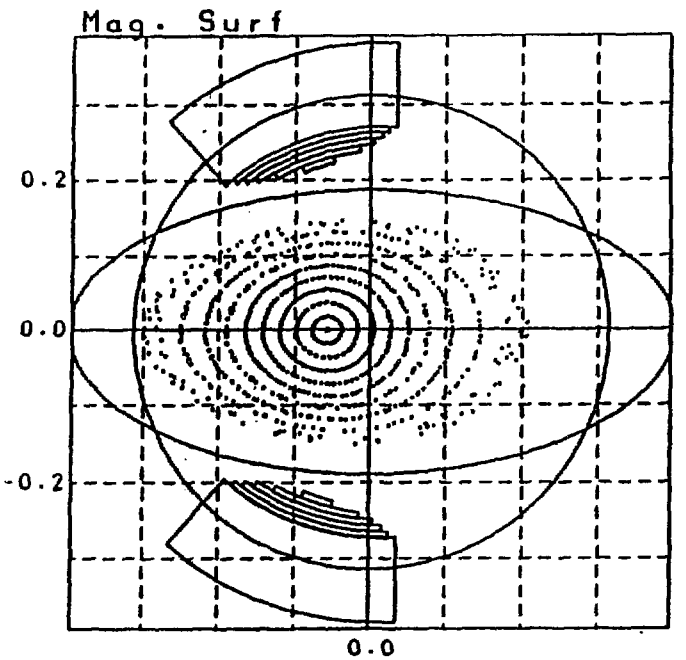

displacement
±1.5mm

displacement
±3mm

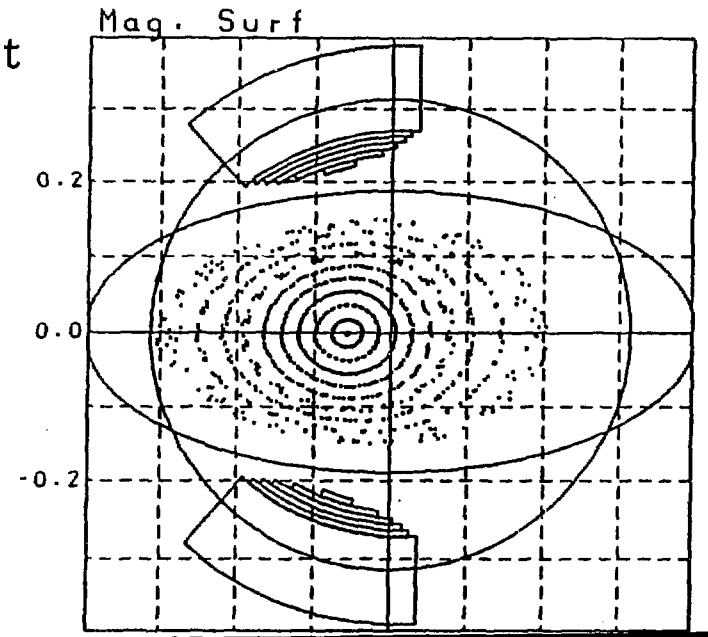

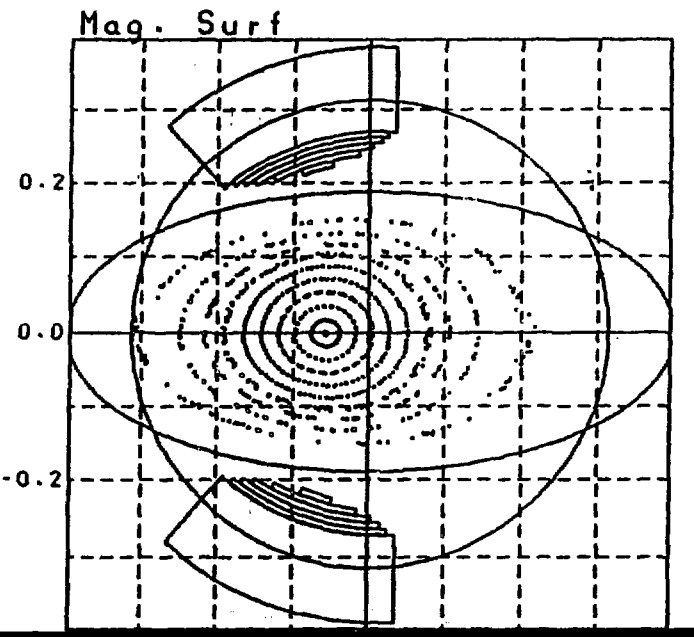

displacement
±1.5mm
and
tilt
±1mm

B_r and B_z measurement
(±3mm tilt)

Br at z = -0.200

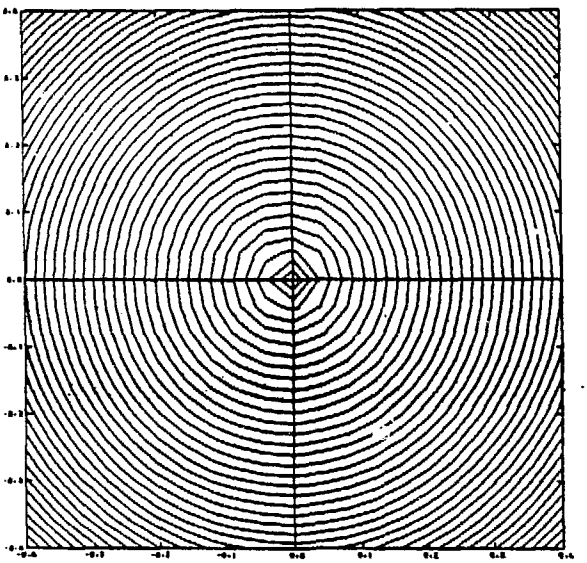

Br max = 0.000026
BR MIN = -0.002325

Bz at z = -0.200

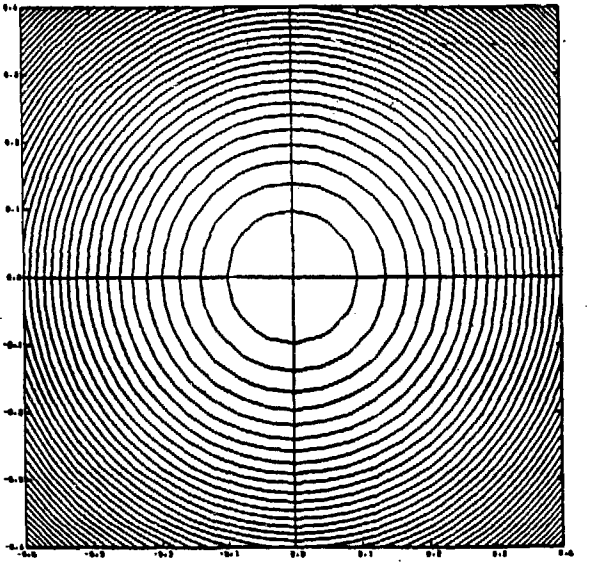

Bz max = -0.001445
Bz min = -0.002169

Br at z = -0.150

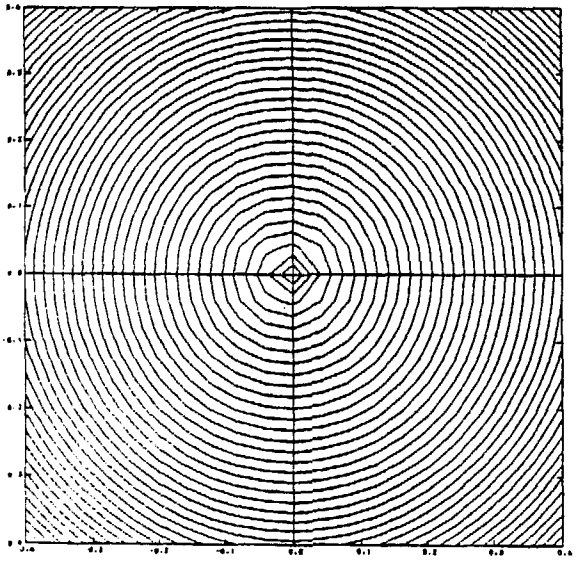

Br max = 0.000026
BR MIN = -0.002464

Bz at z = -0.150

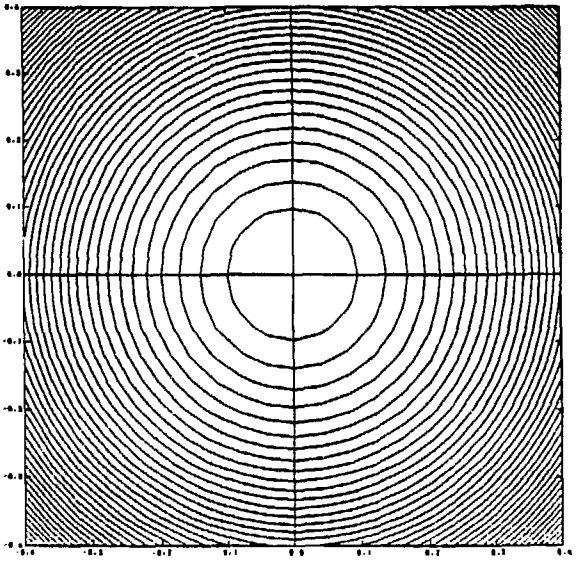

Bz max = -0.001100
Bz min = -0.001662

CHS Experimental Program and Diagnostics

S.Okamura (IPP Nagoya)

1. Research Topics of CHS Experimental Program

2. Experiment Schedule

3. CHS Diagnostics

CHS Experimental Program and Diagnostics

S. Okamura (IPP Nagoya)

Experimental Program : The most important problem we will study in CHS experiment is to evaluate the confinement characteristics of low aspect ratio Torsatron/Heliotron configuration. For this purpose, we made efforts to have high accuracy of the magnetic field by reducing various error field components. As well as to get the global confinement scaling of low aspect ratio system, we will investigate the problem of high energy particle confinement and the stability of high beta plasma which are especially important for the low aspect ratio design. In this direction, we made the experimental program of CHS as following. (1) Global confinement study. Basic confinement scaling will be obtained for both an ECH plasma and NBI and/or ICRF heated plasma. (2) Configuration study. The effects of poloidal multipole field control will be studied in the relation with the transport ($\iota/2\pi(r)$, $\varepsilon_h(r)$) and MHD stability (magnetic shear and well). (3) Special topics of the confinement. Some selected problems will be studied — the effects of the radial electric field, high energy particle orbit loss, anomalous rate of edge region diffusion. (4) MHD physics. Stability will be investigated for high beta equilibrium. (5) Heating. Technical and physical problems will be studied. Special features are neutral beam injection angle variation and ICRF plasma production. (6) Particle control and impurity control. (7) Helical axis configuration.

Experimental schedule : We made five years schedule (1987 - 1991) to study these topics. Experimental phases for these years are 1987 : machine construction, 1988 : basic ECH plasma, 1989 : additional heating I, 1990 : additional heating II, 1991 : advanced study. Two tangential NBI systems and 3MW ICRF heating will be ready for the full heating experiment in 1990. The necessary diagnostics will be developped also till 1990.

Diagnostics : It is necessary to get the profile information of plasma parameters for the quantitative argument of confinement. Diagnostics of CHS for the basic plasma parameters are designed to give profile data — HCN laser interferometer, Thomson scattering, CXRS, SX detectors array, etc. We are preparing also the monitoring diagnostics which are generally easy handling and maintenance free but not always capable of profile measurement — Microwave interferometer, SX PHA, ECE, Diamagnetic loop, etc. As the diagnostics for special research topics, it is planned to develop HIBP for the plasma potential measurement and the probe surface analysis for the high energy ion orbit loss measurement.

Important Items of Experimental Program

1. Confinement Characteristics
   - (i) Basic Confinement Scaring (n, Te, Ti, B)
   - (ii) Confinement Scaling with Strong Additional Heating (NBI, ICRF)
   - (iii) Power Balance Studies
2. Magnetic Field Configuration Studies
   - (i) Plasma Shape Control with Poloidal Multipole Field
   - (ii) Control of Rotational Transform and Magnetic Well
   - (iii) Detailed Studies of Ergodic Layer Structures
3. Special Topics of Confinement Studies
   - (i) Confinement of High Energy Particles
   - (ii) Effects of Radial Electlric Field on Confinement
   - (iii) Anomalous Diffusion in Edge Region
   - (iv) Impurity Control for High Power Heating
4. MHD Studies
   - (i) Characteristics of High Beta Plasma
   - (ii) Stabilization Effects of Magnetic Shear and Magnetic Well
5. Plasma Heating
   - (i) High Te Plasma with Various Scheme of ECH
   - (ii) Effects of Variation of Neutral Beam Injection Angle
   - (iii) Balanced Injection of Two Tangential Neutral Beam
   - (iv) ICRF Heating with Various Propagation Modes
   - (v) Plasma Production by ICRF Heating
6. Particle Control and Impurity Control
   - (i) Pellet Injection and Pump Limiter
   - (ii) Thermal Load Profile on Vacuum Wall and Impurity Control
7. Studies of Helical Axis Configuration

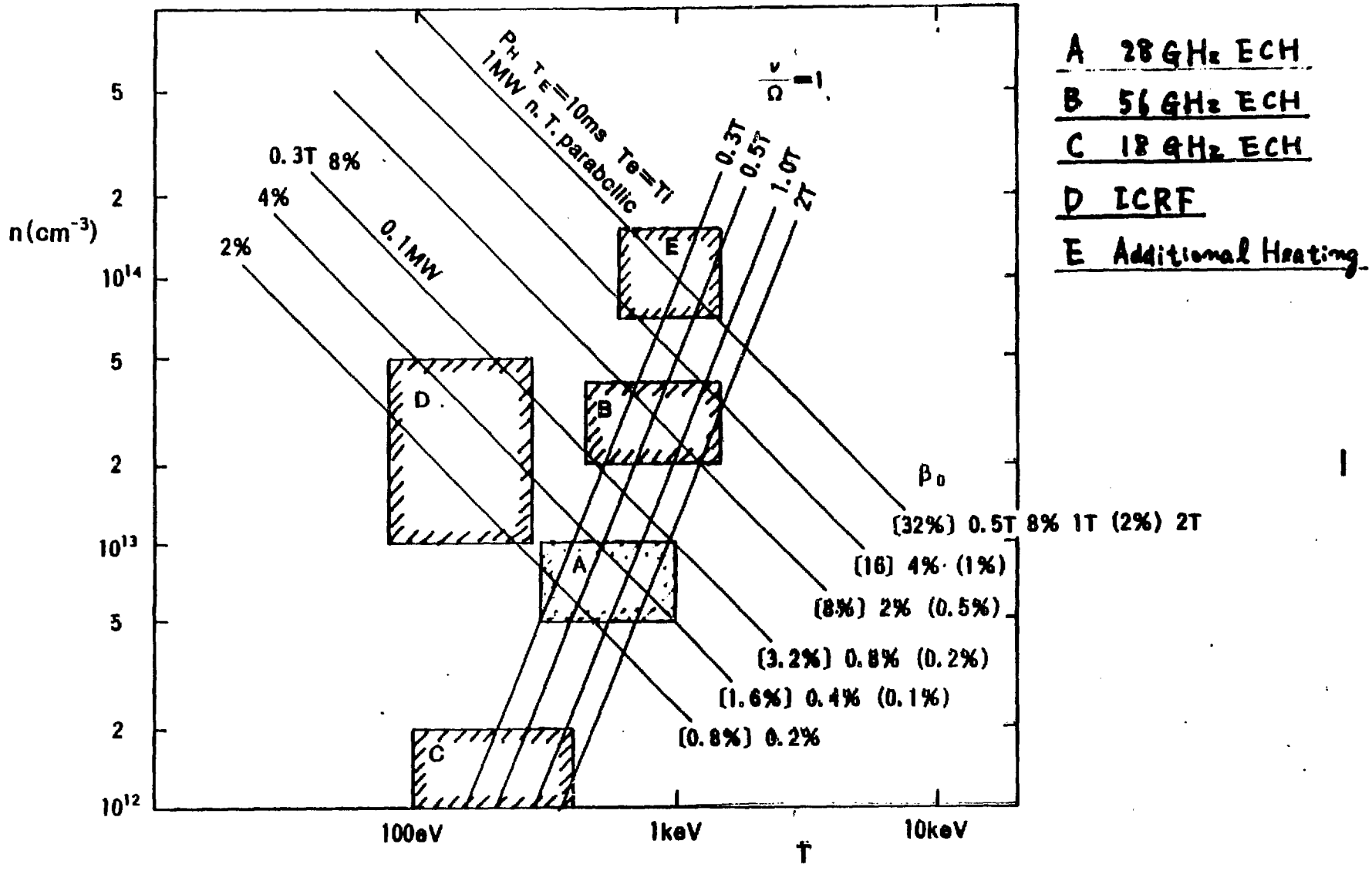
A 28 GHz ECH
B 56 GHz ECH
C 18 GHz ECH
D ICRF
E Additional Heating
n(cm⁻³)
5
2
10¹⁴
5
2
10¹³
5
2
10¹²
100eV
1keV
10keV
T
P_H τ_E=10ms Te=Ti
1MW n. T. parabolic
ν/Ω=1
0.3T
0.5T
1.5T
2T
0.3T 8%
4%
2%
0.1MW
β₀
[32%] 0.5T 8% 1T (2%) 2T
[16] 4% (1%)
[8%] 2% (0.5%)
[3.2%] 0.8% (0.2%)
[1.6%] 0.4% (0.1%)
[0.8%] 0.2%
A
B
C
D
E

Schedule of Machine Construction

FY		1987	1988	1989	1990	1991
Experiment Phase			ECH Plasma Confinement Plasma Production with ICRF	Additional Heating with NBI, ICRF Phase I	Additional Heating with NBI, ICRF Phase II	High Beta Plasma Helical Axis
Magnetic Field Vacuum Vessel		Coiles, Vessel and Power Supply for 1.5 Tesla Field	Modification of Power Supply for 2.0 Tesla Field	Carbon Tile Pump Limiter	Pellet Injector	Helical Axis Configuration
Heating Systems	ECH	28 ~~26~~ GHz (200KW)	56 GHz (200KW)		112 GHz (500KW)	
	NBI		40 keV (1.5MW) #1	40 keV (1.5MW) #2		
	ICRF	Transmitter 1 MW Antennas (Phase I)		Transmitter 3 MW Antennas (Phase II)		
Diagnostics		Basic Diagnostics Thomson Scattering HCN Interfercmeter Fast Neutral Particles Visible Spectroscopy Magnetic Measurement Data Acquisition System	Additional Diagnostics ECE, SX High Energy Particles X Ray Spectroscoopy Edge Region Diagnostics	Electric Field Diagnostics Heavy Ion Beam Probe Doppler Shift	CX Reconbination Spectroscopy	

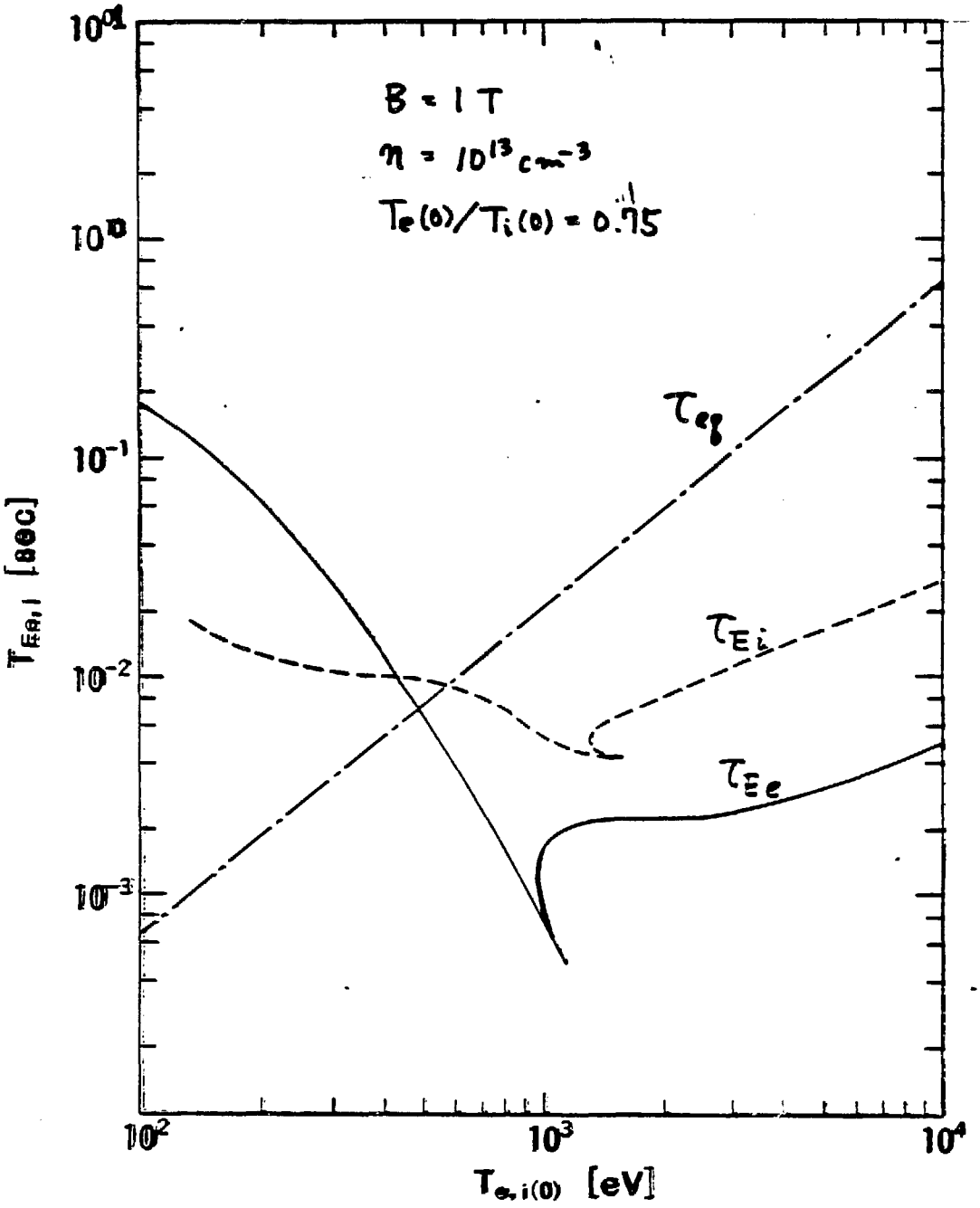
B = 1 T
n = 10^13 cm^-3
Te(0)/Ti(0) = 0.75
τeq
τEi
τEe
10^1
10^0
10^-1
10^-2
10^-3
10^2
10^3
10^4
τE,i [sec]
Te,i(0) [eV]

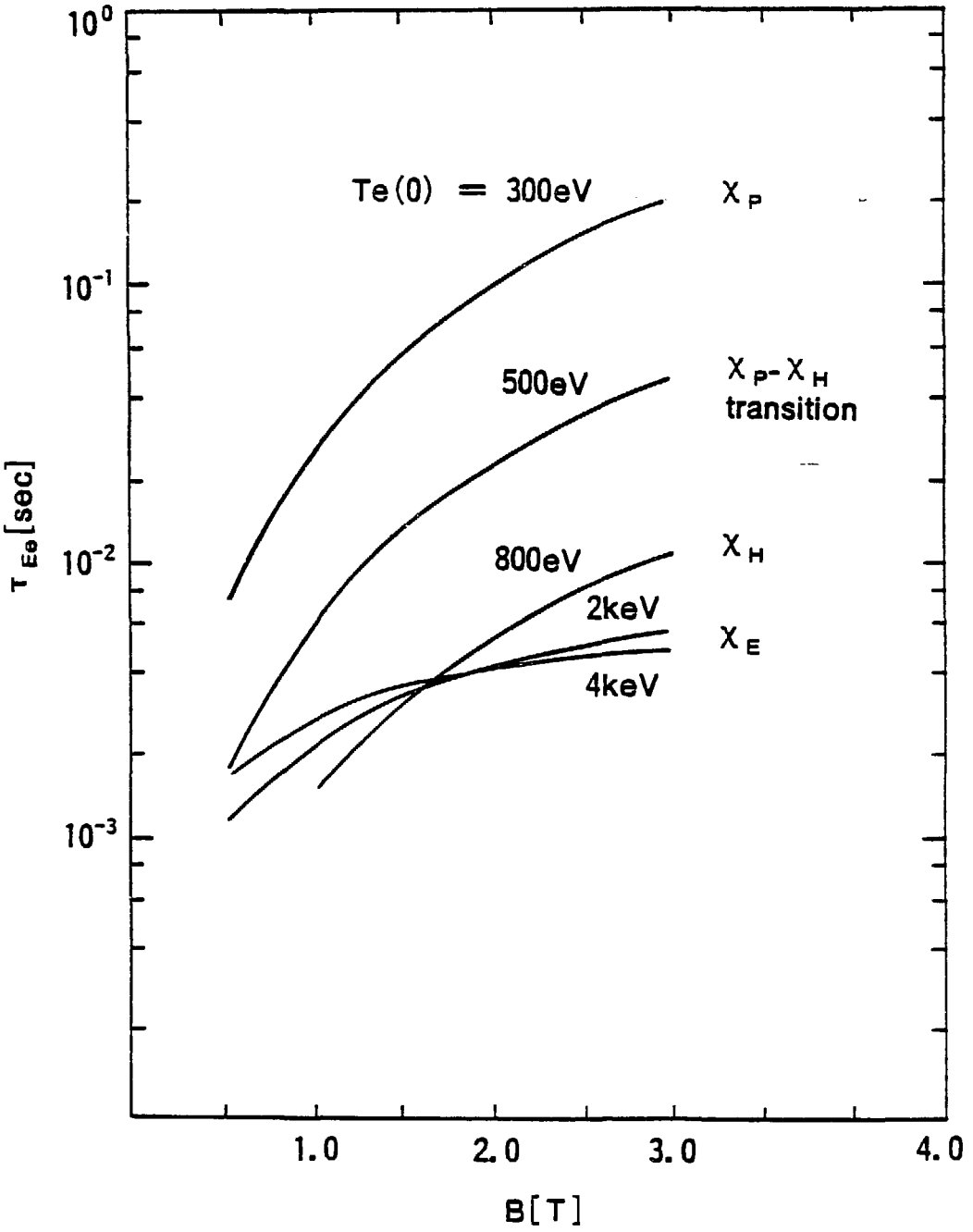
10^0
10^{-1}
10^{-2}
10^{-3}
T_{Ee}[sec]
Te(0) = 300eV
χ_P
500eV
χ_P-χ_H
transition
800eV
χ_H
2keV
χ_E
4keV
1.0
2.0
3.0
4.0
B[T]

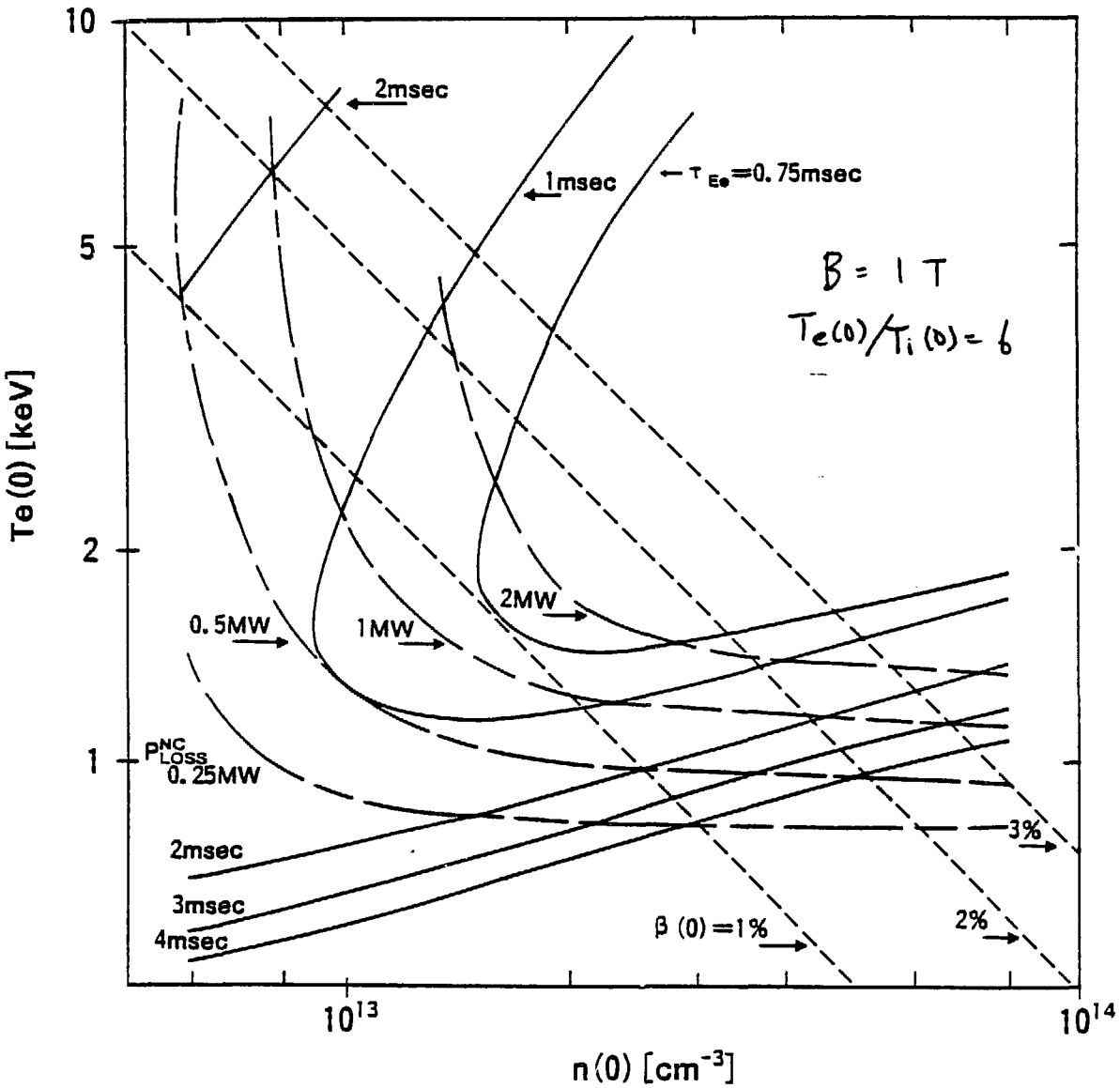
10
5
2
1
Te(0) [keV]
2msec
1msec
τ_{Eo}=0.75msec
B = 1 T
$T_e(0)/T_i(0) = 1$
2MW
0.5MW
1MW
P^{NC}_{LOSS}
0.25MW
3%
2msec
3msec
4msec
β (0)=1%
2%
10^{13}
10^{14}
n(0) [cm^{-3}]

Cace		Ne (cm^{-3})	B	P_{NBI} P_{ECH}	global τ_E	electrons			ions			⟨β⟩ (beam ioms)
						τ_E	$T_e(o)$	$\langle T_e \rangle$	τ_E	$T_i(o)$	$\langle T_i \rangle$	
I	Reference	5×10^{13}	1.5 T	2 MW 0.2 MW	8.1 ms	24 ms	1.9 keV	0.8 keV	4.2 ms	1.9 keV	0.6 keV	3.0% (2.0%)
II	Lower density	3×10^{13}	1.5 T	2 MW 0.2 MW	7.3 ms	13 ms	2.0keV	0.8keV	4.0 ms	1.7keV	0.5keV	2.7% (2.2%)
III	Anomaly only No ripple	5×10^{13}	1.5 T	2 MW 0.2 MW	15 ms	23 ms	2.0 keV	1.1 keV	11 ms	1.9 keV	1.0keV	3.4% (1.4%)
IV	Anomaly and Ripple	5×10^{13}	1.5 T	2 MW 0.2 MW	7.1 ms	13 ms	1.6 keV	0.7 keV	4.4 ms	1.6 keV	0.6 keV	2.9% (2.0%)

(1) Beam absorbed power is approximately 1MW

(2) Anomaly is set as a half of INTOR scaling : $D=5\times10^{16}.\ n_e^{-1}$ (cm/s), $\chi_e=2.5\times10^{17}.\ n_e^{-1}$ (cm/s)

(3) Ripple profile : $\varepsilon_h=0.2\left(\frac{r}{a}\right)^2$

<<< Field Line Topography >>>

Raxis = 97.77

30.0 turns

Bvert = 0.2124 (94.00)
Bquad = 0.0164 (50.00)
Bhexa = 0.0000 (0.00)

NT2 CHS Coil (6pts)
Bv Scanning

Bh0= -1.5001 T Bref= 1.00 T
Bmax= 2.8623 T delB= 0.10 T

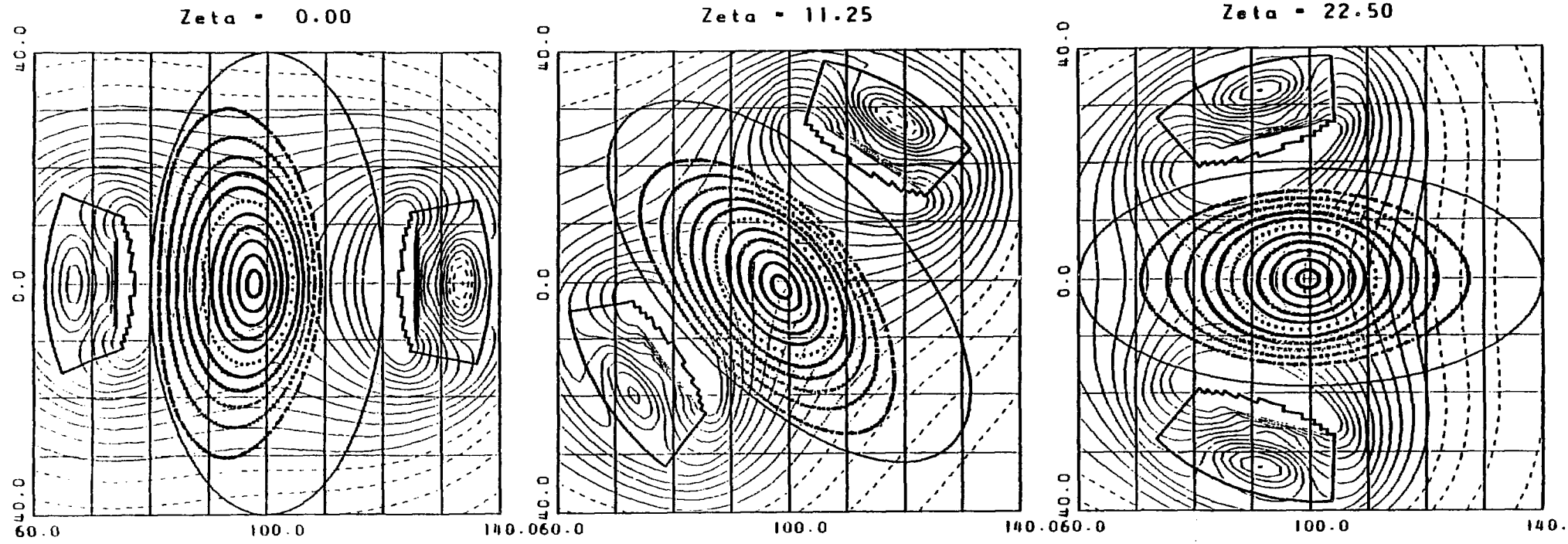

⊙ : Rst= 96.50 30.0 turns
△ : Rst= 95.00 30.0 turns
+ : Rst= 93.50 30.0 turns
× : Rst= 92.00 30.0 turns
◇ : Rst= 90.50 30.0 turns
✳ : Rst= 89.00 30.0 turns
⋈ : Rst= 87.50 30.0 turns
Z : Rst= 86.00 30.0 turns

✱ : Rst= 81.50 30.0 turns

<<< Field Line Topography >>>

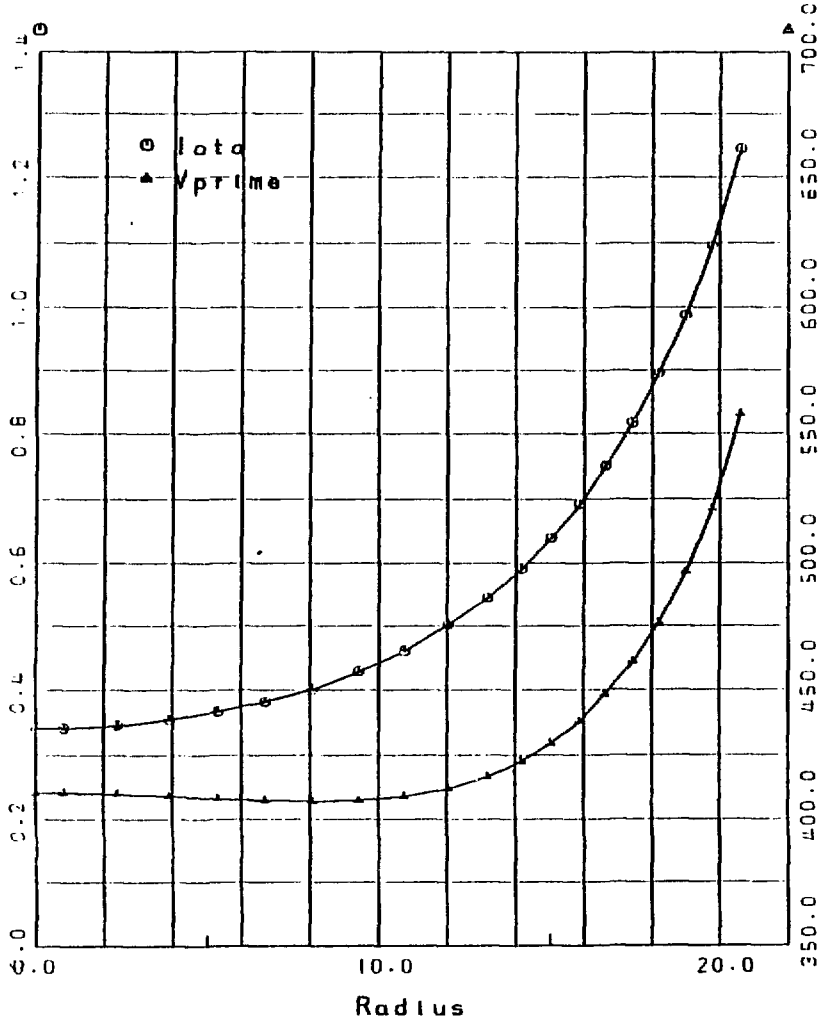

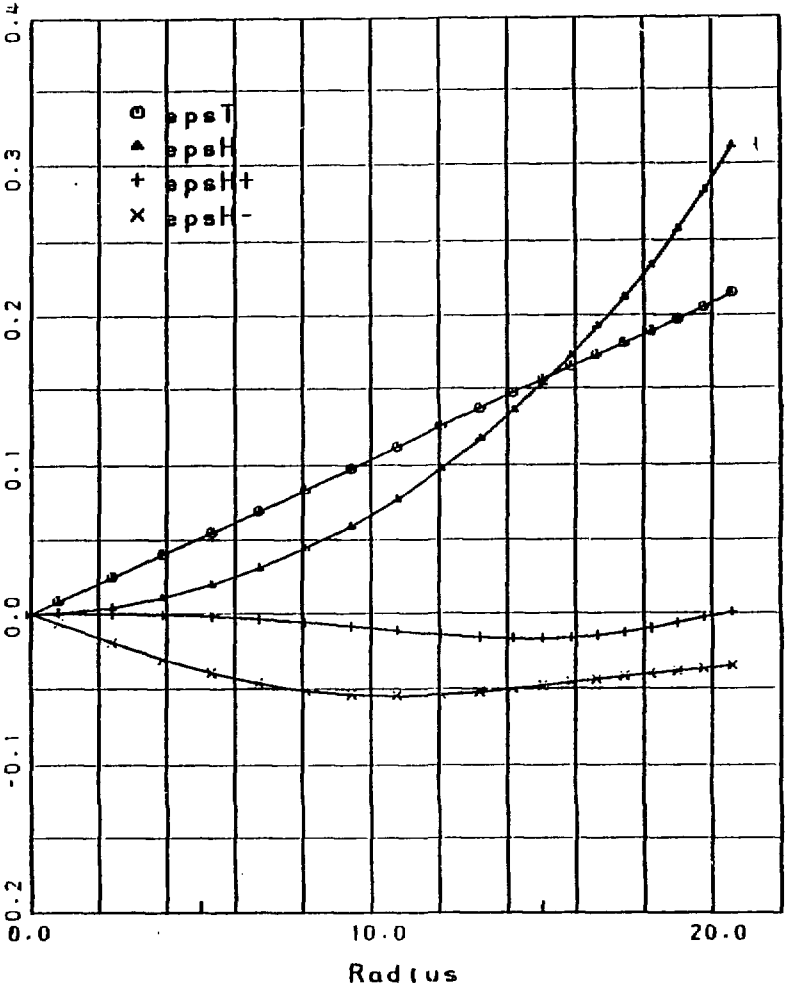

Raxis	=	97.774
radius	=	20.591
iota-0	=	0.341
iota-S	=	1.244
Rbig-0	=	98.710
Rbig-S	=	93.562

epsT	=	0.215
epsH	=	0.312
epsH+	=	0.001
epsH-	=	-0.035

<<< Field Line Topography >>>

Raxis = 101.46

30.0 turns

Bvert = 0.1898 (84.00)
Bquad = 0.0164 (50.00)
Bhexa = 0.0000 (0.00)

NT2 CHS Coil (6pts)
Bv Scanning

Bh0= -1.5001 T Bref= 1.00 T
Bmax= 2.8673 T delB= 0.10 T

Zeta = 0.00

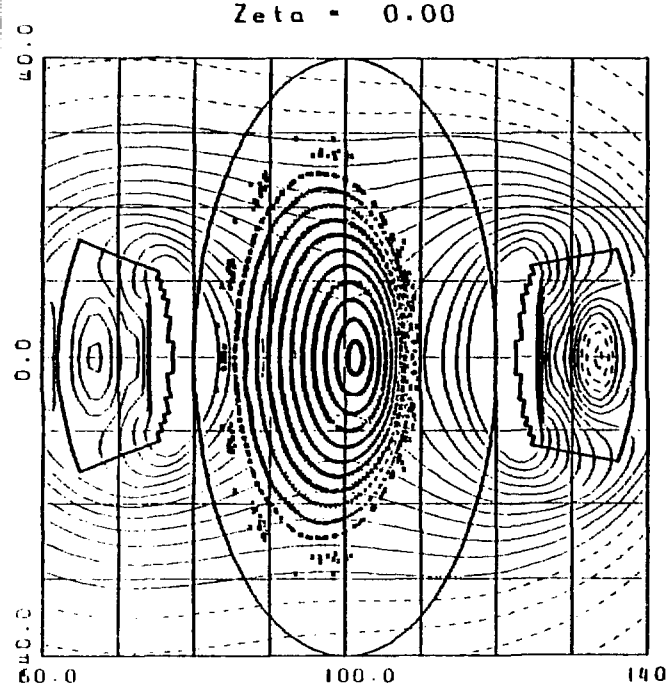

Zeta = 11.25

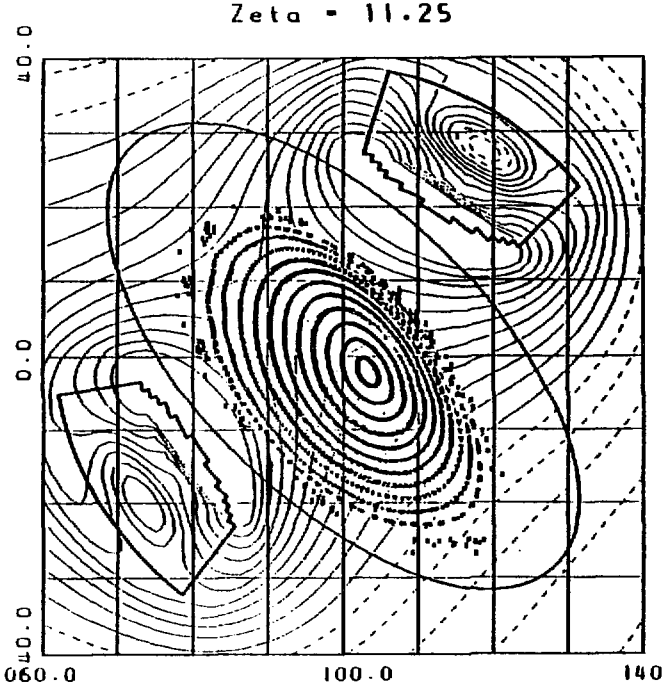

Zeta = 22.50

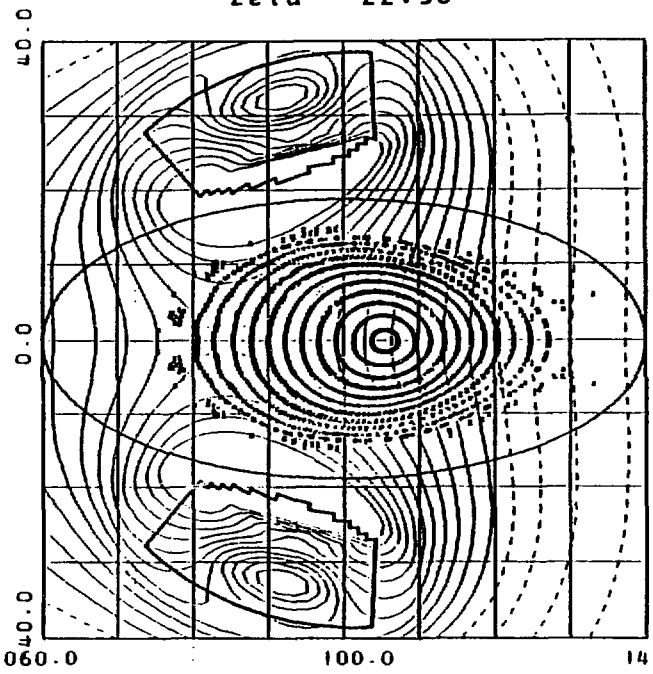

⊙ : Rst= 100.40 30.0 turns
△ : Rst= 98.90 30.0 turns
+ : Rst= 97.40 30.0 turns
× : Rst= 95.90 30.0 turns
◇ : Rst= 94.40 30.0 turns
✝ : Rst= 92.90 30.0 turns
⧖ : Rst= 91.40 30.0 turns
Z : Rst= 89.90 30.0 turns

✳ : Rst= 85.40 30.0 turns
⧗ : Rst= 83.90 6.5 turns

<<< Field Line Topography >>>

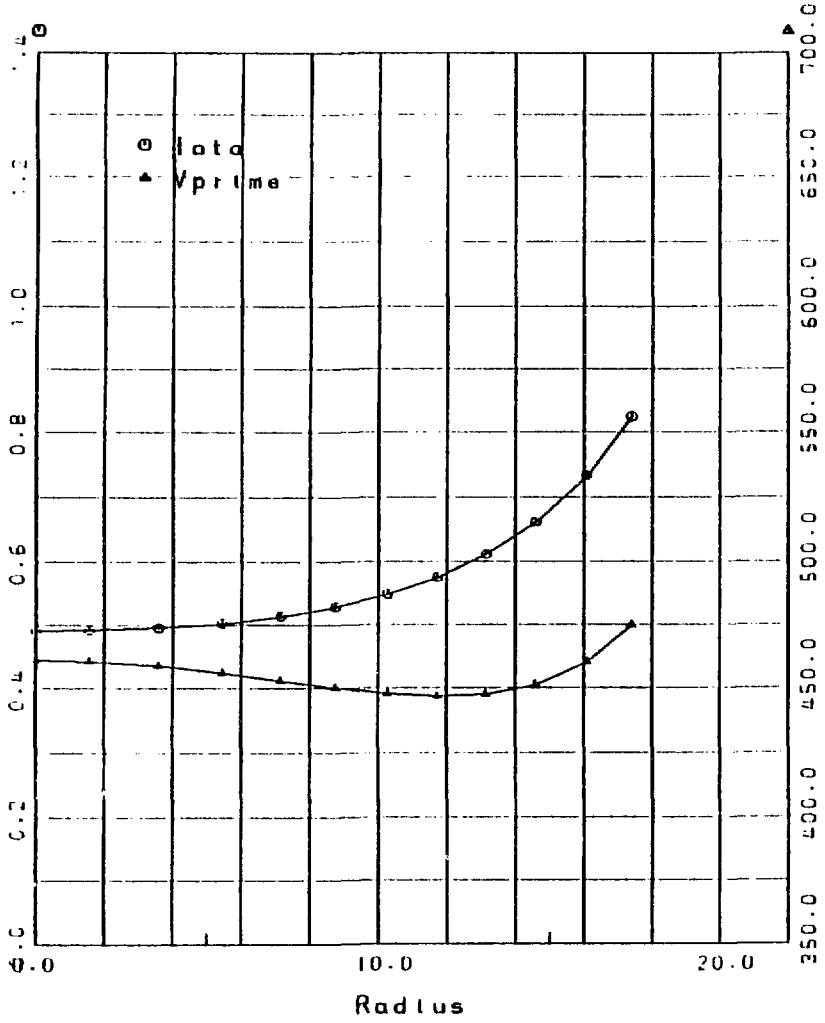

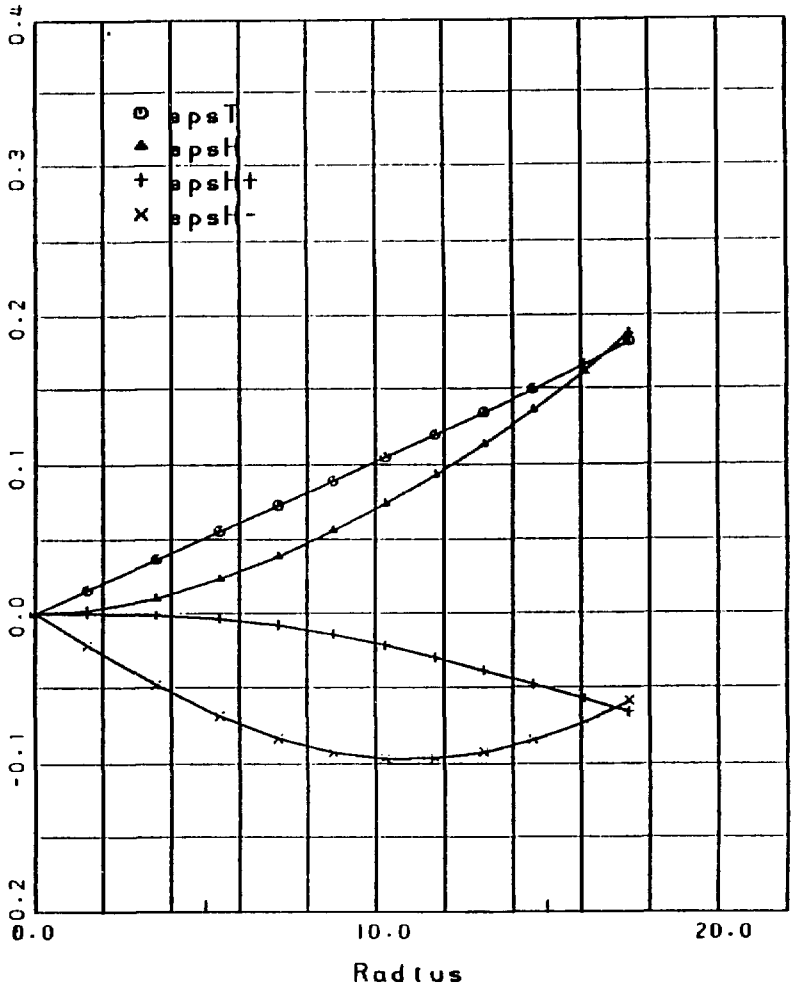

Raxis	=	101.457
radius	=	17.408
iota-0	=	0.491
iota-S	=	0.824
Rbig-0	=	103.481
Rbig-S	=	94.830

epsT	=	0.182
epsH	=	0.188
epsH+	=	-0.066
epsH-	=	-0.059

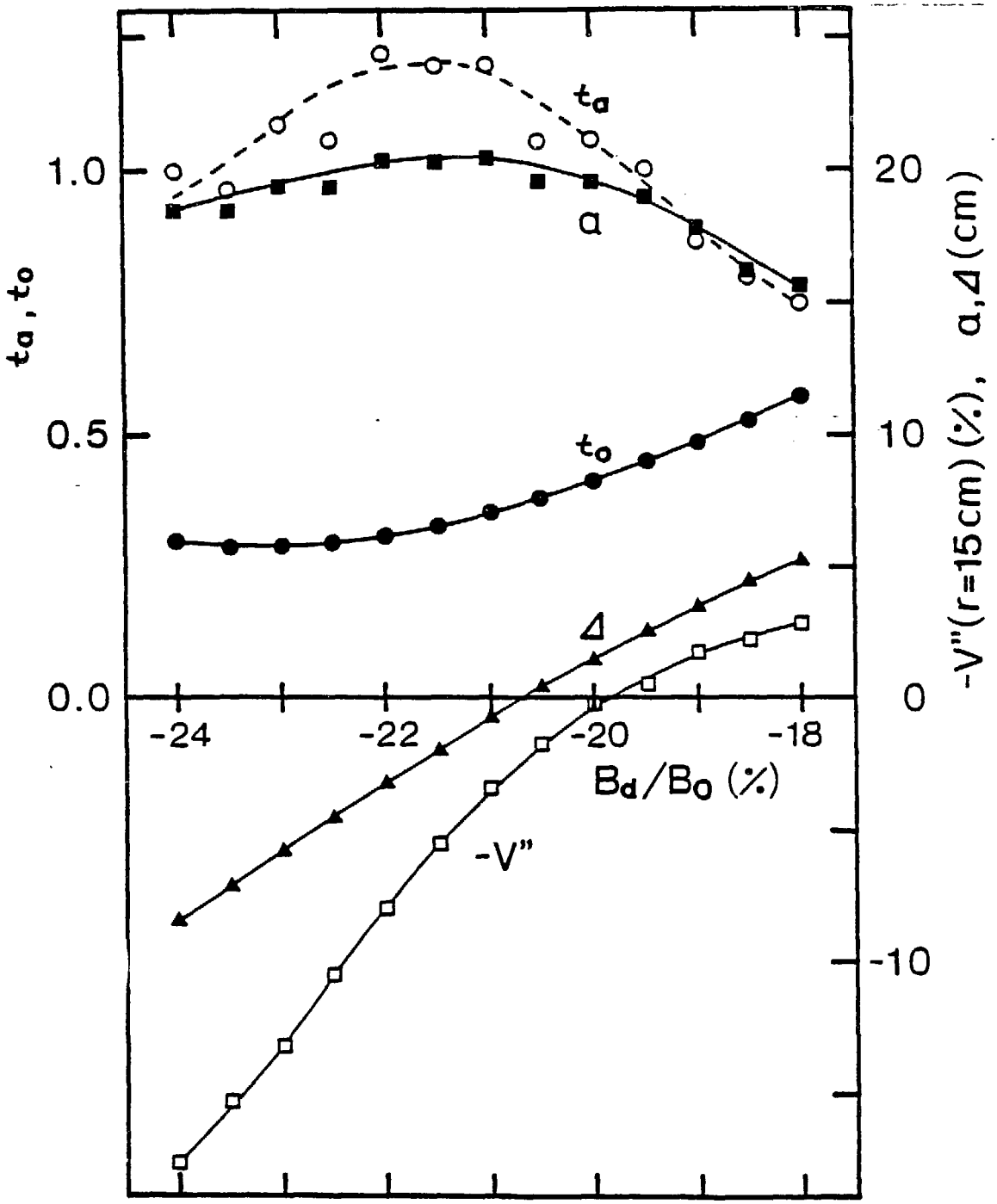
1.0
0.5
0.0
20
10
0
-10
-24
-22
-20
-18
t_a
a
t_o
Δ
-V"
B_d/B_o (%)
t_a, t_o
-V"(r=15cm)(%), a,Δ(cm)

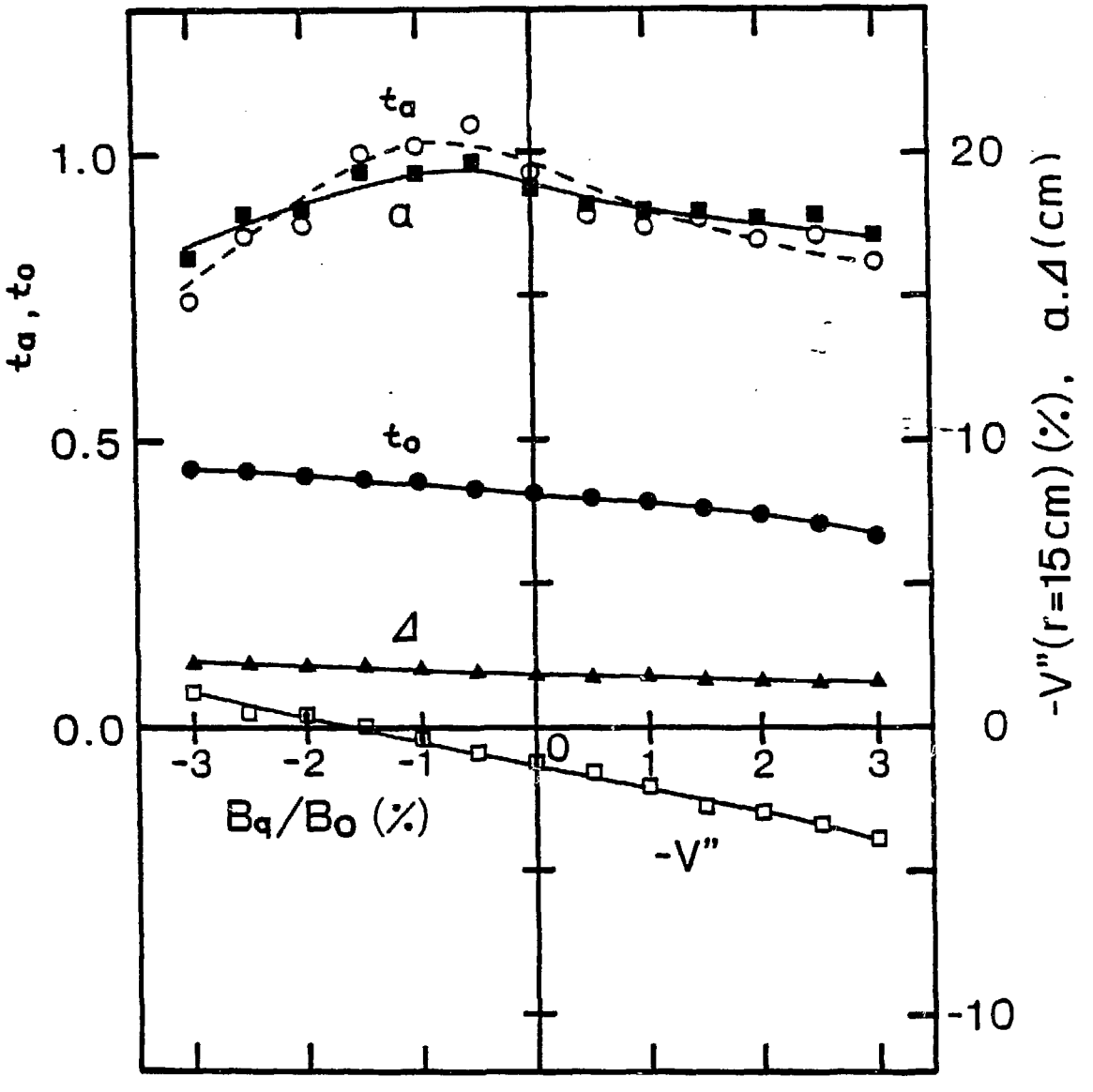
t_a
a
t_o
Δ
-V"
1.0
0.5
0.0
20
10
0
-10
-3
-2
-1
0
1
2
3
B_q/B_o (%)
t_a, t_o
-V"(r=15cm) (%), a.Δ(cm)

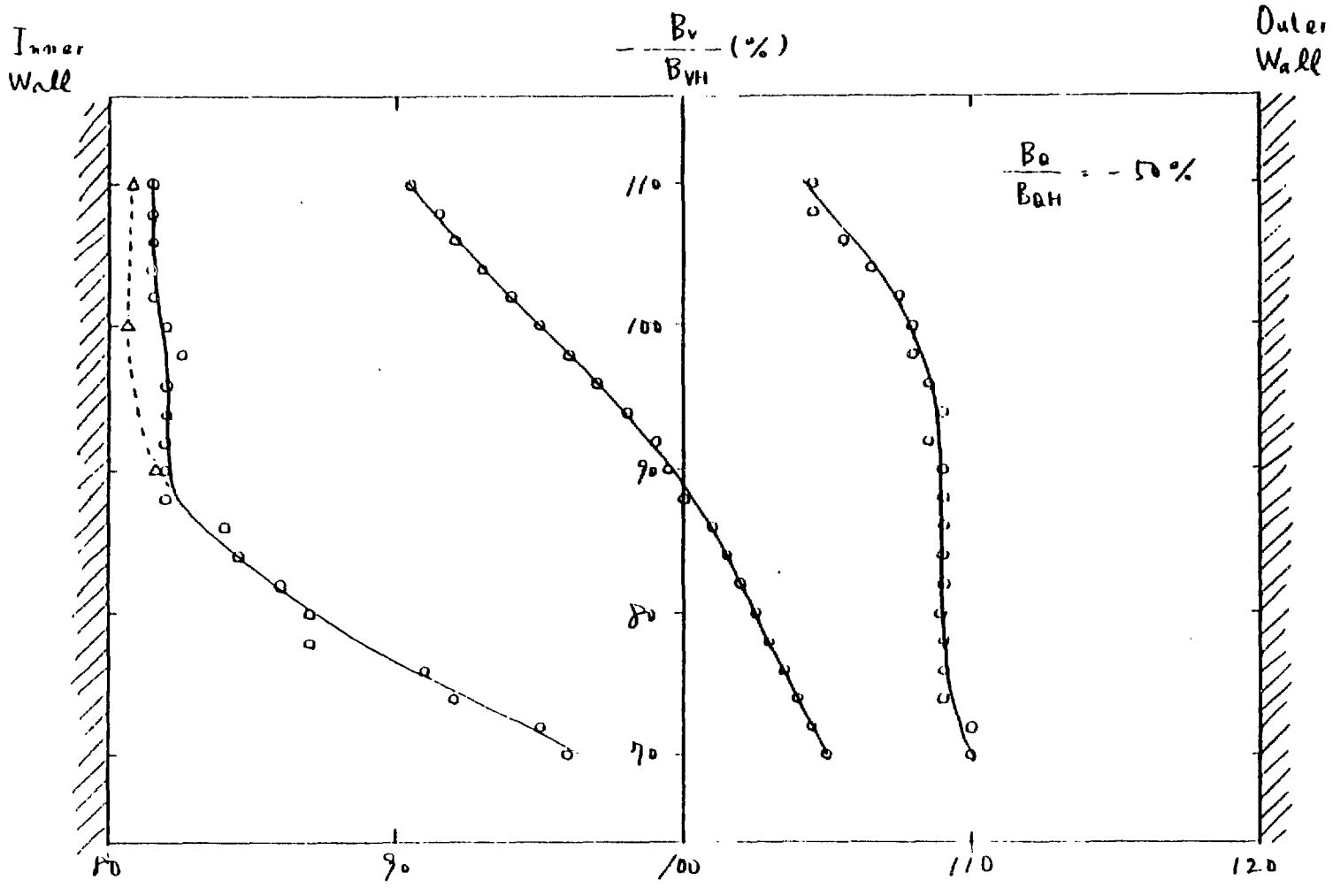
Inner Wall
$\frac{B_V}{B_{VH}}$ (%)
Outer Wall
$\frac{B_\theta}{B_{\theta H}} = -50\%$
110
100
90
80
70
80
90
100
110
120

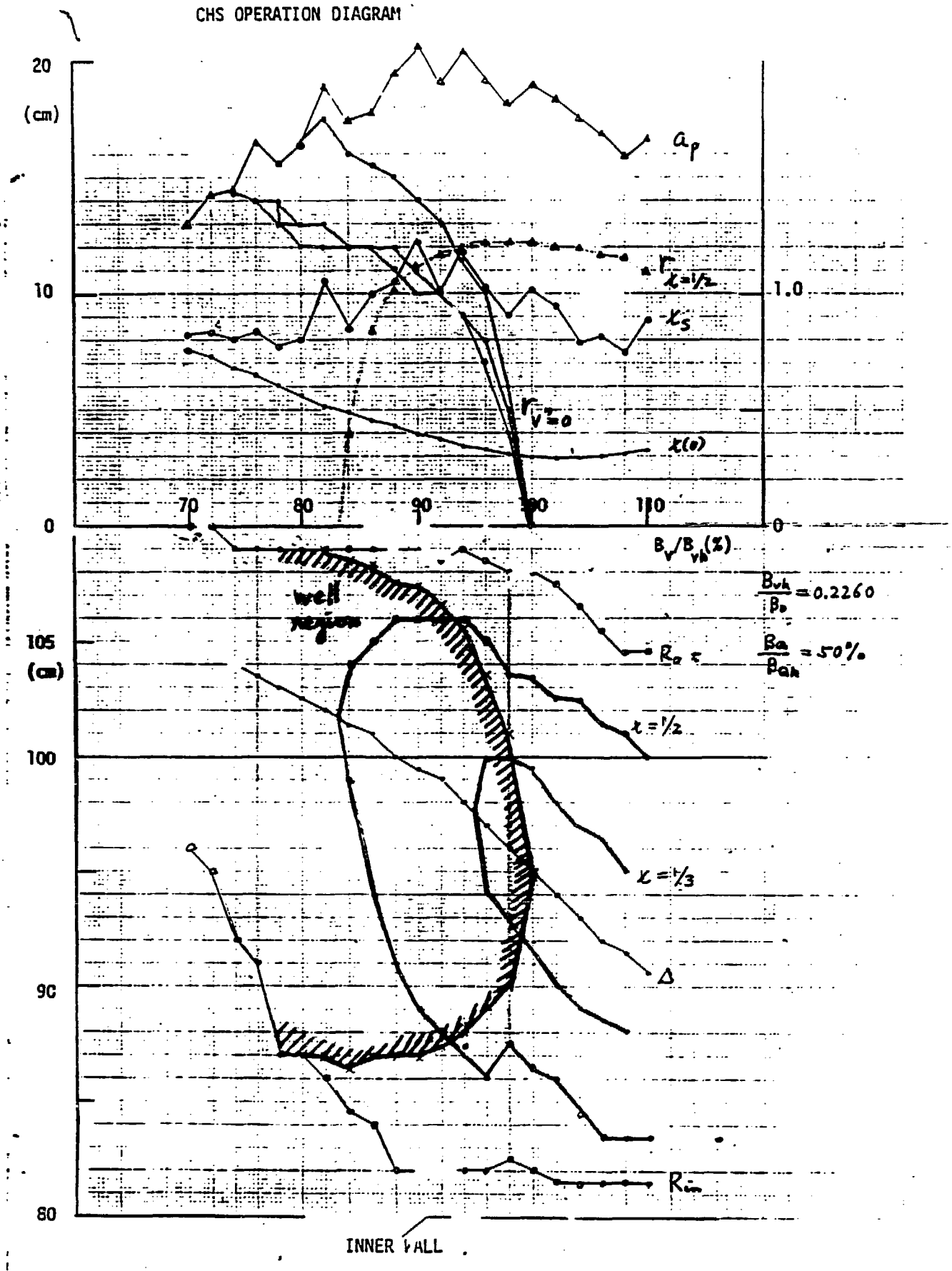
CHS OPERATION DIAGRAM
20
(cm)
10
0
70
80
90
100
110
B_v/B_{vh}(%)
a_p
$r_{x=1/2}$
1.0
x_s
$r_{v=0}$
$x(a)$
$\frac{B_{vh}}{B_o}$ = 0.2260
$\frac{B_a}{B_{ah}}$ = 50%
well region
R_a
$x=1/2$
105
(cm)
100
$x=1/3$
Δ
90
R_i
80
INNER WALL

C.H.S. (M=8) (15cm*18cm)

•NTRACE•V-68(1987/06/10) IADAMS(6), INTPOL(12)0

DDIV • 0.5000
TDIV • 0.0000

Bvert • 0.1875 (83.00) Delta • 3.962
Bquad • 0.0164 (50.00)
Bhexa • 0.0000 (0.00)

ZETA • 0.00

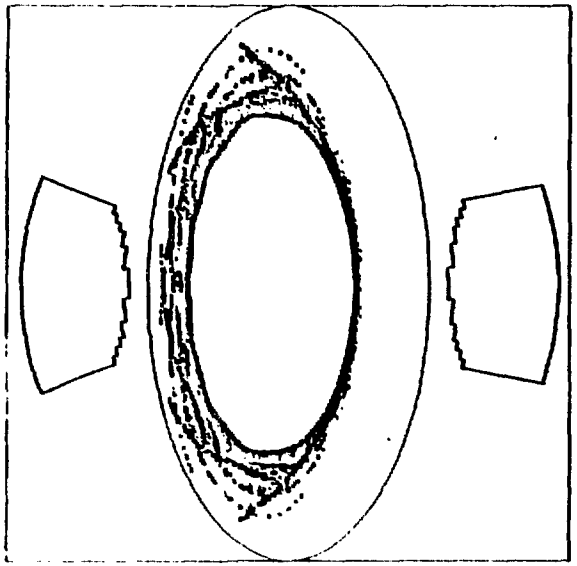

ZETA • 11.25

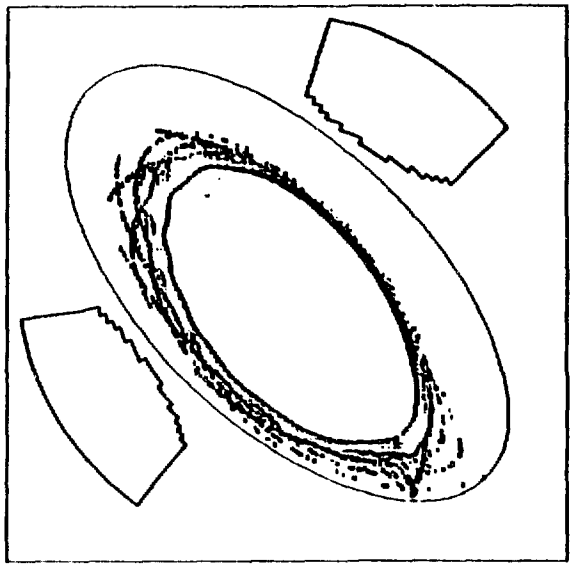

ZETA • 22.50

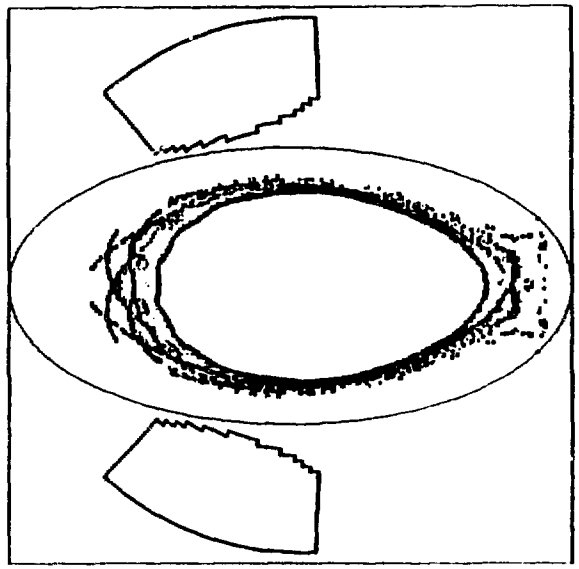

L.H.S. (M-B) (15cm*18cm)

Bvert = 0.1875 (83.00) Delta = 3.962

Bquad = 0.0164 (50.00)

Bhexa = 0.0000 (0.00)

	ODIV	TDIV
□	0.5000	0.0000
○	1.0000	0.0000

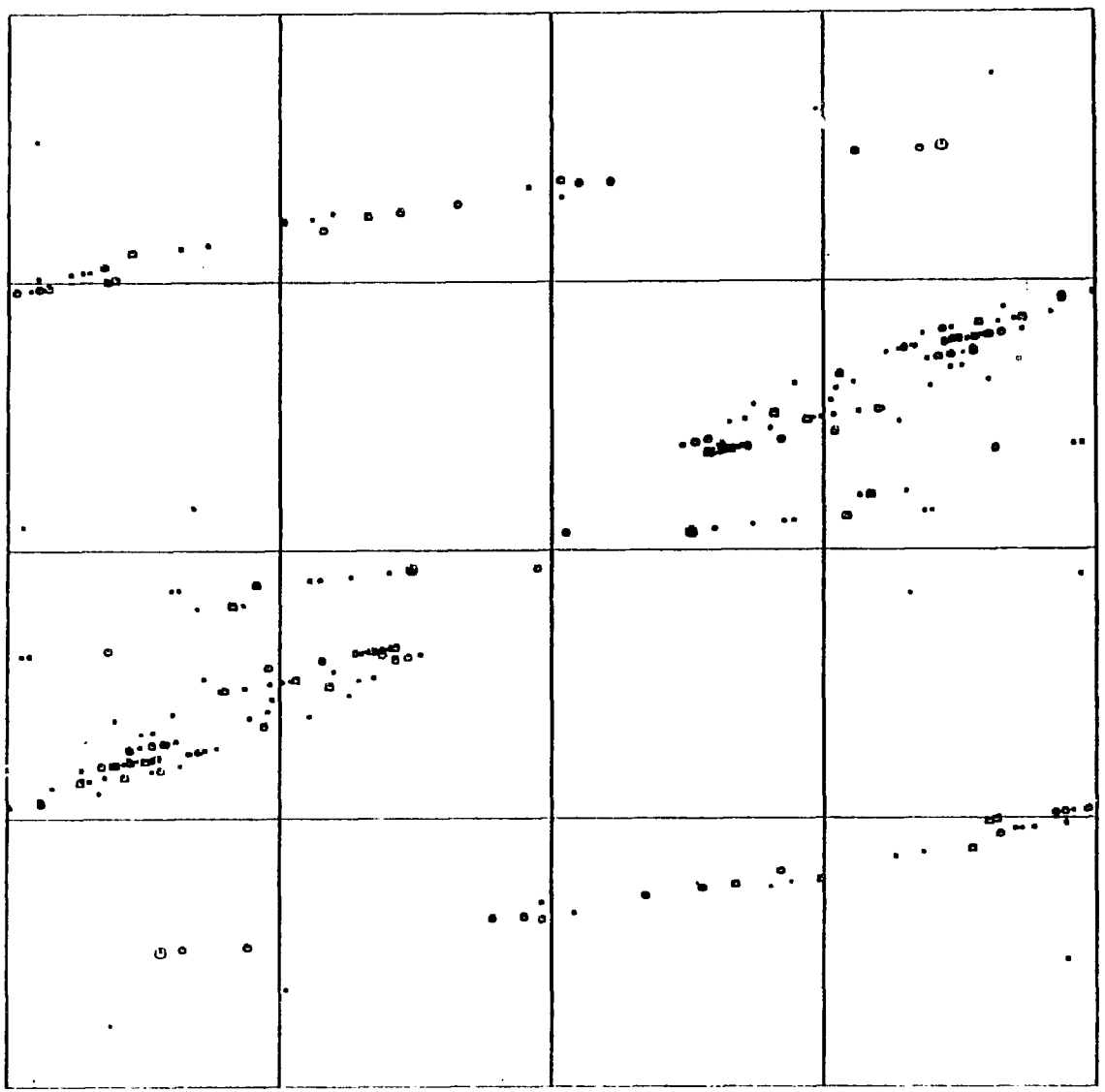

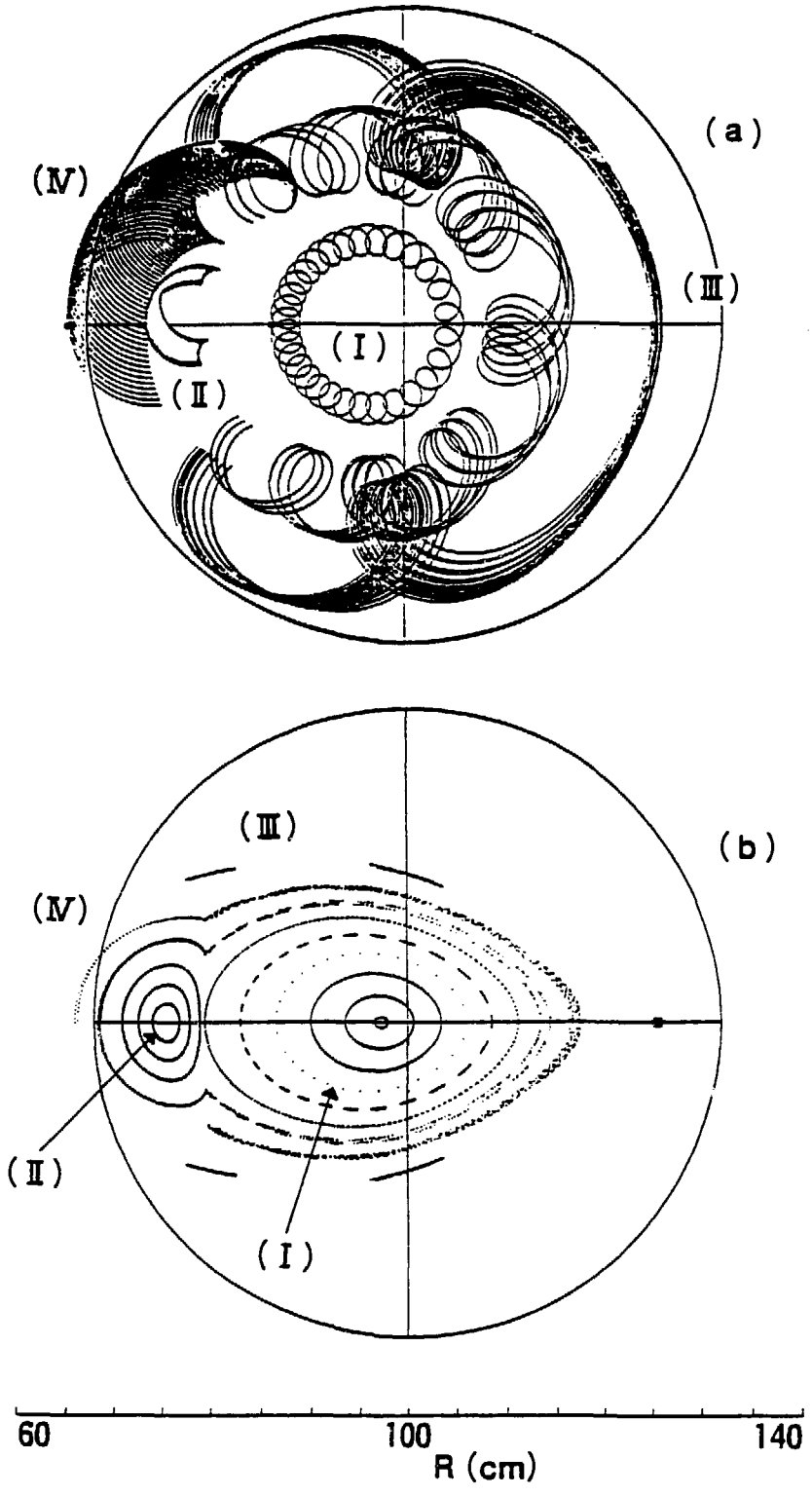
(a)
(Ⅳ)
(Ⅲ)
(Ⅰ)
(Ⅱ)
(b)
(Ⅲ)
(Ⅳ)
(Ⅱ)
(Ⅰ)
60
100
140
R (cm)

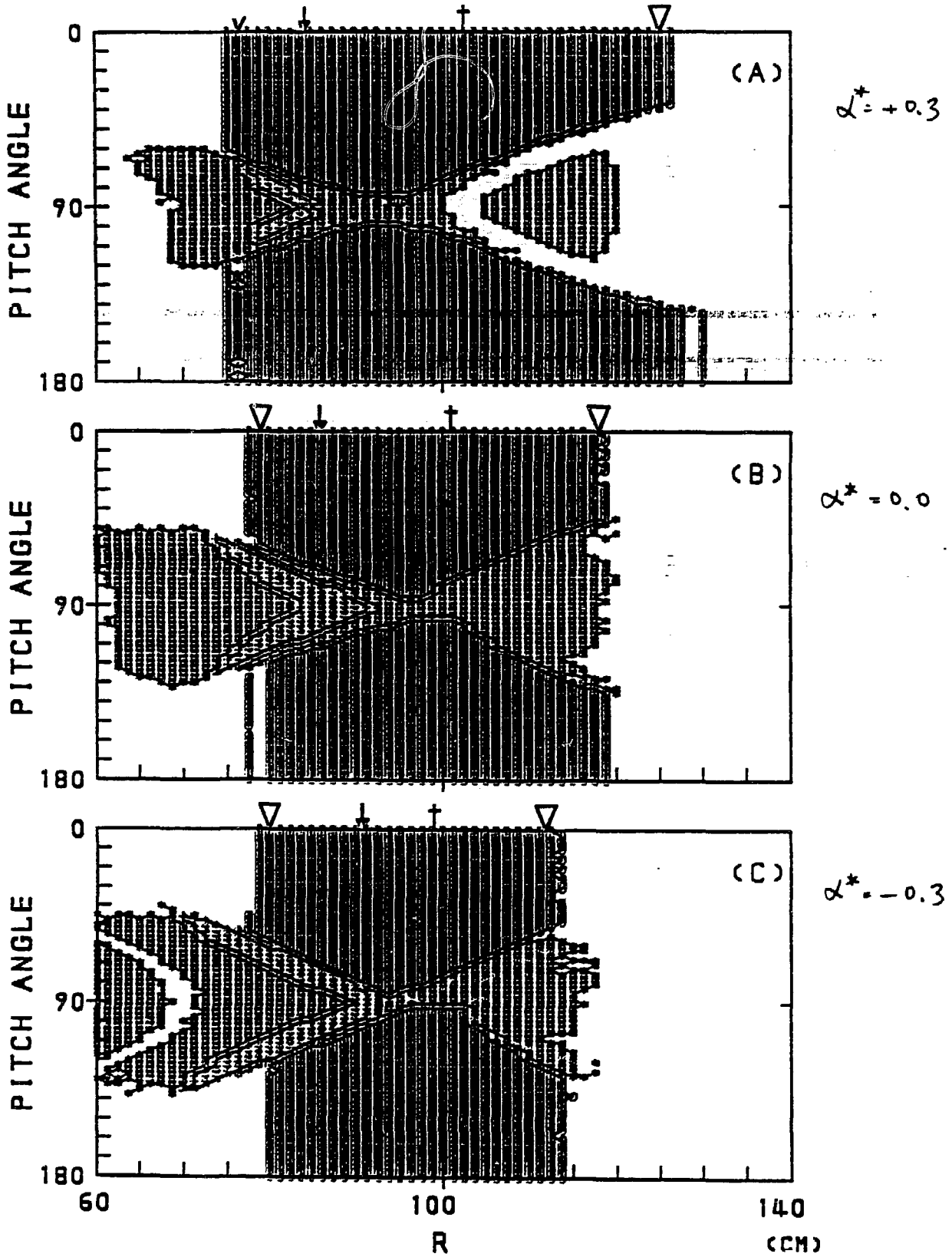
PARTICLE ENERGY 1000. (EV)
PITCH ANGLE
0
90
180
(A)
α* = +0.3
(B)
α* = 0.0
(C)
α* = −0.3
60
100
140
R
(CM)

$\langle\beta\rangle = 0\,\%$

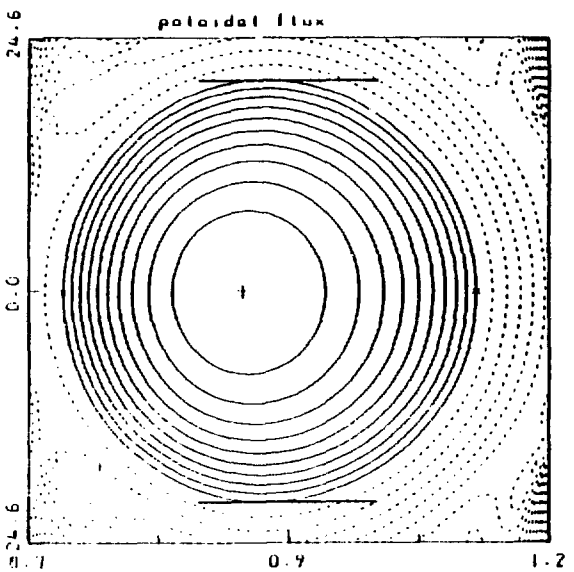

$\langle\beta\rangle = 2\,\%$

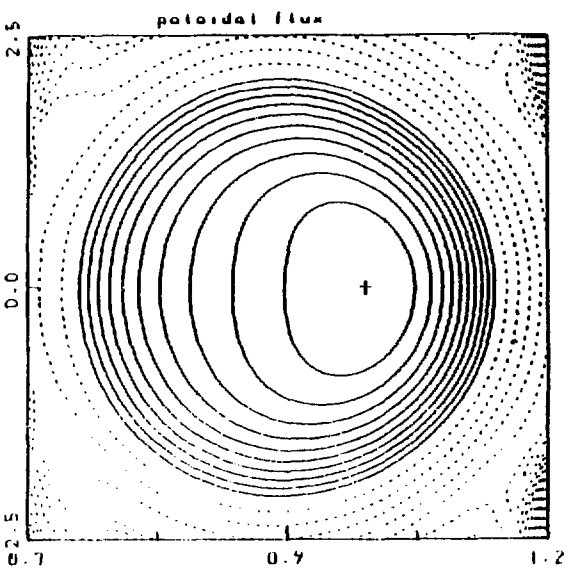

$\langle\beta\rangle = 5\,\%$

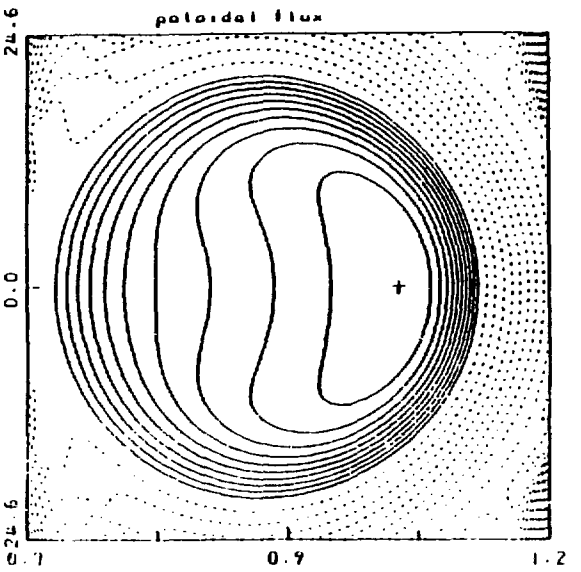

$\langle \beta \rangle = 2\%$

Zeta = 0.00

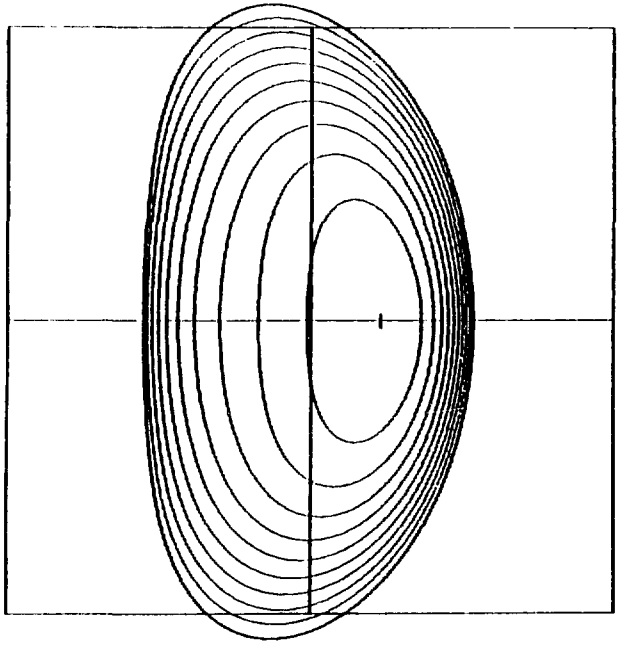

Zeta = 11.25

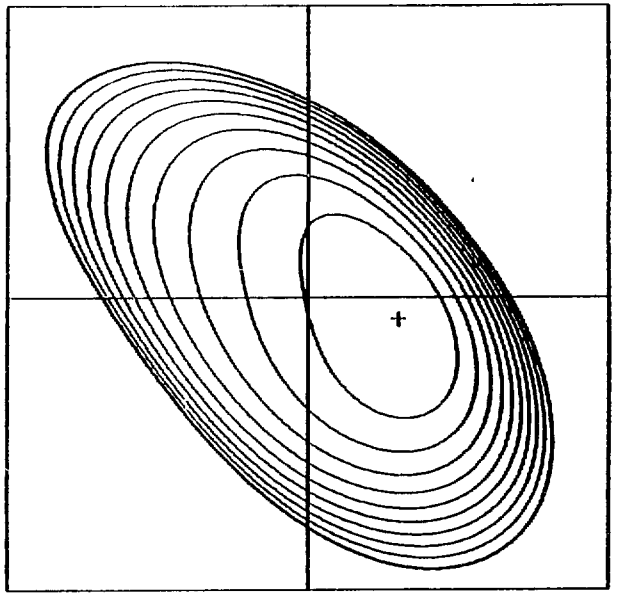

Zeta = 22.50

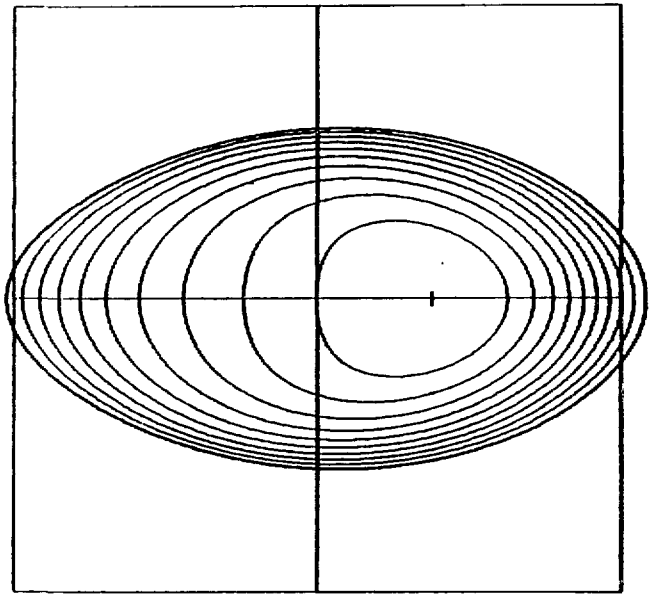

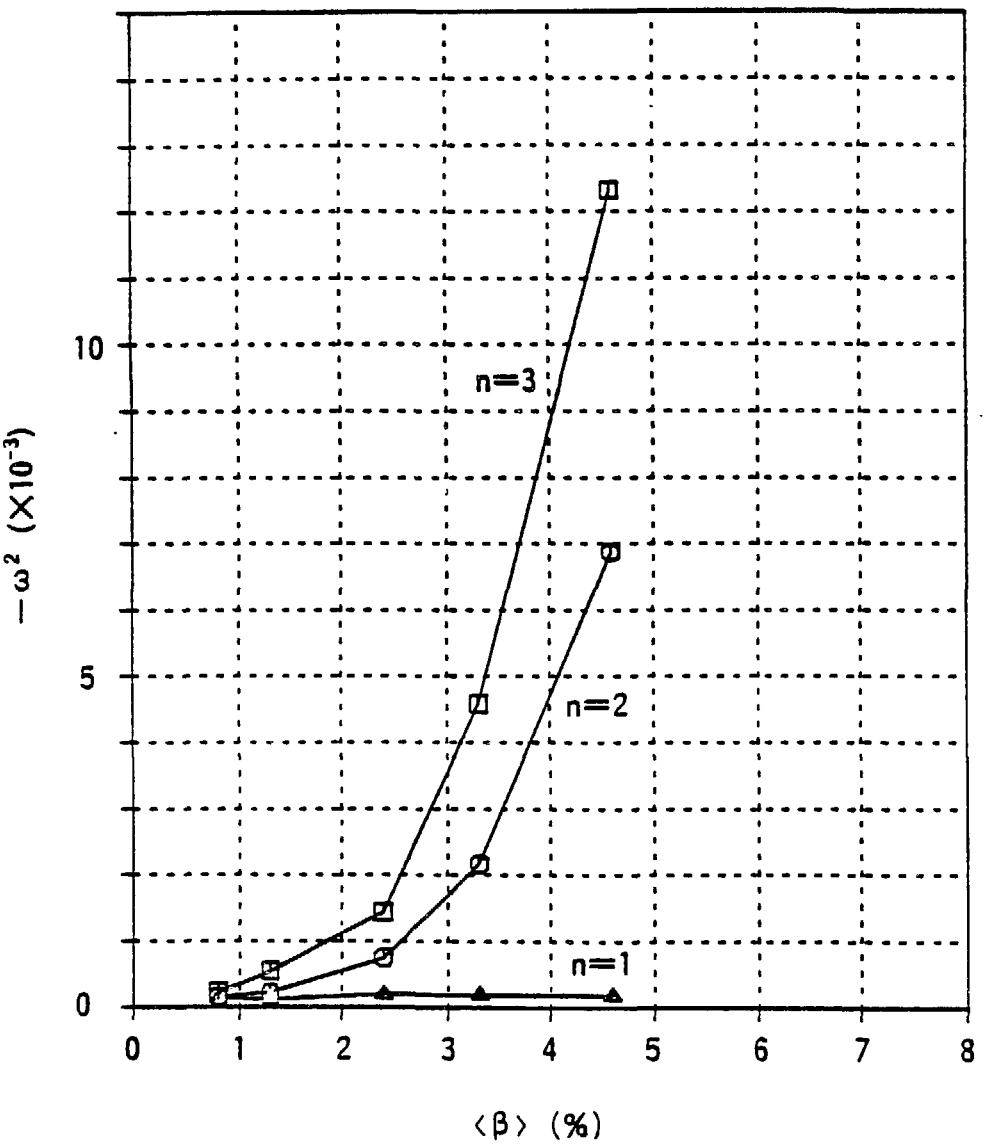
10
5
0
n=3
n=2
n=1
0
1
2
3
4
5
6
7
8
$-\omega^2$ ($\times 10^{-3}$)
$\langle\beta\rangle$ (%)

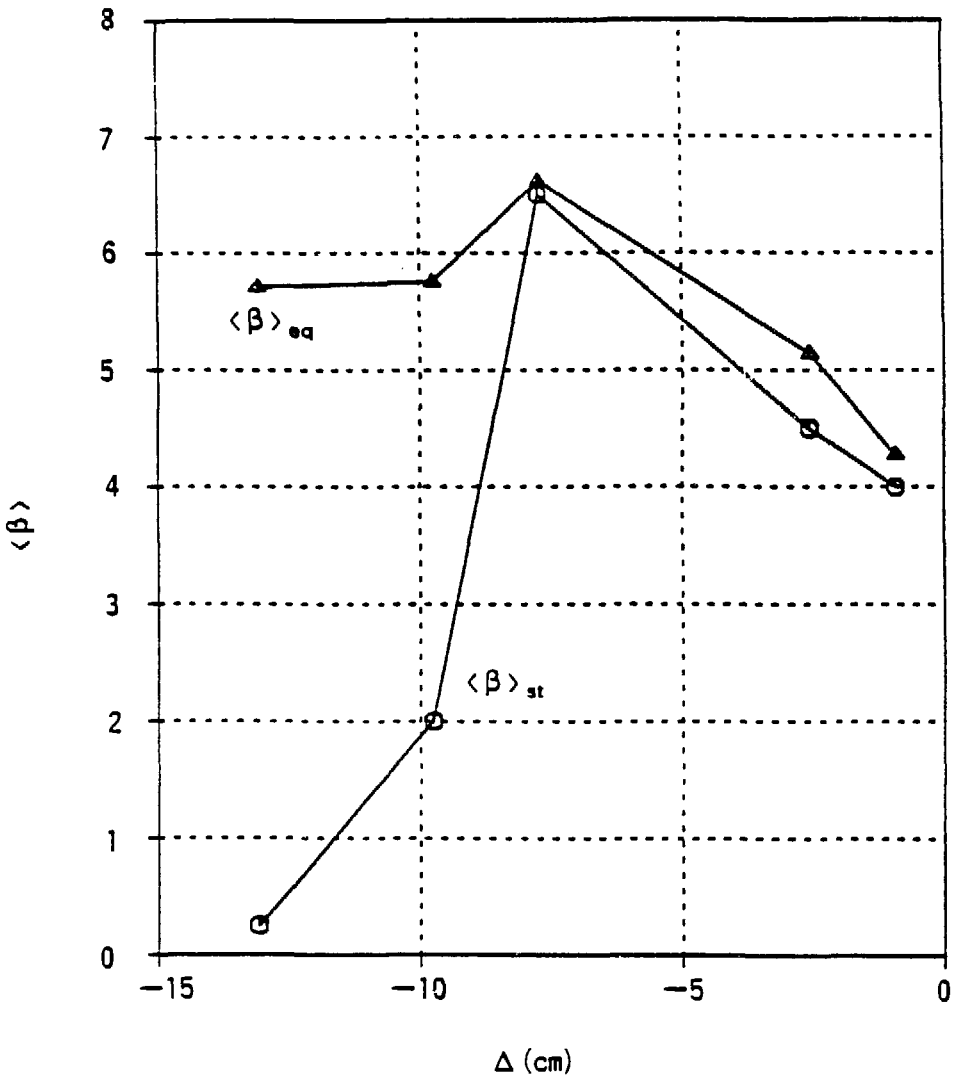
8
7
6
5
4
3
2
1
0
−15
−10
−5
0
⟨β⟩
Δ (cm)
⟨β⟩ eq
⟨β⟩ st

Schedule of Machine Construction

FY		1987	1988	1989	1990	1991
Experiment Phase			ECH Plasma Confinement Plasma Production with ICRF	Additional Heating with NBI, ICRF Phase I	Additional Heating with NBI, ICRF Phase II	High Beta Plasma Helical Axis
Magnetic Field Vacuum Vessel		Coiles, Vessel and Power Supply for 1.5 Tesla Field	Modification of Power Supply for 2.0 Tesla Field	Carbon Tile Pump Limiter	Pellet Injector	Helical Axis Configuration
Heating Systems	ECH	~~28~~ ~~20~~ GHz (200KW)	56 GHz (200KW)		112 GHz (500KW)	
	NBI		40 keV (1.5MW) #1	40 keV (1.5MW) #2		
	ICRF	Transmitter 1 MW Antennas (Phase I)		Transmitter 3 MW Antennas (Phase II)		
Diagnostics		Basic Diagnostics Thomson Scattering HCN Interfercmeter Fast Neutral Particles Visible Spectroscopy Magnetic Measurement Data Acquisition System	Additional Diagnostics ECE, SX High Energy Particles X Ray Spectroscoopy Edge Region Diagnostics	Electric Field Diagnostics Heavy Ion Beam Probe Doppler Shift	CX Reconbination Spectroscopy	

Experimental Schedule

FY		1987	1988	1989	1990	1991
Machines	Bmax		Bmax=1.5 Tesla	Bmax=2.0 Tesla		
	ECH		28 GHz	28 GHz+56GHz		56 GHz+112 GHz
	NBI			40 keV 1.5 MW	40 keV 3 MW (2 Injectors)	
	ICRF		ICRF 1 MW		ICRF 4 MW	
Experimental Scenario		Installation Performance Vacuum Pumping	Discharge Cleaning Magnetic Surface Measurements 28 GHz ECH Parameter Survey Poloidal Coil Control ICRF Plasma Production ICRF Wave Measurements	56 GHz ECH NBI, ICRF Heating Impurity Control Injection Angle Control for NBI High Energy Particles Measurements	Strong Additional Heating Detailed Magnetic Measurements Particle Control NBI Balanced Injection Elec. Field Measurements	Parameter Survey for Te, Ti Electric Field Control High Beta Experiments Helical Axis Experiment
Related Subjects			Confinement Scaling I Configuration Studies Ergodic Layer Structure	High Te Plasma with ECH χe Profile ICRF Heating Physics Pitch Angle and Confinement	Additional Heating Scaling MHD Stability High Energy Particle Confinement Toroidal Rotation Particle Balance Wall Loading	Confinement Scaling II Radial Electric Field High Beta Physics Helical Axis Physics

Initial Phase Schedule

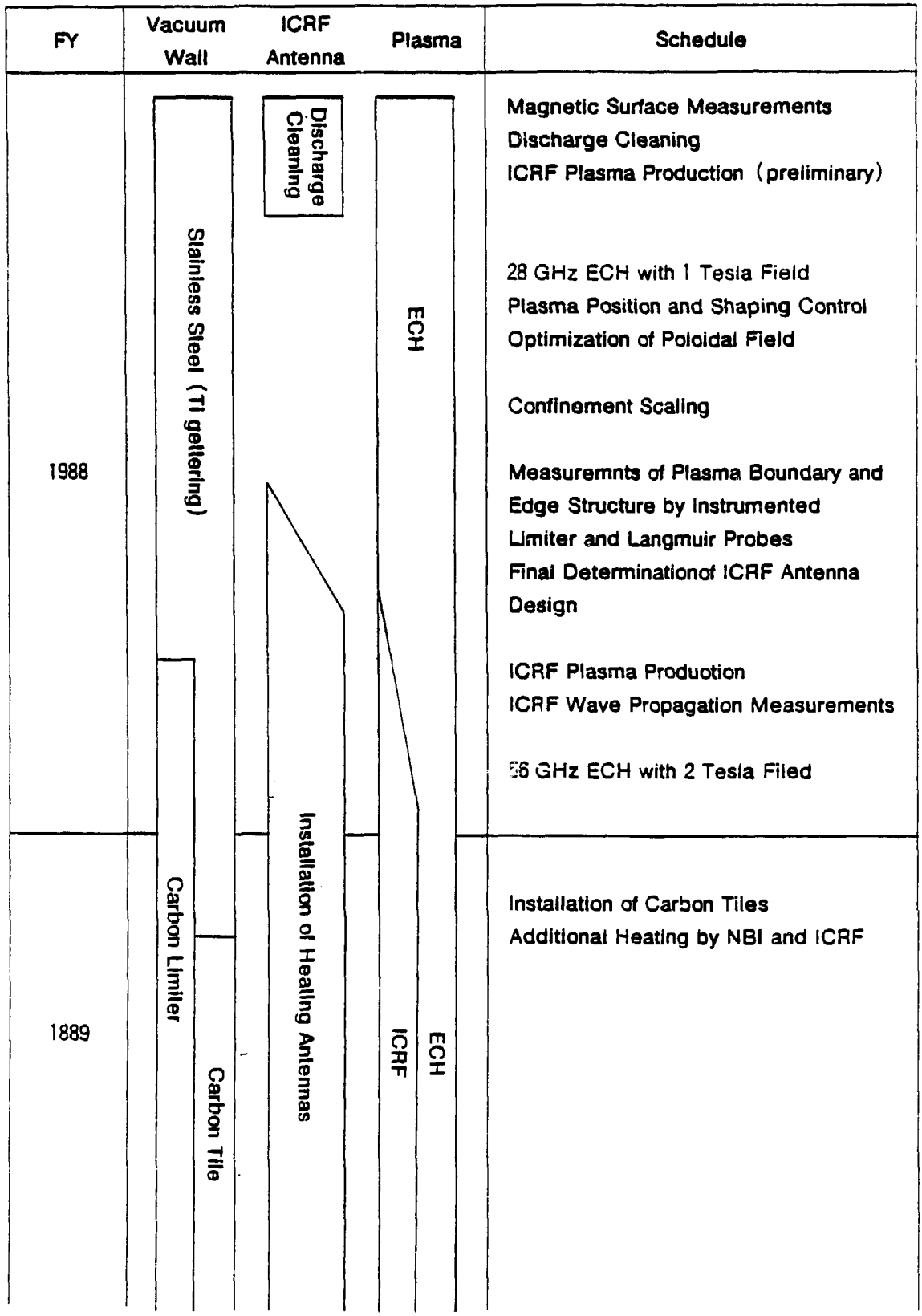

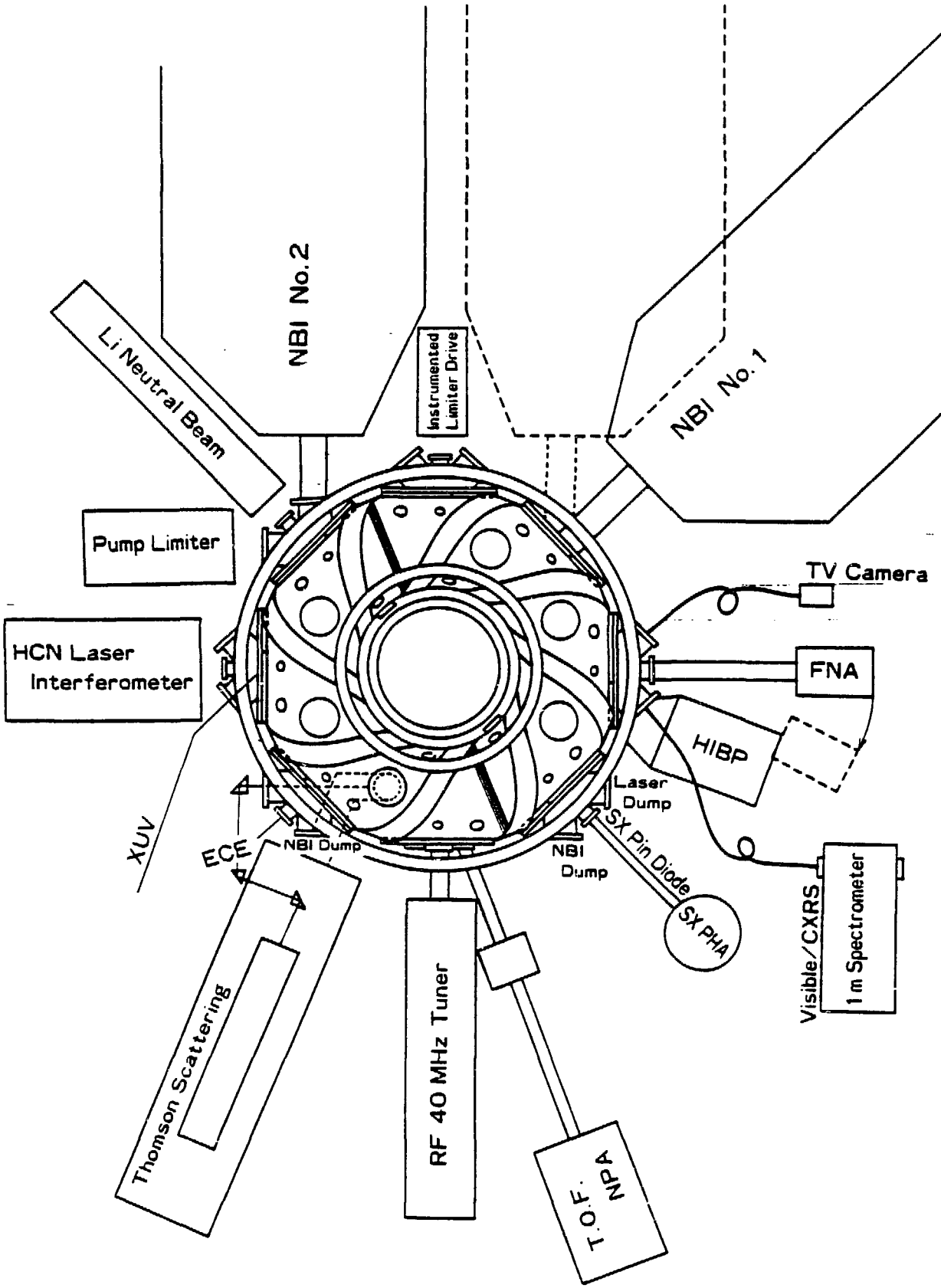
NBI No.2
Instrumented Limiter Drive
NBI No.1
Li Neutral Beam
Pump Limiter
TV Camera
HCN Laser Interferometer
FNA
HIBP
Laser Dump
SX Pin Diode
SX PHA
Visible/CXRS
1 m Spectrometer
XUV
ECE
NBI Dump
NBI Dump
Thomson Scattering
RF 40 MHz Tuner
T.O.F. NPA

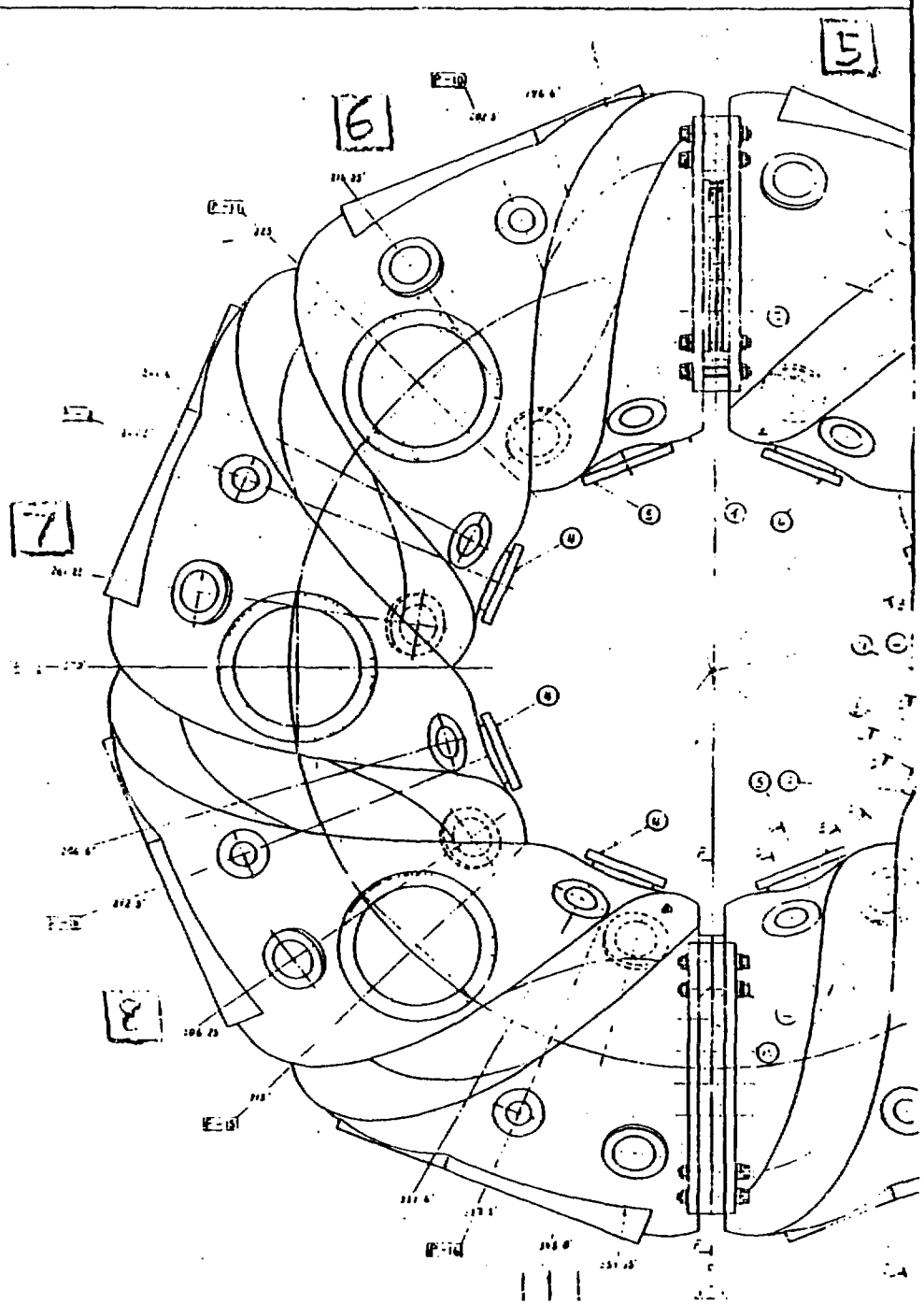
6
5
7
8

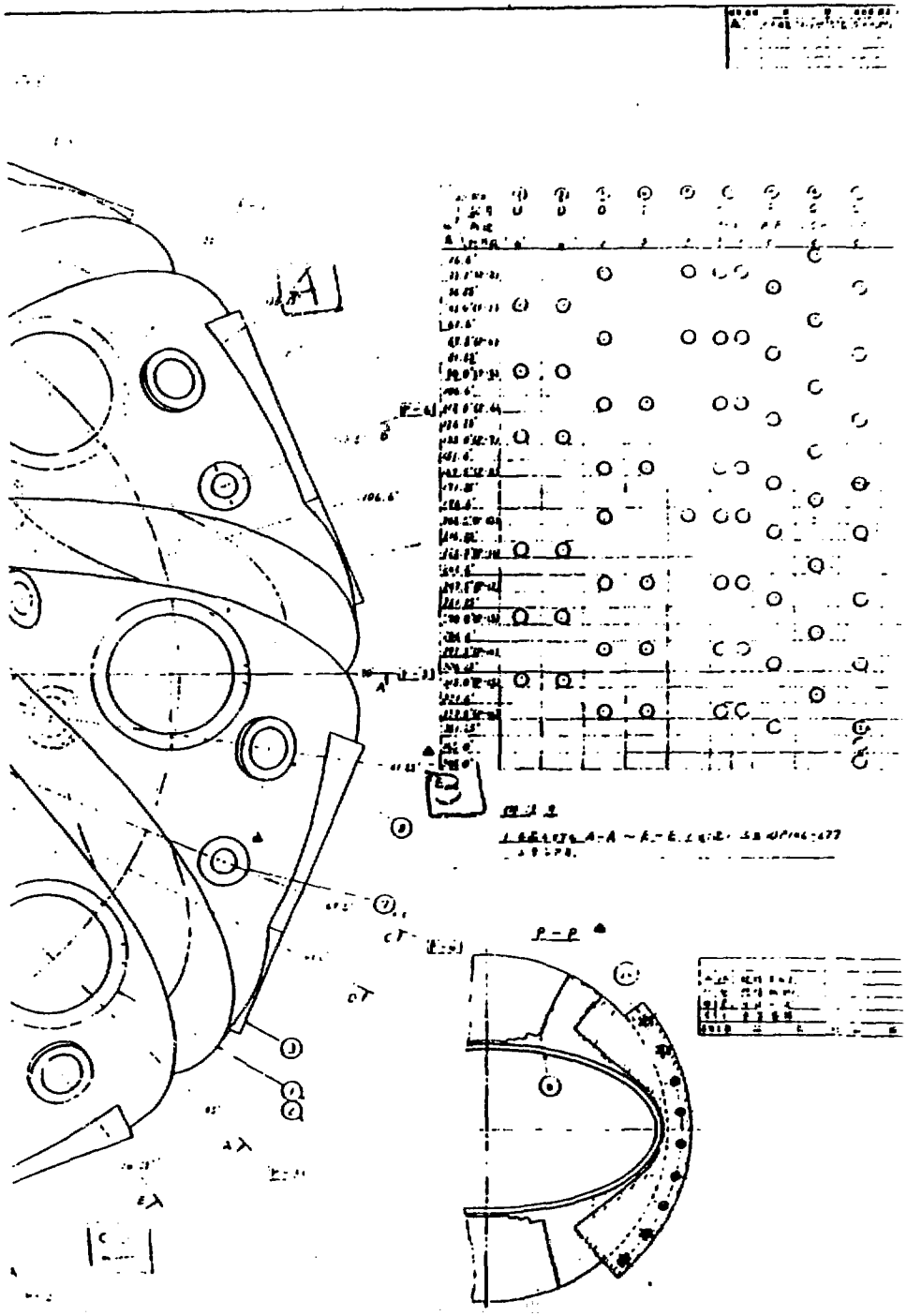
A
B
C
D
A-A
B-B

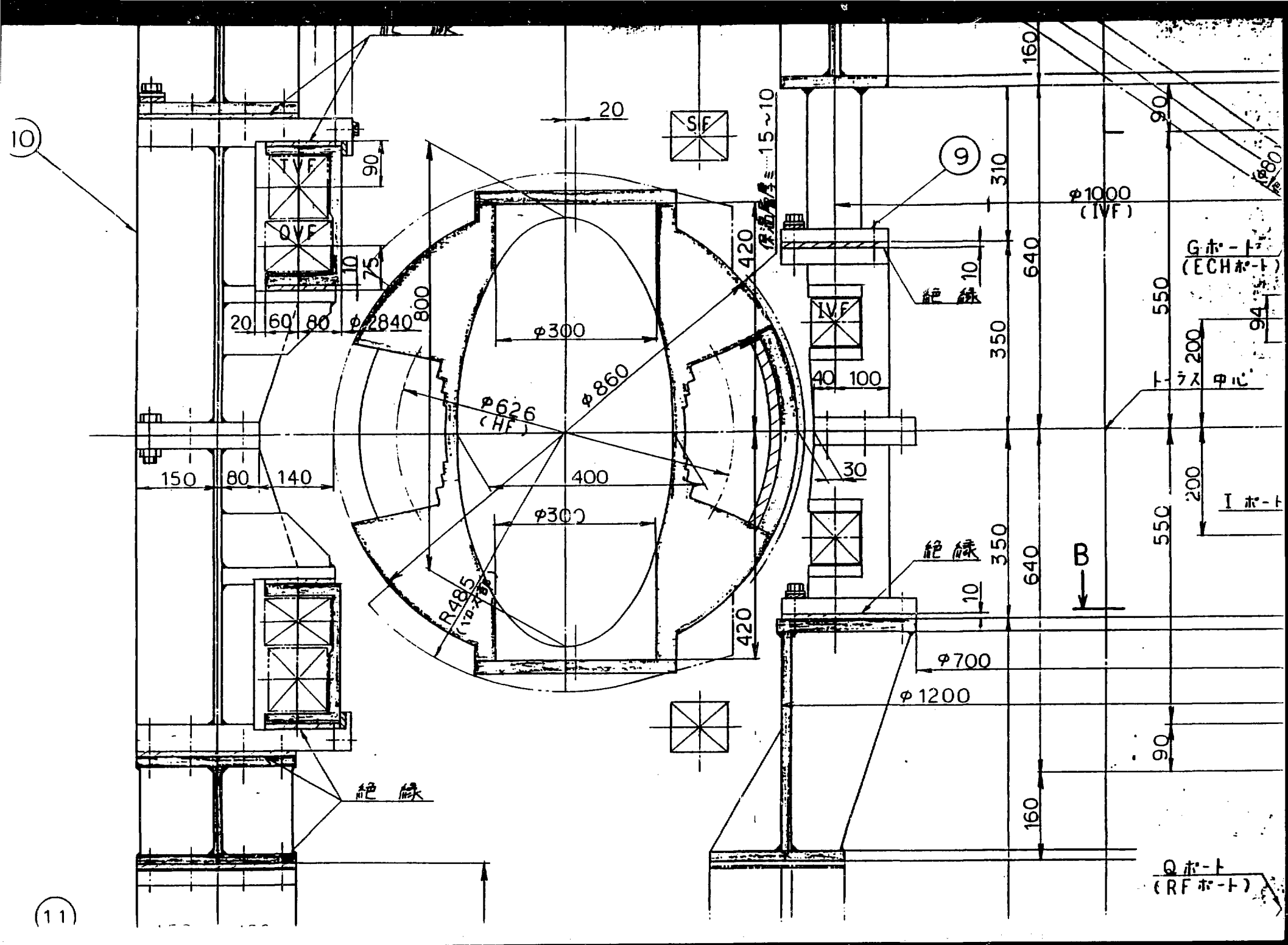
10
11
9
SF
TVF
OVF
IVF
20
90
75
10
800
420
15~10
φ2840
φ300
φ860
φ626
(HF)
400
φ300
R485
150
80
140
60
40
100
30
310
640
350
550
200
94
160
φ1000
(IVF)
φ700
φ1200
絶縁
絶縁
絶縁
B
Gポート
(ECHポート)
トラス中心
Iポート
Qポート
(RFポート)

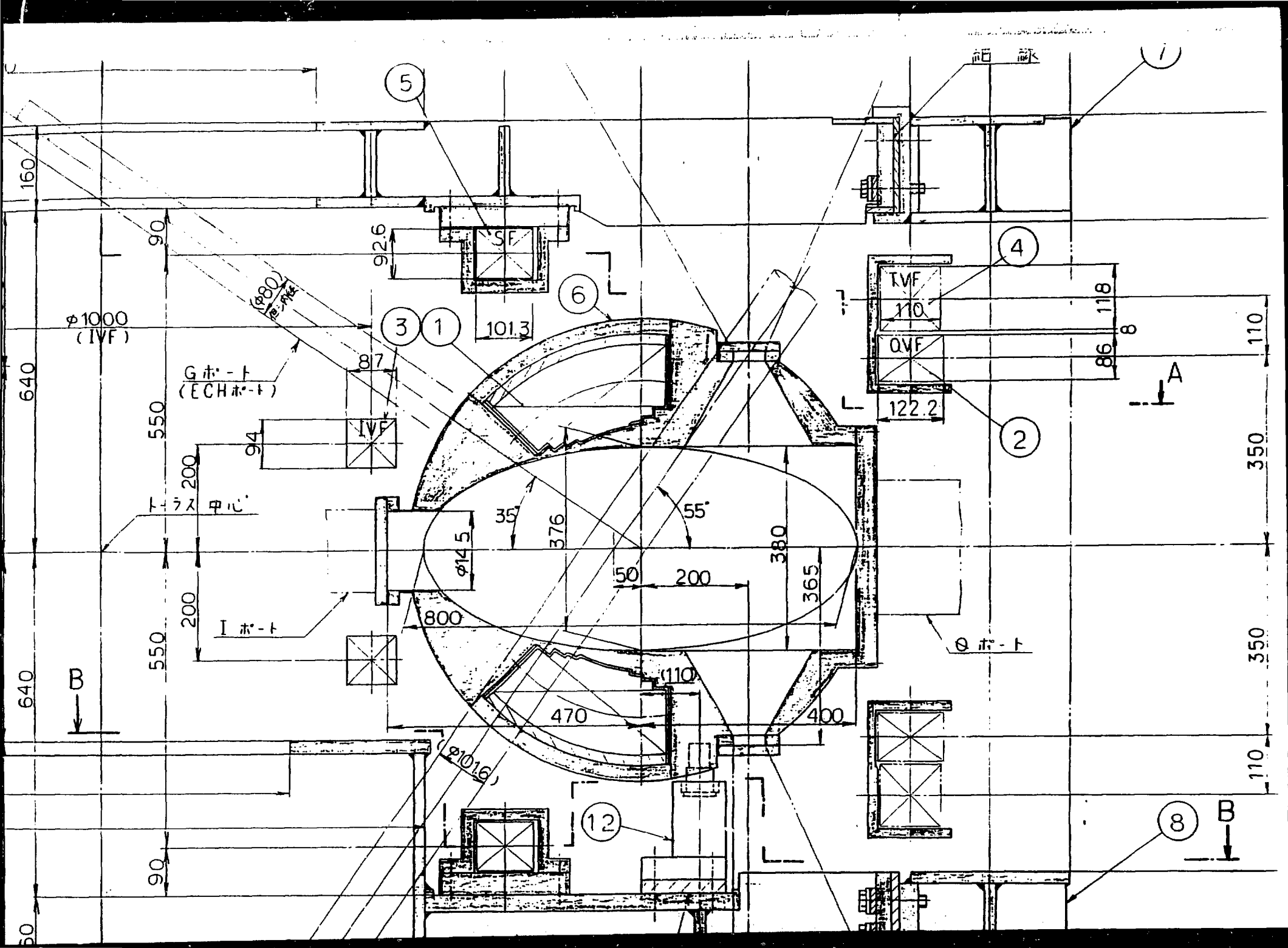
5
SF
92.6
6
3
1
101.3
87
φ1000
(IVF)
(φ80)
Gポート
(ECHポート)
IVF
94
200
トーラス中心
φ145
35°
376
55°
380
50
200
365
800
Iポート
Qポート
(110)
470
400
(φ1016)
12
4
TVF
110
118
8
86
QVF
122.2
2
A
B
8
160
90
640
550
200
350
110

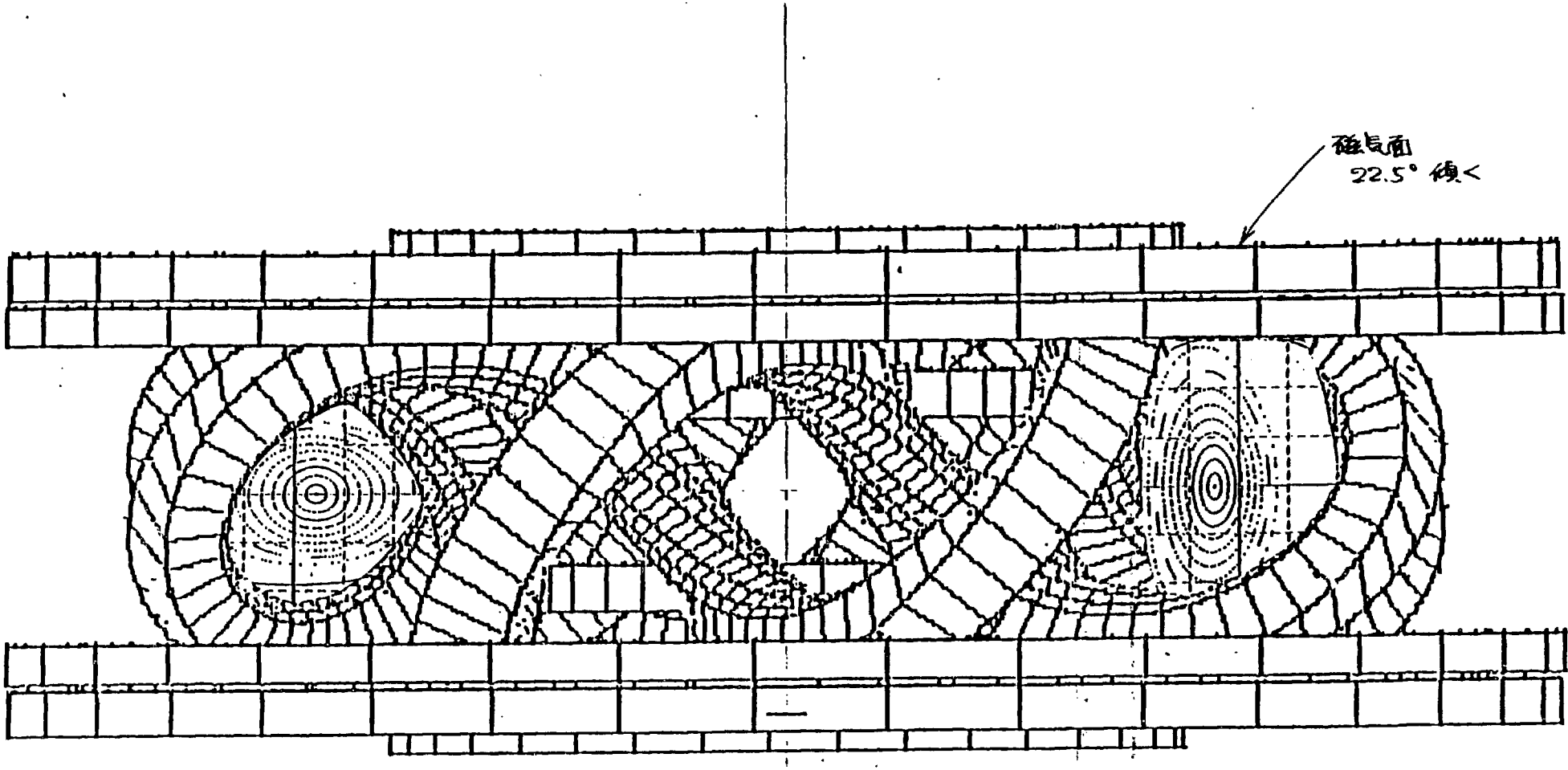
磁気面
22.5° 傾く

CHS Diagnostics

Quantity	Diagnostics	Space Resolution
	Monitoring Diagnostics	
N_e	4 mm Microwave Interferometer	Line Average
T_e	Soft X-ray Pulse Height Analysis	
T_i	Time-of-Flight Neutral Particle Analyzer	
Energy	Diamagnetic Loop	Area Average
N_o	H_α Light Monitor	Chord Average
Impurity	VUV Spectrometor	Chord Average
Radiation	Bolometer	Chord Average
Shape	TV Camera	2 D Image
Current	Rogowskii Coil	Area Average
	Profile Diagnostics and others	
N_e	HCN Laser Interferometer	2 D
T_e	Thomson Scattering	Pointwise
	Electron Cyclotron Emission	1 D
T_i	Charge Exchange Neutral Particle Analyzer	
	Charge Exchange Recombination Spectroscopy	Pointwise
Fast Ion Loss	Ion Beam Surface Analysis	Plasma Surface
	Charge Exchange Neutral Particle Analyzer	Pitch Angle
Potential	Spectroscopy (Doppler Shift)	Chord Average
	Heavy Ion Beam Prove	Pointwise
Magnetics	Soft X-ray Detector Array	2 D
Radiation	Bolometer Array	2 D
Diffusion	Instrumented Limiter	Cross section
Edge Region	Lithium Beam Probe	Pointwise

(B) New method

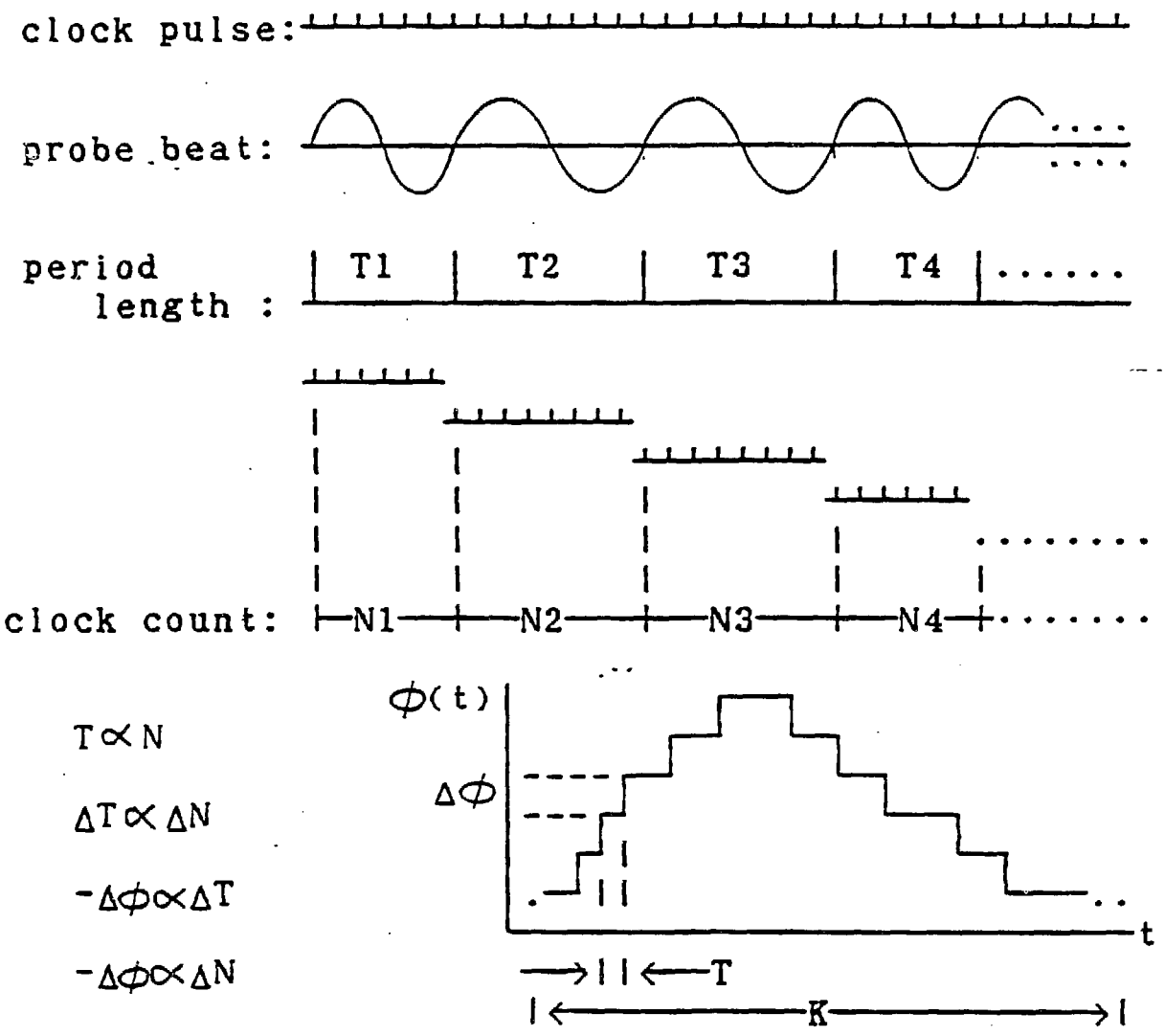

signal from heterodyne detector . $\cos(\omega_m t + \phi)$

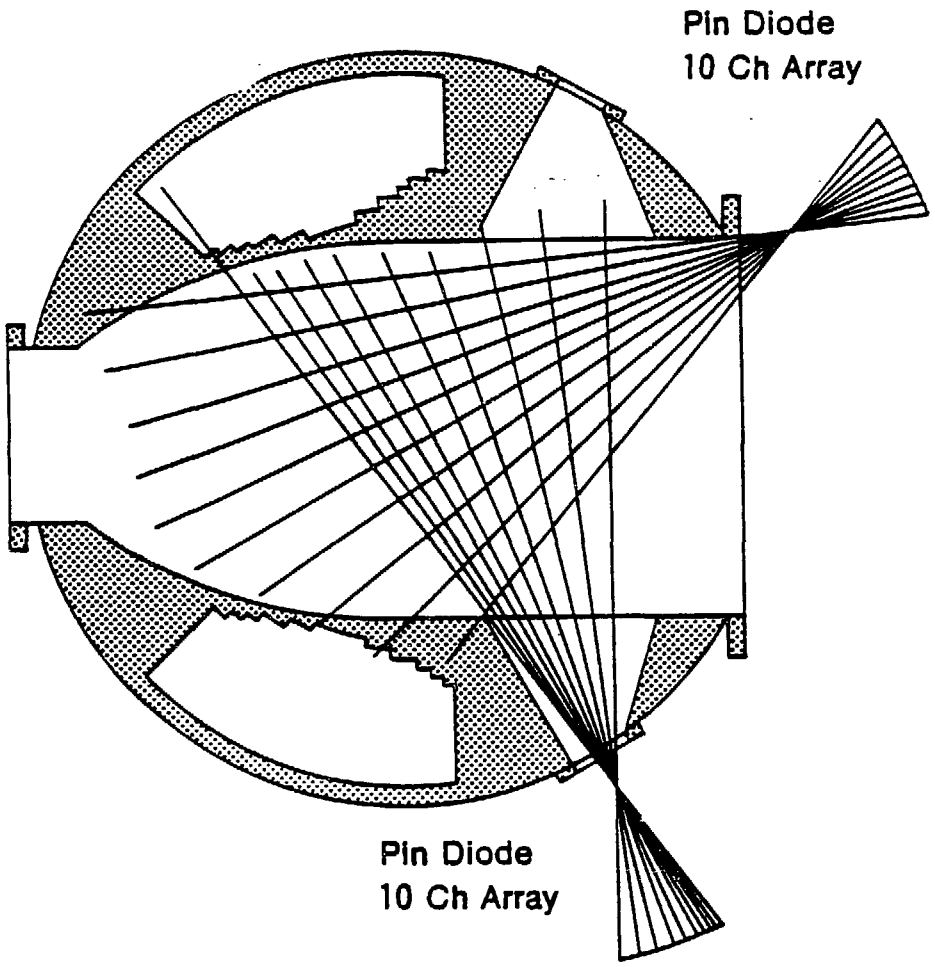
Pin Diode
10 Ch Array
Pin Diode
10 Ch Array

<<< Field Line Topography >>>

HF : I= 937.50 kA
OVF: I= -219.30 kA
TVF: I= -153.60 kA
SF : I= -80.40 kA
IVF: I= 19.60 kA

RAXIS = 95.35

15.0 turns

Zeta = 0.00

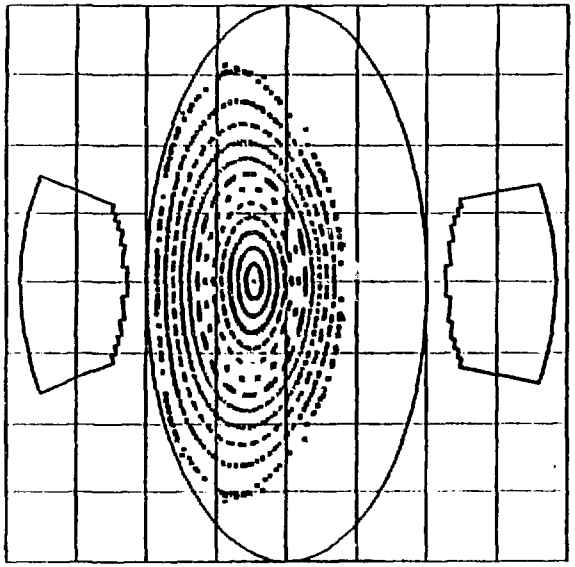

Zeta = 11.25

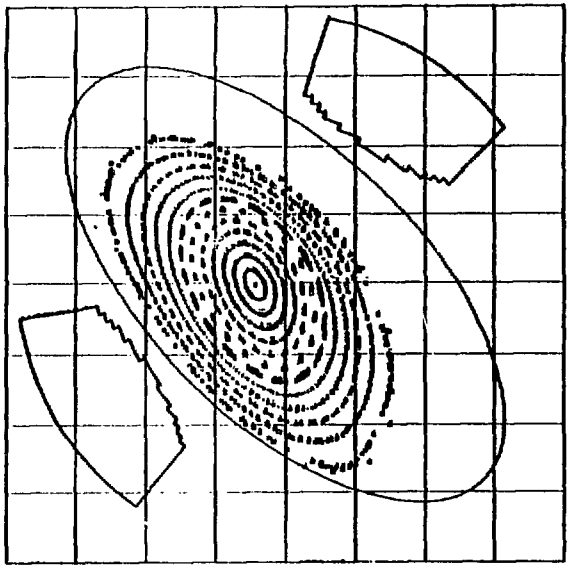

Zeta = 22.50

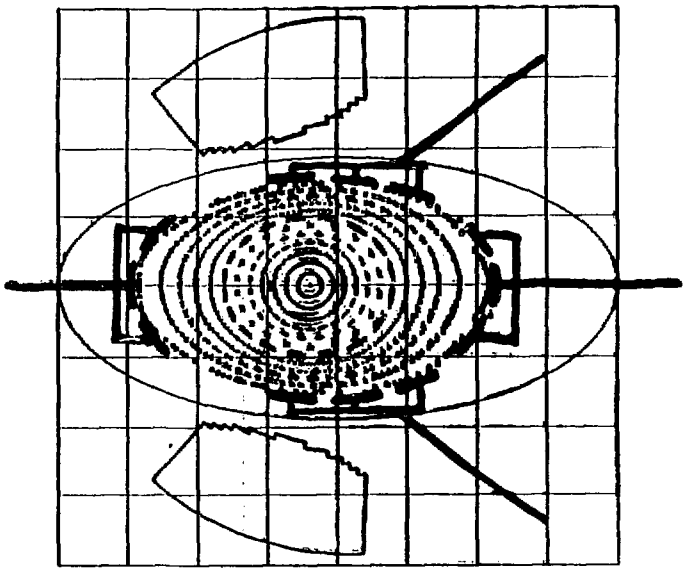

⊙ : Rat= 95.35 15.0 turns
△ : Rat= 94.20 15.0 turns
+ : Rat= 93.05 15.0 turns
× : Rat= 91.90 15.0 turns
◇ : Rat= 90.75 15.0 turns
↑ : Rat= 89.60 15.0 turns
X : Rat= 88.45 15.0 turns
Z : Rat= 87.30 15.0 turns
Y : Rat= 86.15 15.0 turns
H : Rat= 85.00 15.0 turns

✳ : Rat= 83.85 15.0 turns
⧖ : Rat= 82.70 15.0 turns
⊡ : Rat= 81.55 9.8 turns

ANGLE X-Z

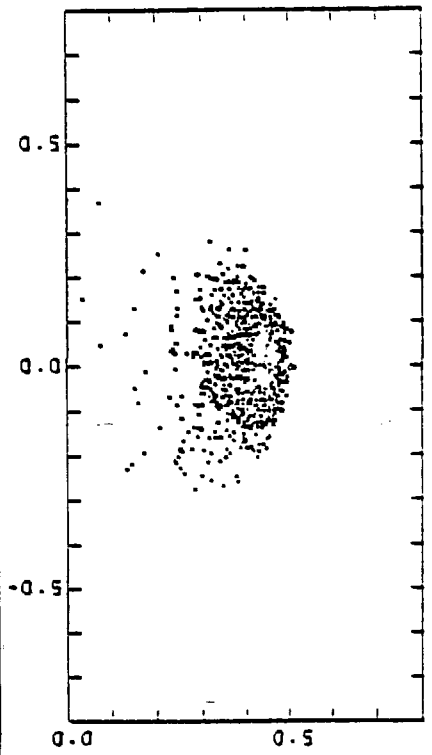

X-AXIS DEPTH (μm)

Distribution of Ions

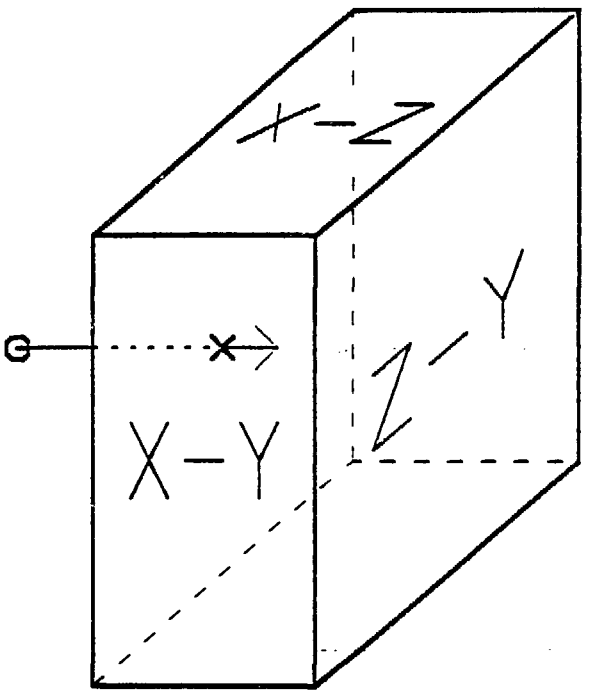

40 keV

ANGLE X-Y

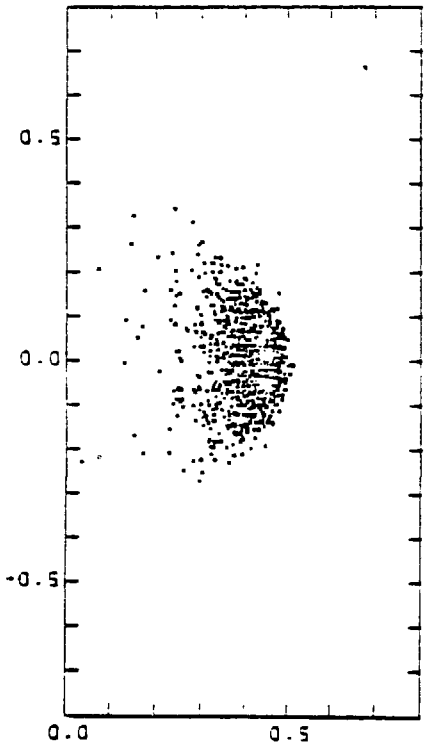

X-AXIS DEPTH (μm)

ANGLE Z-Y

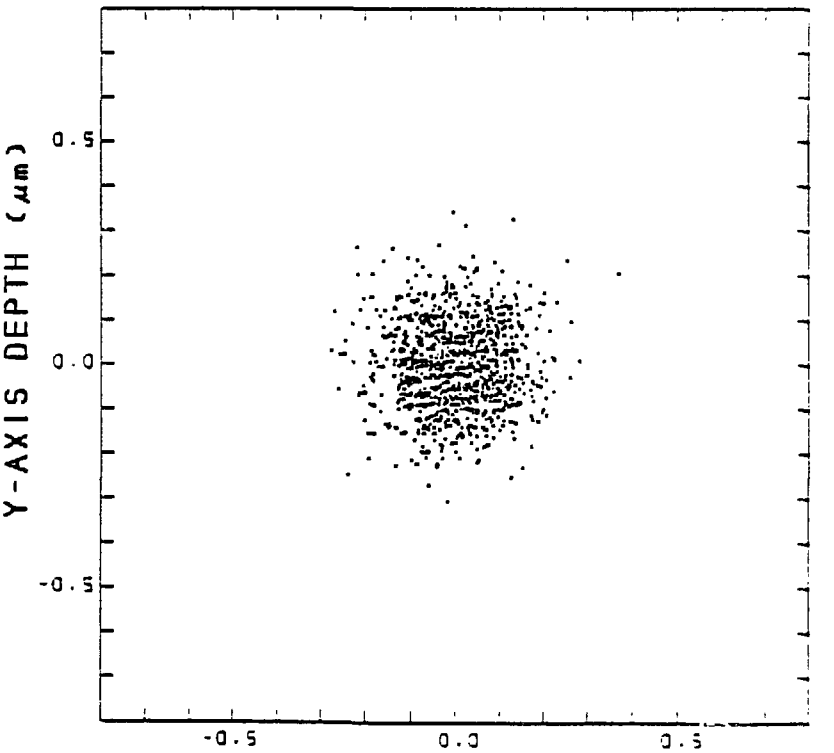

Z-AXIS DEPTH (μm)

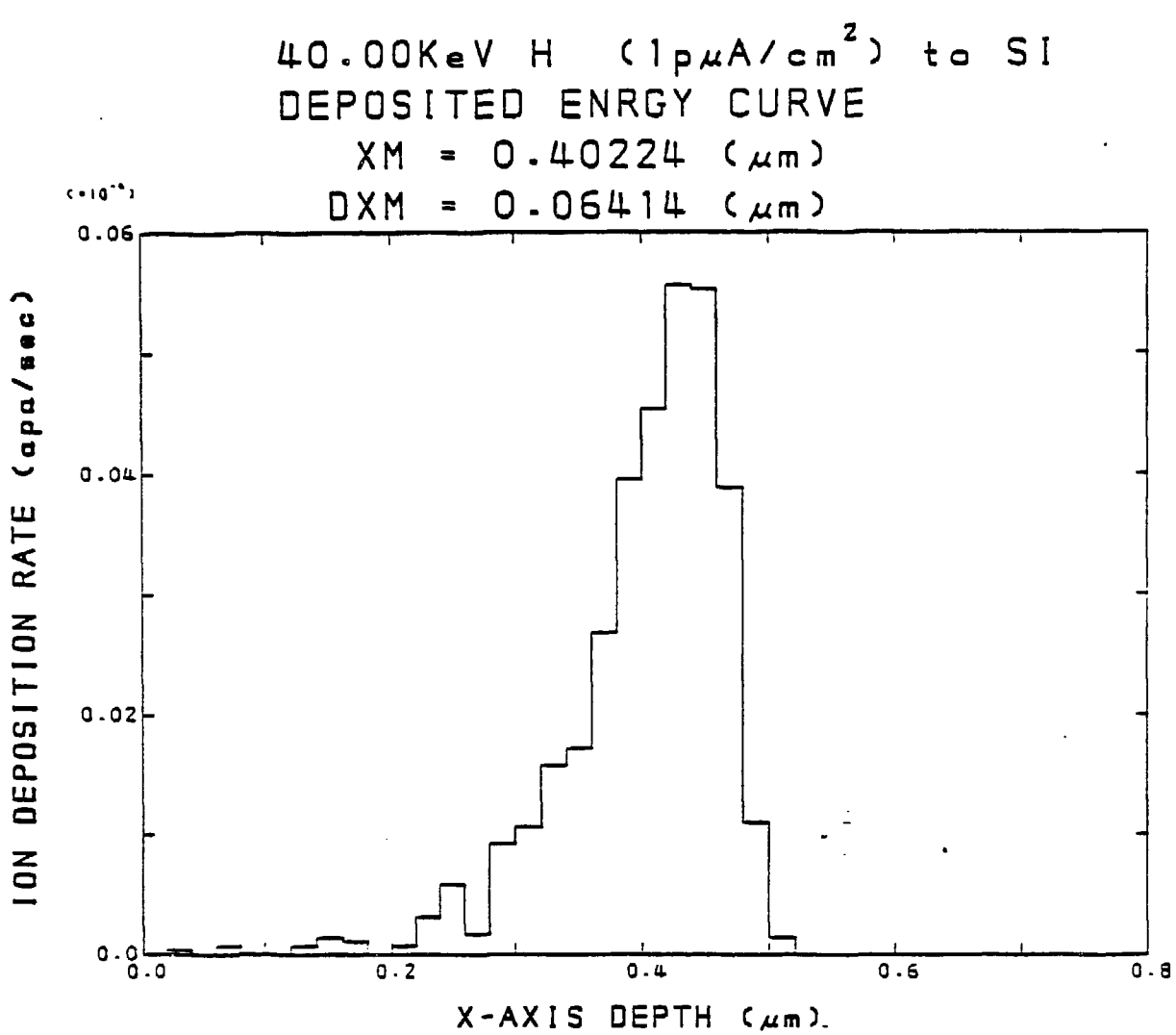
40.00KeV H (1pμA/cm²) to SI
DEPOSITED ENRGY CURVE
XM = 0.40224 (μm)
DXM = 0.06414 (μm)
(*10⁻⁴)
0.06
0.04
0.02
0.0
ION DEPOSITION RATE (dpa/sec)
0.0
0.2
0.4
0.6
0.8
X-AXIS DEPTH (μm)

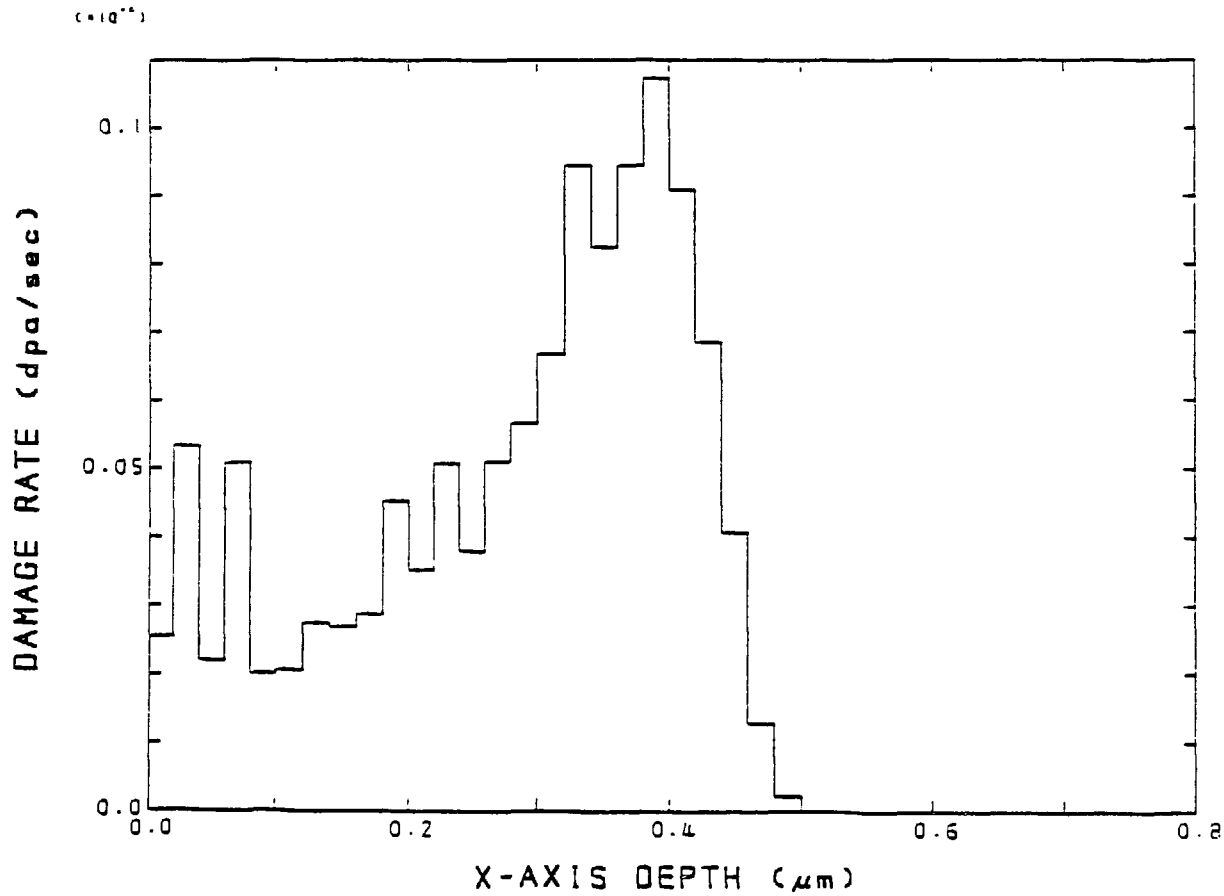
(*10⁻⁴)
0.1
0.05
0.0
DAMAGE RATE (dpa/sec)
0.0
0.2
0.4
0.6
0.8
X-AXIS DEPTH (μm)

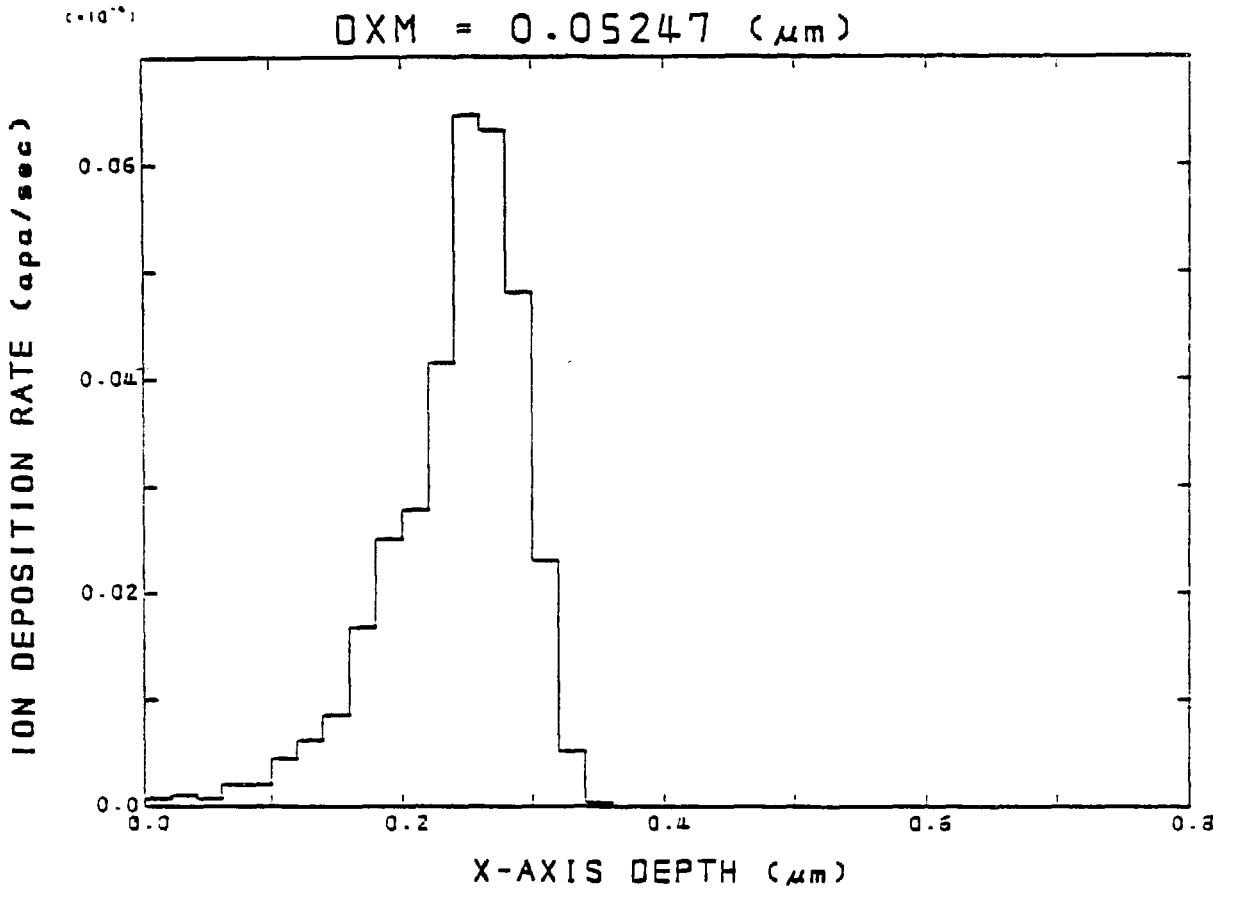
20.00KeV H (1pμA/cm²) to Si
DEPOSITED ENRGY CURVE
XM = 0.24076 (μm)
DXM = 0.05247 (μm)
ION DEPOSITION RATE (dpa/sec)
0.06
0.04
0.02
0.0
0.0
0.2
0.4
0.6
0.8
X-AXIS DEPTH (μm)

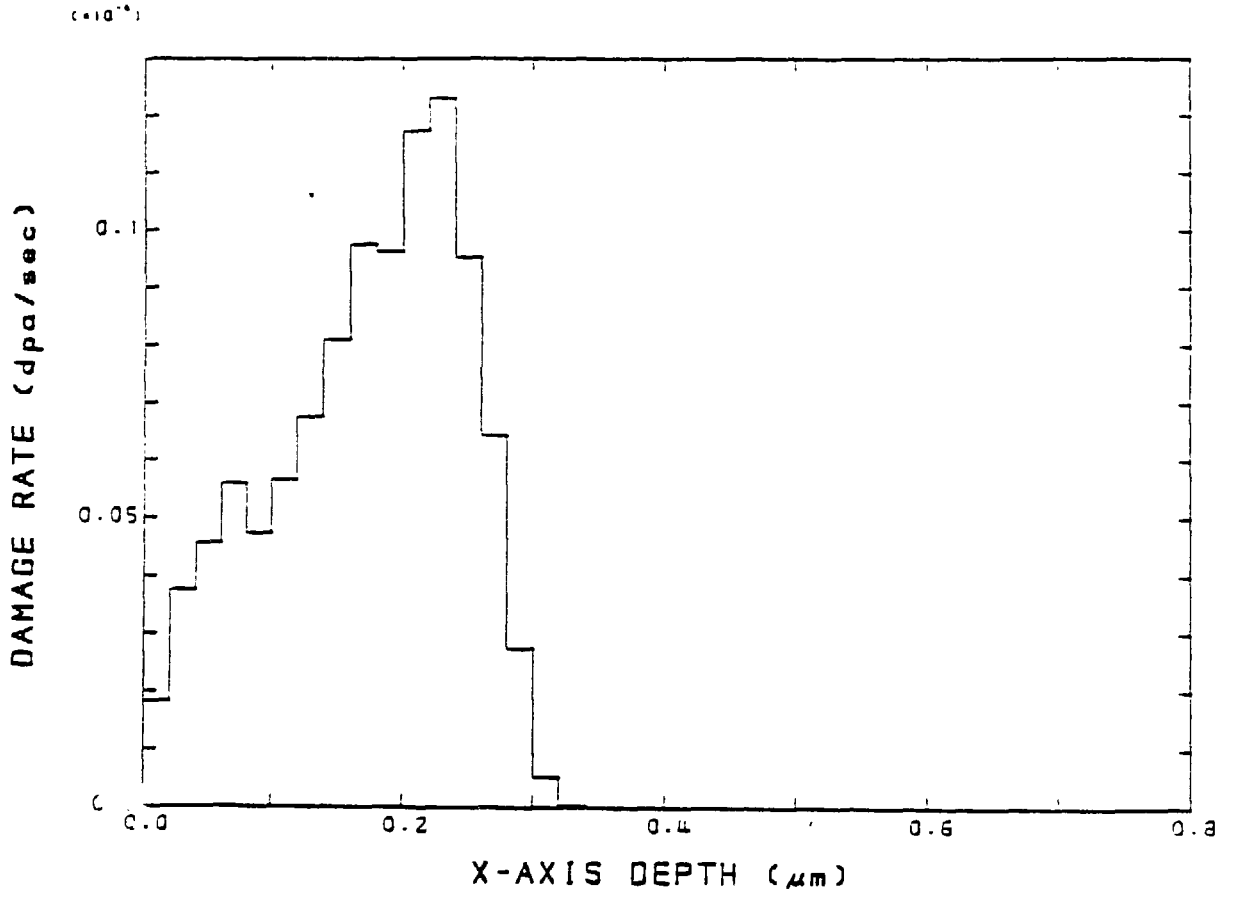
DAMAGE RATE (dpa/sec)
0.1
0.05
0.0
0.2
0.4
0.6
0.8
X-AXIS DEPTH (μm)

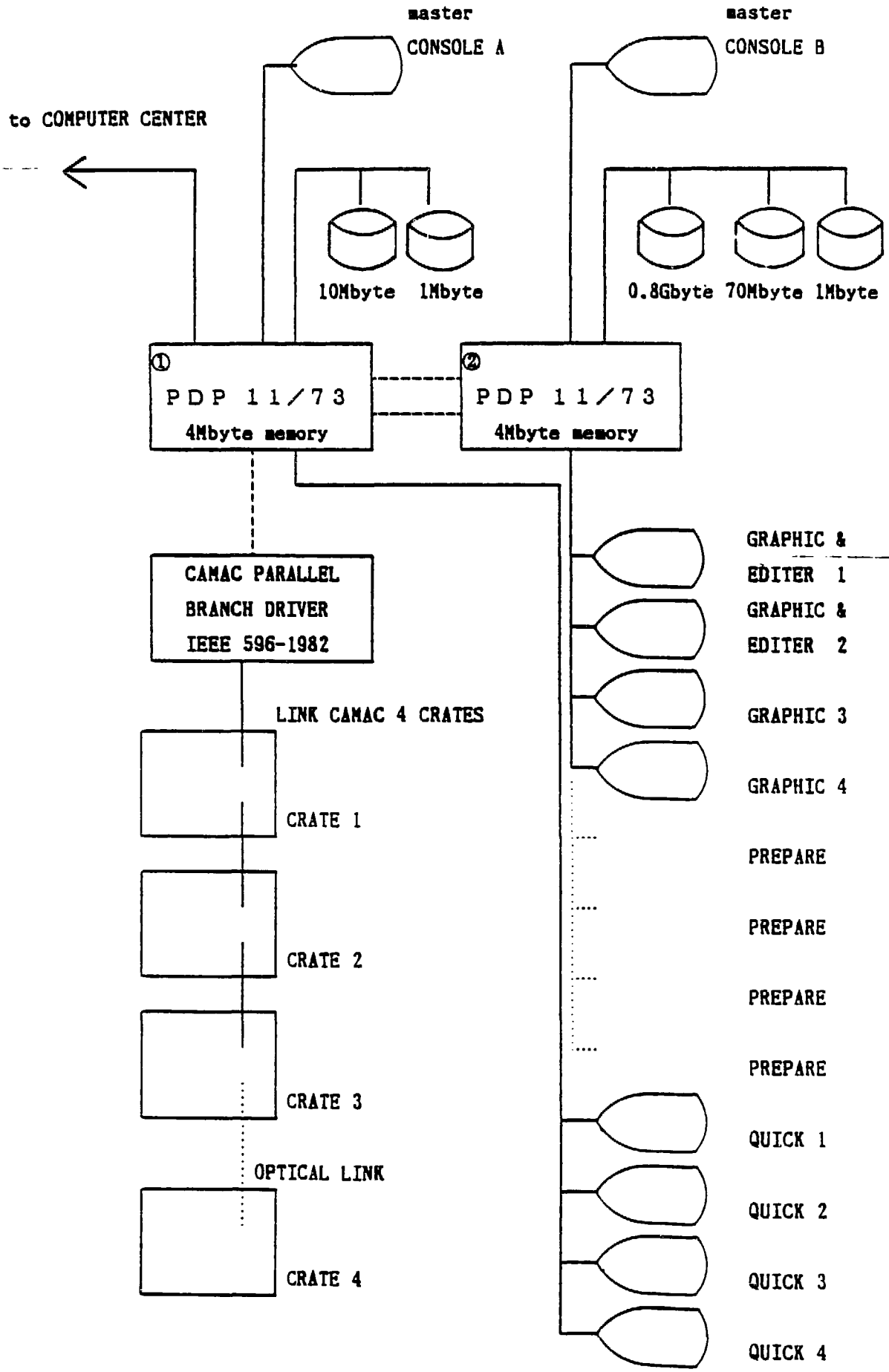
master
CONSOLE A
master
CONSOLE B
to COMPUTER CENTER
10Mbyte
1Mbyte
0.8Gbyte
70Mbyte
1Mbyte
①
PDP 11/73
4Mbyte memory
②
PDP 11/73
4Mbyte memory
CAMAC PARALLEL
BRANCH DRIVER
IEEE 596-1982
LINK CAMAC 4 CRATES
CRATE 1
CRATE 2
CRATE 3
OPTICAL LINK
CRATE 4
GRAPHIC &
EDITER 1
GRAPHIC &
EDITER 2
GRAPHIC 3
GRAPHIC 4
PREPARE
PREPARE
PREPARE
PREPARE
QUICK 1
QUICK 2
QUICK 3
QUICK 4

TRANSPORT STUDIES

IN IMS

J.L. Shohet
F.S.B. Anderson
C. Storlie
R.P. Doerner
W. D'Haeseleer

D.T. Anderson
J.N. Talmadge
W.N.G. Hitchon
K.J.S. Mertens
P.K. Trost

Torsatron/Stellarator Laboratory

University of Wisconsin

Madison, Wisconsin

IMS PARAMETERS

ℓ = 3 MODULAR STELLARATOR

MAJOR RADIUS = 40 CM

MINOR RADIUS = 4 CM

B = 2.6 kG

PLASMA PARAMETERS

$n_e = 1 - 3 \times 10^{11}$ cm^{-3}

$T_e = 8 - 15$ eV

$T_i = 2 - 4$ eV

$\tau_{particle} = 0.5 - 1$ msec

% ionization = 10 - 50%

ECH SOURCE

f = 7.275 GHz

Power = 3 kW

Duration = 10 msec

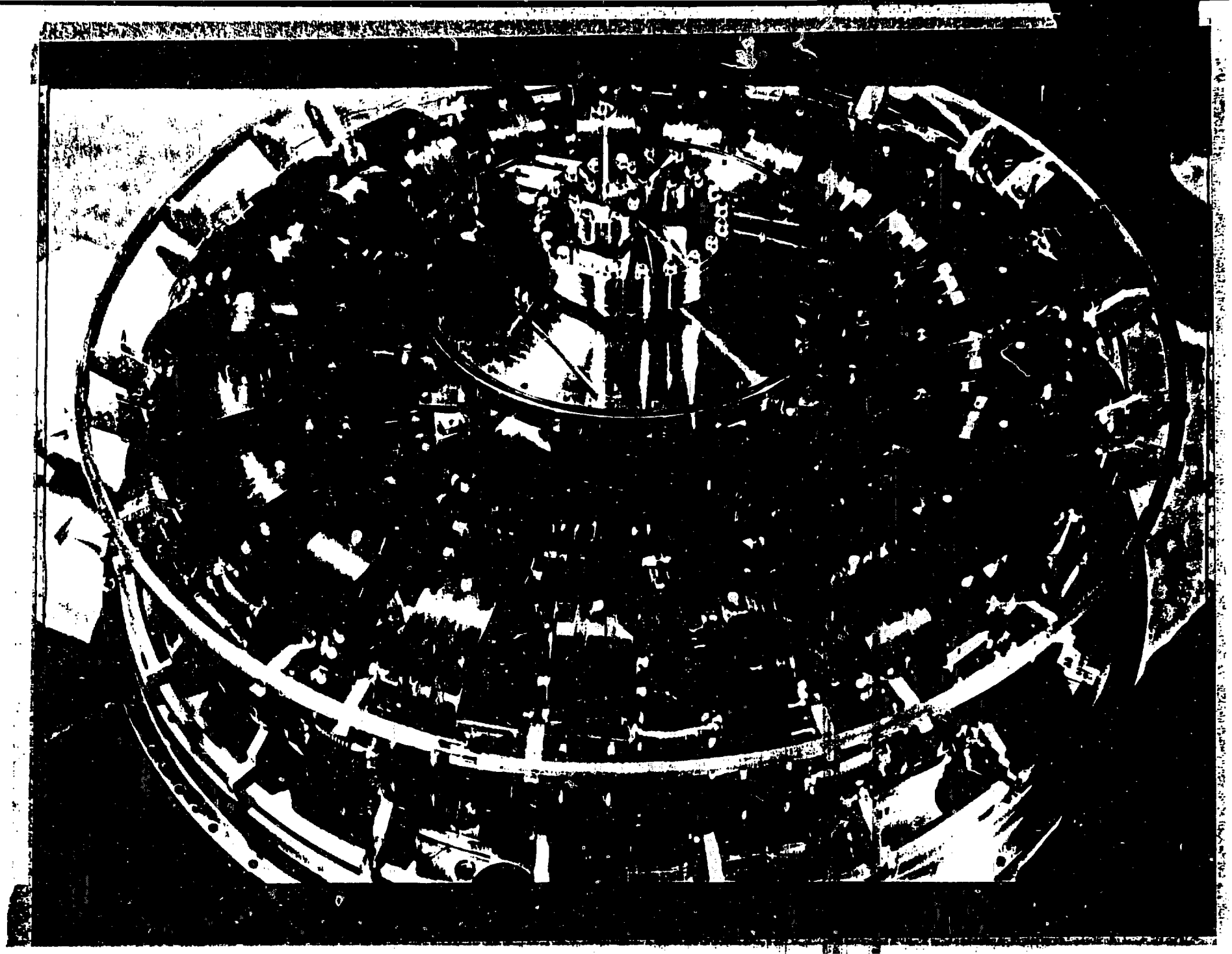

BACKGROUND

- Density profiles in IMS are hollow when the plasma is created and heated with ECRH>
- Hydrogen profiles vary in hollowness from 1.5 to 1 to 10 to 1 (ratio of maximum density at the edge to minimum density in center)
- For cyclotron layer on inboard side, profile is much less hollow than when the layer is on the outboard side

DENSITY PROFILE AS A FUNCTION OF ELECTRON CYCLOTRON RESONANCE LOCATION

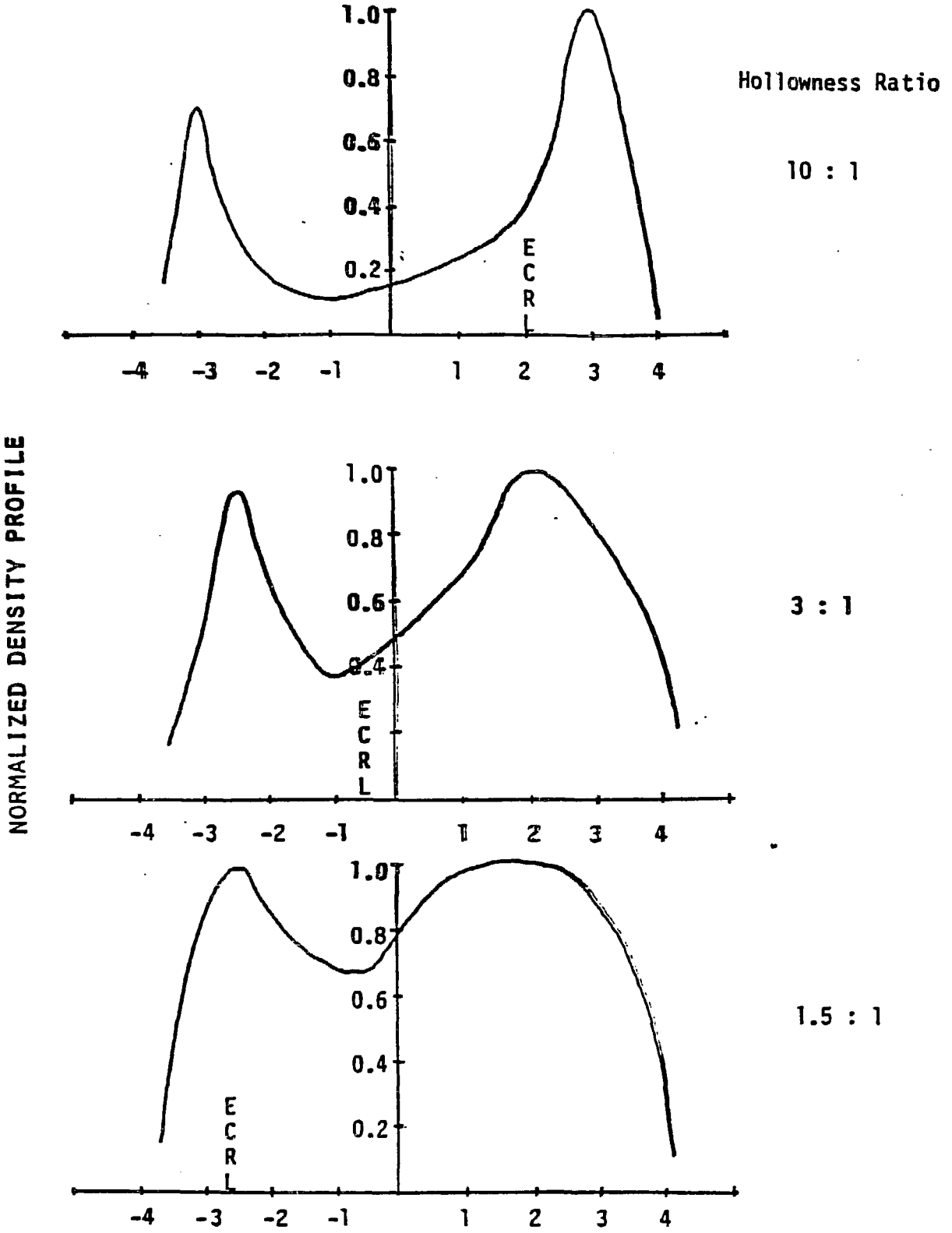

HOLLOWNESS INCREASES AS CYCLOTRON LAYER IS MOVED FROM HIGH FIELD TO LOW FIELD SIDE

NOTE: THERMAL ELECTRON CYCLOTRON EMISSION PEAKS WHEN THE CYCLOTRON LAYER IS LOCATED ON THE OUTBOARD SIDE OF THE DEVICE. THIS CORRESPONDS TO WHEN THE DENSITY PROFILES ARE THE MOST HOLLOW.

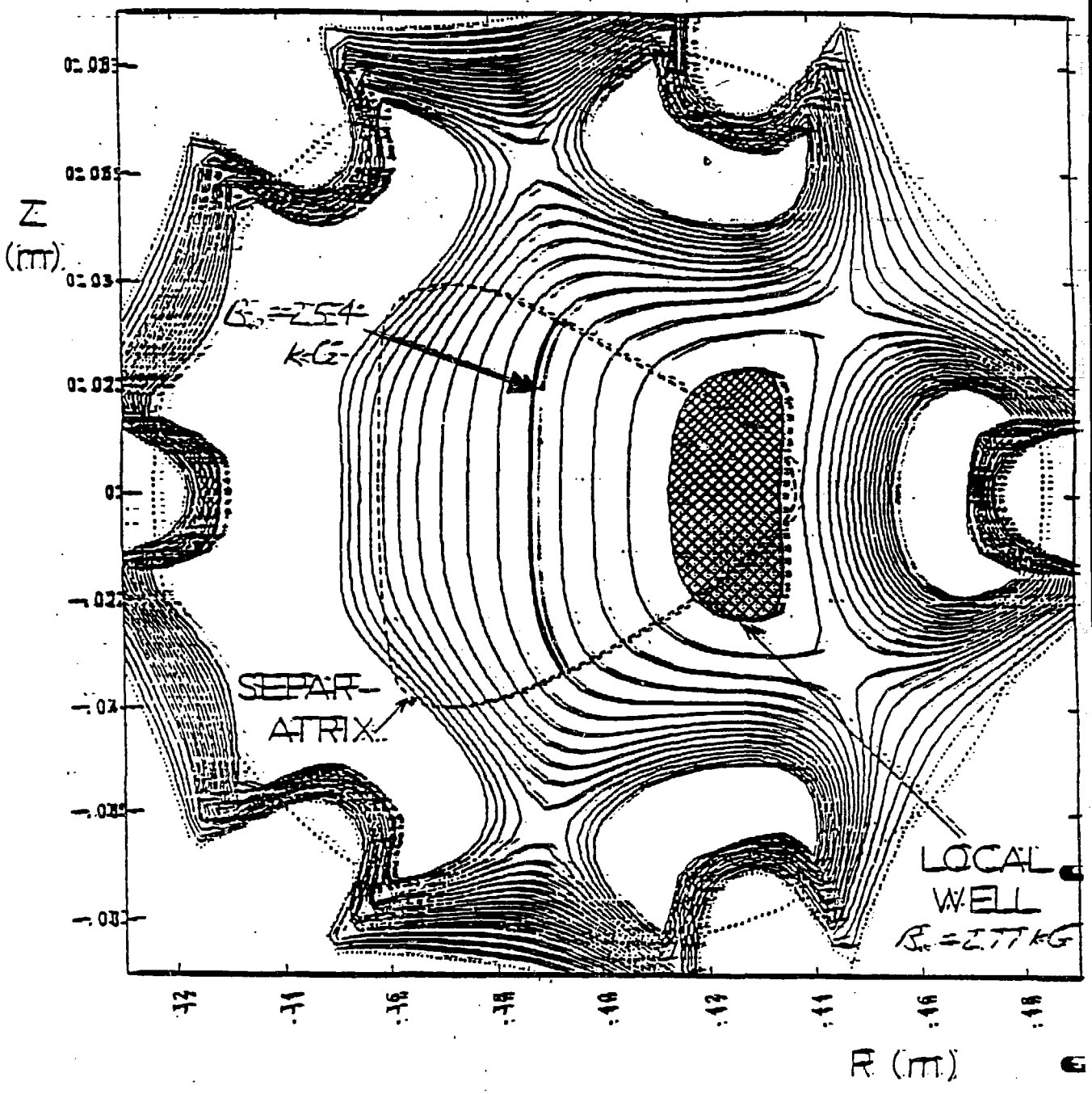

LOCATION OF ECE RESONANCE LAYER FOR DIFFERENT CENTRAL MAGNETIC FIELD VALUES.

EDGE RIPPLE WITH VERTICAL FIELD

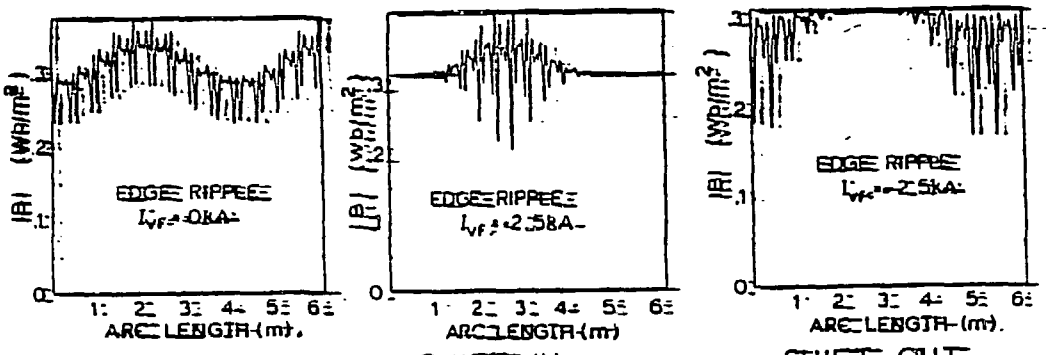

BASE CASE

SHIFT IN. (HILL)

SHIFT OUT (WELL)

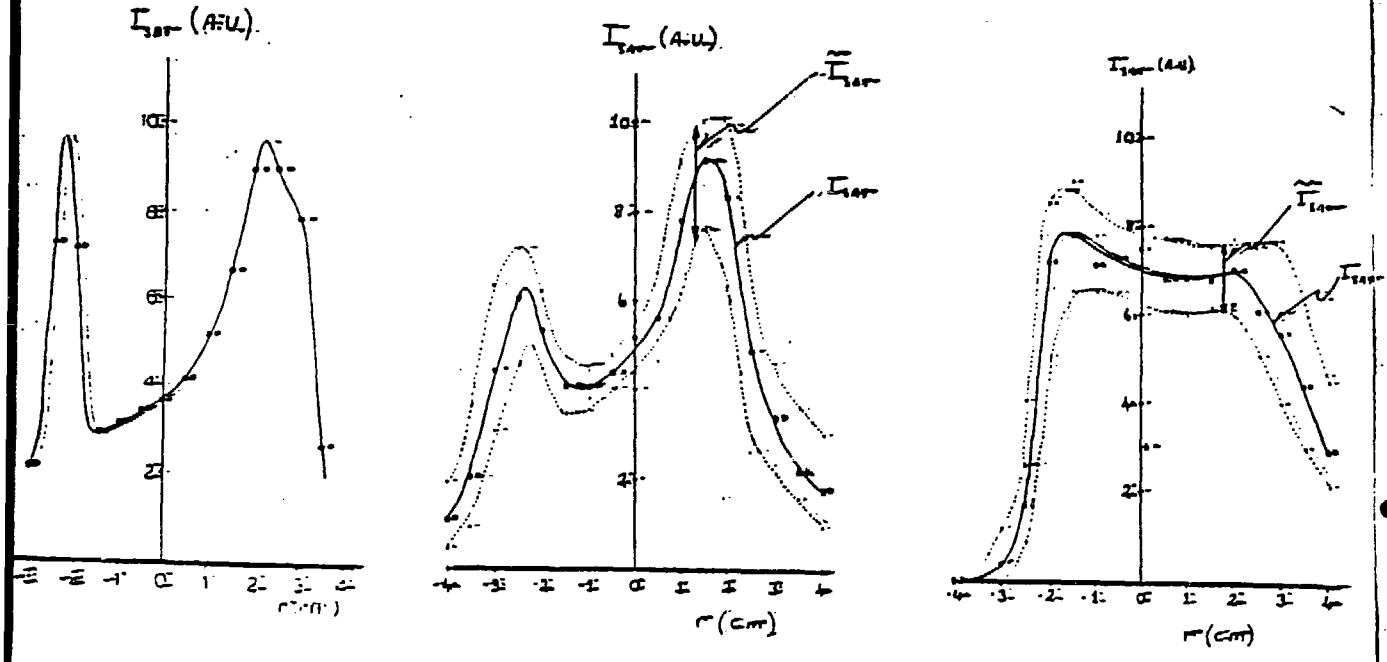

WITH AN APPLIED VERTICAL FIELD THAT MOVES THE MAGNETIC SURFACES TO THE OUTBOARD SIDE OF IMS THE RIPPLE IN THE MAGNETIC FIELD DECREASES AND THE DENSITY PROFILE IS LESS HOLLOW

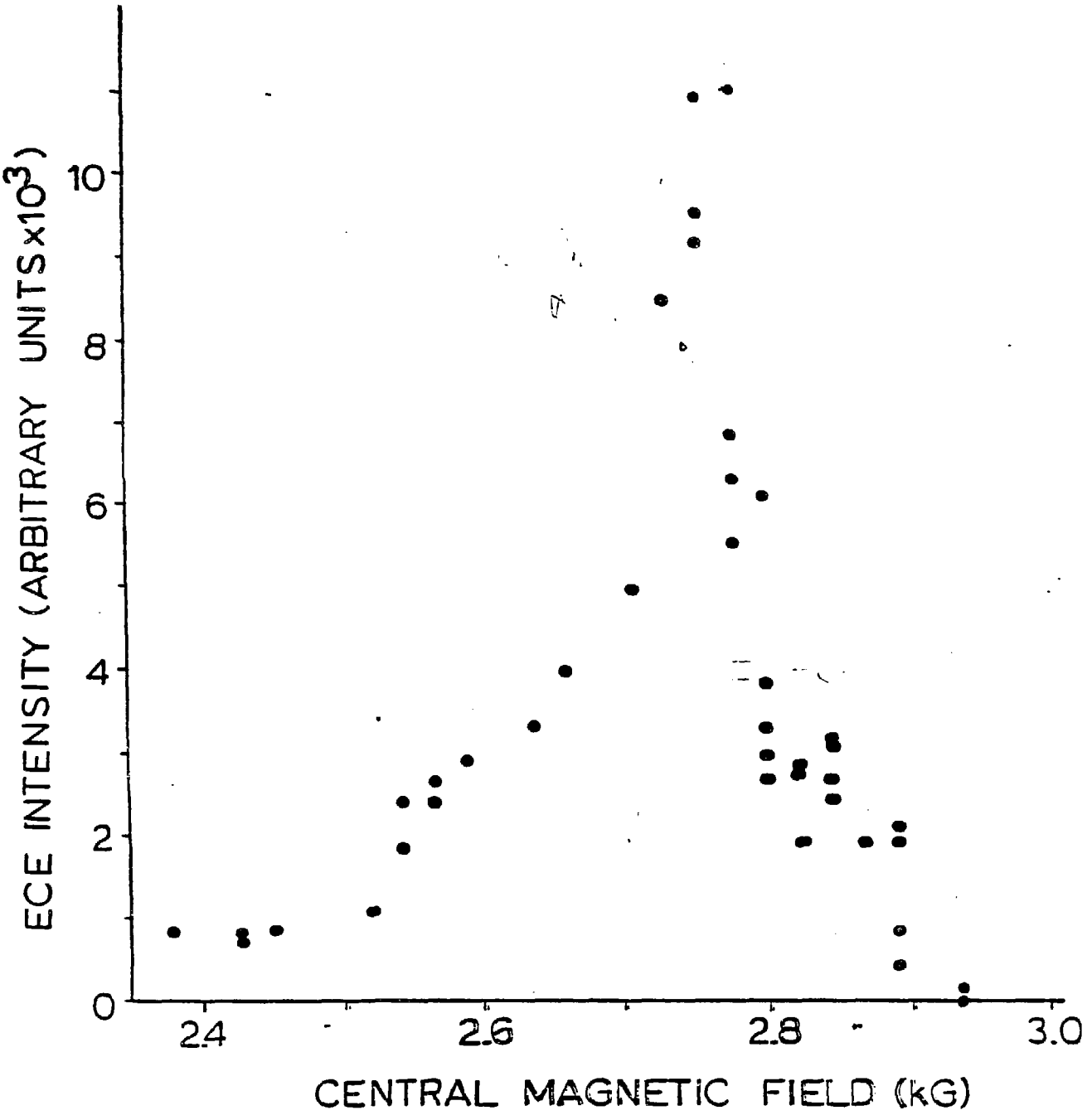

ECE INTENSITY AT 15.0 GHz SHOWS PEAK WHEN CENTRAL MAGNETIC FIELD IS 2.77 kG.

ECH LAYER IS AT PLASMA CENTER WHEN B_0 = 2.54 kG.

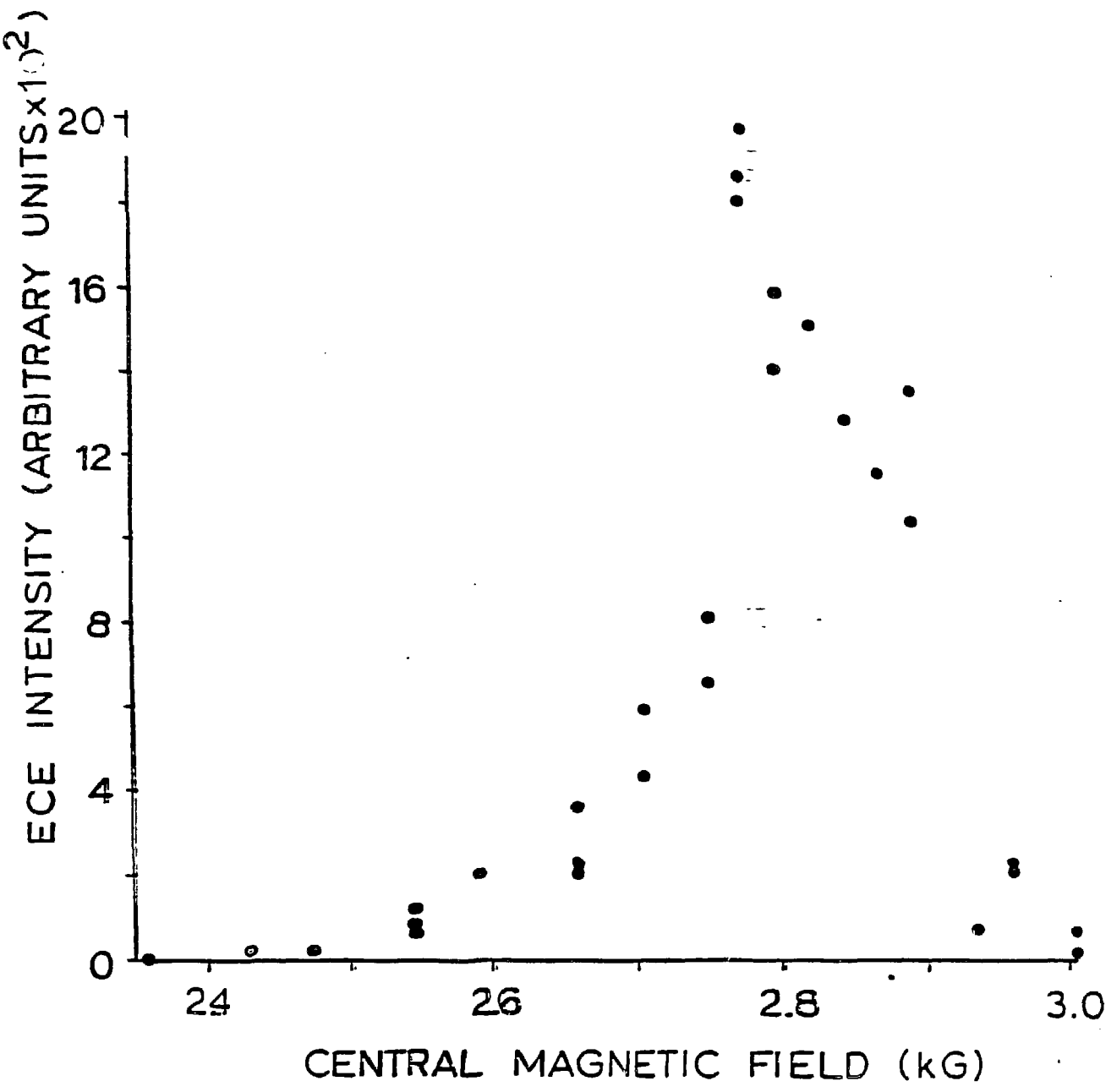

ECE INTENSITY AT 16.0 GHz ALSO SHOWS PEAK WHEN B_0 = 2.77 kG..

- Experimental Observation of Hollow Profiles

  Hollowness is less in Ar than H
  Hollowness increases as cyclotron layer moves to low-field side
  Hollowness decreases with vertical field that pushes surfaces to low-field side
  Hollowness appears to decrease with ECRH at B=6 kG.

THOMSON SCATTERING

- Thomson scattering data is consistent with probe data, except that the temperatures are nearly a factor of two larger, probably due to perturbation of the plasma by the probe.

- The distribution function during ECRH is obtained by solving the Fokker-Planck equation which also gives consistent results with the Thomson scattering measurement.

- Multi-point Thomson scattering data obtained for line-averaged densities of 5-6 x 10^{11} cm^{-3}, and electron temperatures of 5-30 eV.

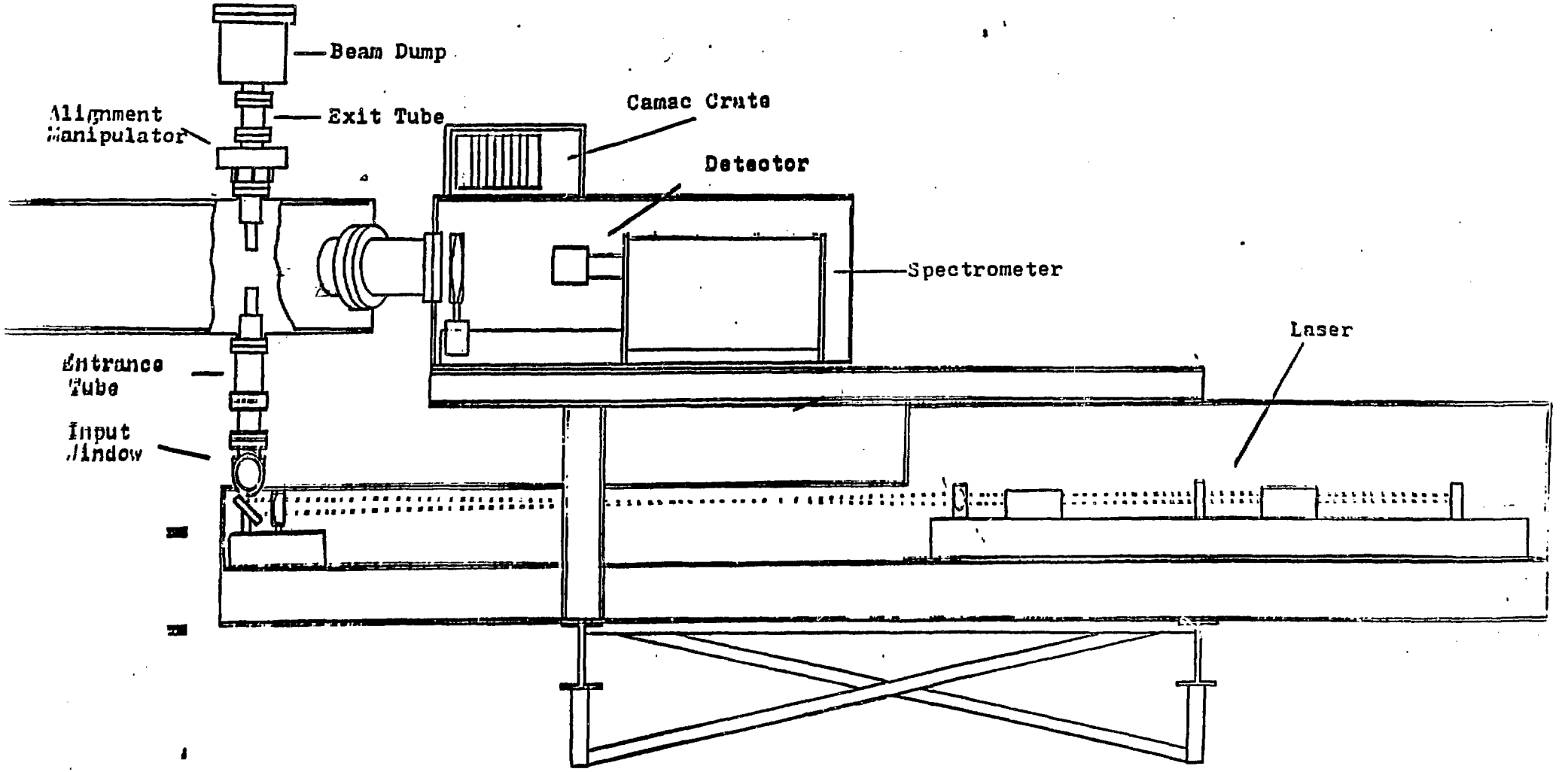
Beam Dump
Exit Tube
Alignment Manipulator
Camac Crate
Detector
Spectrometer
Laser
Entrance Tube
Input Window

IMS THOMSON SCATTERING SYSTEM

A low-density, multi-point Thomson Scattering apparatus which features:

- A 2-d detector (multi-anode micro channel plate PMT) for attainment of multi-point ability.

- A high throughput collection optical system, along with a high gain detection system provides for the necessary sensitivity for low photon counts.

In order to achieve a sufficient signal / noise ratio, the laser light have nearly zero coupling into the collection-detection system.

- The decoupling of the laser from the collection-detection system is done through the design of the laser beam optical system.

SULTS TO DATE

This device has been used to measure electron density and temperature for plasmas with densities as low as 3.e11.

- These densities necessitate averaging several shots for reliable signal/noise.

- **Particle Convection is a good candiate to explain the hollow profiles.**

  Diffusion alone cannot explan steady-state hollow density profiles.

  Inclusion of convection term in steady-state particle balance equation yields hollow profiles in good agreement with experimental profiles.

  Origin of convection term appears to be poloidal electric field which gives good agreement between E x B velocity and pulse propagation experiment.

  Origin of poloidal electric field may be due to tail electrons on direct loss orbits.

  For verification, one must obtain the values for the diffusion coefficent, D, the convection velocity V, and the ionization rate coefficent γ.

PLASMA POTENTIAL MEASUREMENT

- Two-dimensional profiles of space potential have been obtained with an emissive probe
- Equipotential surfaces do not lie on magnetic surfaces
- High-potential region on outboard side of IMS is a closed locallized area which can give rise to a poloidal electric field
- This poloidal field can give rise to radial convection
- Estimates of convection velocity can be obtained by interpolation of the potential on a flux surface to obtain $E_{poloidal}$.
- The E x B drift is found locally and averaged over a flux surface which shows that the radial convection peaks at r=2-2.5 cm and has a magnitude of 500 cm/sec.

HYDROGEN DISCHARGE

PLASMA POTENTIAL

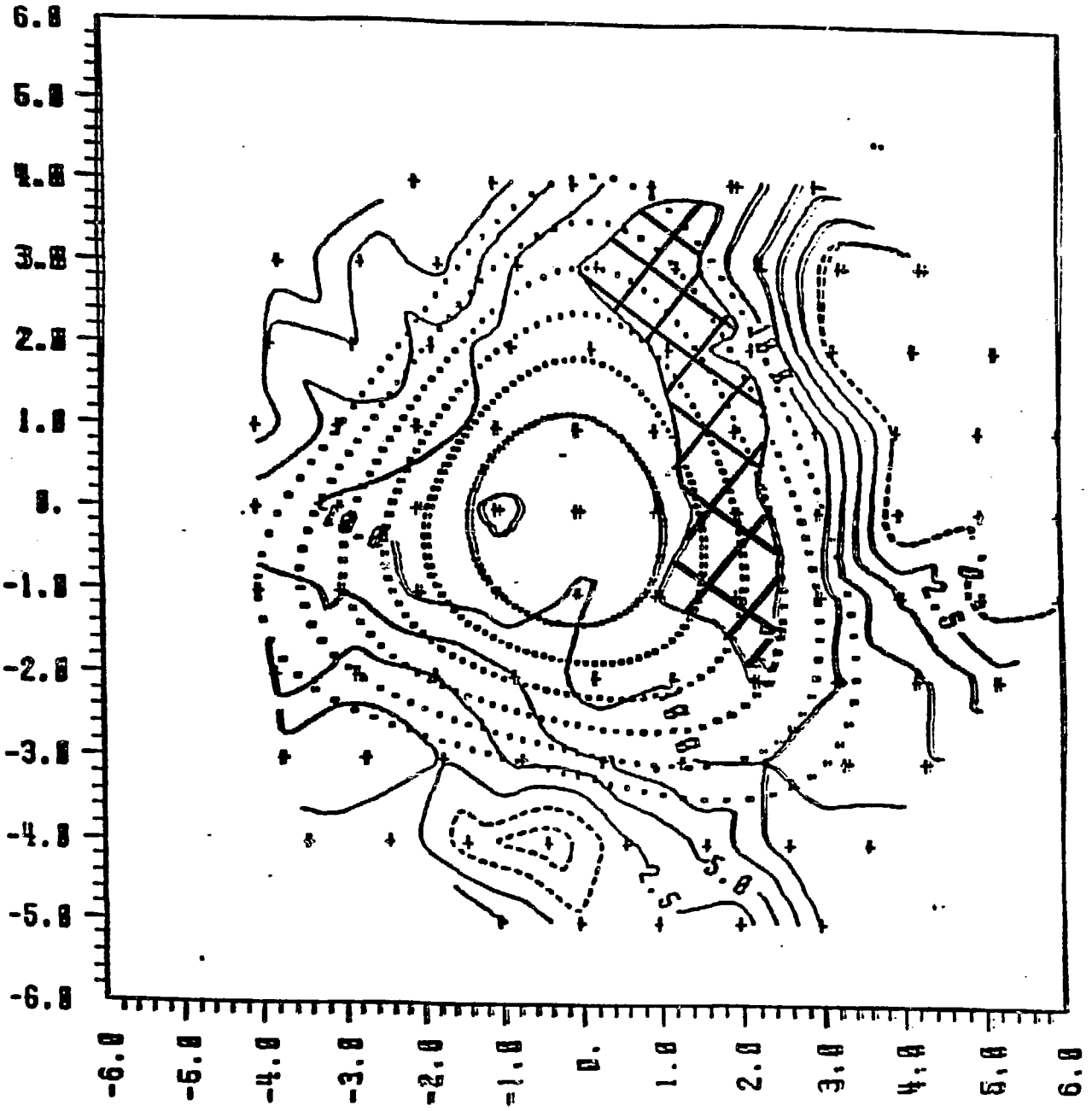

RADIAL DRIFT DUE TO A POLOIDAL ELECTRIC FIELD

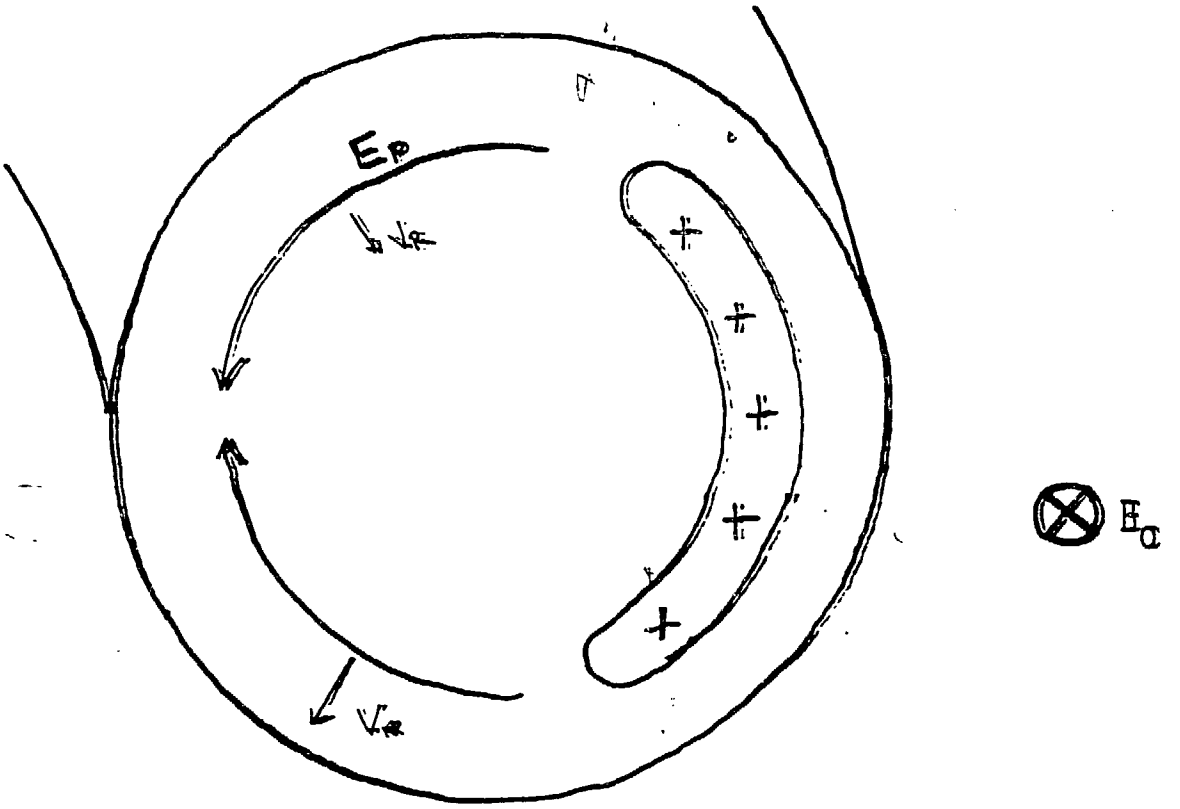

AVERAGE RADIAL VELOCITY

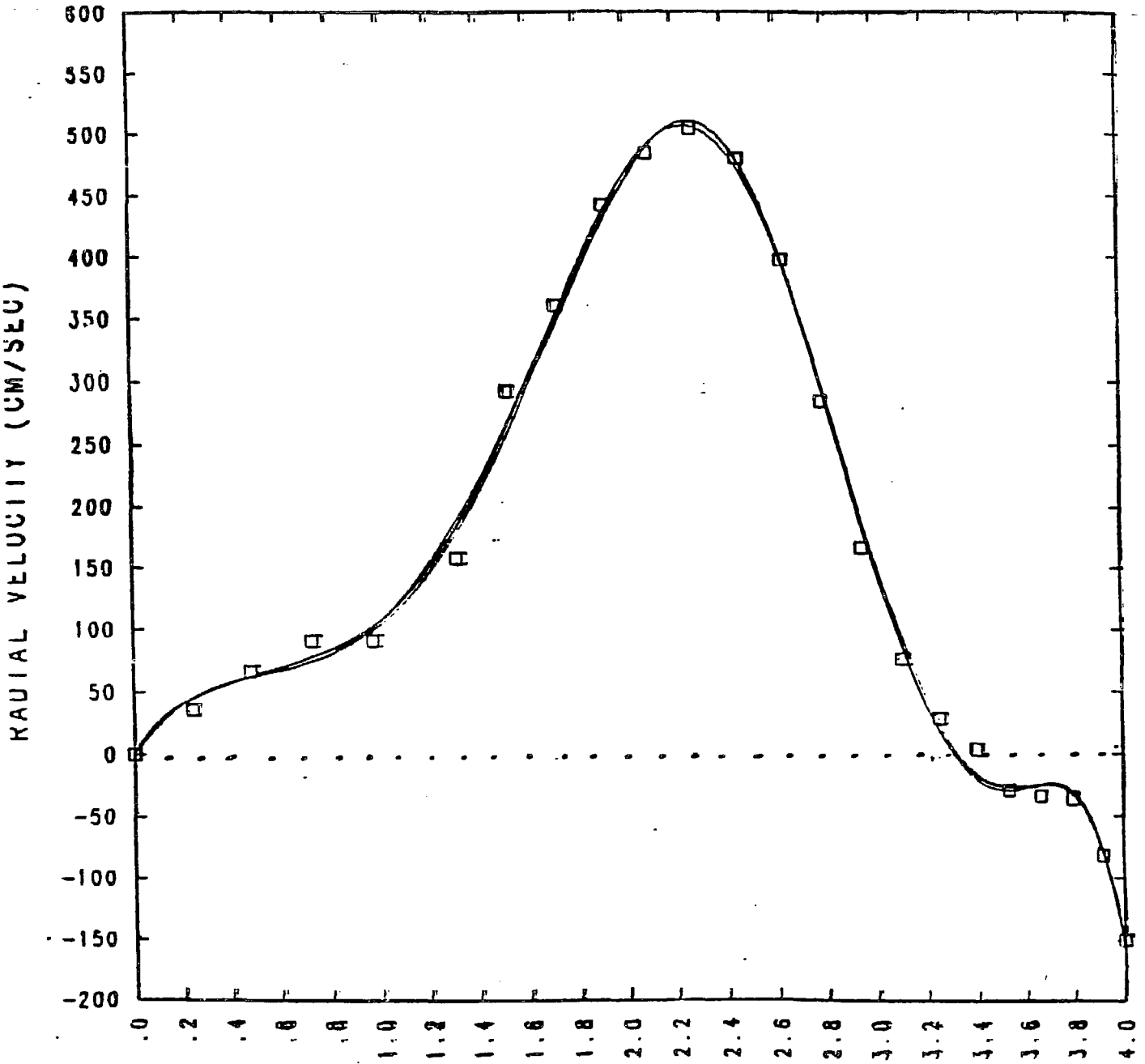

PULSE PROPAGATION EXPERIMENT

- Single disc probe of 0.3cm radius is placed in the center of the plasma
- Biased to -90V into ion saturation with a 1 kHz square wave
- A double probe, also biased into ion saturation is used to measure the perturbation as a function of radius
- A FFT algorithm produces both amplitude and phase shift of the fundamental and its harmonics as a function of radius
- From phase shift and amplitude one can obtain a unique value for D and $K=v^2/4D\gamma$ based on these measurements, but there is significant uncertainty on the phase shifts.

Consider how the analytic solution for the phase shifts and amplitudes in slab coordinates compares to the numerical solution in cylindrical coordinates.

In cylindrical coordinates, solve using Crank-Nicolson method:

$$\frac{\partial n_1}{\partial t} = D \frac{\partial^2 m_1}{\partial r^2} + \left(\frac{D}{r} - v\right) \frac{\partial n_1}{\partial r} + \left(\gamma - \frac{v}{r}\right) m_1$$

1. Boundary condition: $m(r = a, t) = 0$
2. Perturbation is assumed to be uniform from $r = 0$ to $r = r_1$ and is sinusoidal in time.
3. Calculation is performed over sufficient cycles of the perturbation so that the phase shifts and amplitudes converge to unique values.

Conclusion:

(1) The numerical values for the phase shifts deviate only a few percent from the analytic solution in slab coordinates.

(2) For purely diffusive transport, the equation for propagation in a slab $\frac{\partial n}{\partial t} = D \frac{\partial^2 n}{\partial x^2}$, yields $D = \frac{\omega}{2(\Delta\phi/\Delta x)^2}$. Even with the dependence of the diffusion coefficient on the square of the slope of the line plotting phase shift versus distance, the error of the analytic solution is about 5% with respect to the numerical value.

(3) As expected, amplitudes in slab coordinates deviate considerably from amplitudes in cylinders, especially with regard to convection.

Consider time-dependent perturbation equation in slab coordinates,

$$\frac{\partial n_1}{\partial t} = - \frac{\partial}{\partial x} \left[- D \frac{\partial n_1}{\partial x} + n_1 v \right] + n_1 \gamma$$

If D, v and γ are independent of x

$$\frac{\partial n_I}{\partial t} - D \frac{\partial^2 n_I}{\partial x^2} + v \frac{\partial n_I}{\partial x} - n_I \gamma = 0$$

and with $n \sim n_m \exp(jm\omega t + px)$

$$p = \frac{v}{2D} \pm \frac{1}{2D} \sqrt{v^2 - 4D\gamma + j4Dm\omega}$$

If we let $X = \left[\frac{(v^2 - 4D\gamma)^2}{16 D^4} + \frac{m^2\omega^2}{D^2} \right]^{1/4}$

$$Y = 1/2 \tan^{-1} \left[\frac{4Dm\omega}{v^2 - 4D\gamma} \right]$$

Then:

$$n \sim n_m \exp\left(jm\omega t + \left[\frac{v}{2D} \pm (X \cos Y + jX \sin Y)\right] x\right)$$

So phase shift given by:

$$\Delta\phi = X \sin Y \, \Delta x$$

[Reference: Above treatment similar to G. Jahns et al., Nucl. Fusion, 26, (1986) 226].

PULSE PROPAGATION EXPERIMENTAL SET-UP

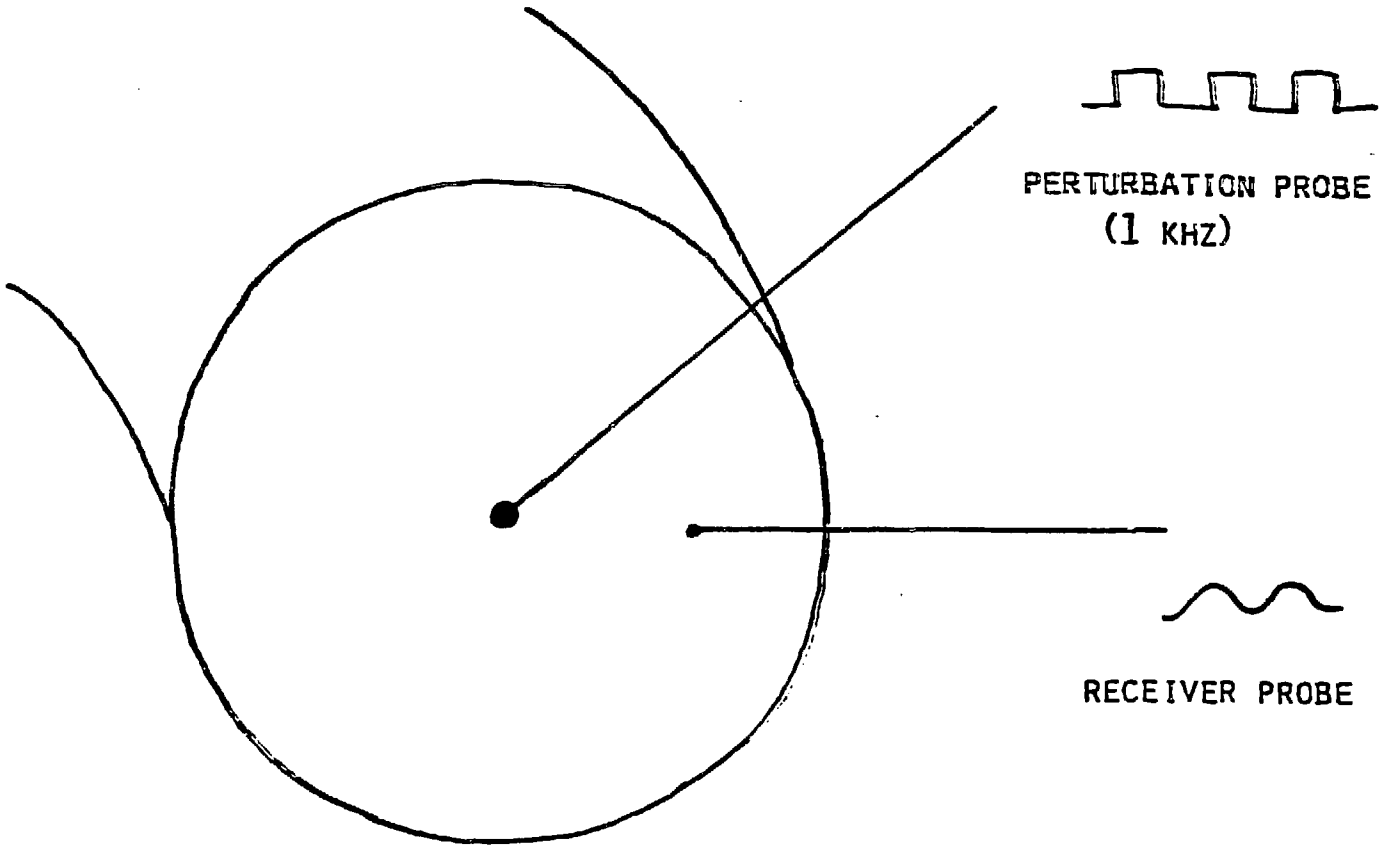

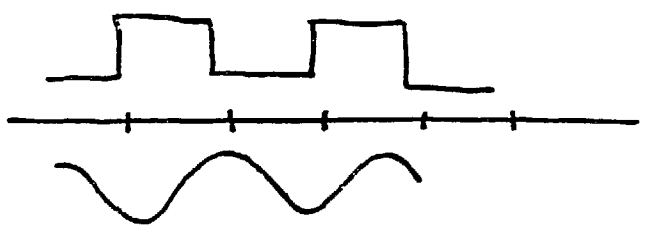

MEASURE PHASE SHIFT BETWEEN SIGNALS

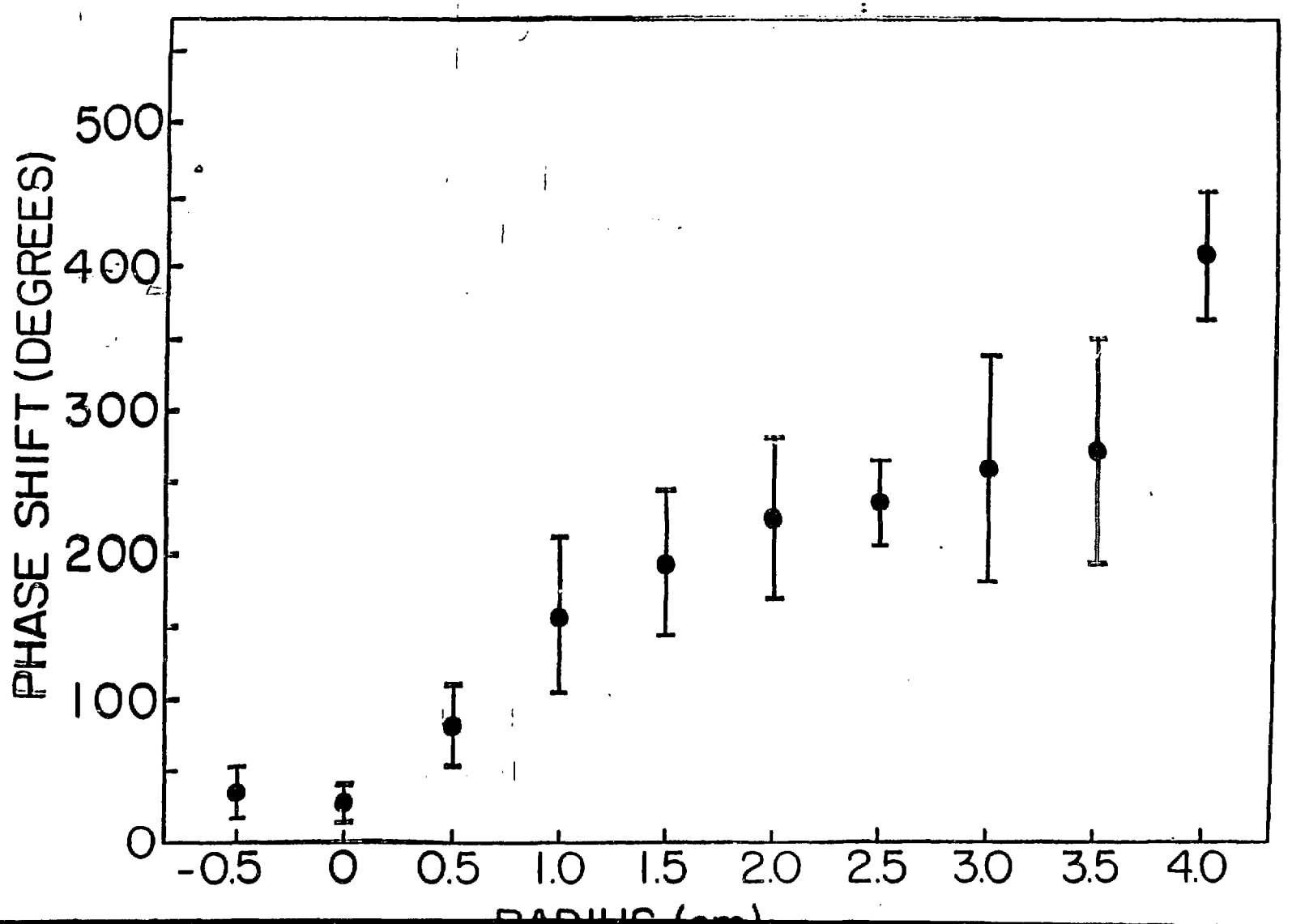
PHASE SHIFT VERSUS RADIUS AT THE
FUNDAMENTAL PERTURBATION FREQUENCY
(1 KHZ)
PHASE SHIFT (DEGREES)
0
100
200
300
400
500
-0.5
0
0.5
1.0
1.5
2.0
2.5
3.0
3.5
4.0

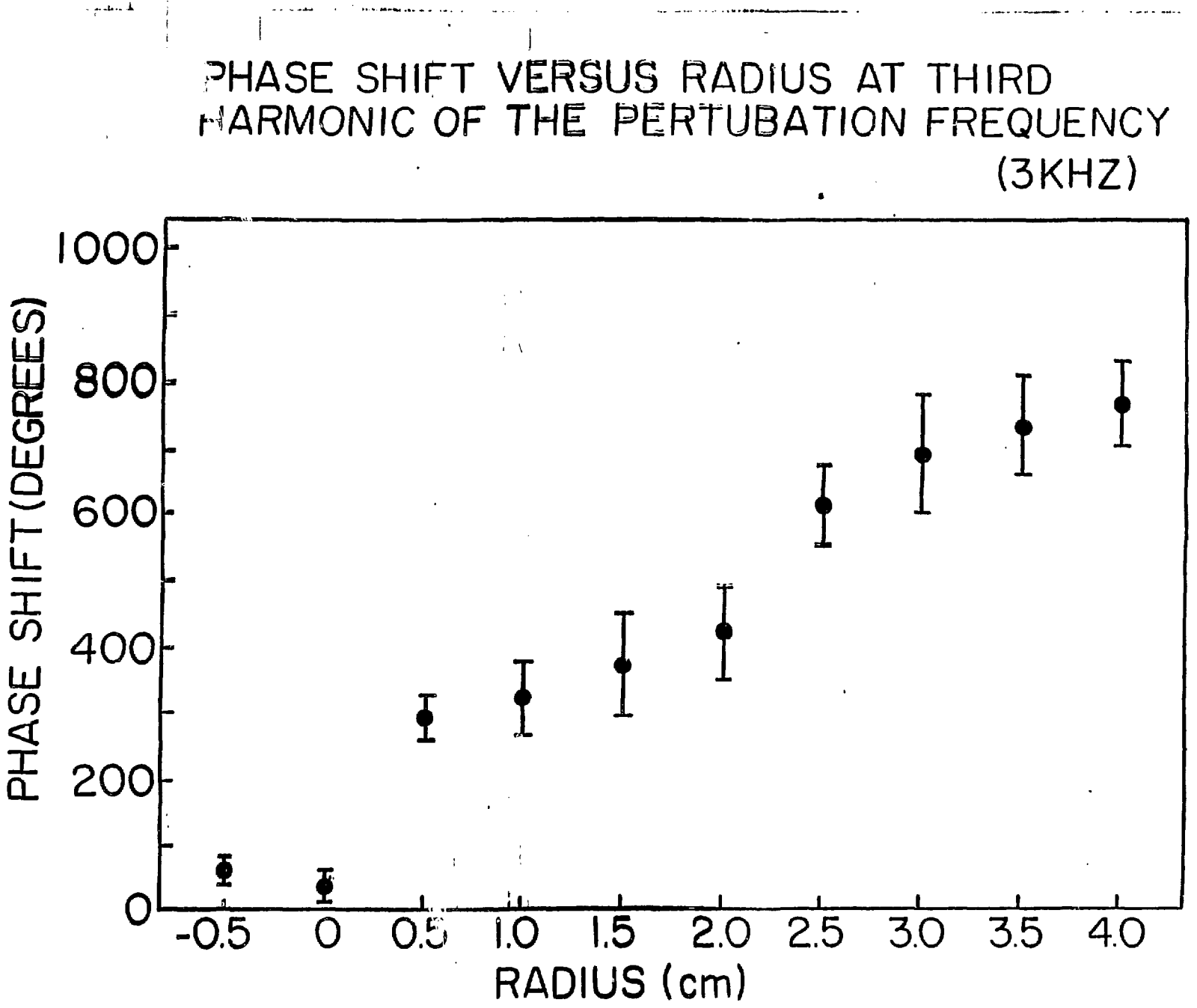
PHASE SHIFT VERSUS RADIUS AT THIRD HARMONIC OF THE PERTUBATION FREQUENCY (3KHZ)
PHASE SHIFT (DEGREES)
1000
800
600
400
200
0
-0.5
0
0.5
1.0
1.5
2.0
2.5
3.0
3.5
4.0
RADIUS (cm)

VARIATIONS OF K VERSUS D FOR THE FUNDAMENTAL AND THIRD HARMONIC OF THE PERTUBATION FREQUENCY

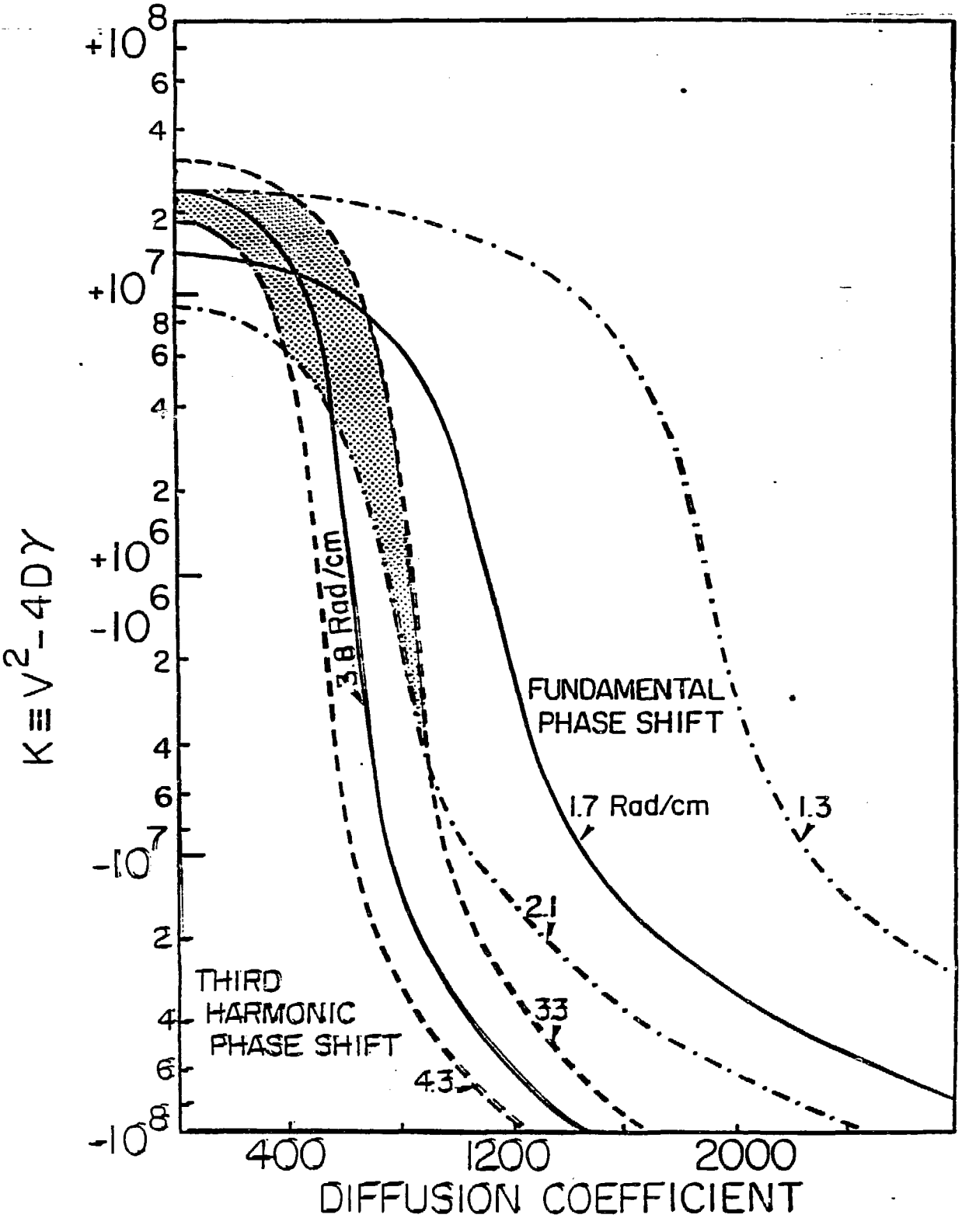

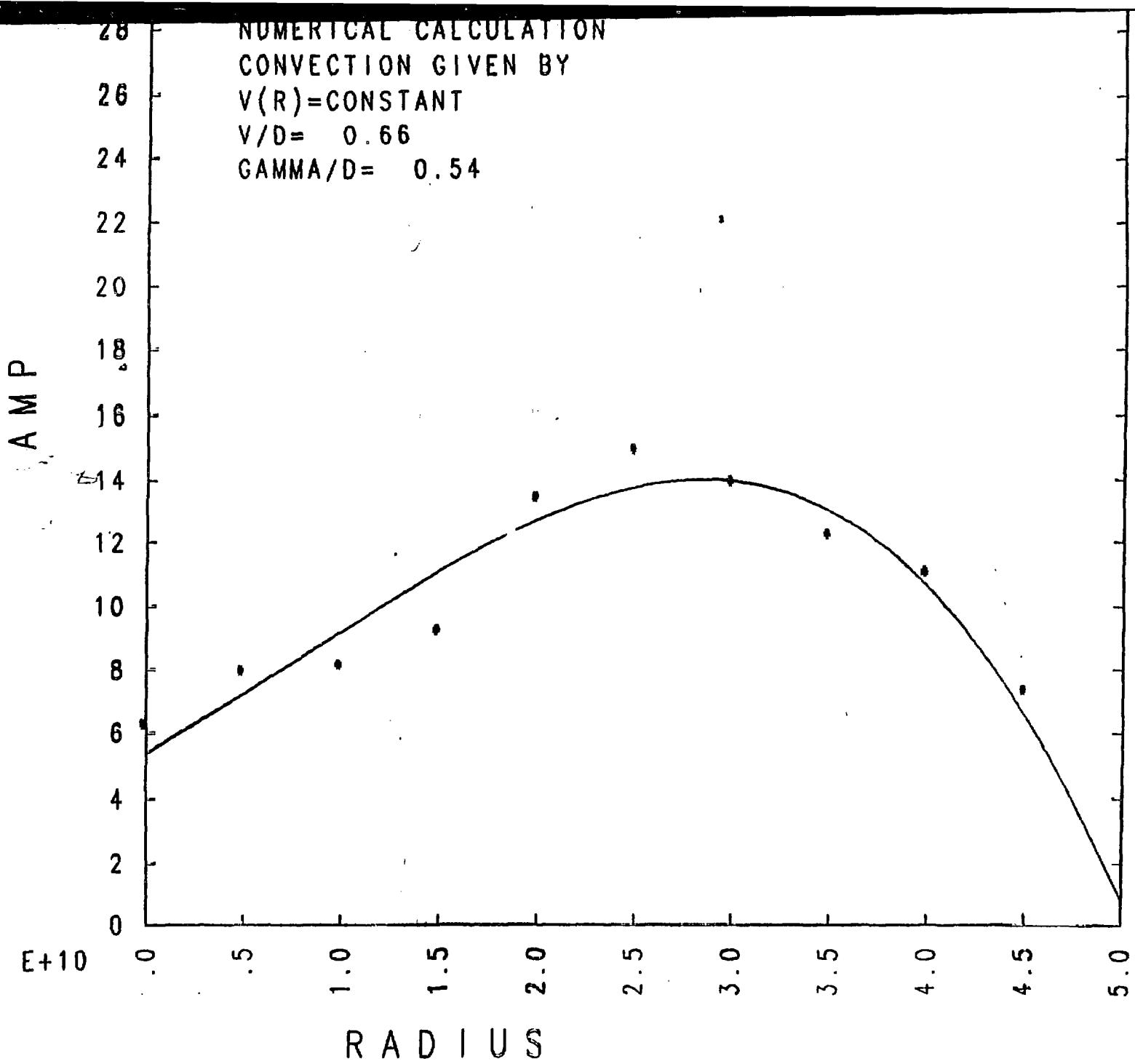
NUMERICAL CALCULATION
CONVECTION GIVEN BY
V(R)=CONSTANT
V/D= 0.66
GAMMA/D= 0.54
AMP
E+10
28
26
24
22
20
18
16
14
12
10
8
6
4
2
0
.0
.5
1.0
1.5
2.0
2.5
3.0
3.5
4.0
4.5
5.0
RADIUS

SUMMARY

- Density profiles in IMS are hollow and can be modelled by the inclusion of a convective term in the equilibrium particle balance equation

- Poloidal E field appears to be responsible for the convection. Hot electrons may be responsible for the poloidal electric field

- Phase shift and amplitude of a perturbation of the potential in the plasma may be related to the diffusion coefficent, convection velocity and ionization rate, but because of high uncertainties, it is hard to obtain good results

- Instead, using the steady-state density profile to obtain the ratios of V/D and γ/D we obtain:

$$D = 800 - 2200 \text{ cm}^2/\text{sec}$$

$$V = 500 - 1500 \text{ cm/sec}$$

$$\gamma = 400 - 1200 \text{ sec}^{-1}$$

INITIAL REDUCED-Q OPERATION OF THE PROTO-CLEO STELLARATOR

- Both reduced and enhanced-Q operations were made by shifting the magnetic axis with an external vertical field.

- Pfirsch-Schluter Currents were measured under both operating conditions in the L=3 Proto-Cleo stellarator. The currents decreased in both directions of shifting the magnetic axis.

- This is consistent with an L=3 device, since the transform is zero on the magnetic axis with no shift and the Pfirsch-Schluter current is inversely proportional to the value of the rotational transform.

- Shifting of the axis causes a non-zero transform on the axis and hence a decrease in Pfirsch-Schluter currents.

- Plans are being made to install the L=2 winding in Proto-Cleo to measure the effect here. In this case, the reduced-Q effect should be observed.